The hauterivian-lower aptian sequence stratigraphy from Jura platform to vocontian basin : a multidisciplinary approach / Field-trip of the 7th International symposium on the Cretaceous (September 1-4, 2005) ; [organized by] Université Joseph Fournier, Grenoble 1 Université de Neuchâtel, UNINE

Thierry Adatte, Annie Arnaud Vanneau, Hubert Arnaud

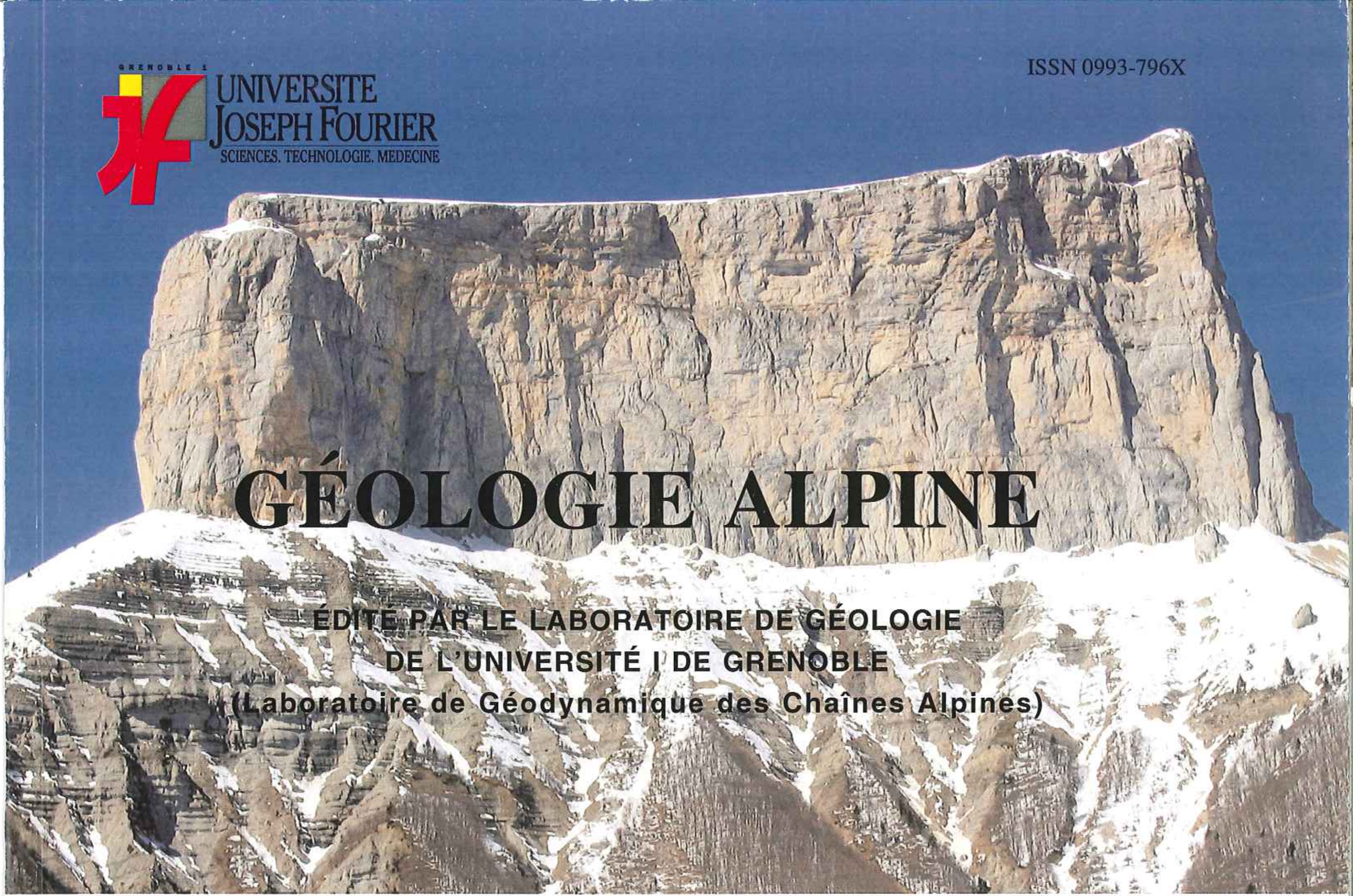

UNIVERSITE JOSEPH FOURIER
SCIENCES. TECHNOLOGIE. MEDECINE

ISSN 0993-796X

GÉOLOGIE ALPINE

ÉDITÉ PAR LE LABORATOIRE DE GÉOLOGIE
DE L'UNIVERSITÉ I DE GRENOBLE
(Laboratoire de Géodynamique des Chaînes Alpines)

SÉRIE SPÉCIALE «COLLOQUES ET EXCURSIONS» N° 7

THE HAUTERIVIAN - LOWER APTIAN SEQUENCE STRATIGRAPHY FROM JURA PLATFORM TO VOCONTIAN BASIN: A MULTIDISCIPLINARY APPROACH

Field-trip of the 7th International Symposium on the Cretaceous (September 1-4, 2005)

Thierry Adatte, Annie Arnaud-Vanneau, Hubert Arnaud,
Marie-Caroline Blanc-Alétru, Stéphane Bodin, Elisabeth Carrio-Schaffhauser,
Karl B. Föllmi, Alexis Godet, Mohamed Chaker Raddadi et Jean Vermeulen

Université de Neuchâtel unine

GRENOBLE 1 UNIVERSITÉ
JOSEPH FOURIER
SCIENCES, TECHNOLOGIE, MEDECINE

Université
de Neuchâtel unine

THE HAUTERIVIAN - LOWER APTIAN SEQUENCE STRATIGRAPHY FROM JURA PLATFORM TO VOCONTIAN BASIN: A MULTIDISCIPLINARY APPROACH

Field-trip of the 7th International Symposium on the Cretaceous (September 1-4, 2005)

Thierry **Adatte** [1], Annie **Arnaud-Vanneau** [2], Hubert **Arnaud** [2],
Marie-Caroline Blanc-Alétru [3] Stéphane **Bodin** [1], Elisabeth **Carrio** [4], Karl B. **Föllmi** [1],
Alexis **Godet** [1], Mohamed Chaker **Raddadi** [5], Jean **Vermeulen** [6]

[1], Université de Neuchâtel, 11 rue Emile Argand, Neuchâtel, Suisse
[2], Laboratoire de Géodynamique des Chaînes Alpines, Maison des Géosciences, 38041 Grenoble cedex, France
[3], 181A Huntingdon Road, Cambridge CB3 0DH, United Kingdom
[4],Laboratoire de Géophysique Interne et de Tectonophysique, Maison des Géosciences, 38041 Grenoble cedex, France
[5],Laboratoire Dynamique de la Lithosphère, Université de Montpellier 2, 34095 Montpellier cedex 5, France
[6], Grand'rue, 04330, Barrême, France

2005

Cover : Mont Aiguille, 50 km south from Grenoble, Glandasse limestones Fm. Photo H. Arnaud

INTRODUCTION

These four days are devoted to the Barremian-Lower Aptian series both in the vocontian trough, characterized by basinal facies with ammonites (one day), and on the Urgonian platform which coresponds to its northern margin (three days).

The first three days, sediments deposited in the shallow marine environment of the so-called Urgonian platform are observed in two main areas : 1) the Swiss Jura corresponding to the inner part of the platform and 2) the Vercors massif, belonging to the Northern Subalpine Chains (Grenoble region) where nice outcrops allow us to detail the lateral change from platform to basin. These days are devoted to facies analysis and distribution, sequence stratigraphy and geochemistry of the Urgonian carbonate platform (Barremian-early Aptian).

The Vercors mountain near Grenoble is one of the most interesting place in the world to analyse the 3D organisation of sedimentary bodies from the inner platform (Gorges du Nant and Les Ecouges section) to the outer shelf which will be observed near Chichilianne on the Glandasse Plateau and the deep marine basin in the eastern Diois.

The last day is devoted to the Barremian stratotype which has been defined in the famous Angles section. This section, complete from Lias to Upper Cretaceous, is one of the best section of the vocontian trough (SE France). It could be considered as a **reference for the Barremian tim**e as detailed biostratigraphic and geochemistry studies are now available.

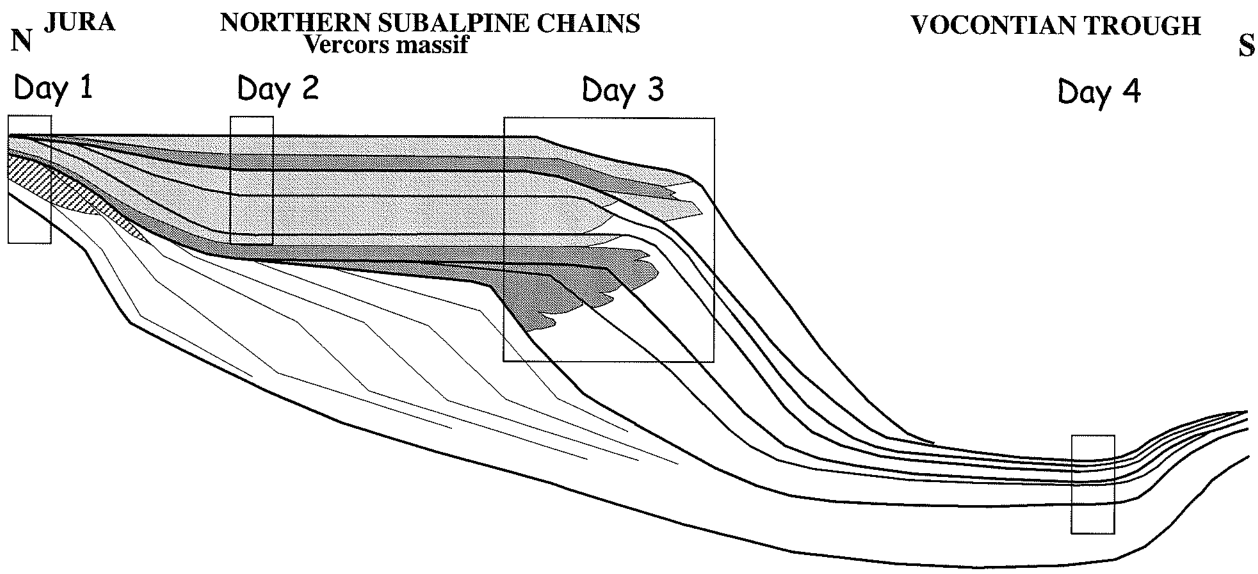

FIG. 1.- Schematic section of the Urgonian platform and vocontian trough showing the regions visited during the excursion.

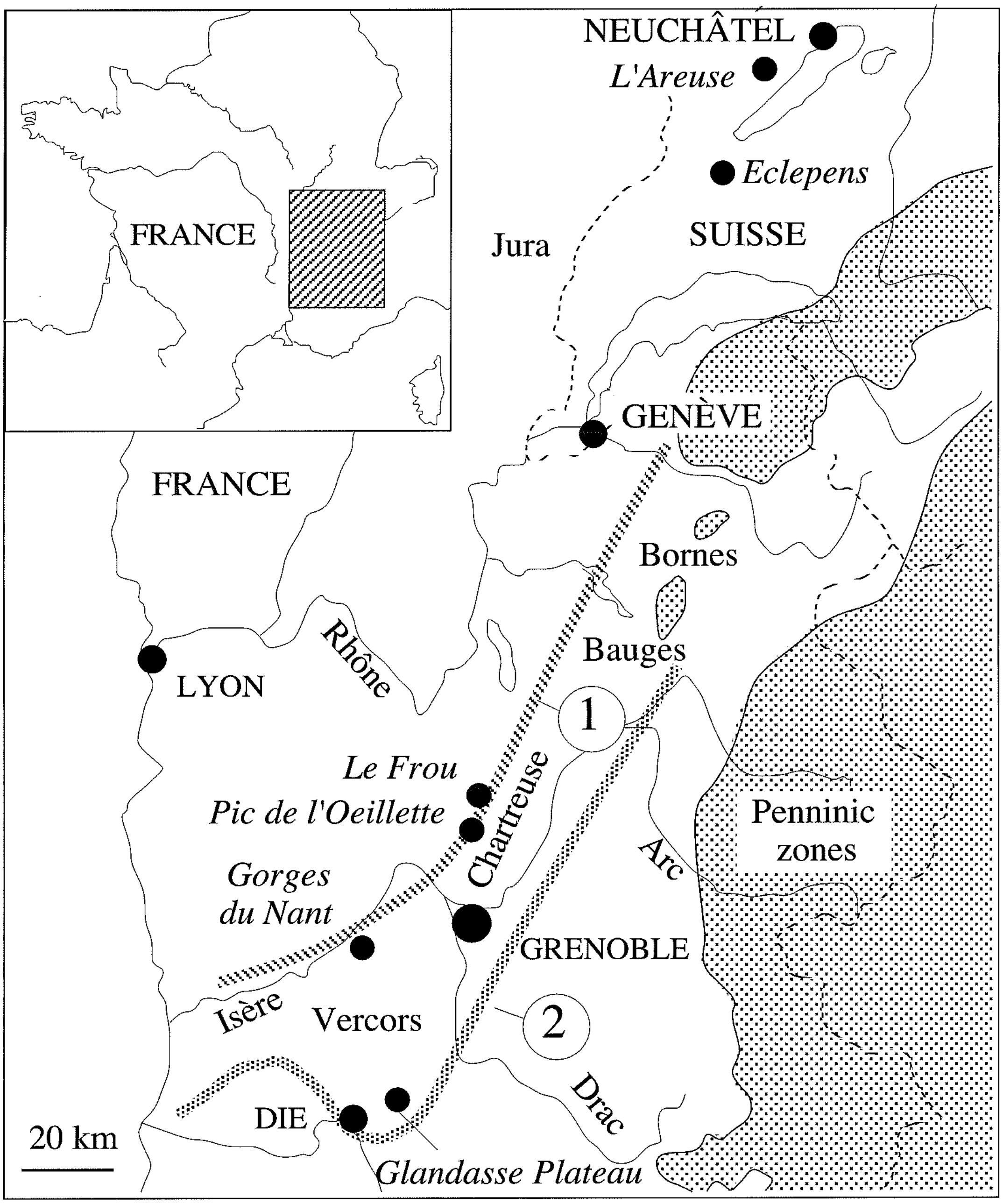

FIG. 2.- Geographical map of the Jura and the Southeastern France showing the location of the studied areas.

THE SOUTH-EAST FRANCE BASIN (SFB) AND ITS MESOZOIC EVOLUTION

Hubert Arnaud *

The Atlantic ocean comprises three main sections. The **South Atlantic** lies between Africa an South-America, to the south of the major transform faults (St Paul, Romanche, etc.) of the Equatorial Atlantic. Between the latter and the Azores fault zone, the **Central Atlantic** separates North-America from Africa. North of the Azores line, the **North-Atlantic** (linked with the **Bay of Biscay** between Europe and Iberia) separates North-America from Iberia and Europe.

About 250 my ago, at the end of Paleozoic times, all continents were grouped to build a single continent called Pangea. The **breakup of Pangea** began in the Jurassic, giving birth progressively to present day oceans such as the Atlantic or the Indian, and also to vanished ones, such as the Tethyan ocean. During this breakup, the different sections of the Atlantic did not open at the same time :

1) the Central Atlantic in Late Middle Jurassic times, 160-170 my,

2) the South Atlantic in the early Cretaceous, 120-130 my,

3) the North Atlantic in the Middle of Cretaceous times, 100-110 my (with the exception of its northermost part, between the Gibbs fracture zone and Iceland, early Tertiary).

Except for the birth of the South Atlantic, which concerns only the relative motions of Africa and South America, all these events governed the relative motions of Africa (more or less linked with Apulia), Iberia and Europe, and therefore the history of the Ligurian Ocean. In this respect, **three main changes** need to be considered during the Mesozoic kinematic evolution.

1) **160-170 my (Bathonian-Callovian)**: the break-up of Pangea occurred along a zigzag ("bayonet") fracture. From this time on, the Central Atlantic opened and began to spread, with the initiation of left-lateral strike-slip motion between Africa and Europe (to which Iberia and Corso-Sardinia were still attached). Apulia, like Africa, moved eastward with respect to the European continent. As a consequence, the opening of the Ligurian Tethys ocean might have occurred at the same time as that of the Central Atlantic from which it was separated by the complex, partly continental and partly oceanic, Gibraltar-Maghreb transform zone.

We may therefore predict (a) that on both sides of the developing Ligurian Tethys, continental rifting might have occurred prior to 170 my, i.e. at Liassic and Middle Jurassic times, possibly also in the Triassic, and (b) that the Ligurian ocean might have opened and then continued to spread on and after 170 my.

2) **100-110 m.y. (Mid Cretaceous)**: the opening of both the North Atlantic and the Bay of Biscay introduced a complication in the previous picture : Iberia began to move eastward, with the possible beginning of closure of at least a part of the Ligurian Tethys. A second rifting episode ("*Atlantic rifting*") in the Late Jurassic and the Early Cretaceous might have been superimposed upon the Tethyan spreading stage, at least in a part of the Iberian and European blocks.

3) **80 or 70 m.y. (Late Cretaceous)**: an important change in the motion of Africa occurred. Africa henceforth moved northwards towards Europe initiating narrowing and disappearance of the Ligurian ocean, followed by continental collision.

As will be demonstrated below, all of these events are recorded in the Mesozoic sediments of the Alps.

1.– THE SOUTH-EAST FRANCE BASIN (SFB) : LOCATION AND SHAPE

The **SFB** is a Mesozoic basin that lies between the internal zones of the Western Alps and the outer-Alpine French Central Massif.

In the South, it is bounded by the Mediterranean sea (fig. 9); its northern limit is conventionally located between the latitudes of Grenoble and Lyon cities, but the basin continues north-eastwards into the Helvetic part of the external zone of the Alps (Savoy in France, Switzerland), where it is fringed in the North-West by the Jura platform.

In the following, this basin will be considered in a broad sense, **including the carbonate platforms areas** that lie around the deep pelagic basin, as well as its transition to the East, towards the internal zones of the Western Alps (fig. 9).

Considering its Jurassic surrounding platforms (fig. 9), this basin displays on a map a more or less **triangular shape** : it was fringed (1) to the West or North-West by the carbonate platform that is the sedimentary cover of the Central Massif (Causses, Cévennes), (2) to the South

* These pages correspond to a short adaptation of Arnaud and Lemoine (1993).

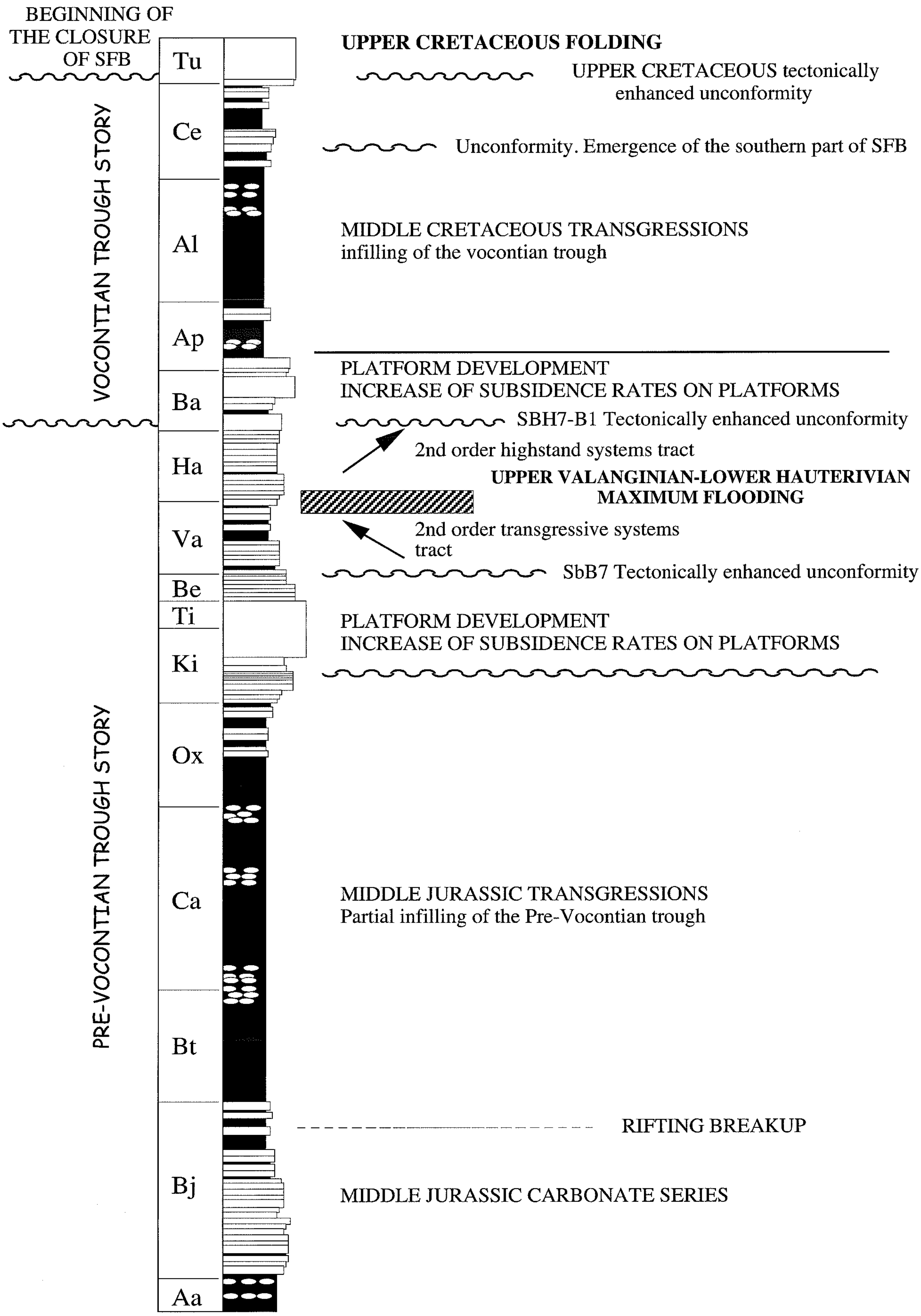

FIG. 3.- Schematic log of the Pre-vocontian and Vocontian series.

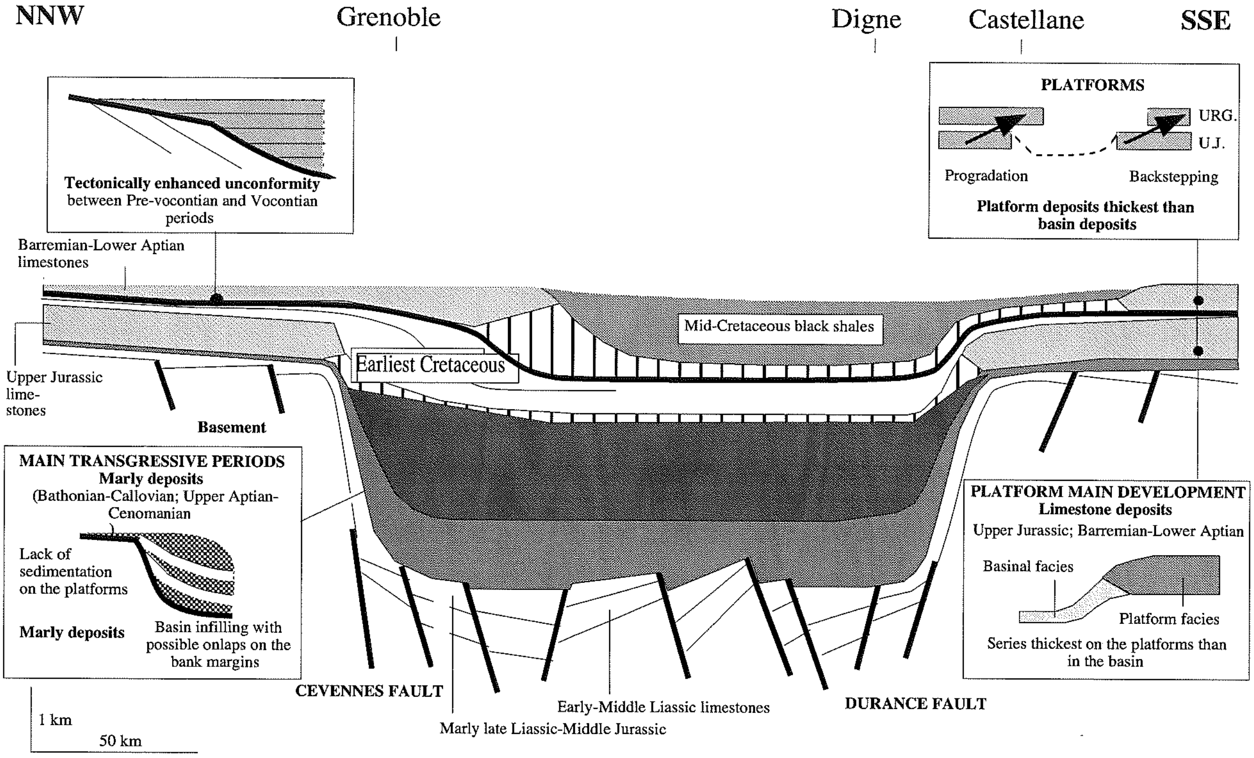

Fig. 4.- A highly schematic section across the SFB, showing the relationships between the main formations. Note (1) the presence of two black-shales episodes, a Jurassic one and the well known Mid-Cretaceous one, and (2) the shift of the platform-basin boundary that occurred at the end of the Hauterivian (more or less 115 my), i.e. at the transition from the pre-Vocontian period to the Vocontian one.

by the Provence platform (at that time connected to the Corsican-Sardinian platform), (3) to the East by the internal zones of the Alps (mostly deep sea basinal). The area of the basin has been reduced and its shape is somewhat different in the late Early Cretaceous, after the "Hauterivian revolution" (fig. 9), as a result of the shift of its North-Western and South-Western platform limits.

1.1. Predominant role of the Cévennes fault zone, close to the Central Massif

South of Valence city, the border of the crystalline basement of the Central Massif trends approximately NE-SW. The boundary is the narrow zone of the **NE-SW trending Cévennes faults**, which were normal faults linked with the Jurassic, syn-rift extensional tectonics, and were later inverted into strike-slip faults during the Cenozoic. This limit played a role since the Triassic. It has been later, in the Liassic and in the Middle Jurassic, the site of normal faulting, and the NE-SW trending major faults extend into the External zone of the Alps, where they bound the major syn-rift tilted blocks. On the other side, the Durance fault plays a symmetrical role (fig. 9).

During the Jurassic and a part of the Early Cretaceous, before the Hauterivian revolution (fig. 9), this narrow NE-SW Cévennes fault zone was also the limit between the carbonate platform of the sedimentary cover of the Central Massif (Causses, Cévennes) and the basinal sediments of the **SFB**.

1.2. Thickness of the sedimentary infilling and deep structure

The Mesozoic and Cenozoic sediments of the basin rest above a **pre-Triassic basement** which is the extension of that of the surrounding basement massifs (fig. 9), namely the Central Massif (West), the external crystalline massifs of the Alps (East), and the Maures-Esterel massif of Provence (South-East). Small Carboniferous coal basins and Permian ones are known in these pre-Triassic massifs. Whether or not such basins are present in the basement of the basin itself remains conjectural, except for two small outcrops in the North and North-West of Digne.

The thickness of the sediments varies considerably. In the centre of the basin, it reaches 10 to 11 kilometres (Triassic, > 900 metres ; Jurassic, 6000 metres ; Early Cretaceous, 2000 metres ; Late Cretaceous, 0 to 600 metres, Tertiary, 0 to 2500 metres).

1.3. Short summary of the Mesozoic sedimentary series and of its evolution

The Mesozoic-Cenozoic cover displays important lateral facies and thickness (maximum of 10 to 11 kilometres, but in some places a few hundred metres only) variations. These sediments, their evolution and their lateral variations will be discussed in the forthcoming sections. In this section we only summarise the most prominent features of the Mesozoic sediments.

Triassic, not yet the basin, but its foreshadowing.

The Triassic evaporites and carbonates (mainly dolomites) were deposited in subaerial to very shallow environments. Not a true marine basin, but only a strong subsidence (900-1000 metres of sediments) with mainly evaporite deposition. This history is therefore only the foreshadow of the future Jurassic-Cretaceous marine basin.

Jurassic-Cretaceous : succession of major, thick, marly and calcareous episodes in the basin

The Jurassic-Cretaceous series will not be described here in details. But an important feature, which is characteristic both of the Atlantic and the Tethyan series, has to be yet emphasized (fig. 3 and 4). The whole series displays an alternation of relatively long episodes of either mainly calcareous or mainly argillaceous-marly sedimentation. In particular, marls devoid of calcareous beds, but for some scarce cases, occur in the Late Liassic-Early Middle Jurassic, in the Late Middle Jurassic-Early Late Jurassic (a kind of "Jurassic black shales" episode), and in the middle of the Cretaceous (Cretaceous black shales, which are widespread, from the Atlantic to the Tethyan domain).

During the Mesozoic (duration : 180 my), several steps, most of them resulting from tectonic changes ("revolutions") are to be distinguished. They are more or less related with the evolution of the European passive margin of the Ligurian Tethys ocean. These steps are as follows.

(1) ***Triassic*** (40 my) : relatively strong subsidence in the center of the future basin, deposition of evaporites, but not yet the true marine basin.

(2) ***Jurassic and a part of the Early Cretaceous*** (80 my) : this is the so-called "**prevocontian period**" ; the basin is broad, the fringing platforms do not significantly shift basinwards.

(2a) *Liassic-Middle Jurassic* (40 my) : opening then early evolution of the basin, with a network of shoals and deep basinal areas, bounded by active normal faults : this is the time of the **Tethyan rifting.**

(2b) *Late Middle Jurassic, Late Jurassic* (25 my): a relatively quiet period, coeval with the **opening then spreading of the Ligurian Tethys ocean**. Note that the several hundred metres of "Jurassic black shales" which are visible in the **SFB** are coeval with radiolarian cherts (at some places missing, often a few metres, rarely a few tens of metres thick) that rest directly upon the new born oceanic crust of the Ligurian ocean.

(2c) *First part of the Early Cretaceous* (15 my) : continuation of the "Tethyan spreading stage", but with superimposition of the **Atlantic-Biscay rifting.**

(3) ***Late Hauterivian revolution (= "Barremian crisis"): shift of the platform***, beginning of the "**Vocontian period**" (fig. 9).

(4) ***Late Early Cretaceous, Barremian-Early Aptian*** (5 my): this is the time of the Vocontian period; the basin has narrowed, as a result of the rapid basinward shift of the platform (now the **Urgonian platform**, fig. 11)

(5) ***Late Aptian to Early Cenomanian*** (15 my): time of deposition of the **Cretaceous black shales.**

(6) ***Late Cretaceous*** (25 my): levelling of the basins sediments, **beginning of inversion,** i.e. of the closure of the basin.

(7) ***Tertiary*** (65 my): Pyrenean and Alpine folds, detrital sediments (flysch and molasse), i.e. **final closure of the basin.**

1.4. Inversion of the basin : folds, thrusts and the Tertiary deposits

Let us only remind here that the inversion of the basin is the result of several phases of folding and thrusting that occurred from the Late Cretaceous up to the Pleistocene.

(1) The basin has been first affected by folding, as early as in the Late Cretaceous, and also in the Middle Eocene : this is the birth of East-West trending folds, which are an Eastern extension of the Pyrenean ones ;

(2) later on, younger folds of Oligocene and above all Neogene and Pleistocene age, that belong to the Alpine history were born; at the same time, earlier, Pyrenean E-W folds were reactivated.

2.– Pre-vocontian period

The proper history of the **SFB**, before its Late Cretaceous and above all Cenozoic closure, can be divided into two main periods. The youngest one is the well-known **vocontian period** (Latest Hauterivian to Cenomanian, about 20-25 my) during which the deep basinal part was relatively narrow, being surrounded by the Urgonian limestone platforms.

But before the Late Hauterivian change, a first step of the history of the **SFB**, which is here called the **pre-vocontian period**, is the time when the deep, basinal part of the basin was much broader between the Jura-Cévennes-Causses (North-West) and Provence (South) border platforms. From the Rhaetian-Hettangian up to the Late Hauterivian, this pre-vocontian period lasted about 90-95 my. In this abstract, the early Cretaceous period is only discussed.

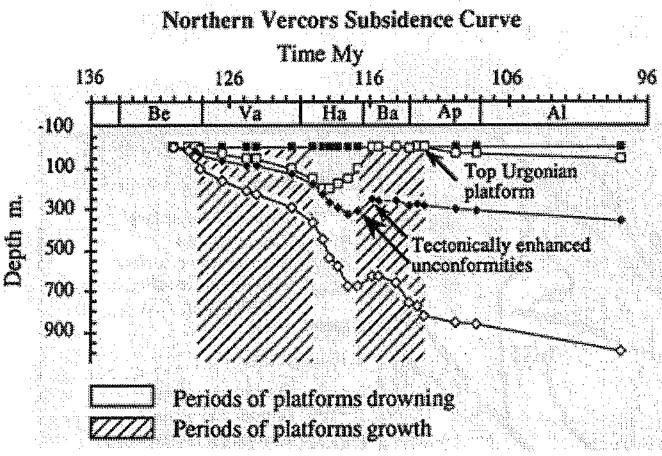

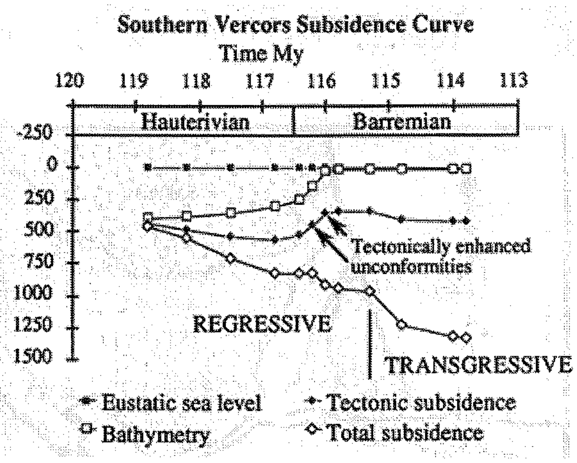

FIG. 5.- Geohistory diagrams for the Northern Vercors (composite section) and the Southern Vercors (Archiane valley) showing the paleobathymetric history, the total subsidence (water depth and decompacted thickness) and the tectonic subsidence (total subsidence corrected for sediment loading). The sea level is assumed to be constant. The stratigraphic data which are plotted are the sequence boundaries. An uplift is assumed for the Late Hauterivian-Early Barremian when the sequence boundaries HA7 and BA1 occurred (tectonically enhanced unconformities). Note that the drowning of the Berriasian-Valanginian platform results from high rates of tectonic subsidence, which indicate that accomodation space of tectonic origin was being created at a greater rate than the carbonates could fill, causing them to drown. On the contrary, the drowning of the Barremian-Aptian platform seems not so well related to the tectonic history. The long term rising of the Lower Cretaceous eustatic sea level is probably significant for the Aptian drowning [Jacquin *et al.*, 1990].

Earliest Cretaceous, before the Late Hauterivian change or "Barremian crisis" (135-120 my)

This period is characterized by four main features, viz. (1) subsidence globally weaker than in the Late Jurassic, (2) abundant terrigenous detrital supply, (3) deposits thicker in the pre-vocontian trough than on the border platforms, and (4) generalized transgression, with a maximum at the base of the Hauterivian.

The detrital supply, mainly clays, with minor siltose quartz, occurs from the very base of the Cretaceous and increases progressively until the Valanginian, during which time it reaches a maximum before a slight decrease in the Hauterivian. Therefore, the deposits of the pre-vocontian trough are mostly marls and limestones and rather thick.

On the border platforms, the deposition of the argillaceous material depends on the different epochs. They may occur as thin argillaceous levels that mark the maximum floodings in the standard platform deposits, or as marly formations on the drowned platforms (e.g., the **Marnes d'Hauterive Fm.** in the Lower Hauterivian of the Jura, or the Upper Valanginian and the Hauterivian of the Castellane arc. These abundant fine-grained detrital supplies gave birth to **deposits whose thickness is greater in the pre-vocontian trough than on the border platforms,** contrary to the Late Jurassic situation.

The subsidence rates are weaker than in the Late Jurassic, as deduced from the global thicknesses of shallow water sediments on the drowned platforms. The rates probably increased during Late Valanginian-Early Hauterivian throughout the SFB. This probably resulted in the important local transgression at that time, a transgression which seems unknown in other Tethyan areas.

From a stratigraphical point of view, the Berriasian-Hauterivian interval can be subdivided into about twenty depositional sequences, known both in the trough and on the Northern border platform. These sequences are well individualized and complete in the pre-vocontian trough series, whereas on the platforms they are reduced to both transgressive and highstand systems tracts. On the Northern platform, our knowledge about the Late Valanginian is too poor because of the lack of deposits. On the Southern platform, no stratigraphic sequence analysis is possible for the Berriasian in the present state of knowledge. For this reason, the events will be described using mainly the study of the Northern platform.

The platforms were still well developped in Berriasian times, but progressively drowned in the Valanginian, then in the Hauterivian. They are well known in the North of the **SFB**; their main features are the following:

1) weak progradation until the beginning of the Valanginian, followed by a continuous facies retrogradation,

2) progressive change of the morphology of the borders (by-pass margin at the base of the Berriasian beds, rimmed shelf in the Valanginian, ramp in the Hauterivian),

3) presence of an important tectonically enhanced unconformity at the top of the Upper Berriasian (BE6-BE7 sequence boundaries),

4) depositional sequences whose general features are similar to those described in figure 6, but vary

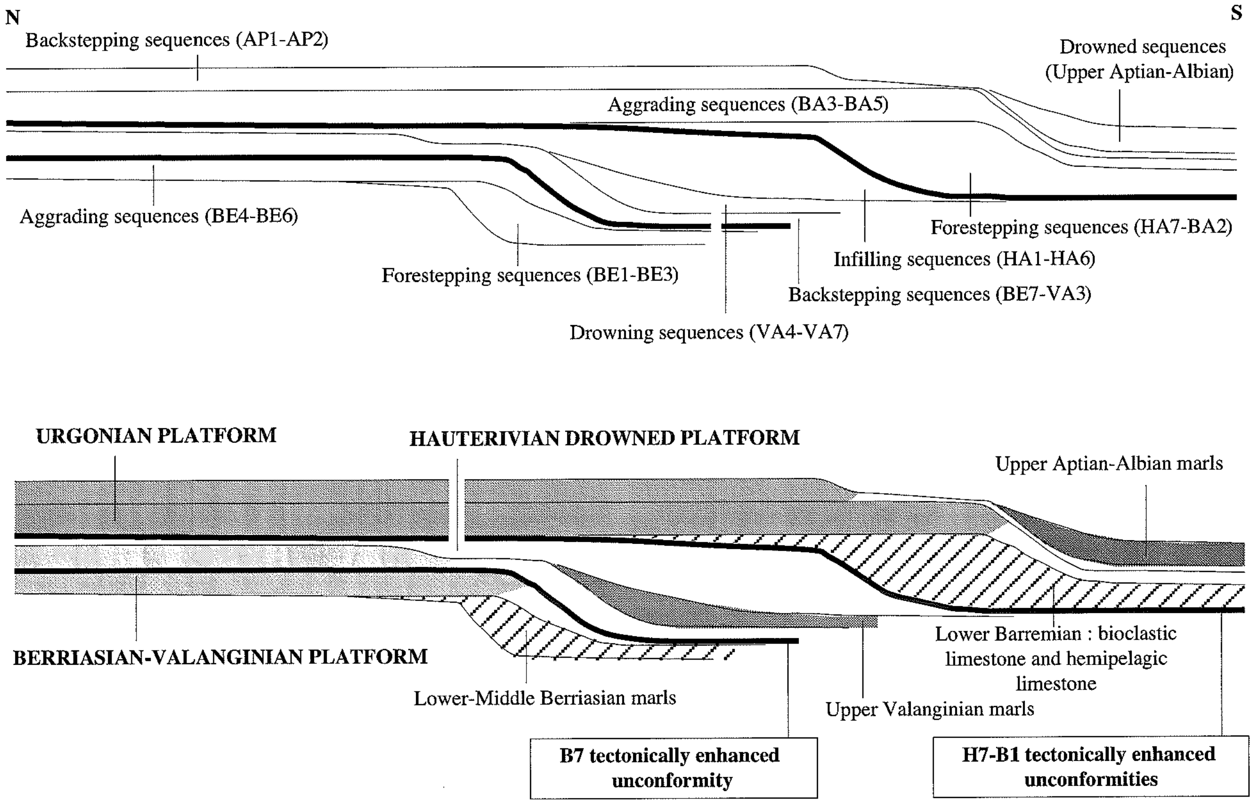

Fig. 6.- Organisation of the depositional sequence sets (Berriasian-Albian) on the northern border of the SFB.

significantly from bottom to top according to the available space.

Five successive stages may be distinguished in the Berriasian-Hauterivian interval.

(1) ***Lower-Middle Berriasian***. The paleogeographic situation was very similar to that of the latest Jurassic, although characterized by emersions and important breaks. In the North of the SFB, the platform were emerged (mostly sedimentary breaks), and the deposits are only those of the so-called "purbeckian facies", formerly interpreted as fresh or brackish water deposits, marking the emersion at the Jurassic-Cretaceous boundary. We know now (Mojon, 2002) that they correspond to transgressive deposits. Parasequences are made up of sediments deposited either in fresh water (lacustrine), charophyta-bearing environments, or in shallow water marine environments (oolithic facies, or with benthic foraminifera); they are overlaid by the maximum flooding deposits that contain ammonites of the Jacobi-Grandis zones (Jurassic-Cretaceous boundary).

In the South of the **SFB**, similar "purbeckian facies" have the same significance, but they do not characterize the same sequence of the earliest Cretaceous (Late Berriasian). On the steep edges of the Northern platform, the hemipelagic sedimentation continues.

(2) ***Late Berriasian***. Both in the North and in the South of the **SFB**, it displays carbonate deposits. In the North, the inner facies are well developped in the Jura, whereas the external facies occur only along a narrow and rather steep border. There are two transgressive systems tracts, the first one in the Paramimounum zone (*Keramosphaera allobrogensis* level, now *Pavlovecina allobrogensis* level), the second in the *picteti* subzone. The depositional sequences are aggrading sequences, and the progradation of the facies towards the centre of the the **SFB** is very weak. On the platform borders, the hemipelagic infilling continues.

(3) ***Latest Berriasian***. A complex tectonically enhanced unconconformity groups the sequence boundaries SbBE6 and SbBE7. It resulted in a regional unconformity, in a sudden fall down of the relative sea level, and in a more or less long emersion of the platforms. Along the edge of the Northern platform, the fall down of the relative sea level resulted in the formation of a lowstand wedge made up of coarse grained bioclastic sediments which were located on SbBE7 and in the lower part of the slope.

On the Southern platform, this tectonically enhanced unconformity corresponds to the great erosional surface that separates the platform carbonates from the Valanginian hemipelagic argillaceous limestones and marls (Point Sublime and Pont de Carajuan sections). This very rapid uplift of the whole **SFB** resulted, on a sedimentological point of view, in the great limit that

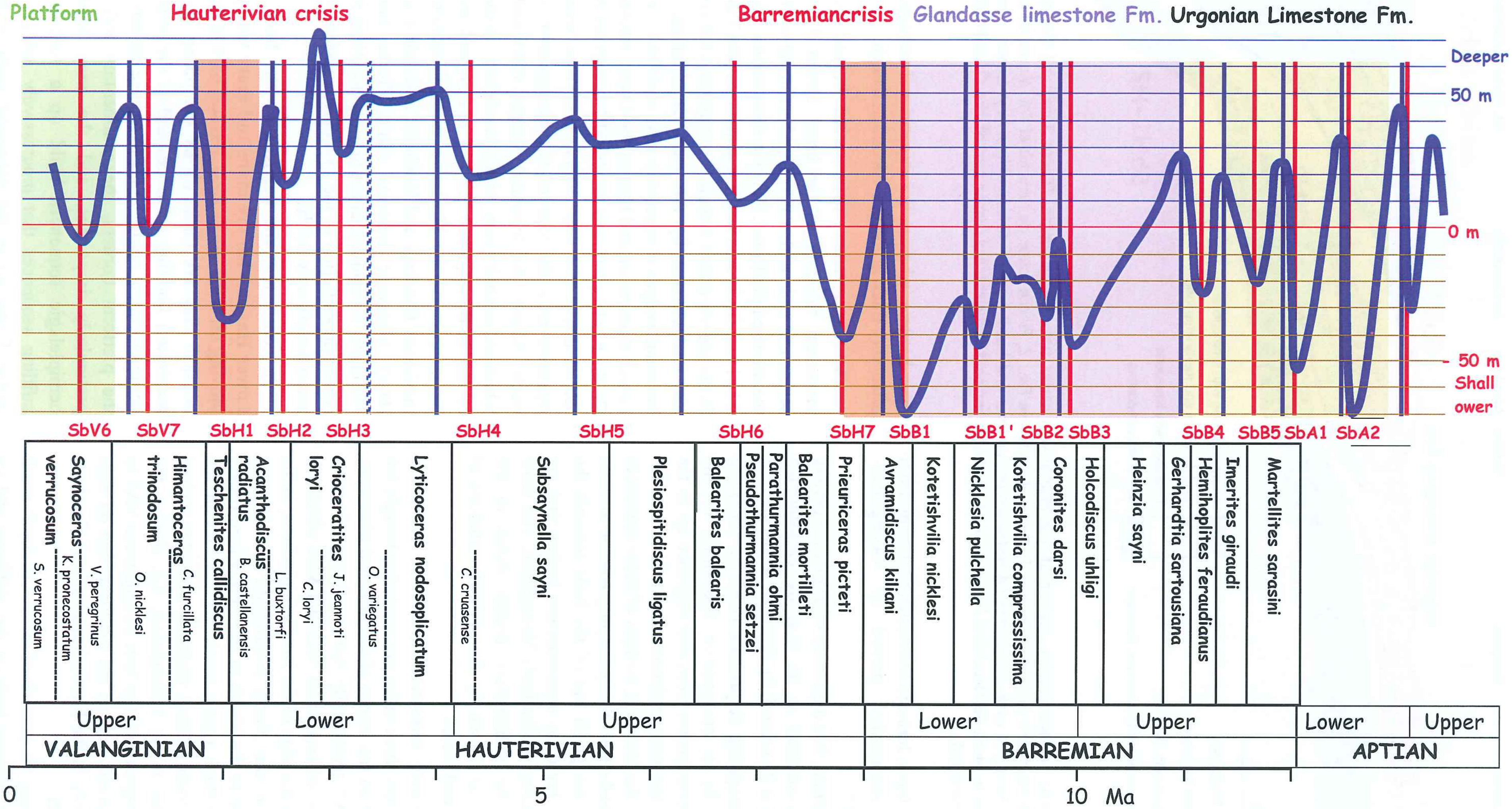

FIG. 7.- Sea-level variations (Upper Valanginian-Aptian).

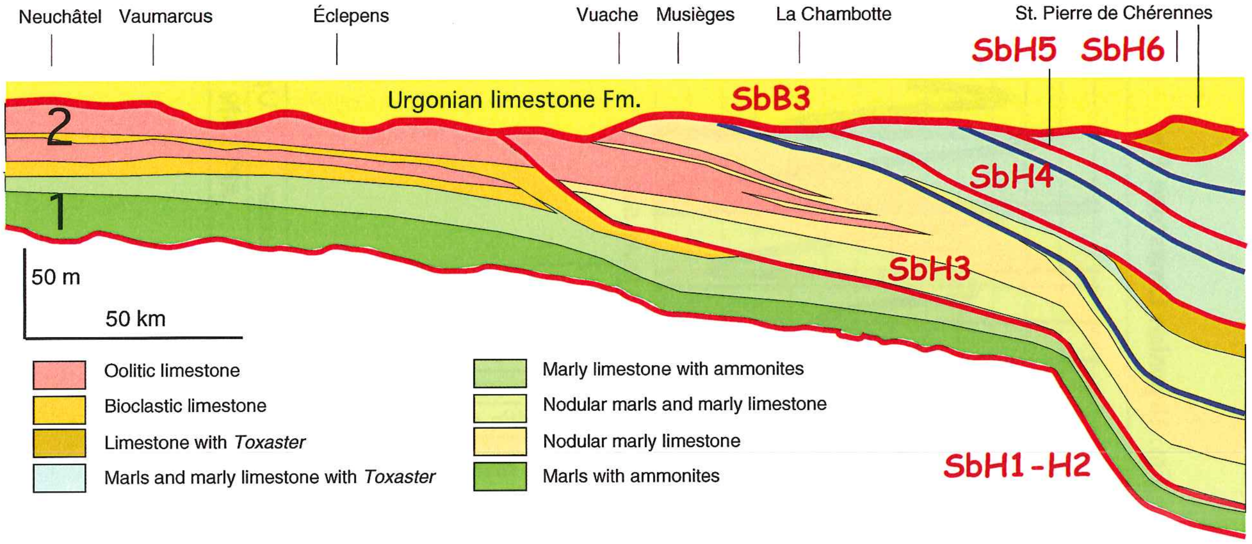

FIG. 8.- Schematic paleogeographic section of the Hauterivian series between Neuchâtel (Swiss Jura) and the northern Vercors (French Northern Subalpine Chains). 1, Marne d'Hauterive Fm.; 2, Pierre jaune de Neuchâtel Fm. Marne d'Hauterive Fm coresponds to marls with ammonites (*Acanthodiscus radiatus* and basal part of *Crioceratites loryi* zones, Lowermost Hauterivian). Pierre jaune de Neuchâtel Fm. is made of bioclastic and oolithic limestones (upper part of the *Crioceratites loryi* zone, early Hauterivian).

separates the Upper Jurassic-Berriasian platforms from the great transgressive period of Valanginian-Hauterivian age.

(4) ***Valanginian.*** It is a globally transgressive period, which is characterized at its base by backstepping sequences and at its summit by drowned sequences.

The backstepping sequences (BE7 to VA2) are characterized by a progressive deepening of the depositional environment from one sequence up to the other, and by the retrogradation of the facies. In the Grenoble area, the lowstand wedges of these sequences are numerous and show clearly the progradation towards the basin and the pinch out of the beds towards the platform; they build up superimposed bodies that are retrograding during all the Early Valanginian. The same geometry of the sedimentary bodies exists in the Castellane arc, as shown by the vertical variations of both lithology and facies.

The drowned sequences (VA3 to VA7) are complete and very thick in the pre-vocontian trough, but they disappear on the slopes of the drowned platforms, below the VA7 tectonically enhanced unconformity. This is the case of sequences VA3 and VA4 which are still present on the edge of the Northern platform, in the Vercors and in the North (Chartreuse massif), but disappear more to the North in the Jura, where only a few decimetre-thick marly levels are portions of the transgressive systems tracts, probably trapped in incised valleys. In the latest Valanginian, i.e. during the maximum transgression, the lack of sequences VA5 to VA7 is widespread both on the platforms and on their borders, not only in the North, but also in th Southern part of the **SFB**.

Summarizing, the periods of maximum depth result in the greatest hiatuses both on the platforms and on their borders, whereas the depositional sequences are often very thick in the pre-vocontian trough.

(5) ***Hauterivian.*** This period begins with the maximum flooding of the basal Lower Cretaceous series, and ends with a very rapid sediment-infilling on the drowned platforms. Hence a succession of drowned (HA1 and HA2) then infilling sequences (HA3 to HA6). In the pre-vocontian trough, the sequences are complete and characterized by the great development of the lowstand wedges of sequences HA3 and HA4 (top of the Lower Hauterivian and base of the Upper Hauterivian). On the border platforms, the basal Hauterivian deposits are all marly, and they display numerous breaks and represent only the tops of the transgressive systems tracts. Above, the lowstand wedges HA3 and HA4, which are normally very thick, are missing : in the North of the **SFB**, sequence HA3 is represented by marls (upper part of the Hauterive marl formation, HA3 maximum flooding) and bioclastic and oolitic deposits (HA3 highstand systems tract, Pierre Jaune de Neuchâtel formation); in the South (Castellane arc), the coeval deposits (top of the *Lyticocers nodosoplicatum* zone) remain only marly.

In conclusion, **the deposits of the base of the Lower Hauterivian are more and more marly when moving off from the central, basinal part of the SFB, because they are made up by the piling up of the maximum flooding** sequences and of the beds which lay immediately below and above these sequences. On the platform borders, the sedimentary infilling is particularly important, and the very thick and hemiplelagic sequences build up a succession of infilling sequences that progressively led (1) to the partial filling up of the peripheral parts of the pre-

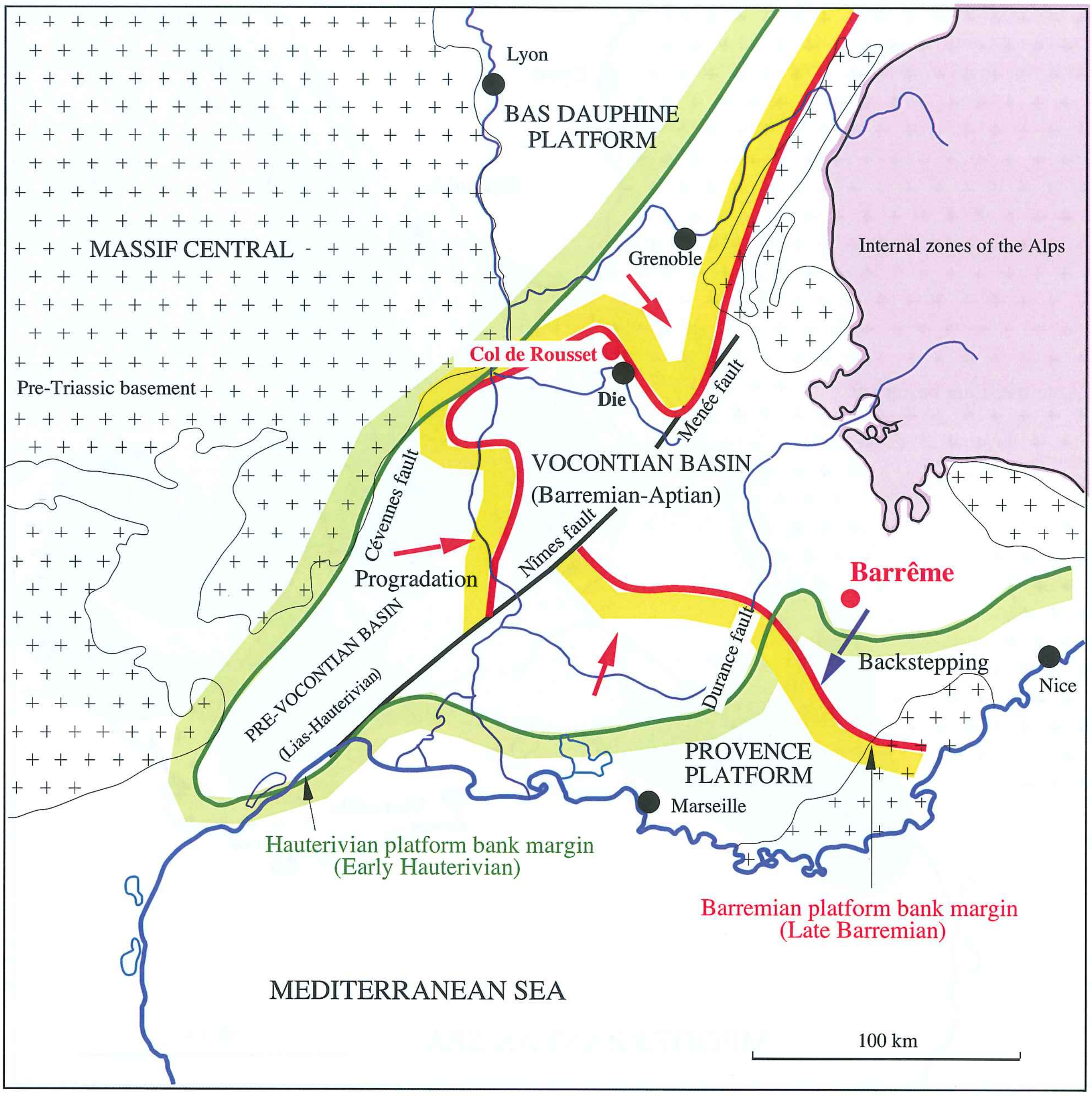

FIG. 9.- Sketch-map of the South-East France basin (SFB). Note the shift of the platform boundary after the late Hauterivian change (the so-called "*Barremian crisis*", transition from the pre-vocontian to the vocontian basin).

vocontian trough, and (2) to the individualization of a weakly inclined ramp.

The gravity derived sedimentary reworkings were frequent at every level in the pre-vocontian trough, but globally displayed a vertical evolution. In Berriasian times, they were mainly thick debris flows that went down along several submarine canyons most of which are inherited from the Late Jurassic. In the Valanginian, the gravity resedimentations are mainly fine grained turbidite or contourite bundles. During the Hauterivian, slumped beds were particularly numerous, especially at the base of the depositional sequences.

The paleogeography is still that of the pre-vocontian period. It is characterized by a very weak progradation of the platforms boundaries during the whole Berriasian and the Early Valanginian (in the latter case, the progradation is coeval with the backstepping), and by a change of the submarine morphology as a result of the Valanginian-Hauterivian infilling.

3.- VOCONTIAN PERIOD

3.1. Late Early Cretaceous, the time of the Urgonian limestones (120-110 my)

Two major events are characteristic of this period, viz. (1) a latest Hauterivian-Lowermost Barremian

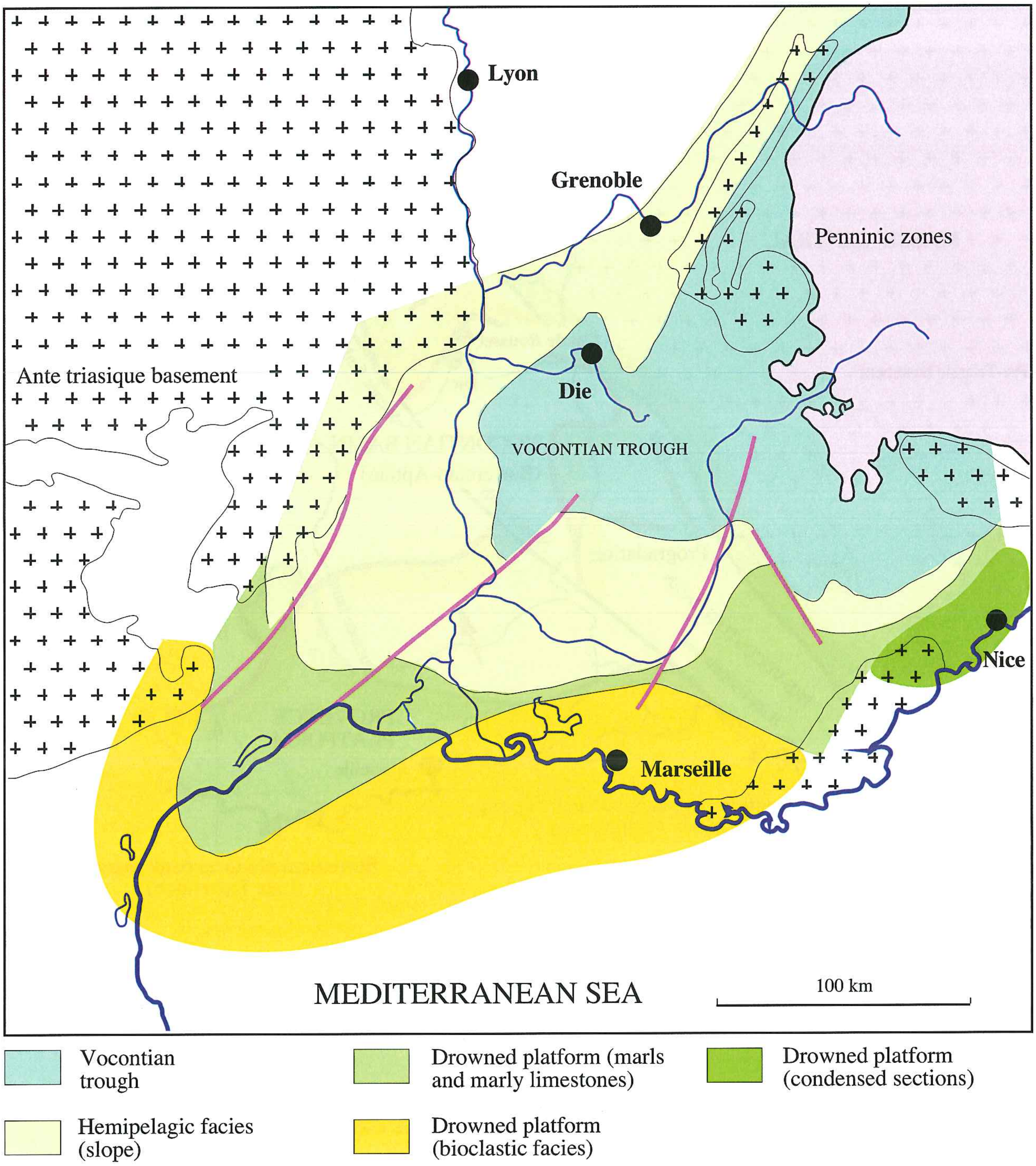

FIG. 10.- Paleogeographical sketch of the Hauterivian (South-East France).

tectonically enhanced unconformity, and (2) the evolution of the Urgonian platforms.

3.1.1. The Hauterivian-Barremian tectonically enhanced unconformity

The tectonically enhanced unconformity of the Hauterivian-Barremian boundary is located between the twin sequence boundaries Sb H7 and Sb B1. It marked the time-limit between the pre-Vocontian and the Vocontian periods of the SFB. This limit resulted from an important uplift which can be seen on the different subsidence curves, and which was responsible of the general tilting of the SFB (emersion in the West, submersion in the East).

In the Western part of the SFB, the emergence resulted in a shift of the shoreline towards the East of the Hauterivian ramp; this caused an important shift, often exceeding 50 kilometres, of the area which was the site of platform carbonate sedimentation (in other words, an apparent progradation jump). At the beginning of the

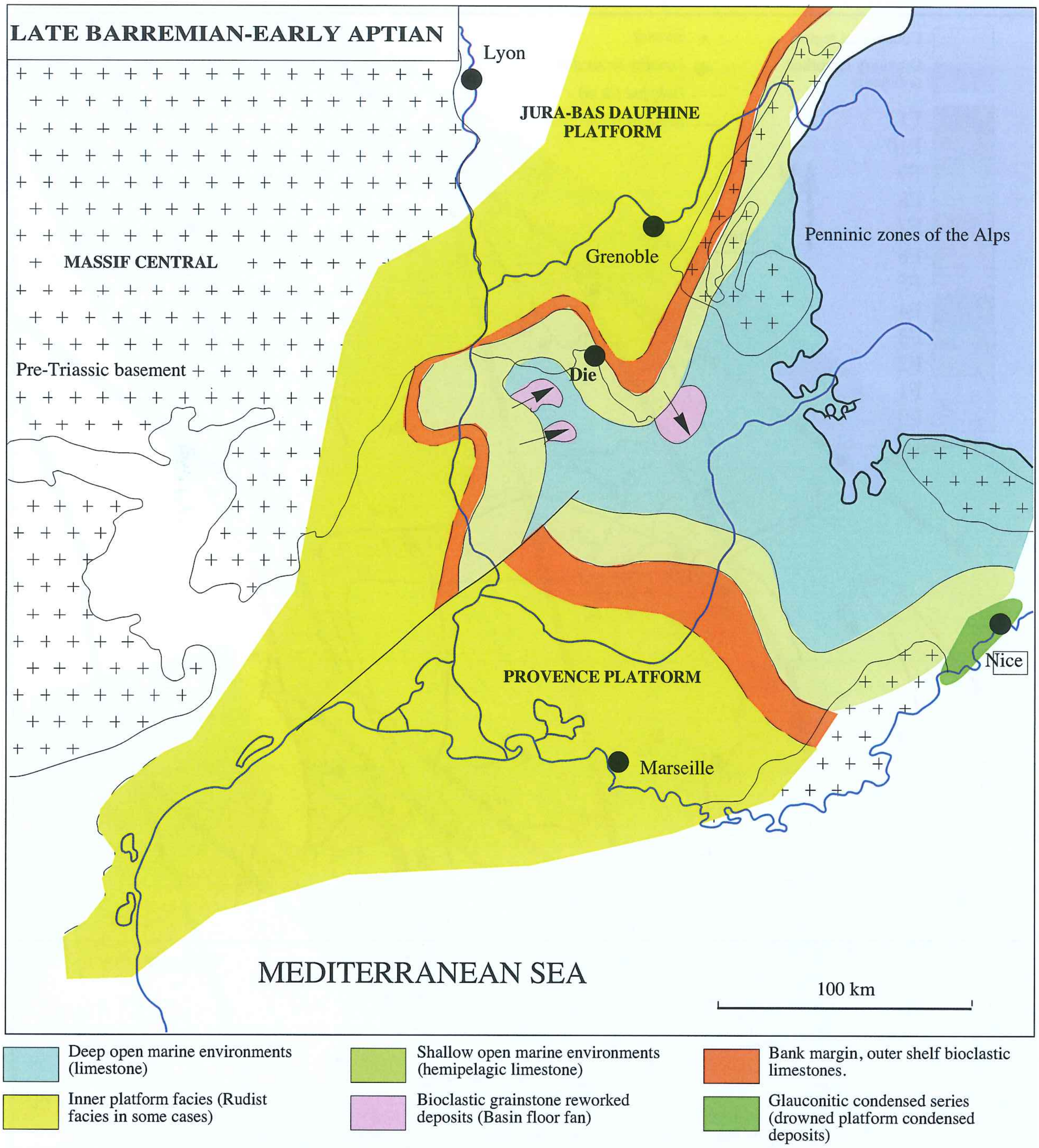

FIG. 11.- Paleogeographical sketch of the late Barremian-early Aptian (South-East France).

Barremian, the first platform sediments deposited above the Hauterivian infilling sequences were laid down in areas that were, from the Jurassic on, the deep parts of the Pre-Vocontian trough.

In the Eastern part, the tectonic tilting resulted in a deepening of the depositional environments, causing the retrogradation of the platform facies of the Barremian with respect to those of the Late Jurassic-Berriasian.

In the North of the SFB, as also probably in the South of the Castellane arc, the tectonically enhanced unconformity shows (1) an oblique truncation of the beds that lie just below the Hauterivian (the disappearance of the Hauterivian upper sequences can be observed between the Grenoble and the Neuchâtel (Swiss Jura) areas, and (2) a disposition in successive onlaps of the beds that lie above the Urgonian platform.

3.1.2. The Urgonian platform deposits

Above the tectonically enhanced unconformity Sb HA7-BA1, the Urgonian platform is characterized by (1) a resumption of the subsidence, mostly from the Late

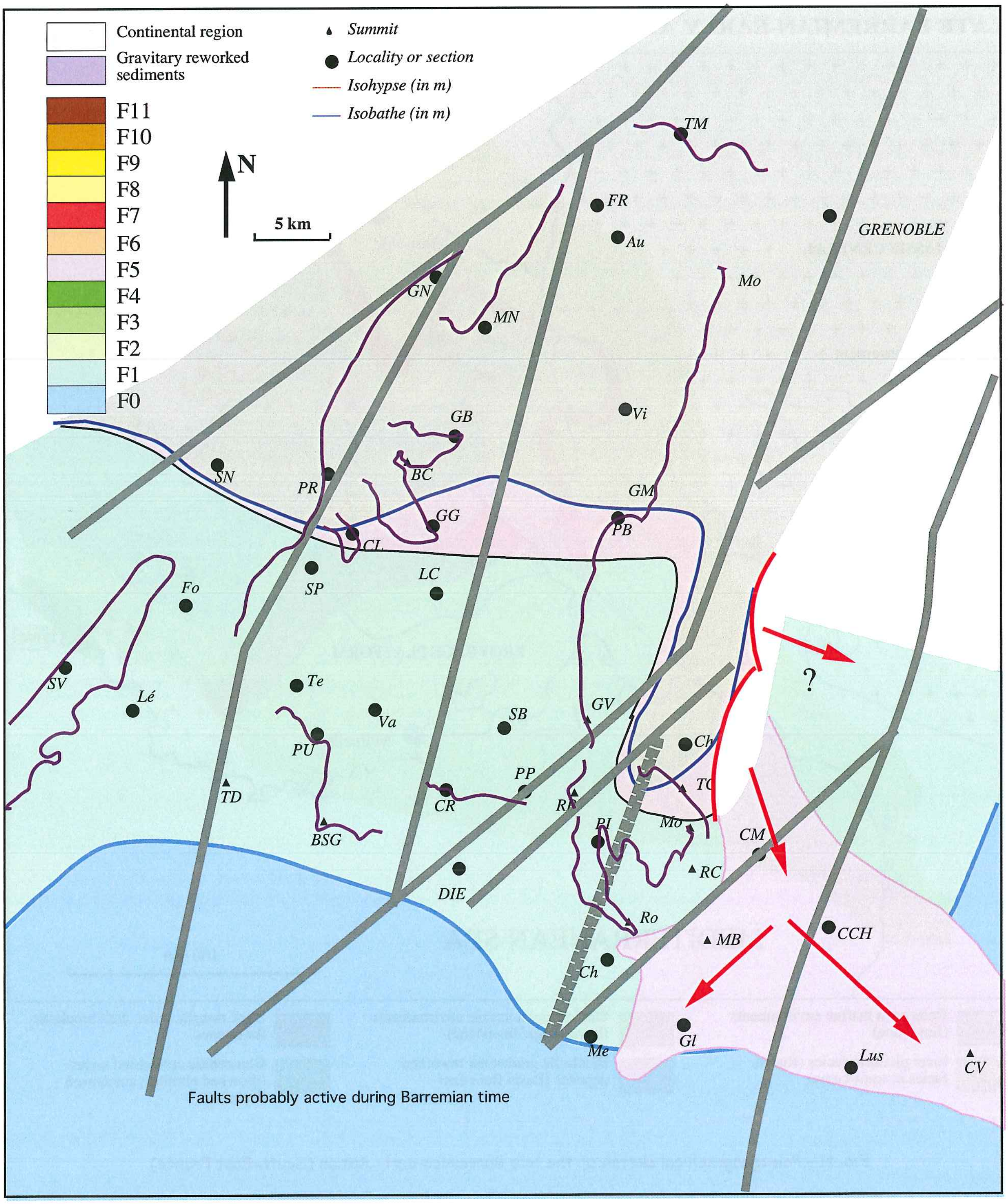

Fig. 12.- Paleogeographical map of the late Lowstand Prograding Wedge (LPW) of the depositional sequence BA1 (early Lower Barremian, probably *Avramidiscus kiliani* zone).

Barremian on, (2) a moderate progradation of the facies during the Early Barremian, (3) a retrogradation coeval with the development of the Late Barremian inner facies, and (4) the transition to a drowned platform from the Early Aptian. In the North of the SFB, the first carbonate facies of external platform type were deposited at the top of the distally steepened Hauterivian ramp, a location that favoured the gravity resedimentation of the bioclastic sands in the Vocontian trough from the beginning of the Barremian (basin floor fan of sequence BA1), but unknown during the Hauterivian.

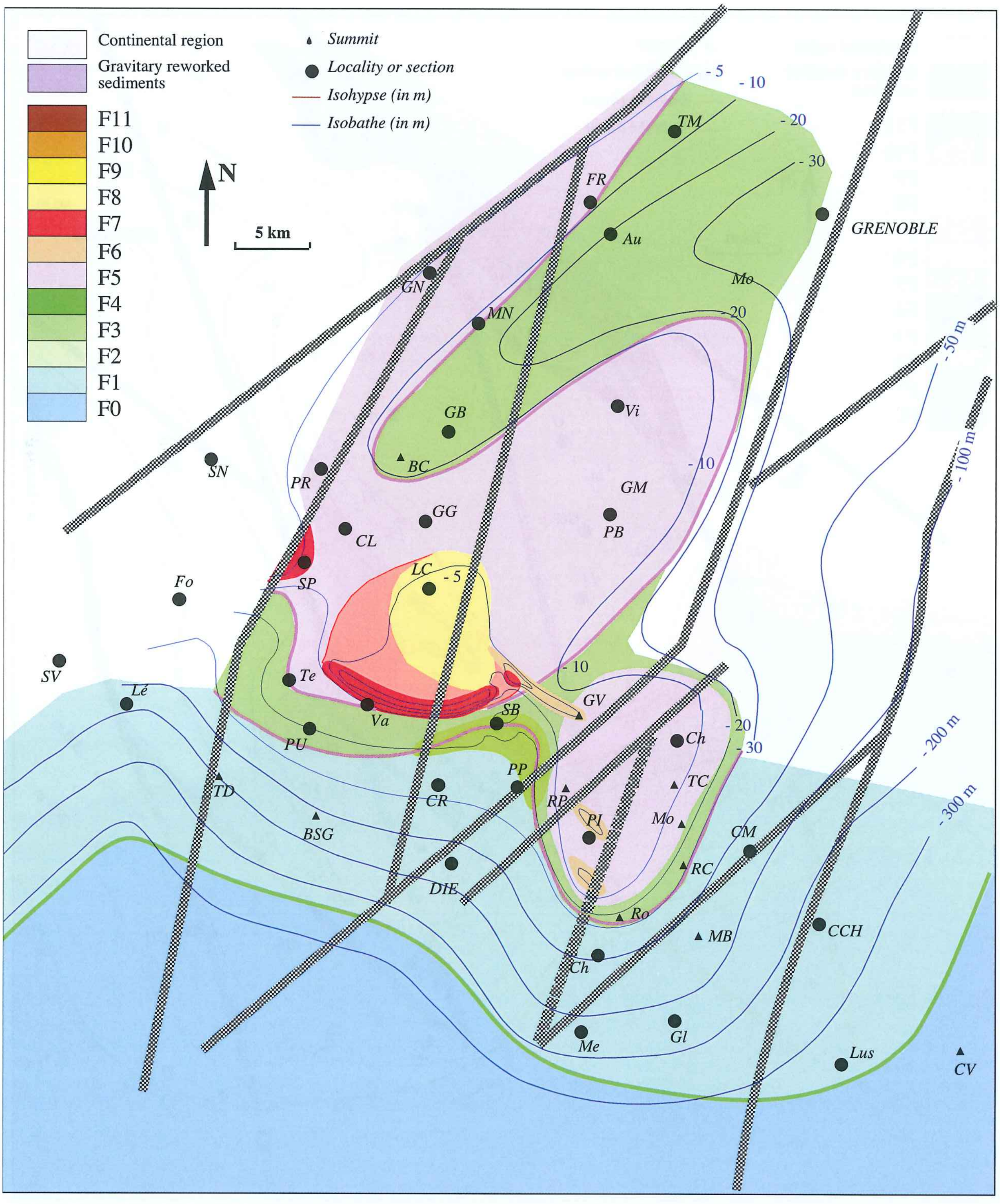

FIG. 13.- Paleogeographical map of the middle Transgressive Systems tract (TST) of the depositional sequence BA3 (early Upper Barremian, probably *Heinzia sayni* zone).

Early Barremian (sequences BA1 and BA2).

In the North of the SFB, forestepping sequences were deposited. They display a moderate to important progradation of the facies, and are only build up of coarse grained bioclastic facies deposited in open marine environments. They form large lobes with always thick but highly laterally variable thicknesses. Lowstand prograding wedges are well developed, as are the slope fans. Transgressive systems tracts and highstand systems tracts do not display important overlaps on the previous Hauterivian ramp.

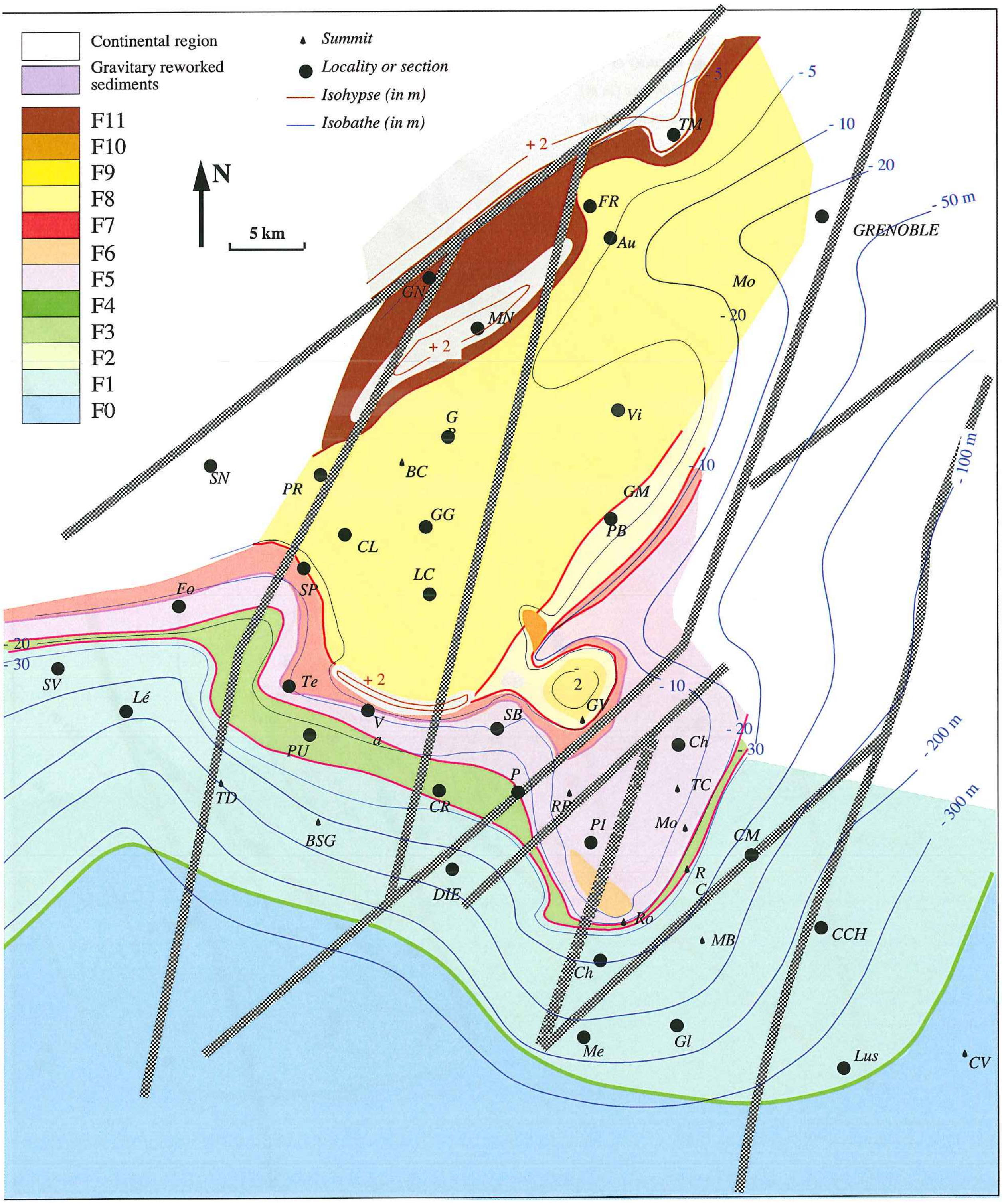

Fig. 14.- Paleogeographical map of the middle transgressive Systems tract (TST) of the depositional sequence BA4 (Upper Barremian).

In the South of the SFB, data are presently too poor to allow such a detailed interpretation.

Late Barremian (sequences BA3 to BA5)

Backstepping sequences were deposited during a globally transgressive period. The basal part of the BA3 sequence still belonged to the Early Barremian prograding body, but the overlying transgressive systems tract and above all the maximum flooding, mark the transition from a prograding general tendency up to a retrograding general tendency, which is the beginning of the highly transgressive median part of the Cretaceous. After the BA3 sequence maximum flooding, three major features must be emphasized.

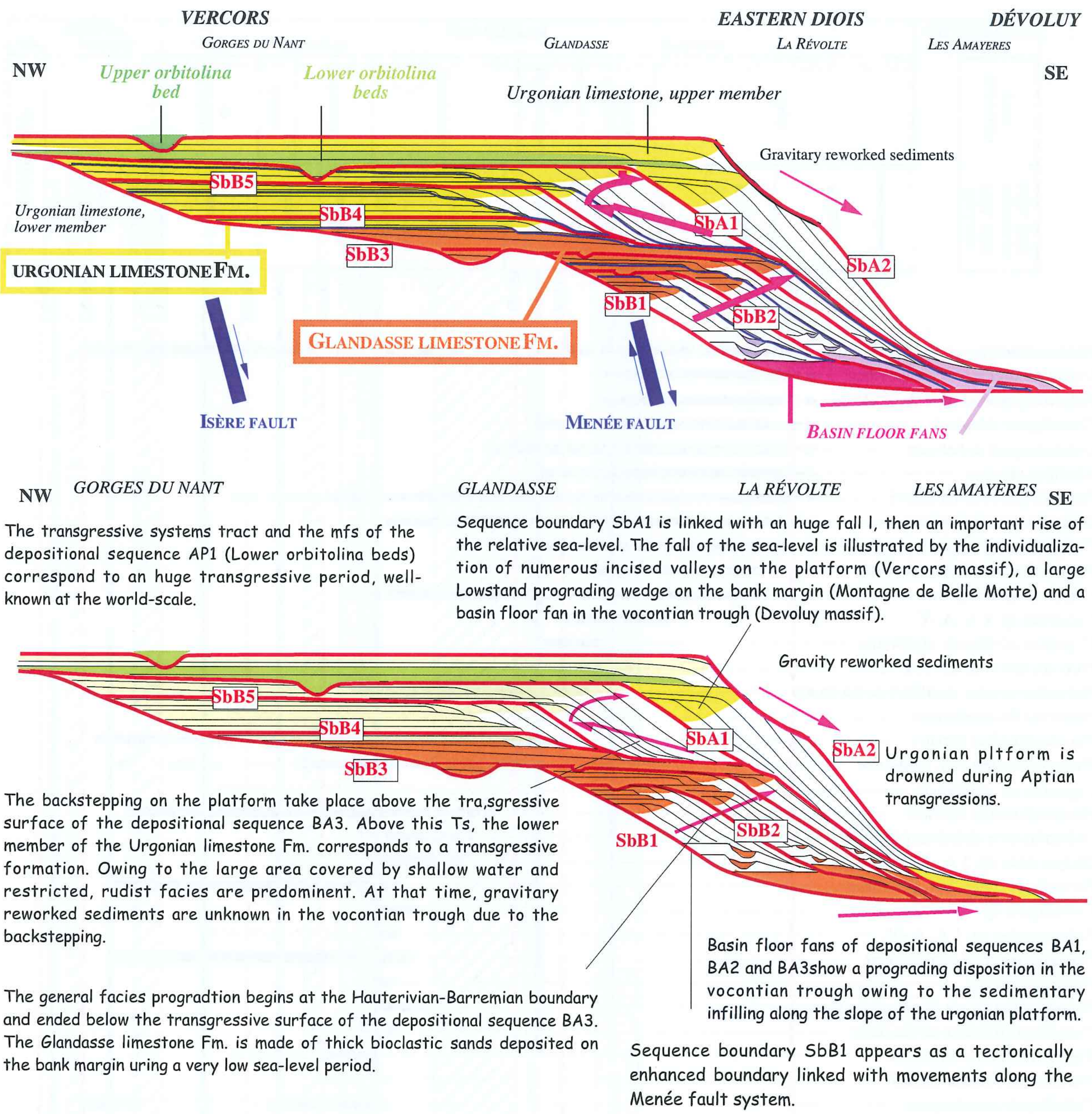

FIG. 15.- Lithologic units of the Urgonian platorm deposits and general trend of the evolution during Barremian and early Aptian time. In the Northern subalpine chains, carbonate platform deposits correspond to two main lithologic formation: the **Glandasse limestone Fm.** and the **Urgonian limestone Fm.** The first one is only developped on the bank margin and could be interpreted as a 2nd order lowstand systems tract, while the second is extensively present on the platform and could be interpreted as the transgressive systems tract and the highstand systems tract of the Barremian cycle.

(1) The backstepping begins with (a) an increase in the depositional depth, (b) a progressive submersion of the upstream emerged part of the former Hauterivian ramp, and (c) the appearance on this ramp of the inner platform facies. **The Urgonian limestones formation appears therefore as a transgressive formation** characterized by the appearance and the development of the inner platform facies that were then spread over large areas, for the first time since the Berriasian. At that time, the large area characterized by very shallow marine environments allowed the appearance of more and more confined environments and therefore of a longitudinal zonation of the facies.

(2) The deposition of the Urgonian limestones is coeval with a predominant marly sedimentation in the Vocontian trough.

(3) The backstepping of the Upper Barremian is also accompanied by a decrease and a nearly complete disappearance of the gravity resedimentation of the bioclastic sands in the Vocontian trough.

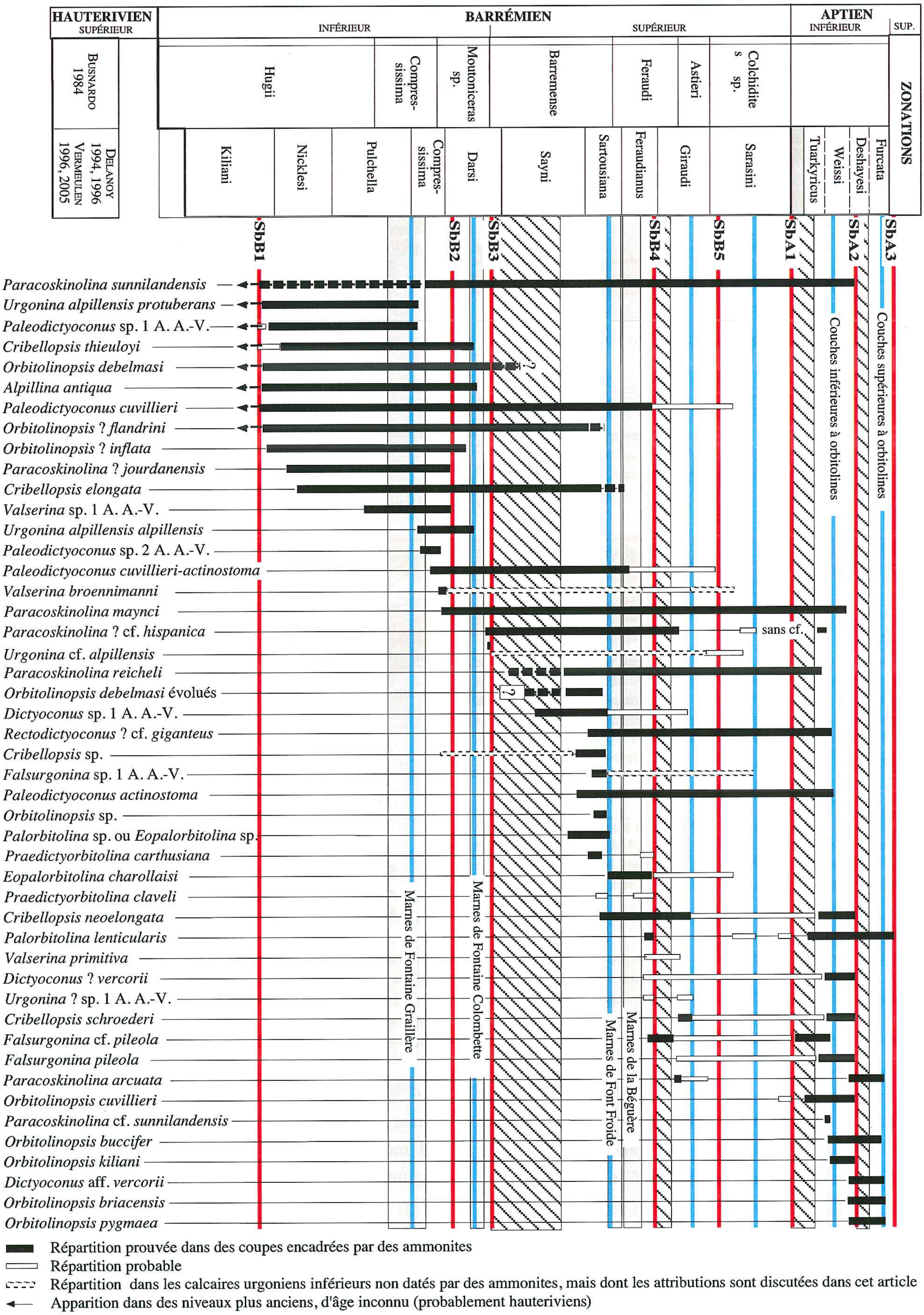

FIG. 16.- Distribution of Orbitolinids in the Northern subalpine chains (Arnaud *et al.*, 1998).

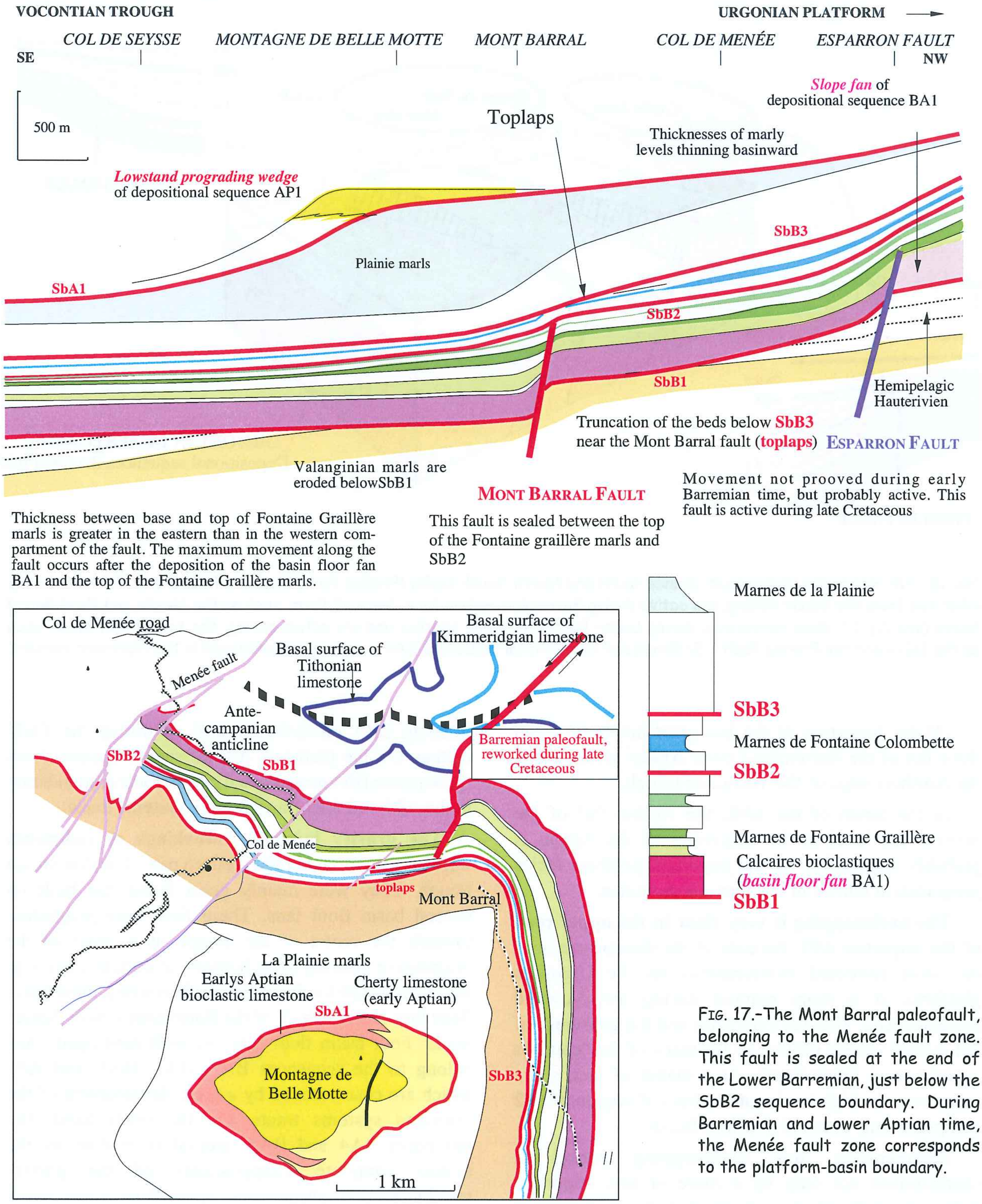

FIG. 17.-The Mont Barral paleofault, belonging to the Menée fault zone. This fault is sealed at the end of the Lower Barremian, just below the SbB2 sequence boundary. During Barremian and Lower Aptian time, the Menée fault zone corresponds to the platform-basin boundary.

Early Aptian (sequences AP1 and AP2)

This time was characterized first by an emergence of the platforms, then by an important backstepping of the facies that finally led, during the latest Early Aptian, to the complete disappearance of the platform facies in the North of the SFB. The ermersion of the platforms at the Barremian-Aptian boundary resulted in :

(1) the grooving of a system of incised valleys, which were infilled by the argillaceous carbonate sediments of the AP1 depositional sequence transgressive systems tract (the so-called "couches inférieures à Orbitolines"),

(2) the individualization on the platform borders of a very important lowstand prograding wedge (e.g. that of the Montagne de Belle-Motte),

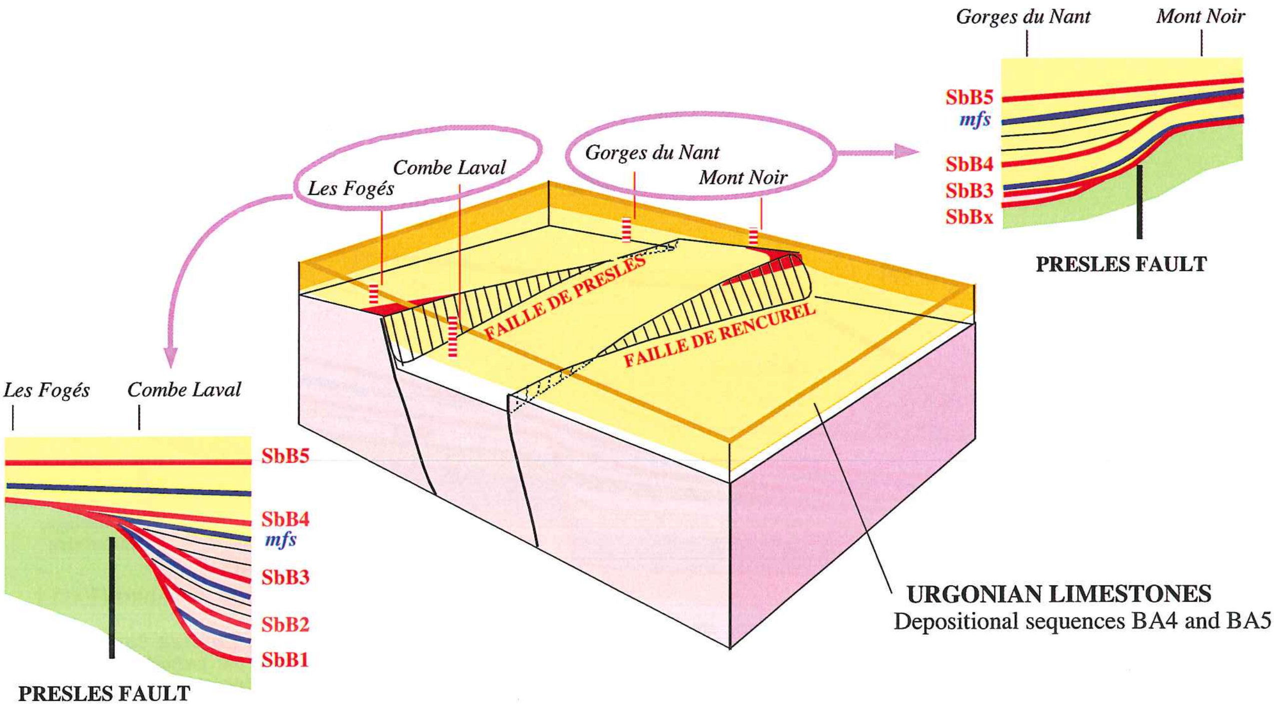

FIG. 18.- NE-SW faults (Isère fault, Menée fault) and North-South faults (Presles fault, Rencurel-Rochers de Chironne fault), inherited from the liassic rifting, are active during Barremian-Aptian time. Some of them, such as the Menée and Mont Barral faults (see fig. 17) show movements during Lower Barremian while another one are active during the Upper Barremian, such as the Isère and the Presles faults. Sediments of depositional sequences BA4 are especially affected in the Northern Vercors.

(3) the formation of the last great bioclastic basin floor fan of the Barremian-Lower Aptian series, along the Northern edge of the Vocontian trough.

In the South of the SFB, the sudden fall of the relative sea level in the beginning of the Aptian is probably responsible for the important platform facies progradation known in the Ventoux mountain.

The backstepping is very clear in the upper part of the sequence AP1, because of the disappearance of the most restricted environments on the Urgonian platform. It is more marked during the drowned sequence AP2, after the emersions and the groovings of the incised valleys infilled by the marls of the "couches supérieures à Orbitolines". As a matter of fact, when preserved, the highstand systems tract of sequence AP2 comprises only external platform facies.

Summarizing, this backstepping period is characterized not only by a more or less important retirement of the platform facies, but also by important variations of the relative sea level resulting in two close emergences (base of AP1 and AP2), with grooving of incised valleys (Les Rimets for example). As during the Berriasian and the Valanginian, it seems that the globally transgressive periods also correspond to those that are characterized by the greatest relative sea level variations (fig. 7).

The detrital supply is poor during the Early Barremian. It increases in the Vocontian trough during the Late Barremian, especially from the maximum flooding BA3 onwards, as well as during the Early Aptian. On the platform, detrital supply appears from the sequence BA4 onwards, and may become preponderant in the AP1 and AP2 transgressive systems tracts.

The gravity induced reworkings of sediments were very important in the Western part of the Vocontian trough. They were mainly grain flows that built up several basin floor fans. These fans were prograding towards the centre of the trough, as a result of the progressive infilling of its borders. In certain areas, e.g. the Dévoluy (20 km East from les Nonières), these basin floor fans built the bulk of the Barremian-Lower Aptian series. Four basin floor fans are well developed; they belong to the sequences BA1, BA2, BA3, and AP1 which are characterized by a great development of the lowstand systems tracts. On the other hand, the sequences BA4 and BA5 interval is marked by the almost complete disappearance of the gravity resedimentation phenomena, apart from some small turbidites. These BA4 and BA5 sequences are aggrading sequences coeval with the build up of the internal facies of the Urgonian platform.

3.1.3. Synsedimentary tectonics

From the Barremian on, synsedimentary tectonic movements resulted in :

(1) the activity of some paleofaults, such as the Menée fault (Mont Barral fault, fig.17),

(2) the acceleration of the subsidence rates in the whole SFB, leading to the accumulation of more than 300 metres of Urgonian limestones on the peripheral platforms of the SFB,

(4) the presence of paleofaults in the South of the SFB and Vercors (during Barremian as Aptian time),

(3) the starting of huge submarine slumps coeval with, or slightly subsequent to the SbA2 sequence that marks the end of deposition on the Urgonian platforms.

The latest Barremian paleofaults are responsible for the individualization, amidst the Provence Urgonian platform, of the La Bédoule graben near Marseille, a foreshadow of the "Basse Provence gulf" which will be a characteristic paleogeographic feature of the Southern SFB from the Albian onward. Other paleofaults, that are sealed by Upper Aptian ("Lumachelle") or Aptian-Albian marls are known in Northern subalpine chains and in the Ventoux-Lure mountains (between the Rhône valley and the Sisteron-Digne area). Finally, the geometrical organization of the deposits leads to the admission of a reworking of older faults that already carved all the Centre-South part of the SFB, giving birth to a succession of horsts, grabens and tilted blocks. This foreshadows the paleofaults reworking that resulted, from the Albian on, in the Durance uplifted area ("isthme Durancien").

The submarine slumpings are known in the South-West of the Vercors, among which a single one has been spread over more than 10 km², being responsible of the downward displacement of several km³ of hemipelagic and bioclastic limestones originating from the slope of the Urgonian platform. These mud or debris flows and slumped beds gave birth to the piling up of several huge debris flows that were resedimented at the top of the Lower Aptian beds in the Western part of the Vocontian trough.

3.2. The Mid-Cretaceous black shales episode : Late Aptian to Cenomanian (110-90 my)

This period differs from the Hauterivian to Lower Aptian carbonate formation period (Jura and Northern subalpine chains). It displays (1) a very high relative sea level, which was responsible for the disappearance of the Urgonian platforms, (2) the deposition, in the Vocontian trough, of a very thick marly series, (3) the importance of the coarse grained terrigenous detrital supply, and (4) the increased influence of the extensional tectonics linked with the opening both of the North Atlantic and of the Bay of Biscay. From the beginning of the Early Aptian, the successive transgressive stages resulted in the submersion of the Urgonian platforms, and in the progressive replacement of the carbonate sedimentation by a detrital sedimentation, siliciclastic on the platforms and argillaceous in the Vocontian trough.

3.2.1 Aptian-Albian

Both in the median part of the Early Aptian and in the Late Albian, two major events occurred, viz.: (1) the submersion of the Urgonian platforms and the end of the carbonate sedimentation, and (2) the birth, for the first time in the history of the SFB, of a siliciclastic sedimentation. This great change resulted not only from the actual rise of sea level, but seems also to have climatic causes.

The submersion of the Urgonian platforms followed the Early Aptian emergence and occurred during the transgressive systems tract of the AP2 sequence (Les Rimetsincised valley). During this emergence, the highstand prograding wedge of the AP1 depositional sequence was deeply eroded, and a system of 10 to 60 metres deep incised valleys is well known in the Vercors. These incised valleys were infilled by the marls of the AP2 sequence transgressive systems tract (Upper orbitolina beds); these marls were locally overlaid by a few metres of oolithic and Orbitolina-bearing limestones (highstand systems tract of the top of the Lower Aptian, AP2 sequence). The same situation marked the evolution of the Vocontian trough. At the level of SbA2, a sudden lithological change occurred, from the Barremian-Earliest Aptian limestones up to pelagic foraminifera bearing marls: the SbA2 is often overlaid by a great debris flow with an argillaceous matrix, and the maximum flooding of AP2 sequence gave birth to the first black shales level (Goguel level).

The siliciclastic sedimentation appeared progressively in the Late Aptian, and prevailed in the Albian on top of the former drowned Urgonian platforms (above all, in the Vercors and close to the Central Massif). In the Western part of the Vocontian trough, gravity resedimented green sandstones (sand flows) occur at several levels in the series. The important supplies of quartzose sands deposited at that time resulted from a resumption of the erosion on the basement massifs in the West and North-West of the SFB. This was probably due both to the uplifts that resulted from the extensional tectonics linked with the opening of the North Atlantic, and to a change from a tropical to a temperate climate. This climatic change (cooling), which resulted both from a change of the continental weathering and from a decrease in sea temperatures, is evidenced by the complete lack of platform carbonates in the North of the Vocontian trough, contrary to the Southern border in Provence.

From the beginning of the Late Aptian to the end of Albian times, the organization of the deposits curiously resembles that of the Jurassic, Bathonian-Callovian black shales (Pre-Vocontian period). The very thick marly deposits of the Vocontian trough grade laterally into thin beds, often condensed and with hiatuses, that were deposited on the peripheral drowned platforms. This is typical of the drowning sequences that characterize the major transgressive intervals.

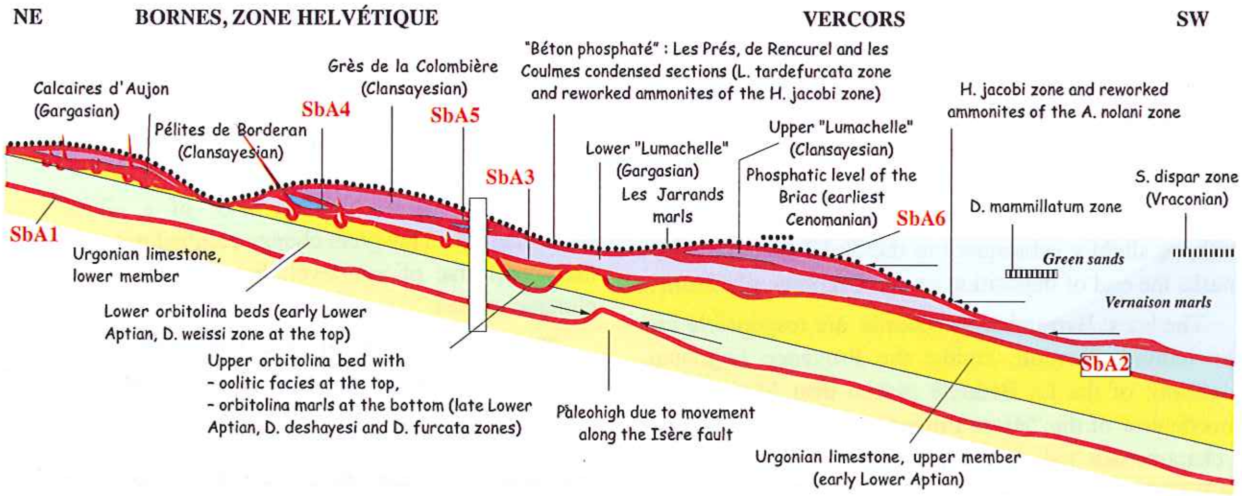

FIG. 19.- Organization of the Aptian deposits in the Northern subalpine chains.

In the Vocontian trough, this interval was that of the deposition of marls whose thickness reached 800 metres. In the Western part of the trough, the series contains gravity resedimented glauconitic sands and several organic-matter rich levels. Several superimposed depositional sequences are known; the generally thick lowstand systems tracts begin in the Western part of the Vocontian trough by gravity reworked green sands; the maximum floodings are decimetric to metric black shales levels, the highstand systems tracts are marly, often less thick than the lowstand systems tracts, and still contain very thin black shales levels. Numerous clastic dykes occur in this series as a result of tectonic or gravity driven instability acting upon sandy beds intercalated within the marls.

On the peripheral drowned platforms (i.e., on the former, drowned Urgonian platforms), the Upper Aptian beds are thin, often with breaks (the lower part is often missing, in particular in the North, in the Northern Subalpine Chains, and in the South, in the Castellane arc). These beds, from Grenoble to Provence, comprise reddish brown bioclastic limestones (drowned platform facies, i.e. the so-called "Lumachelle" formation). On the Western borders of the Vocontian trough, Albian beds are often much more reduced in thickness. In the upstream part of the drowned platforms, they are only in the form of a decimetre-thick condensed level (Northern Subalpine Chains), whereas downstream there are green glauconitic sands that were deposited in shallow marine environments. In these various beds, the Albian condensed levels, rich in ammonites, glauconite and phosphate, mark a maximum transgression of the whole Cretaceous series.

Middle Cretaceous tectonism is not conspicuous. It probably resulted from a stretching of the crust linked with the opening both of the North Atlantic and of the Bay of Biscay, and resulted in the birth of normal faults, and eventually in the reactivation of the Liassic blocks. The first movements, probably an extension of the Barremian faulting, exist at the calcareous Aptian-marly Aptian boundary (small paleofaults on the Northern and Southern borders of the Vocontian trough, gravity induced dismembering of the edge of the Urgonian platform in South Vercors, probable tilted blocks in the Vocontian trough, possible uplift on the peripheral platforms). Things are less clear in the Albian deposits; nevertheless, the clastic dykes are sometimes interpreted as the result of seismic activity linked with the stretching. On the other hand, at the end of Albian times, the tectonic mobility becomes very clear and results in (1) the birth of the early Durance uplift ("Isthme Durancien" of the Provence domain), that emerges and definitively separates the Vocontian trough from the Marseille area where certain areas collapsed, (2) the generalized unconformity of the Cenomanian deposits upon the Albian ones, or upon older beds, (3) the presence of hectometre- to several hectometres-sized glided bodies, which were resedimented, at the Albian-Cenomanian boundary, not very far from the normal faults which existed at least from the Turonian onwards.

3.2.2 Cenomanian

In the deepest parts of the Vocontian trough, the Cenomanian beds are alternating limestones and marls with ammonite and planctonic foraminifera. Their general organization is similar to that of the Albian beds: thick deposits in the Vocontian trough, laterally grading into thin beds deposited on the platforms.

On the platform margins two different cases occur in the North of the Durance uplift : sandy continental (Gard area close to the Central Massif) or coastal (Ventoux-Lure, Vercors) deposits, sandy marls with large Orbitolinas in the East of the Castellane arc. In the South of the Durance uplift, the Cenomanian beds are rudist limestones (a platform that extends towards the Pyrénées). This paleogeographic framework shows the importance of the tectonic changes at the Albian-

Cenomanian boundary: a first step in the disappearance of the SFB.

3.2.3. Conclusion

The Late Aptian to Cenomanian period is both very similar to, and different from the Bathonian-Callovian interval (deposition of the "Terres Noires", i.e. of the Jurassic black shales). The similarities result from: (1) hiatuses and reduced deposits on the platforms versus particularly thick sediments in both the Pre-Vocontian and the Vocontian troughs; (2) beginning of the opening of the Ligurian Tethys ocean in the first case, and beginning of the opening of the North-Atlantic-Bay of Biscay ocean in the second; (3) presence of confined levels amidst the black shales. But there are important differences when comparing the subsidence rates; they were high in the Bathonian-Callovian of the Pre-Vocontian trough, unlike the border platforms, so that in spite of the huge accumulation of sediments, the depth of the Pre-Vocontian trough increased from the Bathonian up to the Oxfordian. On the other hand, the subsidence rate was poor or near zero in the Late Aptian-Cenomanian : in the latter case, the huge accumulation of sediments resulted in the infilling of the Vocontian basin whose Western part almost reached emergence.

4.– Beginning of the closure of the basin in the Late Cretaceous

In a particular area of the External Western Alps, namely the major part of the SFB south of the Vercors, a first compressional phase took place in the Late Cretaceous.

But this phase has nothing to do with the normal evolution of the Alpine compression that resulted from the Europe-Africa collision, just as the Atlantic-Biscay rifting known in the same area is disconnected from the Liassic-Middle Jurassic, Ligurian rifting.

Regarding the Europe-Africa collision, Late Cretaceous compression, probably linked with subduction, began at the same time in the most internal Alpine zones (Apulian margin and a very internal part of the Ligurian ocean). During this collision, the "tectonic wave" that progressively spread upon the former European passive margin reached the External Dauphiné zone only in the Late Paleogene or in the Neogene).

Therefore, the Late Cretaceous folding that occurred both in the Southern part of the External zone of the Alps and in the Provence ranges, and that gave birth to E-W trending folds in the SFB, belonged to the Pyrenean history. It resulted from the relative motions of Iberia (probably also partly of Apulia-Africa?) with respect to Europe.

This not strictly Alpine compressional phase resulted (1) in the individualization of a E-W trending fault bundle in the North-Eastern part of the SFB, and (2) in a major paleogeographical change, namely the retreat of the sea from the Western part of the SFB and the disappearance of the Vocontian trough.

The pre-Senonian folding affected not only the Dévoluy mountains (20 km East from Les Nonières) and their surroundings (where it is clearly evidenced by the presence of unconformable marine Campanian beds, such as in the Glandage area or at the top of the Montagne de Belle-Motte), but also, very probably, the whole Vocontian trough. This latter case cannot be demonstrated, due to the lack of Senonian outcrops, and one may wonder whether or not one or the other among the E-W trending folds may also result from the Middle-Late Eocene Pyrenean-Provence folding.

Whatever the case, a very early, complete tectonic inversion occurred in this part of the SFB, that emerged and has been deeply eroded before the deposition of the Campanian beds. Throughout the Western part of the SFB, the main part of the compressional structure already exists from the Late Cretaceous onwards, contrary to other parts of the SFB where the Cenozoic deformations prevailed.

At the end of the Late Aptian-Cenomanian times, the Vocontian trough and its shallower borders are still clearly seen in the paleogeographic framework. Two kinds of data have nevertheless to be emphasized.

(1) The double influence both of the sediment accumulation which was very important during the Mid-Cretaceous, and of the progressive uplift of this part of the margin, resulted in a nearly complete infilling of the Western part of the Vocontian trough where deep sea graded upwards to shallow sea marine environments.

(2) The reworking of the great Liassic paleofaults was probably responsible both for the birth of the Durance uplift in Provence and for the unconformity of the Cenomanian beds upon the Albian ones, and also for the appearance in the Cenomanian of two depocentres respectively located to the West of the Nîmes fault (West of the lower Rhône valley) and to the North of the Ventoux-Lure fault.

The Turonian-Senonian period is characterized both by the Late Cretaceous folding and by the reappearance of calcareous sedimentation. The Turonian beds lie unconformably upon the Cenomanian ones throughout the Western part of the SFB (Turonian tectonically enhanced unconformity). This unconformity resulted from both a sudden decrease in sea level (uplift of the sea bottom ?), and from a subsequent transgression whose maximum occurred in the Middle-Upper Turonian . This led to three consequences:

(1) The Cenomanian beds are more or less deeply eroded, even in areas where the marine environment was relatively deep .

(2) The base of the Turonian limestones is more and more recent towards the borders of the Vocontian trough.

(3) The boundary of the non-eroded Turonian beds passes beyond that of the Cenomanian deposits. This

evidences the transgressive character of this period after the emergence at the Cenomanian-Turonian boundary.

From a paleogeographic point of view, two marine areas exist at that time in the SFB, which are roughly similar to those of the Cenomanian: in the North, the partly filled up Vocontian trough extends to the East towards the open sea, and to the South towards the Lower Provence gulf which was probably connected with the North-Pyrenean basin. The coarse grained detrital supplies are very abundant in the Western part of the SFB, and the facies grade laterally from pelagic foraminifera bearing limestones in the deepest part, into sandy limestones with bryozoa and crinoids, then into channel deposited sands or sandstones in the shallowest parts. Rudist bearing limestones occur in the North near the Rhône valley and in the South in the Lower Provence gulf.

Both the palaeogeography and the facies organization of *the Lower Senonian* are globally similar to those of the Turonian. Nevertheless, great detail complexities occur in the area of the Late Cretaceous folding.

The Upper Senonian (Campanian-Maastrichtian) period postdates the folding phase (fig. 20), and is characterized by a completely different paleo-geographic framework. The Vocontian trough had completely disappeared, and a Campanian transgression occurred towards the West up to a NNW-SSE shoreline between the Grenoble and Castellane areas: the marine deposits occur in the East of this shoreline, whereas all the Western part of the former SFB is emerged.

The pre-Senonian folding resulted in the emergence of a wide area, from the Pelvoux external crystalline massif down to the South of the Dévoluy, possibly also to the Digne area. But the unconformable Upper Senonian beds outcrop only in the Dévoluy area; elsewhere they are conformable, or absent. Their thickness is laterally variable because the Campanian transgresssion occurred upon an area with a rugged topography due to the erosion of the folds. This erosion went down as deep as the "Terres Noires" (Upper Jurassic black shales). In the North-West of the SFB, the Campanian transgression occurred upon a rather inclined ramp; as a consequence, one can observe a rapid lateral change from planktonic foraminifera bearing limestones into sandy limestones with bryozoans and crinoids (Grenoble area), then to red continental sands. In the South of the SFB, the subsidence was still great in the former Lower Provence gulf where thick continental sediments were deposited (as in its Western Pyrenean extension).

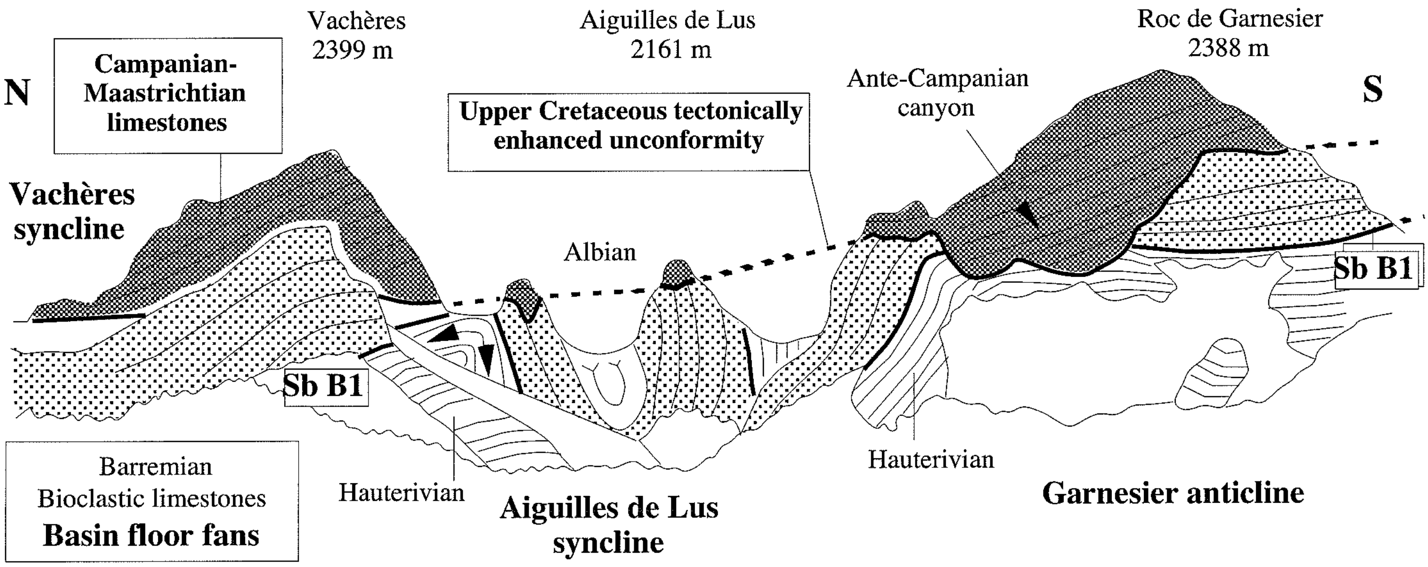

FIG. 20.- Panorama of the Aiguilles de Lus showing the ante-Campanian folds (Dévoluy massif).

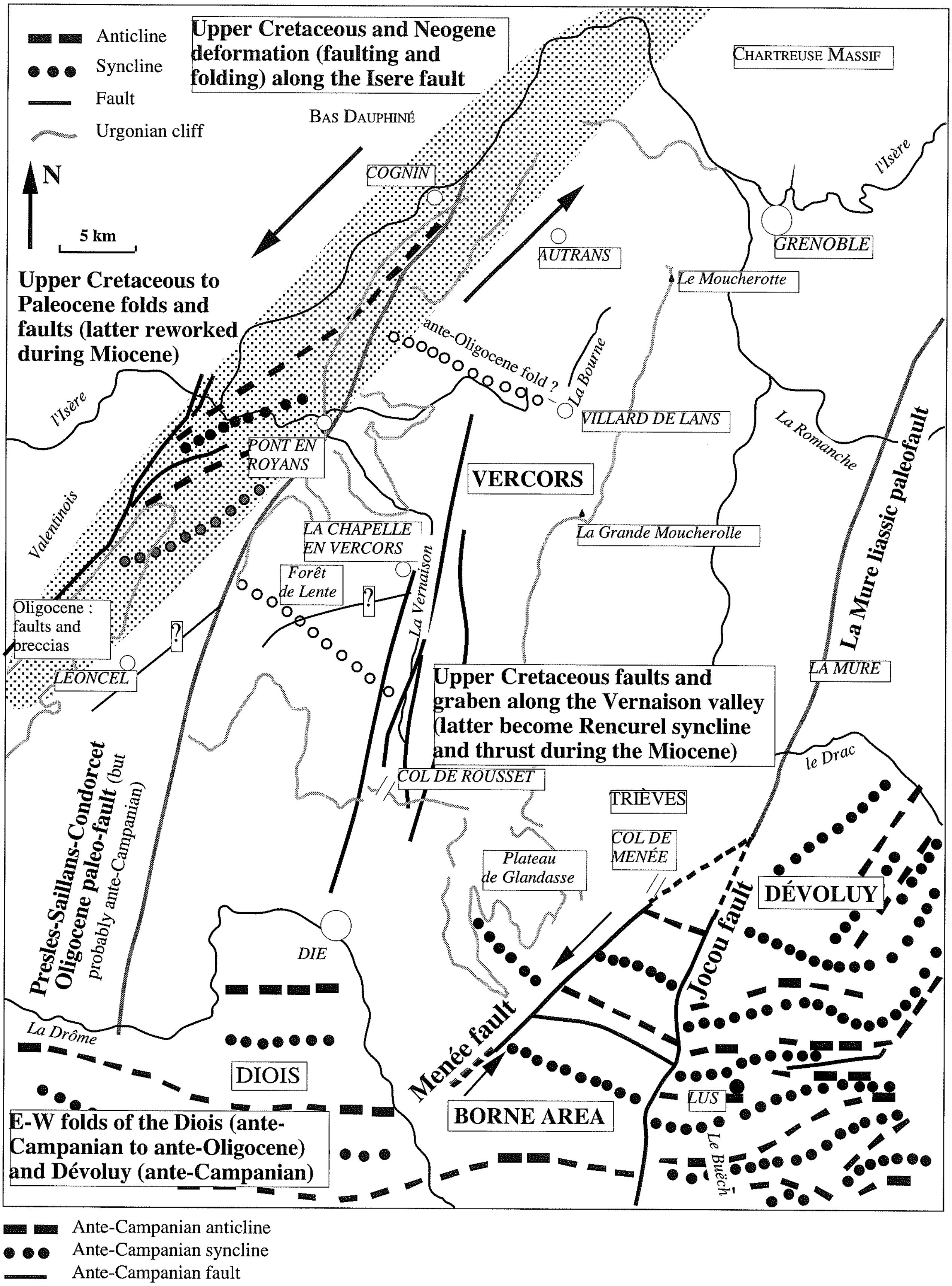

FIG. 21.- Ante-Campanian folds and faults from the vercors massif to the Devoluy.

Selected references

ARNAUD H. (1981). – De la plate-forme urgonienne au bassin vocontien: le Barrémo-Bédoulien des Alpes Occidentales entre Isère et Buëch (Vercors méridional, Diois et Dévoluy). *Géologie Alpine*, Grenoble. **11**, 3 vol., 804 p.

ARNAUD H., CHAROLLAIS J & MEDIONI R. (1984). – Bresse, Jura, Bas-Dauphiné, Chaînes subalpines septentrionales. *In* DEBRAND-PASSARD S. (Ed.), Synthèse Géologique du Sud-Est de la France, Le Crétacé inférieur, *Mém. Bur. Rech. Géol. Min.*, Orléans, **125**, 305-313.

ARNAUD H. (1988). – Subsidence in certain domains of Southeastern France during the Ligurian Tethys opening and spreading stages. *Bull. Soc. géol. France*, Paris, **8**, IV, 5, 725-732.

ARNAUD H., ARNAUD-VANNEAU A., ALETRU M.-C., ADATTE T., ARGOT M., DELANOY G., THIEULOY J.–P., VERMEULEN J., VIRGONE A., VIRLOUVET B. & WERMEILLE S. (1998).– Répartition stratigraphique des orbitolinidés de la plate-forme subalpine et jurassienne (SE de la France). *Géologie Alpine*, **74**, 3-89.

ARNAUD-VANNEAU A. (1980).– Micropaléontologie, paléoécologie et sédimentologie d'une plate-forme carbonatée de la marge passive de la Téthys : l'Urgonien du Vercors septentrional et de la Chartreuse (Alpes occidentales). *Géologie Alpine*, Grenoble, mém. sp. **10**, 3 vol., 874 p.

ARNAUD-VANNEAU A. & ARNAUD H. (1990).– Hauterivian to Lower Aptian carbonate shelf sedimentation and sequence stratigraphy in the Jura and northern Subalpine chains (southeastern France and Swiss Jura). *Spec. Publs int. Ass. Sediment.*, **9**, 203-233.

BAUDRIMONT A.F. & DUBOIS P. (1977).– Un bassin mésogéen du domaine péri-alpin : le Sud-Est de la France.- *Bull. Centres Rech-Explor.-Prod. Elf-Aquitaine*, Pau, **1**, 1, 261-308.

BEAUDOIN B., FRIES G., JOSEPH P. & PATERNOSTER B. (1983).– Sills gréseux synsédimentaires injectés dans l'Aptien supérieur de Rosans (Drôme). *C. R. Acad. Sci. Paris*, **296**, ser. II, 387-392.

BRÉHERET J.G. (1988).– Episodes de sédimentation riches en matière organique dans les marnes bleues d'âge Aptien et Albien de la partie pélagique du bassin vocontien. *Bull. Soc. géol. France*, Paris, **8**, IV, 2, 349-356.

BRÉHERET J.G. (1995).– The Mid-Cretaceous organic-rich sediments from the Vocontian zone of the French Southeast Basin. In: A. Mascle Ed, Hydrocarbon and Petroleum Geology of France . *Spec. Pub. European Assoc. Petrol. Geologists*, Berlin Heidelberg 4, 295-320.

BRÉHERET J.G., & DELAMETTE M. (1988).– Séquences de dépôt et couches riches en matière organique (CRMO) dans les marnes bleues aptiennes et albiennes du Bassin Vocontien, *in* FERRY S. & RUBINO J.-L. eds., Eustatisme et Séquences de dépôt dans le Crétacé du Sud-Est de la France (livret-guide Groupe Français du Crétacé, 25-27 Mai 1988). *Géotrope*, Lyon, **1**, 83-93.

BULOT L. G., ARNAUD-VANNEAU A., BLANC E., ARNAUD H. & THIEULOY J.-P. (1992).– Basin type successions : biostratigraphic tools, stratigraphic gaps and reworked sediments. *In* : "*Transition from Platform to basin in the Subalpine chains*", Platform Margins Symposium Guide-Book, Ed. Arnaud-Vanneau A., Grenoble, 25-41.

CURNELLE R. & DUBOIS P. (1986).– Evolution mésozoïque des grands bassins sédimentaires français (bassins de Paris, d'Aquitaine et du Sud-Est). *Bull. Soc. géol. Franc, Paris*, **8**, II, 4, 529-546.

DELAMETTE M. (1988). – Relation between the condensed Albian deposits of the Helvetic domain and the oceanic current-influenced continental margin of the northern Tethys. *Bull. Soc. géol. France*, Paris, (8), IV, 5, 739-745.

FERRY S. (1984).– Apports détritiques dans le Bassin vocontien, *in* DEBRAND-PASSARD S. (Ed.), Synthèse Géologique du Sud-Est de la France, Le Crétacé inférieur, *Mém. Bur. Rech. Géol. Min.*, Orléans, **125**, 332-334.

FERRY S. (1987). – Le détritisme carbonaté profond dans le Crétacé inférieur du Sud-Est français. Ses rapports avec l'eustatisme. *Géologie Alpine*, Grenoble, Mém. H.S. **13**, 197-202.

FERRY S. (1988). – Contrôle eustatique de la resédimentation calcaire (Valanginien a Aptien de la fosse vocontienne). *In* FERRY S. & RUBINO J.-L. Eds., Eustatisme et Séquences de Dépôt dans le Crétacé du Sud-Est de la France (livret guide Groupe Français du Crétacé en fosse vocontienne), 25-27 mai 1988, *Géotrope*, Lyon, **1**, 40-55.

GRACIANSKY P.C. DE, DARDEAU G., LEMOINE M. & TRICART P. (1989).– The inverted margin of the french Alps and foreland basin inversion. *In* COOPER M.A. & WILLIAMS G.D. (eds) : Inversion tectonics. *Geological society special publication*, London, **44**, 87-104.

GRACIANSKY P.C. DE, ARNAUD H., BUSNARDO R., DARDEAU G., GERLIER A., LEMOINE M., MASCLE G. & PHILIP J. (1987).– Rifting et basculement de blocs au Crétacé inférieur dans les Alpes Occidentales françaises : un écho à l'ouverture du golfe de Gascogne. *C. R. Acad. Sci. Paris*, **305**, II, 711-713.

JACQUIN, T., ARNAUD-VANNEAU, A., ARNAUD, H., RAVENNE. C & VAIL, P.R. (1991).– Systems tracts and depositional sequences in a carbonate setting: study of continuous outcrops from platform to basin at the scale of seismic lines. *Marine Geology*, Amsterdam, **8**, 2, 122-129.

LEMOINE M. (1984).– La marge occidentale de la Téthys ligure et les Alpes Occidentales. *In* BOILLOT G. (ed.), Masson, Paris, 155-248.

LEMOINE M., BAS T., ARNAUD-VANNEAU A., ARNAUD H., DUMONT T., GIDON M., BOURBON M., GRACIANSKY P.-C. DE, RUDKIEWICZ J.-L., MEGARD-GALLI J. & TRICART P. (1986).– The continental margin of the Mesozoic Tethys in the Western Alps. *Marine and Petroleum Geology*, Amsterdam, **3**, 179-199.

LEMOINE M., DARDEAU G., DELPECH P.Y., DUMONT T., GRACIANSKY P.-C. DE, GRAHAM R., JOLIVET L., ROBERTS D. & TRICART P. (1989).– Extension syn-rift et failles transformantes jurassiques dans les Alpes Occidentales. *C. R. Acad. Sci. Paris*, **309**, II, 1711-1716.

MASCLE G., ARNAUD H., DARDEAU G., DEBELMAS J., DUBOIS P., DELPECH P.Y., GIDON M., GRACIANSKY P.-C. DE, KERCKHOVE C., & LEMOINE M. (1988).– Salt tectonics, Tethyan rifting and Alpine folding in the French Alps. *Bull. Soc. Géol. France*, Paris, **8**, 4, 705-716.

MOJON P.-O. (2002).– Les formations mésozoïques à Charophytes (Jurassique moyen-Crétacé inférieur) de la marge téthysienne nord-occidzntale (Sud-Est de la France, Suisse occidentale, Nord-Est de l'Espagne). Sédimentologie, micropaléontologie, biostratigraphie. *Géologie Alpine*, Mém. H.S. n°41.

RUBINO J.-L. (1988). – Organisation des séquences de dépôt de la plate forme au bassin dans l'Aptien et l'Albien du bassin vocontien (SE de la France). *In*: FERRY S. & RUBINO J.-L. Eds., Eustatisme et Séquences de Dépôt dans le Crétacé du Sud-Est de la France (livret guide Groupe Français du Crétacé en fosse vocontienne), 25-27 mai 1988, *Géotrope, Lyon*, **1**, 56-83.

ENVIRONMENTAL CONTROLS ON TROPICAL CARBONATE PLATFORM

Annie Arnaud-Vanneau

Carbonate environments differ substantially from clastic ones because much of the sediment is of biogenic origin and produced in the area in which it is deposited. Biogenic production determines the bioclasts available for transport and sedimentation and so influence the nature of substrat, which in turn may influence the biota that colonizes it. Sedimentary grains are skeletal and non-skeletal origin (ooids, oncolites...), but the majority are skeletal grains. The bioclasts are fragments of shells and carbonate mud may be have an organic origin (algae, bacterial activities...). The bioclastic composition of a limestone reflects the nature of the habitat inhabiting the area. It is the fabric of sediment, which reflects the prevailing ecological conditions. A carbonate platform may be considered as a living factory where shell and skeleton of shallow water organisms contribute to detrital deposits of widely varying grain size.

Benthic organisms are bottom-living organisms and animal may live on the sea floor as **epifauna** or below the sediment surface as **infauna**.

Planckton consists of organisms that float passively in the water. Carbonate tests of microplanktonic organisms constitute the main component of pelagic mud deposited in basin.

1.– Limiting factors on the distribution of organisms

The potential niche of a species is defined by many ecological parameters, but, within a particular environment, some factors have a more important effect in determining the range of the species than others.

1.1. Light (Plate 1 to 4)

Light is the fundamental source of energy for primary producers at the base of the food chain. In most photosynthetic plants, light energy reacts with photosynthetic pigments, such as chlorophylls, and fixes carbon dioxide into organic compounds. The intensity of light decreases exponentially from the sea surface downwards so that most photosynthesis activity has stopped at maximum depths of about 150 m. The highest photosynthetic rates are commonly 10-20 m below the surface. The depth range from the ocean surface through there is a net photosynthetic production is known as the **photic zone (PZ)**.

Many organisms living on carbonate platform are associated to symbiotic green algae (zooxantellae). Organisms gain from the zooxantellae because they absorbed CO_2 during photosynthesis and release carbon compounds that provide energy and promote calcification.

1.2. Nutrients (Plate 5)

Nutrients are the inorganic and organic substances that are essential for the growth of plants. Together with light they exert a dominant control on productivity. Carbonate platform with low level of nutrients supply are referred to as **oligotrophic**. Stable, nutrient-poor systems tend to produce ecosystems that have a high diversity of organisms. The zooxantellate organisms that contribute largely to the framework of platform are adapted to low nutrient level, while filamentous and algae favor high nutrient level. Consequently carbonate platform and reefs flourish under **oligotrophic conditions**.

Abundance of nutrients favors development of sea grasses and algae and affects the oligotrophic factory of carbonate platform.

Consequently, under somewhat more nutrient-rich, **mesotrophic** condition growth tends to be suppressed and bioeroders associated to sea grasses favor a large amount of carbonate mud.

1.3. Oxygen and salinity (Plate 6)

1.3.1. Oxygen

Almost eukaryotic organisms require oxygen for their metabolism. The oxygen content of sea-water is mainly in the range of 6 to 1ml/l which is viable for the majority of marine organisms. The biotic response to low oxygen level is marked by decrease in faunal diversity when dissolved oxygen falls below about 2 ml/l Animals migrate away from the low oxygen area or show adaptations (*Istriloculina* and its thin calcitic test).

1.3.2. Salinity

Most ocean waters have relatively uniform level of salinity to which the majority of marine animals are well adapted. Salinity becomes an important limiting factor in marginal marine environments that are brackish or hypersaline. Animals have a constant concentration of dissolved ions within their cell fluids. Water will enter a cell across its semi-permeable membrane by **osmosis.** Most animal are isotonic with sea water and live within a narrow range of salinities. They are **stenohyaline** such as **corals**, brachiopods, **echinoderms**, ammonoids and **large benthic foraminifers.**

Species, which can tolerate a broader range of salinities are called **euryhaline**. Crustaceans can keep their internal solutions constant in spite of fluctuating levels of salinity.

2.3.3. Conclusion

The two factors produce the same effect. Facies deposited in normal marine waters are characterized by stenohyaline group. Brackish or hypersaline facies generally have a low to very low diversity, contain ostracods and gastropods and species tend to be small.

2.4. Temperature (Plate 7)

Temperature is one of the most pervasive influences on the distribution of organisms and plays a major role in determining the latitudinal partitioning of species into biogeographic provinces. Tropical carbonate platforms extent between 30° South and 32° North. Most marine animals apparently live within a relatively narrow range of temperature that is commonly determined by the optimal temperatures for reproduction and early growth.

Generally, the diversity of faunal assemblage decreases toward high latitudes. The abundance of shell-bearing animals increases towards equatorial regions, so that the presence of thick shelly limestones of carbonate platform is a good indicator of low latitudes. With increasing water temperatures shells tend to be more strongly ornamented.

2.5. Nature of substrate (Plate 8)

The grain size of sediment is one of the most easily assessed physical parameters, but the grain size is one amongst many constituting aspect of substrate. A new population of marine animals may become established by the random settlement of larvae on the sea floor. Larvae select the site where they will settle.

In nearshore environments, the species diversity is generally highest in muddy sands, moderate in sandy muds, low in pure sands and may be near 0 in soft mud. The firmness of the sediment is an important factor in influencing faunal distribution. Sediments vary from soupy mud with a very high water content, to soft loose sediments, to firm grounds and hard grounds. The identification of hard grounds in which carbonate sediment had become at least partially cemented on the sea floor, depends largely on fossil evidence of a hard substrate. Hard ground surface is bored and colonized by epifaunal animals like oysters.

2.6. Substrate mobility, sedimentation rates and turbidity

Sediment mobility and the turbidity of the water are important limiting factors in certain nearshore environments. Epifaunal animals have many difficulties in surviving in very mobile sands. Some infaunal animal have adapted to sediment instability by rapid burrowing. Generally the sands have a low faunal diversity and a low abundance.

Storm-event sands rarely contain indigenous fauna, but have shell concentrations at the base of the bed, winnowed from the underlying sediment. Rapid rate of sedimentation, associated with storms, floods and turbidity currents may be recognized by escape burrows. Low rate of sedimentation may be recognized by firm grounds or hard grounds.

The effect of depth of water on an organism reexperienced through the increase in hydrostatic pressure. Animals, like *Nautilus*, have enclosed pockets of gas in their body. *Nautilius pompilius* lives at depths of about 600 m, and implode at depths between 730-900 m.

Planktonic foraminifers need a certain water depth for reproduction. If the water-depth is not sufficient, the reproduction cycle is interrupted and it is one of the reason why planktonic foraminifers are missing on carbonate platform of represented by small immature and juvenile forms.

But depth alone has relatively little effect on biotic distribution.

However, many of the other ecological factors, such as temperature, substrate, turbulence, light, oxygen, nutrients and salinity are depth related and are commonly used to infer relative depth in environmental reconstructions.

Plate 1

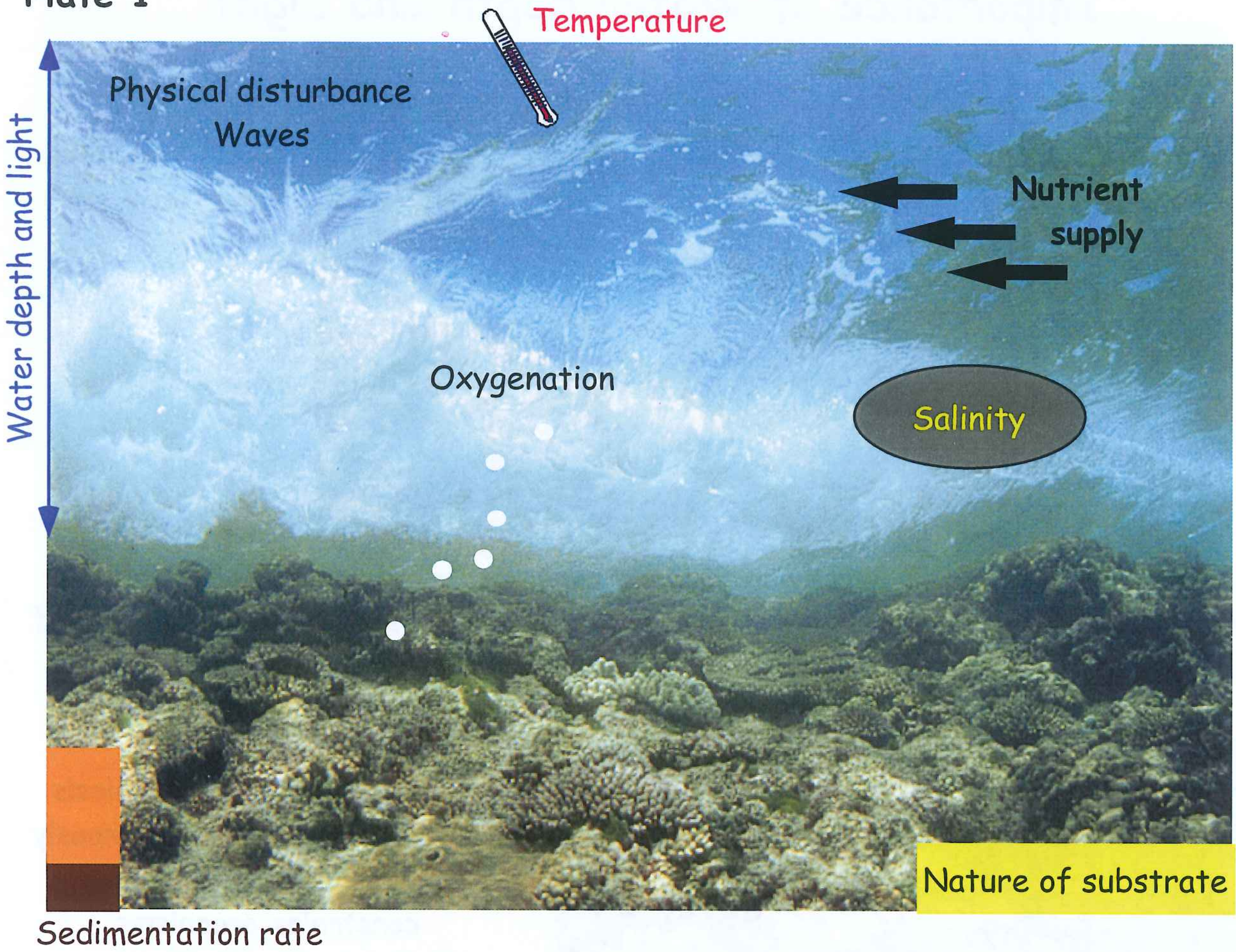

Main ecological factors

Physical disturbance and waves

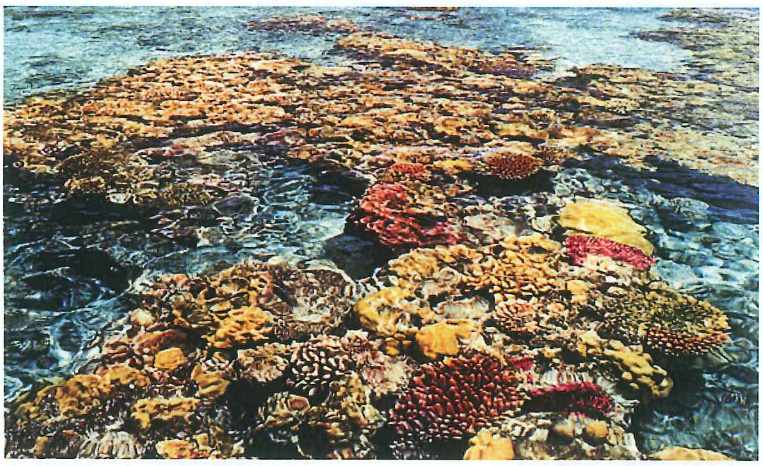

Morea Island (Pacific Ocean)

Aptian Buccicrenata

Barremian Trocholina

High physical disturbance favors robust species with high calcification rate and attached fauna (corals, calcareous sponges, bivalves,..). Benthic foraminifers are frequently conical and have a large size (1-0.500 mm)

Importance of Water depth and Light

A carbonate platform is a living factory composed of organisms that inhabit high water transparency. The depth of the photic zone is linked to clarity of water.

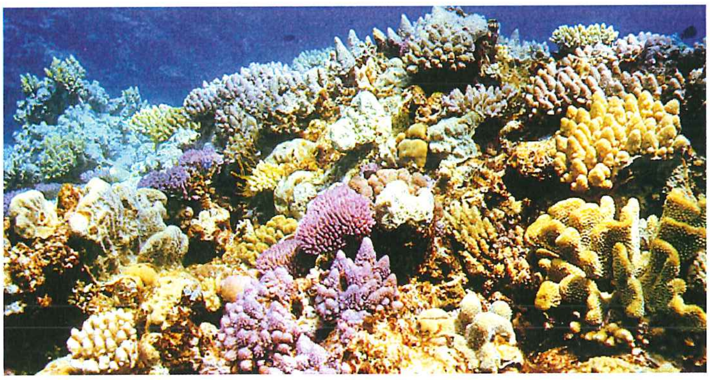

Acquisition of photosymbiosis allows the invasion of previously inhospitable habitats but constrains organisms to live in the photic zone

Benthic foraminifera

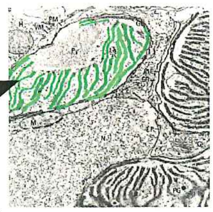

Symbiotic green algae Zooxantellae

Porites- Caribbean sea

Photosymbiosis is the link between light and high calcification rate

Plate 2

Organisms living in the photic zone are usually associated to symbiotic green algae and have a large size

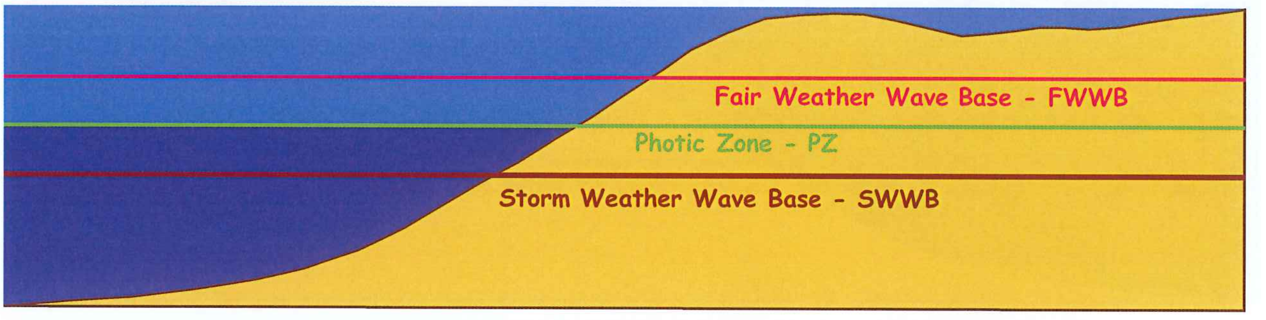

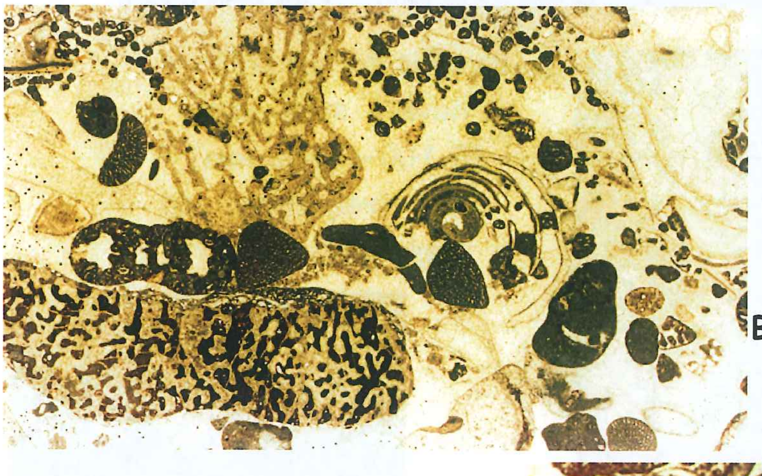

Benthic foraminifers can have a large size (1-0.500 mm)

The most common organisms are corals, large bivalves, large gastropods, large green algae and large benthic foraminifers

Plate 3

Organisms living below the photic zone have a small size and a thin test

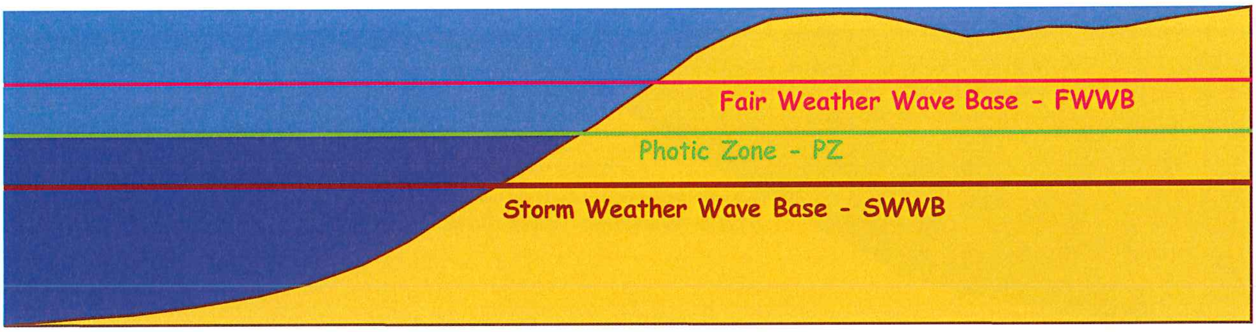

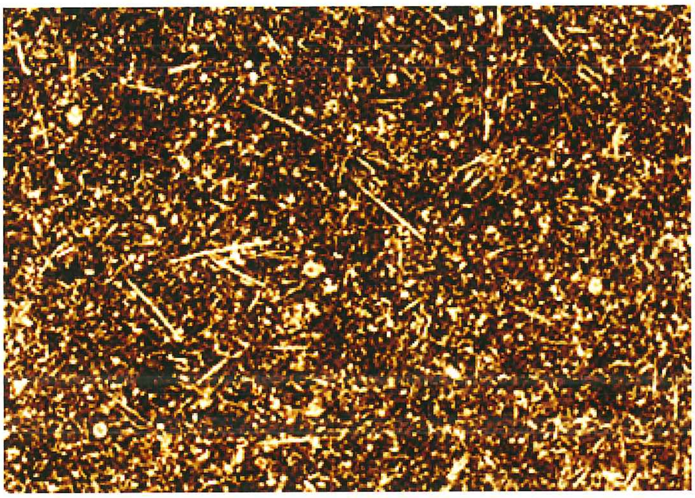

Benthic forаmininifers have a small size (0.100-0.200 mm) and, frequently, an agglutinated test

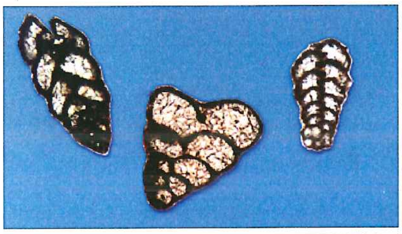

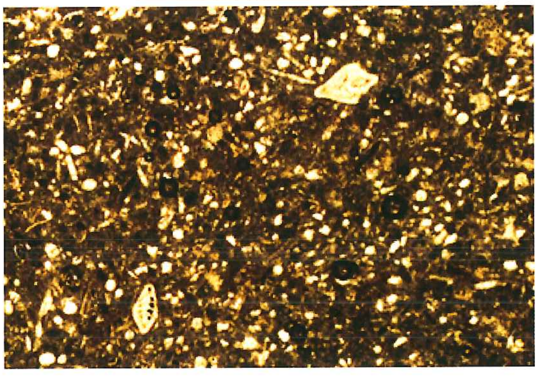

Siliceous sponges are the most abundant organisms

Plate 4

Plate 5 Nutrient supply

Abundance of nutrients favors development of sea grasses and algae and affects the oligotrophic factory of carbonate platform.
Consequently, under somewhat more nutrient-rich, mesotrophic condition growth tends to be suppressed and bioeroders associated to sea grasses favor a large amount of carbonate mud.

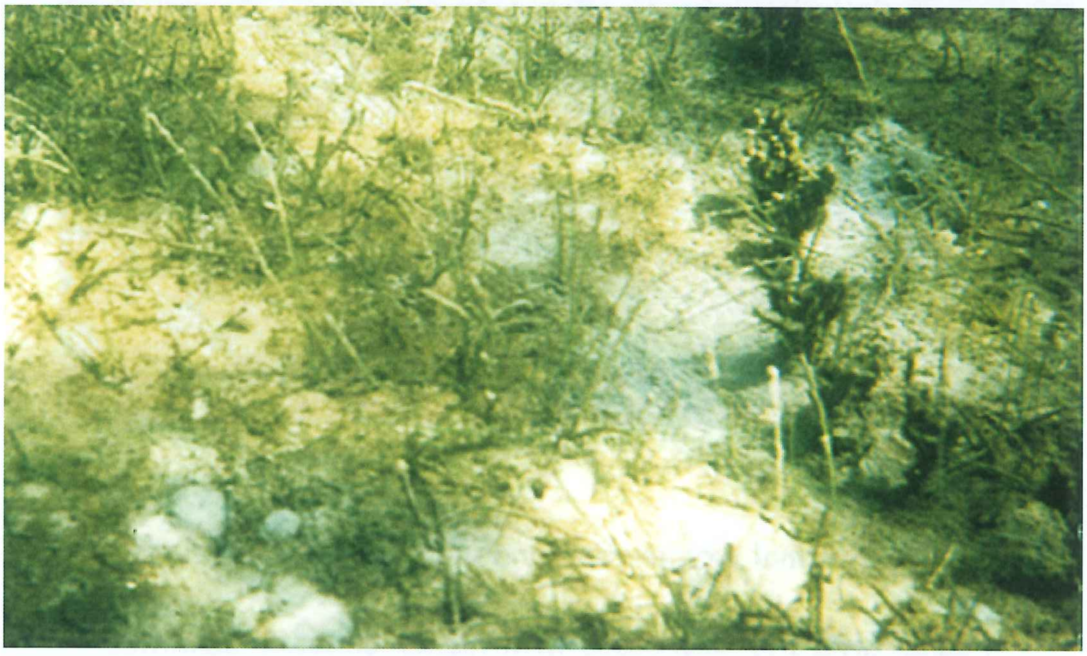

Thalassia and Halimeda, Lagoon of St Barthelemy (West Indies)

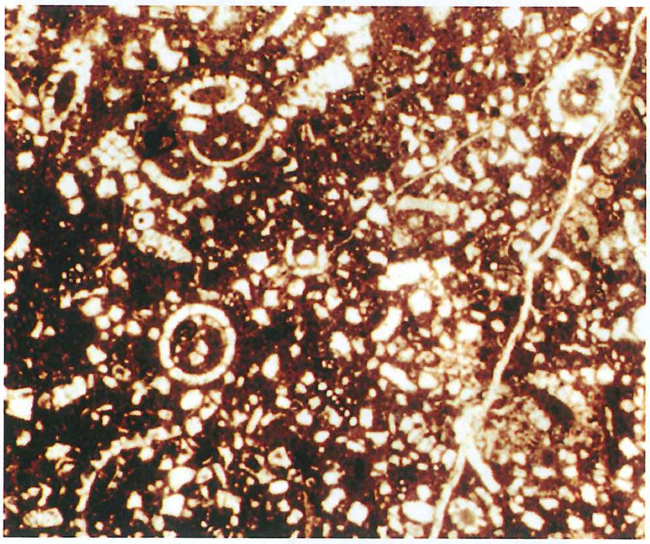

Wackestone with dasycladacean algae
Aptian (Lower Orbitolina Marls, Vercors)

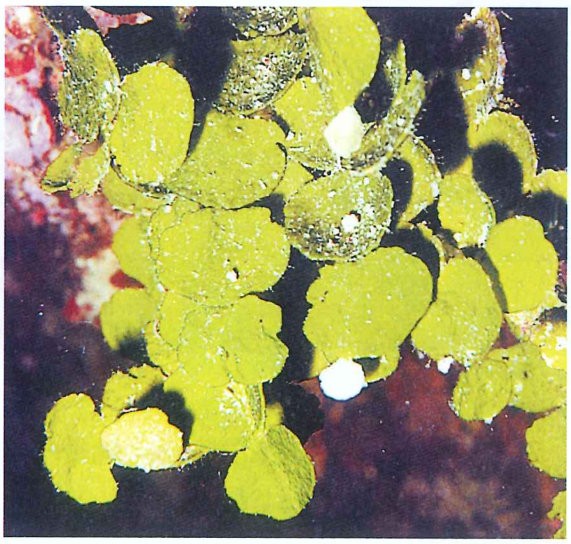

Halimeda sp.

Oxygenation and salinity

Normal oxygenation and salinity favor reef development

Abnormal oxygenation and unstable salinity.

Faunal diversity decreases with higher or lower salinities

Istriloculina (thin shell miliolid) is one of rare organism which is able to live into muddy environment of lagoon

Saint Paul Trois Châteaux- Martinique West Indies

Plate 6

Temperature

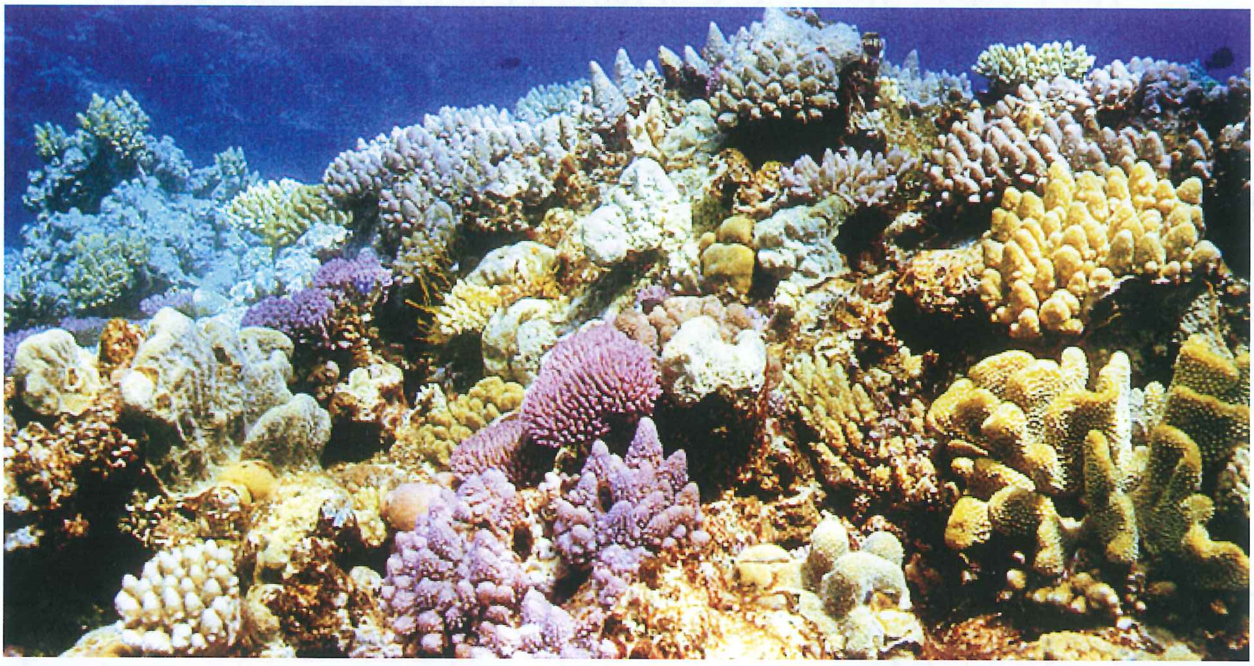

A tropical carbonate platform is a living factory composed of organisms that inhabit shallow and warm-water of the tropical area

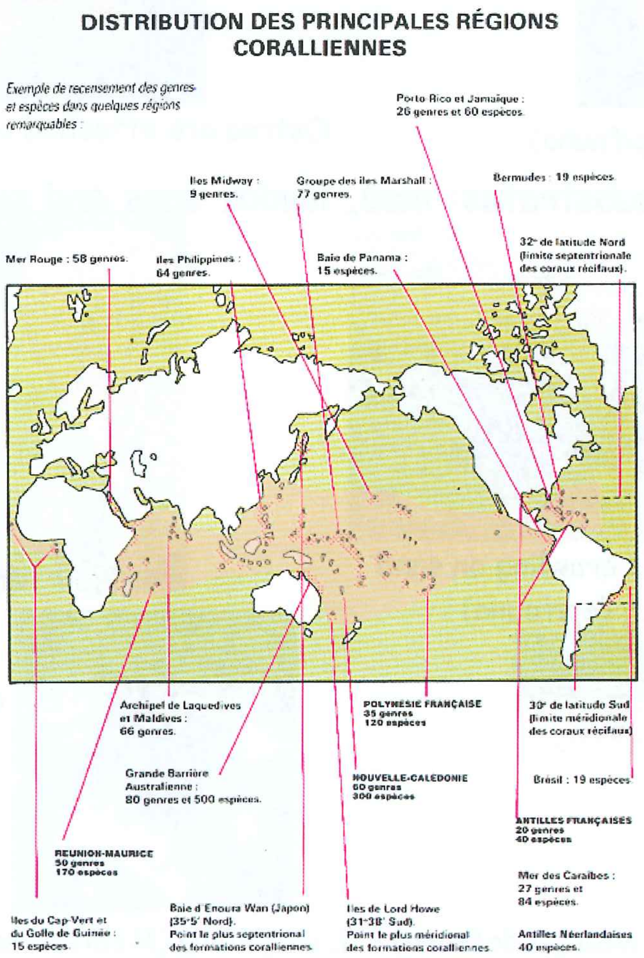

Plate 7

Plate 8 Nature of substrate

Hard substrates: Hard ground, Firm ground, Leaves,...

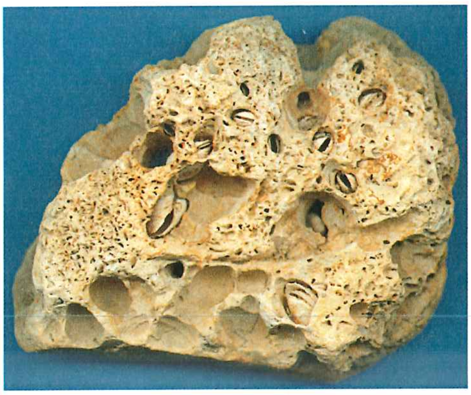

Borings into a pebble (endofauna: Cliona and bivalves) Mediterranean Sea

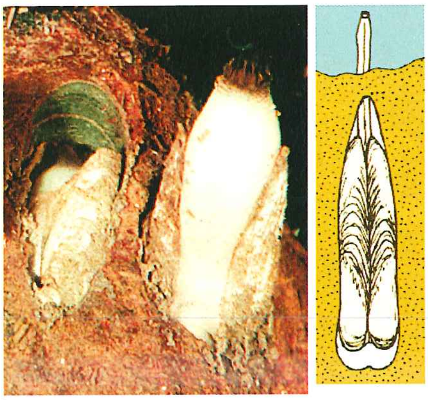

Living bivalves (Pholadomya) into hard substrates

Boring of Pholadomya

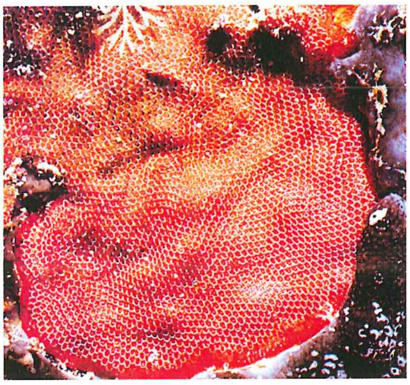

Attached Bryozoan (epifauna)

Ostrea are attached on the firm ground

Soft substrates: mud, muddy sans and sand

Gastropods crawling on sand beach (epifauna)

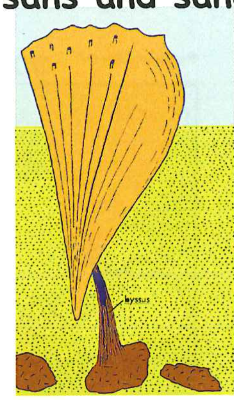

Fossil Pinna

Pinna attached by byssus is living in muddy sand (endofauna)

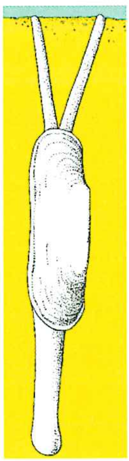

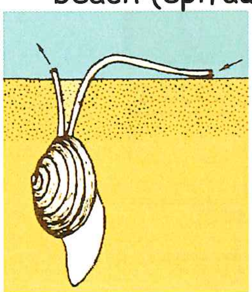

Mobil bivalves living in mud (endofauna)

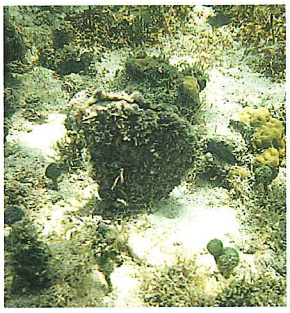

Living Pinna (Mediterranean Sea)

Carbonate facies and microfacies of the Lower Cretaceous carbonate platforms

Annie Arnaud Vanneau and Hubert Arnaud

Considering the range of sedimentological and ecological parameters which control deposition in the marine environment, the organization of microfacies into a limited number of categories is a simplification. In the South-East of France, carbonate platform facies are observed in three different types of environments: standard platforms, drowned platforms, and resedimented deposits in the Basin.

1.– Standard platform

On the standard platforms, which are well developed during periods of relatively low sea level, 12 families of microfacies, classified from F0 to F11, may be distinguished in the early Cretaceous. They constitute a natural but hypothetical continuation between a "basinal" environment characteristic of a deep marine domain, and a restricted marine environment, shallow and sometime emerged. These platforms are sufficiently recognizable to be able to establish vertical evolution curves of facies on the platforms and their margins.

1.1. Facies F0: Mudstone-Wackestone with radiolaria and ammonites (Plates 9, 10, 11 and 12)

This pelagic (or deep hemipelagic) basin facies is characterized:

Macroscopically by alternations of marls and bluish-grey ammonitoid argillaceous limestones;

Microscopically by essentially pelagic organisms: radiolaria associated to planktonic foraminifers. The micritie matrix is made of Coccolithophiridae or Nannoconidae.

This facies comprise varying but sometimes, substantial proportions of clay, silted quartz and glauconite.

1.2. Facies F1: Wackestone with sponge spicules

This hemipelagic facies deposited in sciaphile environments, is characterized (Plate 13):

Macroscopically by marls or by bluish-grey argillaceous limestones with rare macrofauna (a few ammonites and irregular sea urchins [Spatangidae]) made up of 50 to 60% carbonates, 30 to 40% clay, 10 to 20% quartz and glauconite;

Microscopically by a large number of sponge spicules, commonly replaced by calcite and by a fairly dispersed microfauna of small agglutinated foraminifers and Nodosariidae.

1.3. Facies F2: Wackestone with irregular sea urchins (Spatangidae)

This facies deposited in quiet deep subtidal environments is characterized (Plate 14):

Macroscopically by greyish-blue fairly argillaceous limestone (60-70% carbonates, 20-30% clay, 7-10% quartz) including a significant number of irregular sea-urchins (Spatangidae);

Microscopically by a mixture of Spatangidae fragments and peloids.

The microfauna is composed of small agglutinated foraminifers (*Marssonella, Gaudryina, Textularia, Glomospira, Nezzazata*) and some Nodosariidae.

1.4. Facies F3: Packstone-grainstone with echinoderm fragments and small benthic foraminifers

Characteristic of deep subtidal environments, such as the previous facies, these fine grainstone facies are generally well sorted and slightly more calcareous than the facies F2 (about 80% carbonates, 20 to 30% clay, less than 10% quartz) (Plate 15).

Macroscopically, they are characterized by wavy decimeter beds, which correspond to bluish to slightly reddish limestones with a sparse and badly preserved macrofauna.

Microscopically, they are characterized by numerous small rounded fragments of echinoderm, abundant peloids and abundant small deep subtidal foraminifers (specifically similar to those of the facies F2).

The worned grains are well-sorted and beds are bounded by ripple marks. This aspect attests the presence of hydrodynamism (low speed currents).

1.5. Facies F4: Packstone-grainstone with bryozoans and crinoids (Plates 16 and 17)

These facies, deposited in deep subtidal environments under the photic zone, are coarser than the previous ones. They are characterized :

Macroscopically by reddish to yellowish-brown limestone showing either meter-scale cross-bedded beds or as decimeter-sized beds;

Microscopically, sessile populations are predominant or constituted exclusively by bryozoans and crinoids. Foraminifers are absent excepted for some reworked large, robust and generally worn forms (*Lenticulina* and *Trocholina*). These facies are made up of 75-87% carbonates, 7-15% clay and 2-10% quartz.

1.6. Facies F5: Grainstone with large rounded bioclasts (Plate 18)

These limestones (minimum 90% carbonates) were deposited in the photic zone and in shallow subtidal to tidal environments. They are characteristic of high energy level.

Macroscopically, they are characterized by decimeter yellowish beds with oblique or cross-stratifications.

Microscopically, they are characterized by the abundance of rounded bioclasts of metazoans and algae, and, occasionally, by abundant large-sized benthic foraminifers.

The good sorting, presence of alternating fine or coarse-sized laminae, and the richness in dasycladacean algae and corals debris evidence the formation of these facies in shallow subtidal to tidal environments subject to a constant, moderate to strong, hydrodynamism (foreshore for example). On the platform's outer slope, the coarse-grained sands may be transported laterally downward to deep subtidal environments by storm currents or grazvitary currents.

1.7. Facies F6: Grainstone with oolites (Pl. 19)

These limestones (100 % carbonates) were deposited in the photic zone and in shallow subtidal to tidal environments. They are characteristic of medium energy level due to waves and tidal currents.

Macroscopically, they are characterized by decimeter yellowish beds with oblique or cross-stratifications.

Microscopically, they are characterized by the abundance of oolites and absence of non-oolitized fauna and microfauna.

1.8. Facies F7: Grainstone with corals or Boundstone

These facies (Plates 20 and 21), deposited in subtidal to tidal environments were subject to moderate, or even locally strong, hydrodynamism. They contain 88 to 95% carbonates and, at the most, 1% quartz (quartz is often absent).

Macroscopically, they appear either as decimeter-sized levels with oblique or cross-stratified beds (F6) or else in lenticular levels (F7). They are found either on the edge of the platform (their lateral extension is therefore generally reduced), or else in the inner platform, after a considerable submersion episode when the carbonate sedimentation returned to normal standard platform (in this case, which corresponds to highstand systems tract, these facies are observed in very large areas). Aside from the metazoan fauna which accompanies the corals of facies F7, there is no autochtonous fauna except for one or two species of foraminifers (*Reophax ? giganteus* or *Acruliammina neocomiana*).

Microscopically, once again they are biosparites with rounded skeletal debris or oosparites, the elements of which are often well-sorted.

1.9. Facies F8: Packstone-wackestone with large foraminifers and large Rudists

These facies, are related to sediments deposited in lagoonal environments and considered to be "external lagoon" facies. They contain 86 to 95% carbonates.

Macroscopically, they appear as massive beige limestones with much skeletal debris (corals and Chaetetidae among others) and with rudists (mainly large Requieniidae rudists for the Barremian-Aptian).

Microscopically, they often correspond either to fairly coarse grainstone/packstone or to wackestone with large foraminifers. In both cases, these facies are characterized by large foraminifers and algae and by a high percentage of micritized bioclasts (peloids), evidence of microbial activity.

It is also here that are found the species displaying the best stratigraphic definition. Finally, all these bioclasts are regularly accompanied by some echinoderm debris, indication of normal salinity.

1.10. Facies F9: Packestone-wackestone with miliolidae and rudists (Plates 22 and 23)

These facies correspond to sediments deposited in shallow subtidal environments of the inner platform domain. Made up of 95 to 100% carbonates, they contain no quartz.

Macroscopically, they appear as massive, calcareous, meter-thick beds, white to beige in color, and contain small rudists.

Microscopically, all the debris are micritized and the microfauna is largely dominated by miliolidae.

There is not echinoderm fragments, indication of restricted environment.

1.11. Facies F10: Packstone-grainstone with oncolites and Bacinella (Plates 24 and 25)

These facies correspond to sediments deposited in shallow subtidal to tidal environments of the inner platform domain. Made up of 100% carbonates, they contain no quartz.

Macroscopically, they appear as massive, calcareous, meter-thick beds, white to beige in color, and contain oncolites.

Microscopically, all the debris are micritized and oncolites are abundant.

1.12. Family of facies F11 (Plates 26 to 31)

This family of facies corresponds to facies deposited in tidal and supratidal environments.

F11: Mudstone with Istriloculina and bird's eyes (Plate 26).

These facies correspond to restricted environments.

Macroscopically, they appear as beige or white decimeter- or meter-sized beds devoid of macrofauna and, in general, exclusively carbonate (99-100%).

Microscopically, they contain small thin tests of Miliolidae (*Istriloculina*) and a few other species of foraminifers. They are made of algal mats (stromatolites).

F11: Grainstone with keystone vugs and storm deposits, early diagenetic features (Plates 27 and 28)

These facies indicate beach, storms and early dissolution or dolomitisation.

2.– Drowned platform (Plate 32)

During the periods of relatively high sea level, platforms are characterized by the development of "transgression facies". Identification of these particular facies frequently associated with the presence of hardgrounds brings good evidence of periods of marine environment deepening. They present all or a part of the following features.

a) They are very rich in iron oxides, which appear either as black or reddish peloids or oxidized or darkened debris. These oxydes provide the facies with their highly characteristic reddish, yellowish-brown or blue color.
b) They often show a dual granulometry indicating substantial reworking: a first group of small bioclasts may be mixed with a second group of larger, worn and rubefied bioclasts. Sometimes, pebble-sized elements may be reworked.
c) They often contain a very rich and diversified fauna, often a mixture of deep and shallow-water fauna.
d) They sometimes display a mixture of two distinct facies, this mixture having been formed before the two sediments hardened.
e) They often contain fairly high proportions of terrigenous detritic elements (quartz, clays...).

3.– Reworked sediments in the basin (Pl. 33 and 34)

Three types of gravity flow deposits (mud flow, sand flow, turbidites) are observed in the Vocontian trough where they have eroded pelagic and hemipelagic autochtonous substratum. These flows relate to the transport by gravity, all the way to the bottom of the basin, of sandy, sand-mud, or muddy sediments deposited on the margin or outer slope of the platform. However, the nature of the sediments deposited by gravity at the bottom of the basin is directly related to that of the sediments deposited at the same time on the platform margins: this results in the substantial variation in the nature of gravity deposits according to the relatively high or low sea level of the period.

During periods of relatively low sea level, (Lowstand systems tract), the margins and outer shelf slopes are characterized by huge accumulation of bioclastic sands. In the basin, the reworked sediments are deposited in beds sometimes decameter-thick made up of coarse-grained sand with a number of large Foraminifers (*Trocholina*, Orbitolinidae, large agglutinated foraminifers) and dasycladadean algae. In the turbidites, vertically graded bedding is nevertheless poor because of the originally well-sorted sediments deposited on the outer platform slope. These beds form huge basin floor fan, especially for BA1 depositional sequence.

During periods of very high sea level (Transgressive systems tracts), the drowned platforms are the site of sedimentation in a deep environment (Facies Fl or F2). The turbidites present in the basin, generally rare due to the lack of sandy sedimentation on the upper slope, are of two types :
– thin turbidites, centimeter to decimeter-thick, corresponding to a massive remobilisation of sponge-spiculed mud,
– very thin turbidites, millimeter- to centimeter-thick, reddish in colour, made up of very fine packstone-grainstone with small sponge spicules.

During periods of relatively high sea level (Highstand systems tracts, standard platform), the margins and outer platform slopes are characterized by generally fine-grained bioclastic sands and muddy sands, deposited under photic zone, due to the small-scale progradation following the maximum flooding. In this case, the reworked sediments in the basin are often deposited in small, reddish, decimeter-sized beds; they are well-sorted, from fine to very fine, with basal sedimentary structures. One finds mainly fine-grained grainstones with small deep-water benthic foraminifers or fine grainstones with large sponge spicules.

In conclusion, the granulometry, the nature of the bioclasts and the type of facies found in the bioclastic sedimentary bodies reworked in the basin are not directly related to the distance of the re-deposit areas from the source platform margins, but rather to the platform margin environments and thus to the variations in depth there observed. According to this interpretation, the vertical transition in the basin is not from proximal to distal turbidites, but rather from low sea level to high sea level turbidites.

Plate 9 Facies F0

Nannoplankton: Coccolithophorids

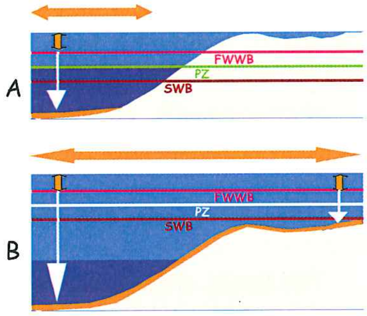

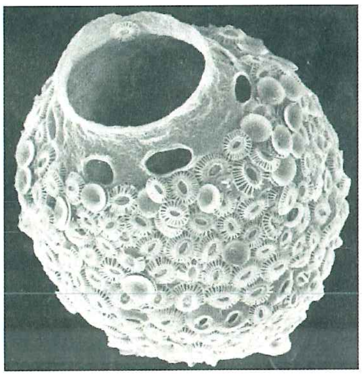

Coccosphaera

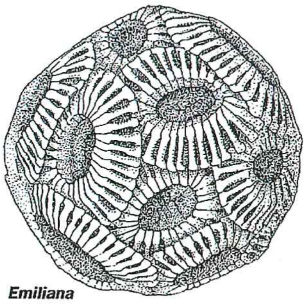

Emiliana huxleyi
5 µm

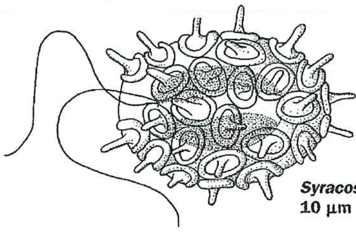

Syracosphaera subsalsa
10 µm

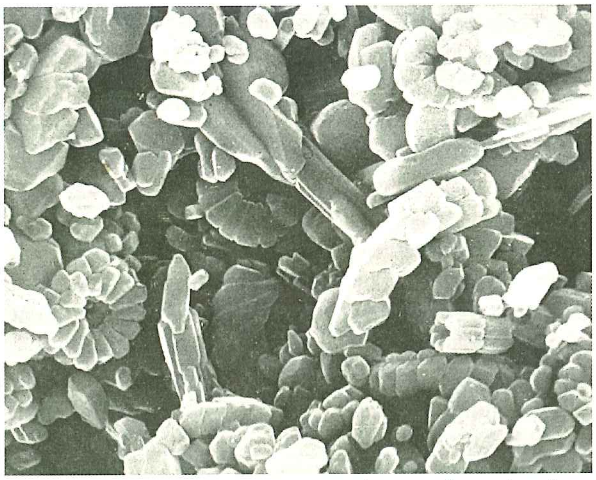

Scanning microscope view of pelagic limestone showing Coccoliths and Nannoconus

Coccoliths

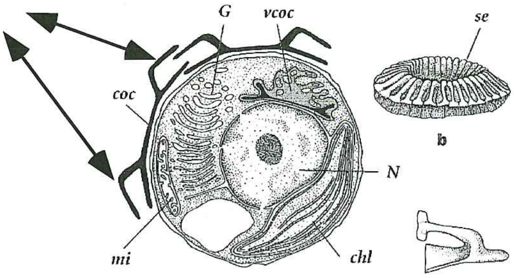

Section of Coccosphaera

Alternating marl and calcareous limestone (Vocontian Basin - France)

Facies F0 - Radiolaria

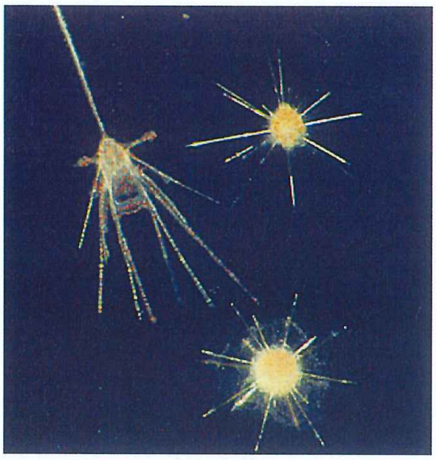

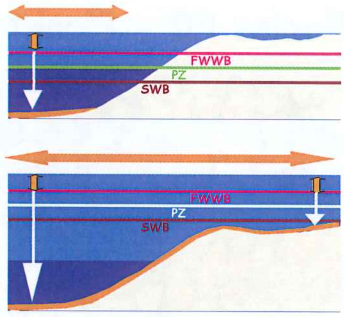

Living radiolaria

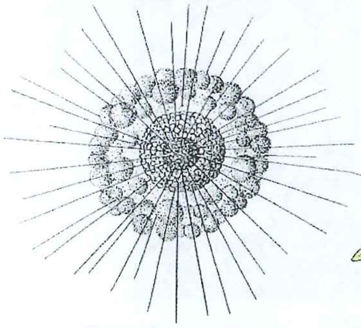

Thalassicola nucleata
70 µm

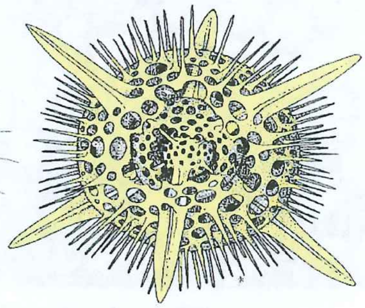

Hexaconthium asteracanthion
200 µm

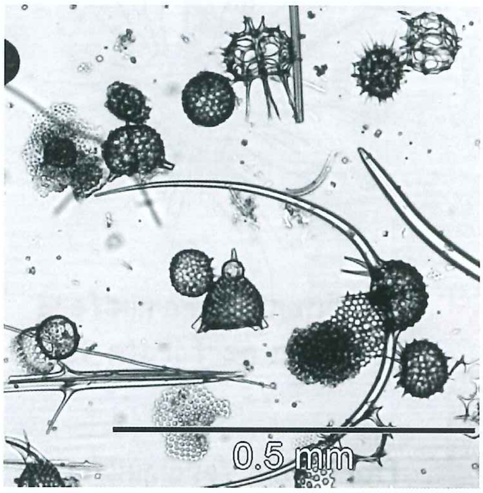

Early Oligocene from the Indian Ocean
(Sarah-Jane Jackett, Univ. Lausanne, 2004)

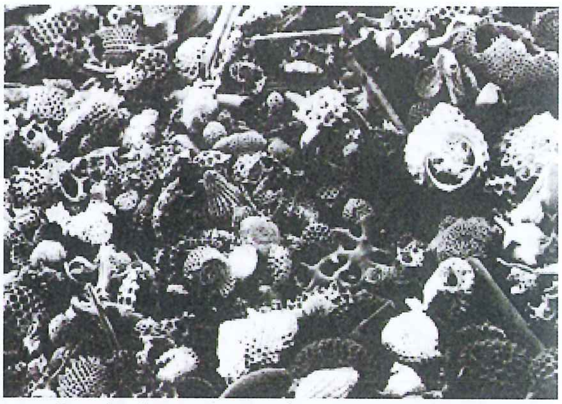

Radiolaria in siliceous oozes

Radiolaria are marine planktonic protozoa in which a central capsule and surrounding spicules consist of silica

Bioturbated pelagic limestone

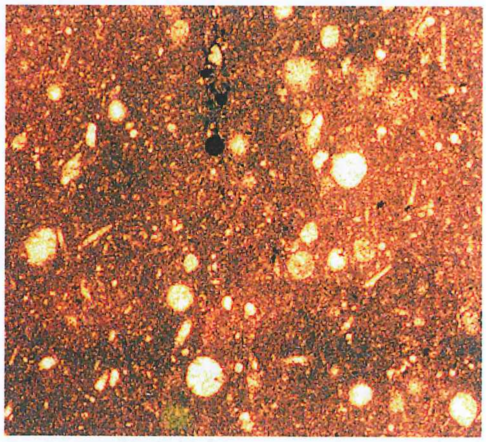

Radiolaria in limestone. Opaline tests are replaced by calcite

Plate 10

Facies F0 - Planktonic Foraminifers

Plate 11

"Pelagic Soup""
Accumulation of planktonic foraminifera tests

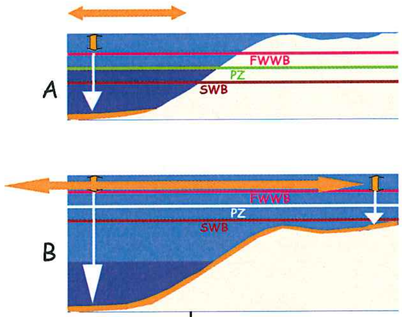

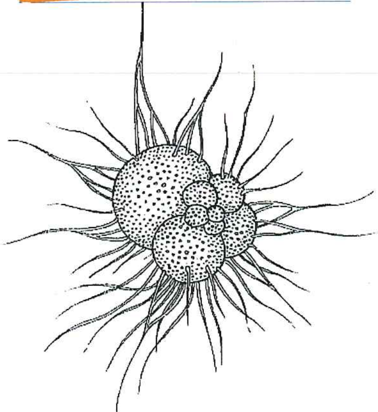

Plancktonic foraminifera showing a perforate test

Planktonic foraminifers can be locally in sufficient number to be the major rock-building constituent

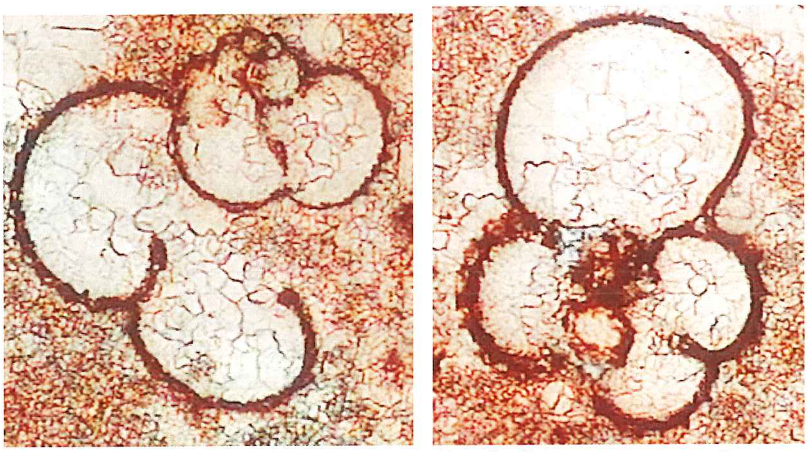

Thin sections of Favusella (Albian - Oman)

Albian-Cenomanian marls from the Vocontian Basin (France)

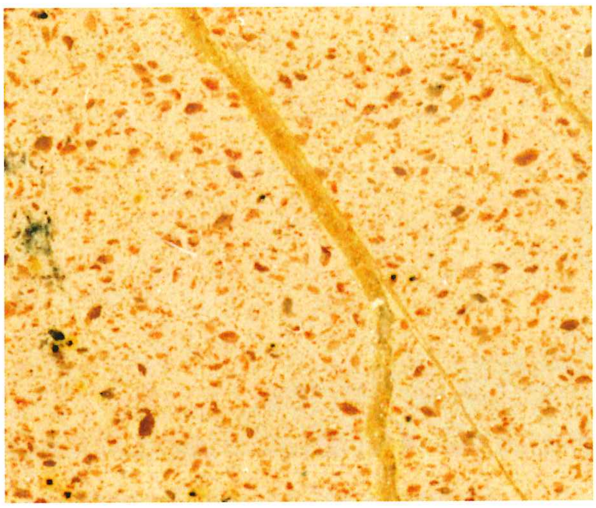

Pelagic limestone with Globotruncana

Facies F0 - Cephalopods: Nautiloidea and Ammonoidea

Nautilus pompilus
Pacific Ocean
(L'évolution animale, 1968)

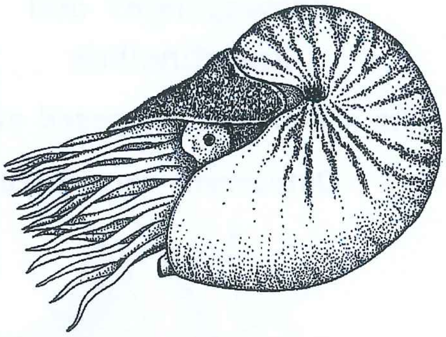

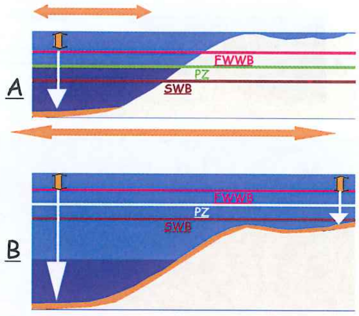

Nautilus can control is own buoyancy by changing the amount of gas and fluid in chamber

Ammonidea is a group which evolved from Nautiloidea and which shows an increase in the complexity of the suture line

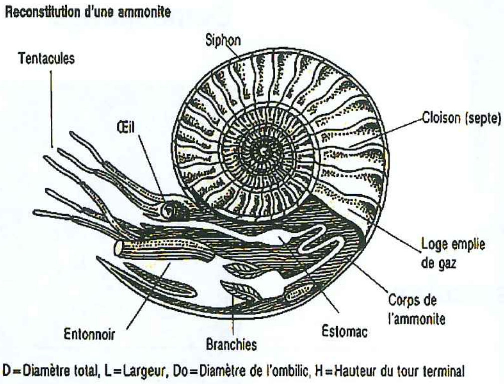

Section of Ammonite
(Les Fossiles)

Small evolute ammonite (Lytoceras sp.) from Valanginian of Vocontian basin

Shell of Spirula

Crioceras sp.
Hauterivian ammonite
from Vocontian basin

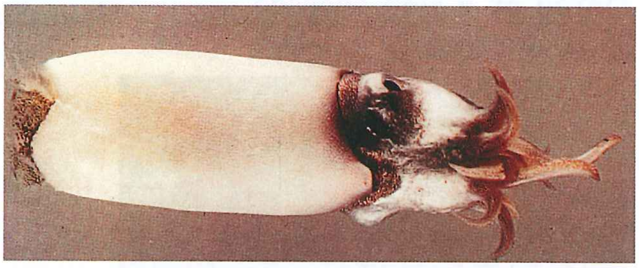

Spirula has an internal shell (Coquilles et Mollusques)

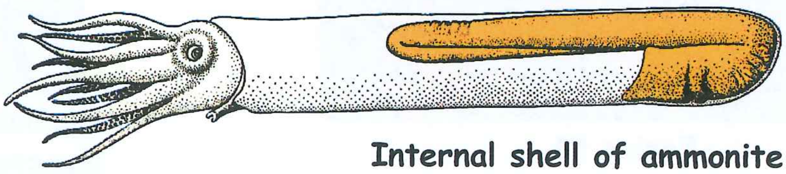

Internal shell of ammonite

Plate 12

Plate 13

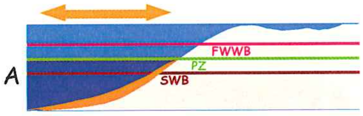

Facies F1
Siliceous sponges; demosponges and hexatinellids

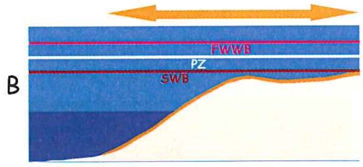

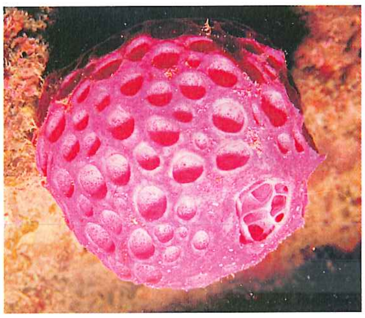

Cinachytra

The skeleton is composed of siliceous spicules

Outcurrent pore (oscule)

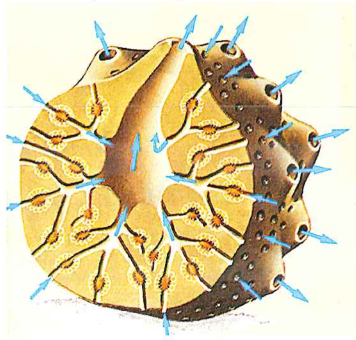

Incurrent pore (ostia)

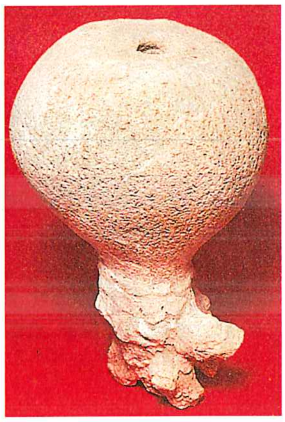

Skeleton of Siphonia Demosponge

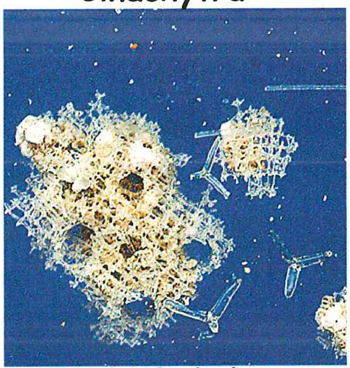

Detail of skeleton

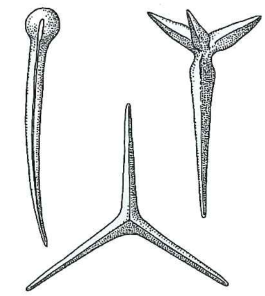

Demosponge spicules

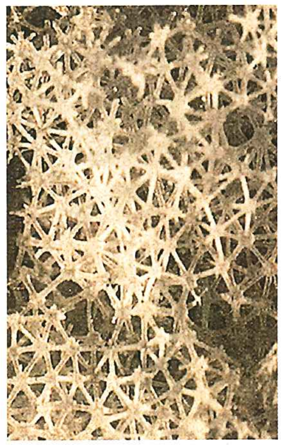

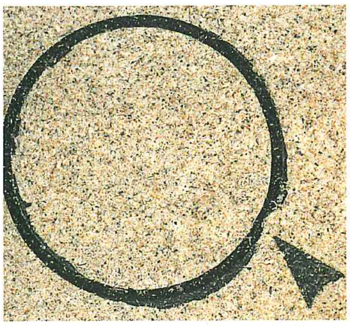

Detail of a slab showing abundant sponge spicules

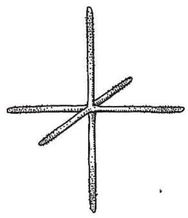

Hexactinellid spicule

Facies F1

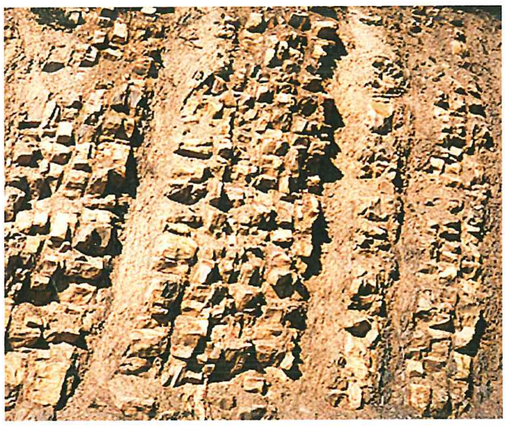

Alternating marl and argillaceous limestone - hemipelagic facies

Facies F2 - Irregular echinoids - Spatangus

Plate 14

A

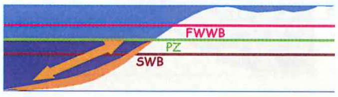

B

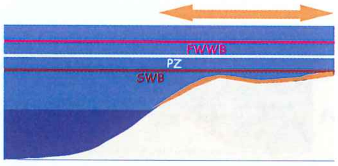

Spatangus are deritivore and normally hidden in a shallow burrow in soft sediment (sand or muddy sand)

The mouth has migrated forward and anus to a lateral position at the posterior side of the test

Fossil and recent irregular sea urchin show the same morphology

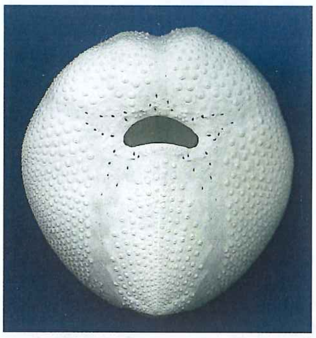

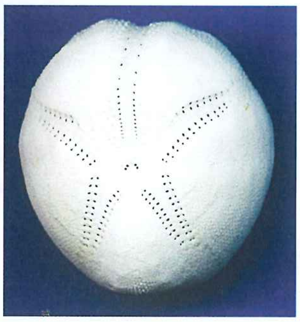

Recent irregular sea urchin

Toxaster amplus (Hauterivian)

Lavenia elongata

The test is surrounded by thin and short blunt spines

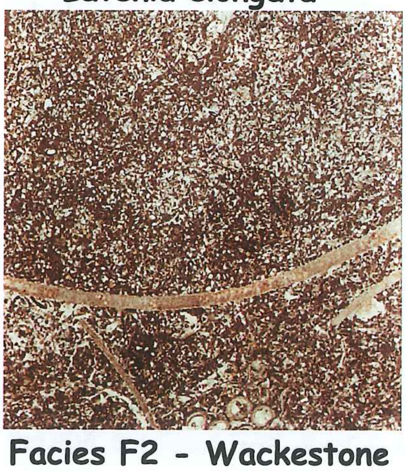

Facies F2 - Wackestone with irregular sea urchin

Wavy limestones - calcaire à miches

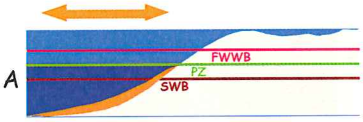

Facies F3
Small benthic foraminifers
and annelids

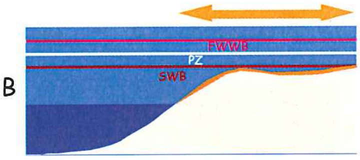

These minute foraminifers normally live in soft sediment (fine-grained sand or muddy sand)

Fossil Nodosariidae

Fossil Valvulineria
Small Nezzazata

Present day Ammonia

Fossil Marssonella
Gaudryina

Fossil Glomospira

Present day annelid

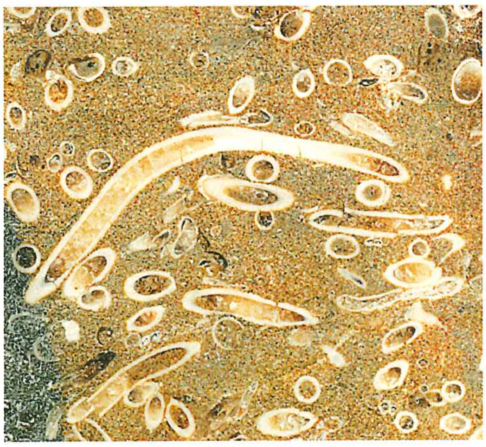

Barremian isolated annelids

Plate 15

Thin section showing annelids

Fine-grained grainstone - Facies F3

Wavy decimeter beds

Plate 16 — Facies F4 - Bryozoans

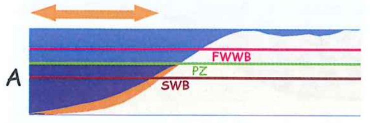

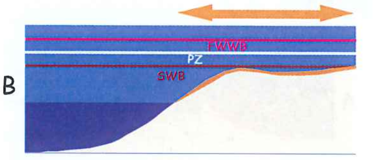

These minute animals live together in colonies and are abundant in obscure areas. They are attached on a substrate.

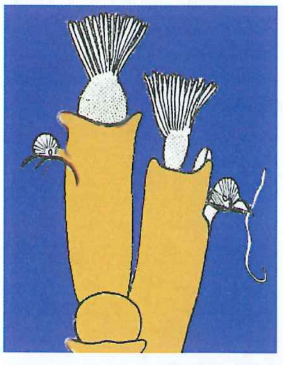

Detail of two living zooecia

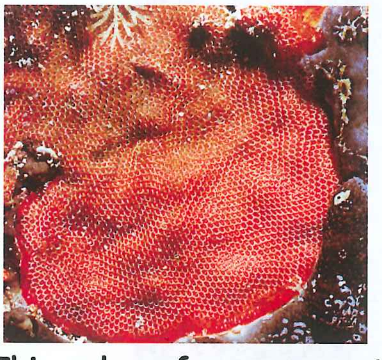

This colony forms a crust on a firm surface

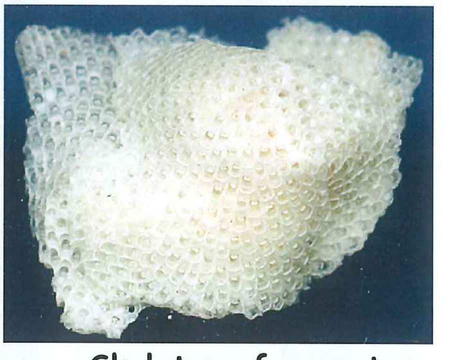

Skeleton of recent bryozoan

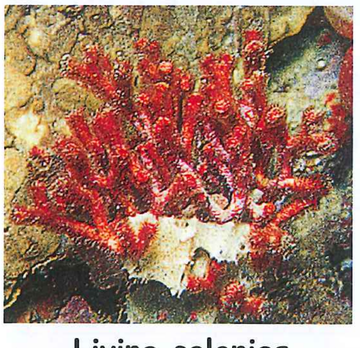

Living colonies
Myriopora truncata
(Mediterranean sea)

Skeleton

Similar morphology found in the Cenomanian of Algeria

Bryozoans attached on a small rounded intraclast

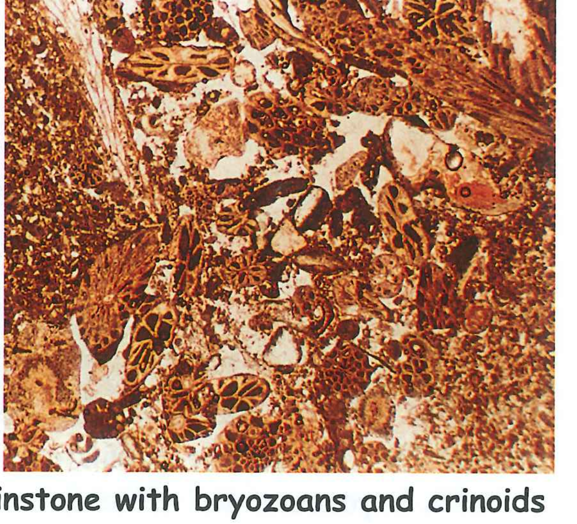

Facies F4
Packstone-grainstone with bryozoans and crinoids

Plate 17

Facies F4 - Crinoids

A

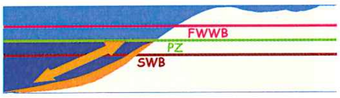

B

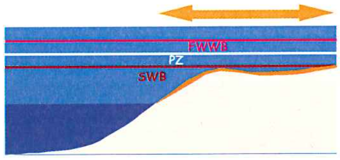

Present day crinoid

Living crinoid

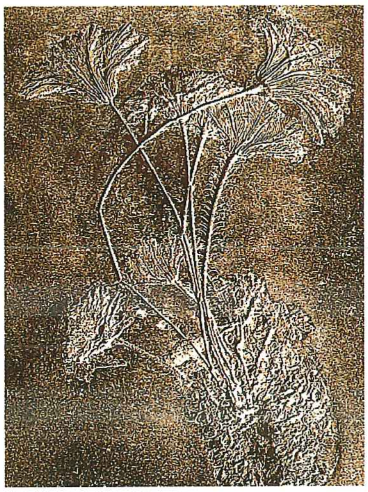

Fossil crinoid

Fossil calyx

Fragments of fossil stem

Fragments of fossil crinoid in limestone

Present day Calyx fragments

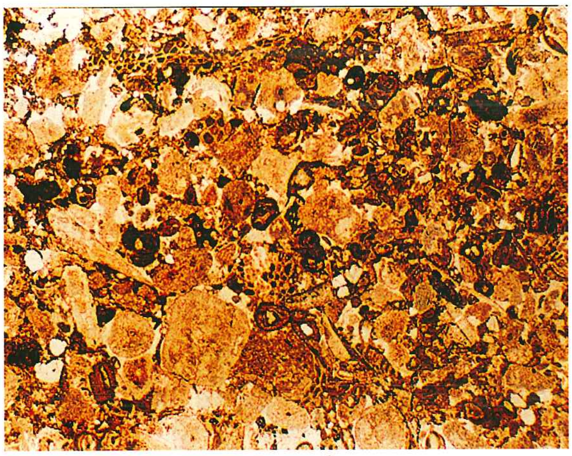

Facies F4 - Packstone-grainstone with bryozoans and crinoids

Cross-bedded festoons in crinoid limestone

Facies F5 - Bioclastic grainstone

A

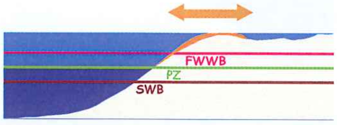

B

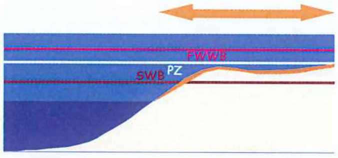

Bioclastic sand containing large benthic foraminifers, green algae, molluscs and fragments of corals can form a belt on platform margin.

Skeleton sand belt from the Belize barrier

Slab of bioclastic limestone (Lower Barremian limestone La Montagnette, Vercors)

Foreset bedding at the front of a sand bar (Barremian, Vercors)

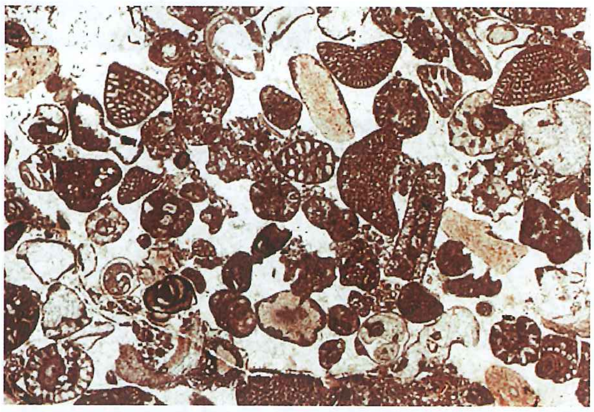

Bioclastic grainstone with large benthic foraminifers and green algae (Facies F5) Lower Barremian limestone - Vercors

Plate 18

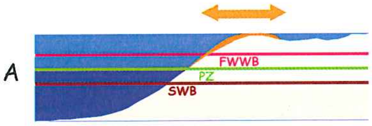

Facies F6
Oolitic grainstone

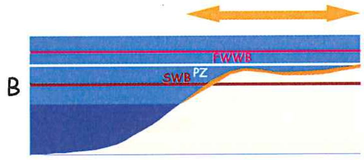

Detail of tidal bars rimming Exuma Sound (Bahamas)

Submarine photograph showing detail of the slope of a sand wave

Present day ooids from the Persian Gulf

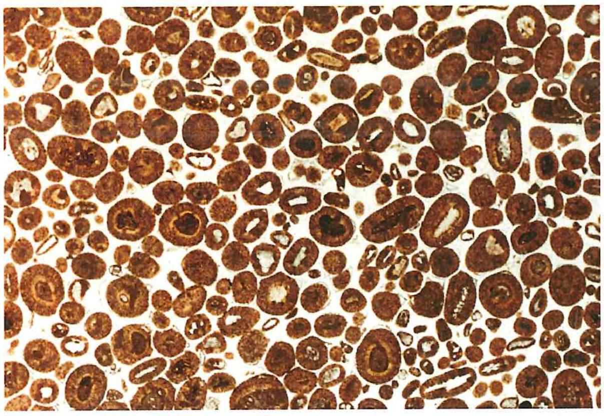

Oolitic grainstone
Facies F6

Slab of oolitic limestone

Plate 19 (Barremian limestone, La Montagnette, Vercors)

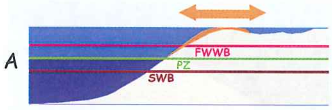

Facies F7 - Corals (1)

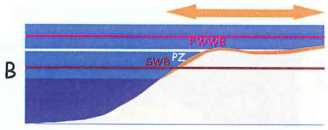

Corals and hard corals are the main reef builders. They live in colonies with Zooxantellae within animal's tissues. They obtain nourishment from photosynthesis where the energy of sunlight is use to convert carbone dioxide and water into carbohydrate and oxygen. Hard corals have usually an aragonite skeleton.

Reef flat and atoll (Maldivia)

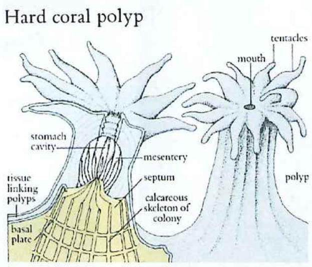

Favia

Types of skeleton

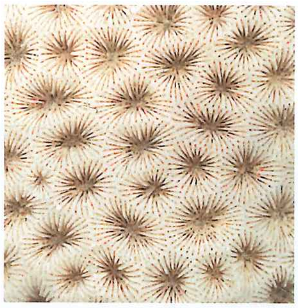

Forms and pattern of corals

Acropora palmata
(Caribbean)

Table and plate coral

Brain coral (Martinique)

Massive corals

Reef front exposed to the influence of winds and full ocean supports a coral community, which resists these forces

Acropora cervicornis
(Caribbean)

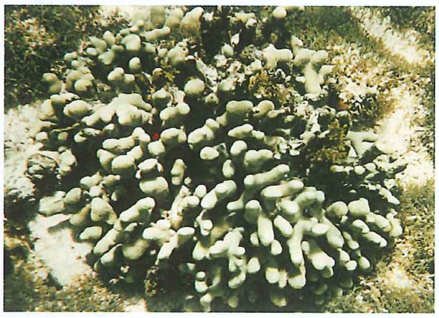

Pocillopora

Branching gives more access to space and allows all the polypes good exposure to the water currents carrying their food

Plate 20

A
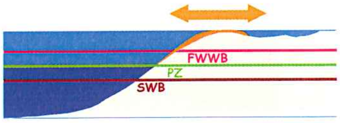

Facies F7 - Corals (2)

B
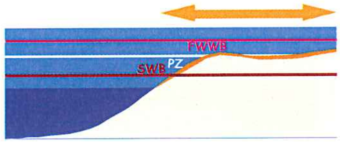

Fossil corals or present day corals show the same morphology if they are found in the same ecological niche

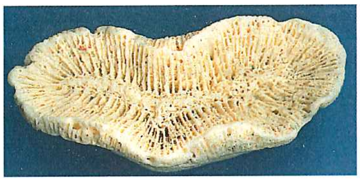

Present day coral Fungia

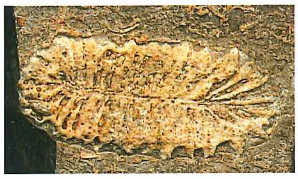

Late Jurassic coral from Slovenia

Isolated coral

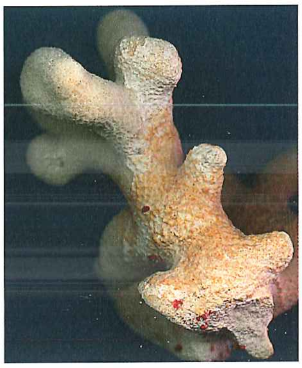

Skeleton of Pocillopora

Aptian form

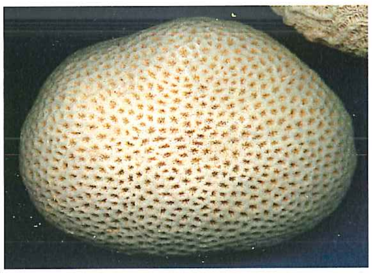

Present day coral - Pavona

Rounded coral

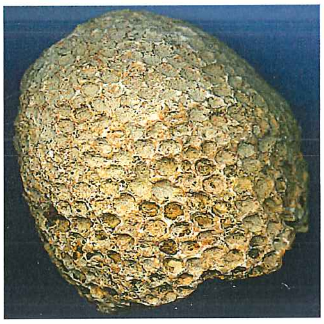

Aptian coral

Close view of the coarse coral-rich limestone

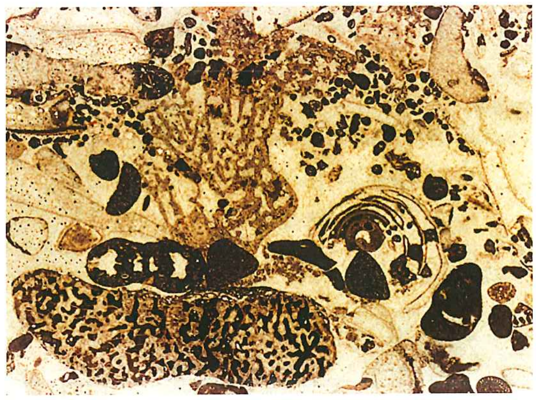

Grainstone rich in corals fragments

Facies F7

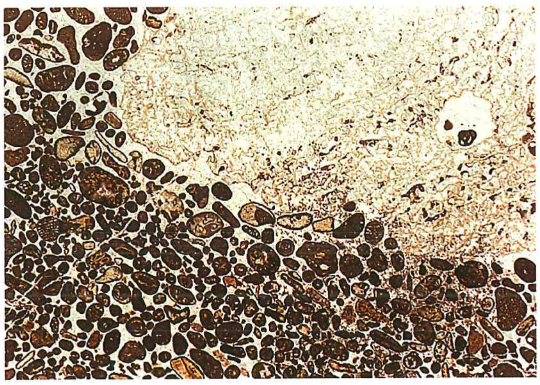

Common organisms: corals, calcareous sponges, large dasycladaceous algae, large foraminifera, fragments of molluscs

Plate 21

Facies F8 and F9 - Rudists (1)

Plate 22

Lizard Island (Australia)

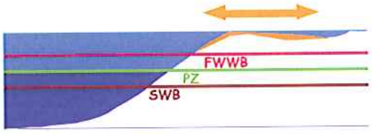

The rudists bivalves were one of the most important biotic constituents of Cretaceous carbonate platforms. They have usually one large valve attached to substrate while the other was a lid or cap.

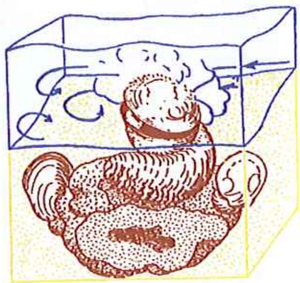

Living Chama (Gulf of Aqaba)
Spiral valve fixed to anchor and keeping aperture more or less parallel to bottom surface during growth

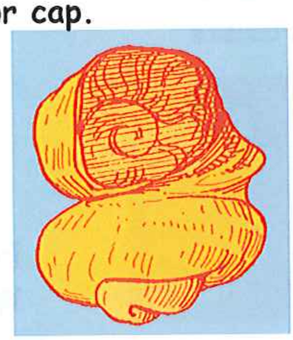

Requienia ammonia
(fossil analog to present day Chama)

Requienia ammonia
Dorsal side

Colony of Hippurites

Small rudists

Monopleura sp.

Monopleura varians

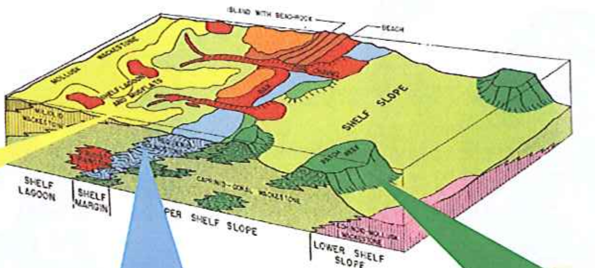

Large rudists

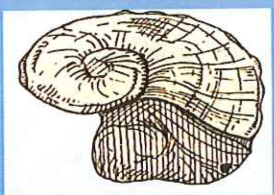

Toucasia carinata

Requienia ammonia

Monopleura varians

Colony of rudists

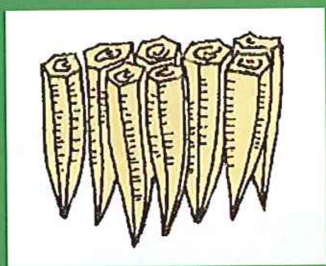

Agriopleura

Pachytraga

Canaliculate rudists

Facies F8 and F9 - Rudists (2)

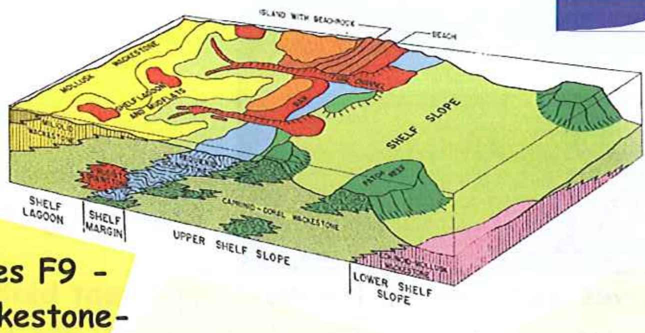

Facies F9 - Wackestone-packstone with small rudists

Small rudists

Facies F8 - Wackestone-packstone with large rudists

Large rudists

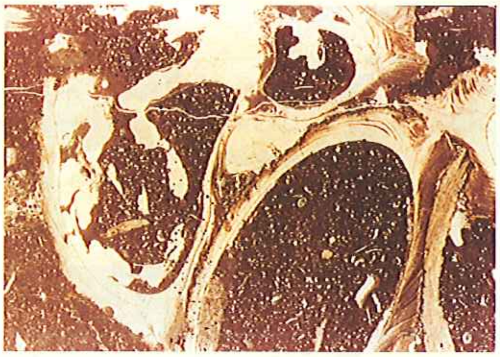

Colony of rudists

Canaliculate rudists

Plate 23

Plate 24 Lagoon - Bacteria

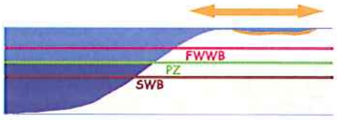

Grass bed vegetation helps stabilize sediment and reduce energy levels of the sediment-water interface. Such a situation promotes the accumulation of organic detritus derived from decaying vegetation and bacterial activity.

Guadeloupe Island - Lagoon of St François

Grains exhibit well-developed constructive and destructive micrite envelopes.

Destructive micrite envelopes

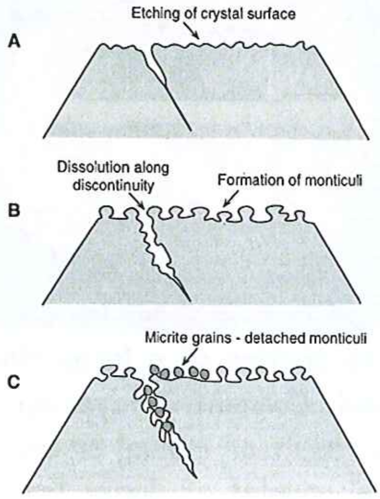

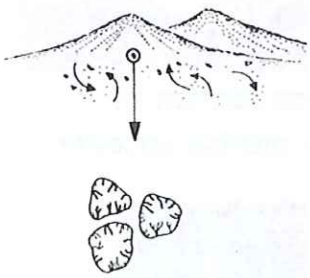

Destructive micrite envelopes develop. Deep sediment reworking prevents accumulation of organic detritus and associated biofilms on grain surfaces.

Constructive micrite envelopes

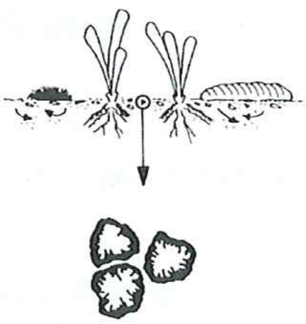

Biofilm comprising epilithic cyanobacteria, diatoms, bacteria and associated mucilage develops on grain surface. Thick constructive micrite envelopes form around grains.

Biofilm

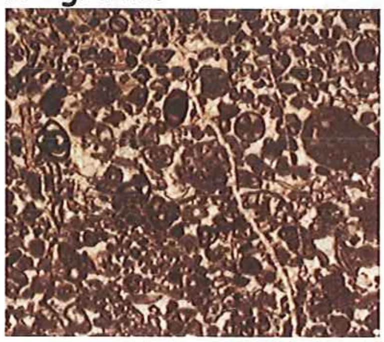

(after C. T. Perry, 1999)

Facies F10 - Inner lagoon: Oncoids-Oncolithes

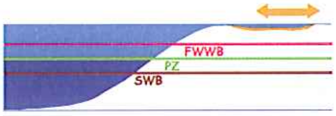

Green Lake, New York-USA

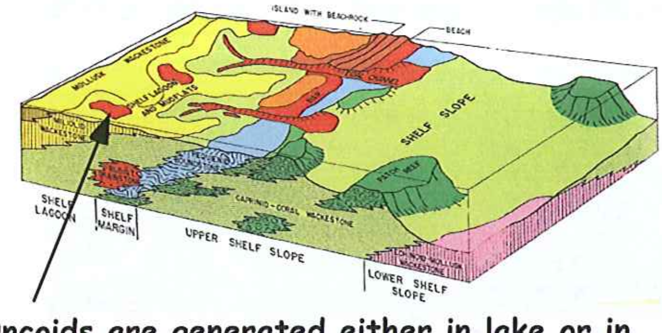

Oncoids are generated either in lake or in shallow-marine subtidal environmements.

The rate of bio-induced carbonate precipitation is greater in littoral zone.

Polished slab showing various sections of oncolites.
Urgonian limestone - Vercors

Cross section of a large marine oncolite

Cross section of a lacustrine oncoid. Concentric layering is the result of annual or seasonal couplet of dense laminae.

Large oncoid in thin section

Plate 25

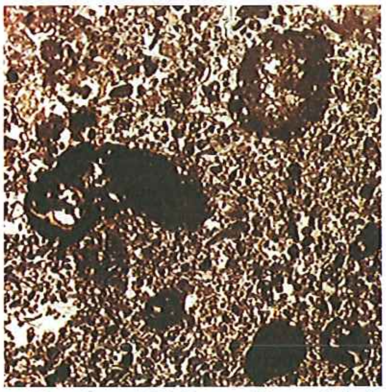

Facies F10 - Oncoidal packstone in thin section
Urgonian limestone - Vercors

(After Wilson, 1975)

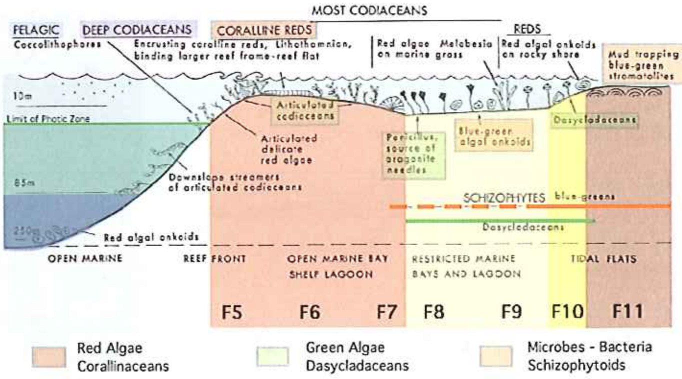

Facies F11 - Inner lagoon: Supratidal environment

Plate 26

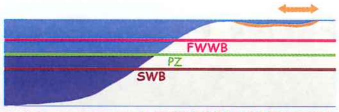

Mud cracks of the Oued Merguellil - Kairouan - Tunisia

Fossil mud cracks from lower Cretaceous carbonate platform of Dj Bou Rhazel - Algeria

Desiccation crack (arrow) in thin section - Barremian (Italy)

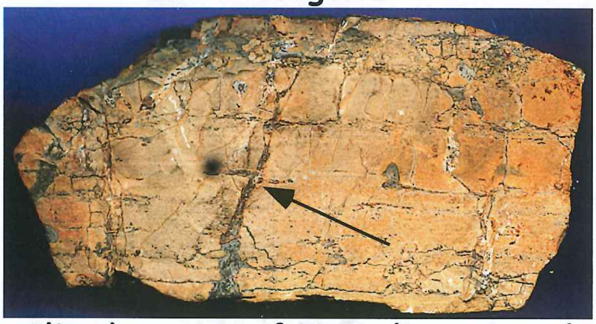

Sliced section of Trias limestone showing desiccation crack (arrow)

Slab of supratidal laminations showing flat pebbles (arrows). Lower Cretaceous - Italy

Escaping gas bubble in a Noirmoutier marsh

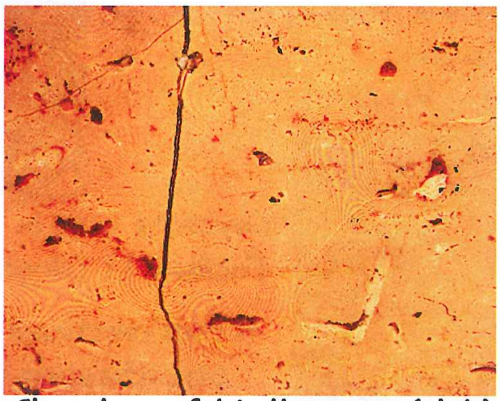

Closed up of bird's-eyes (slab)

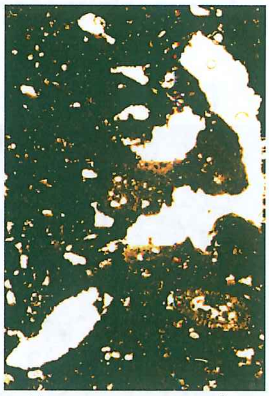

Bird's-eyes in thin section

Facies F11 - Beach

Plate 27

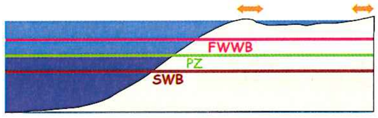

Yucatan beach (Mexico)

Well sorted and rounded medium sized grains (Sunset beach - Honolulu)

Air-bubble holes in uppermost part of swash zone (Island of Noirmoutier)

Air-bubble holes in the uppermost part of swash zone - cross-sectional view of beach (Yucatan, Mexico)

Large elongated keystone vugs in slab of grainstone (Urgonian limestone - Vercors)

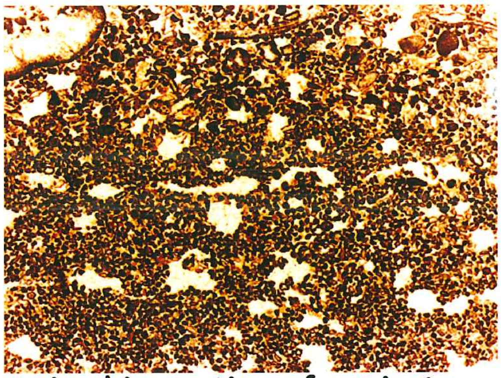

Keystone vugs in thin section of grainstone Facies F11 (Urgonian limestone - Vercors)

Cross-sectional view of Hummocky Cross Stratification (HSV) (Hauterivian lime-stone La Chambotte - Jura)

Facies F11 Beachrock - Storm deposit

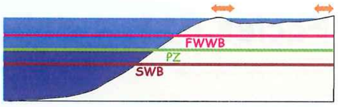

Seaward dipping slabs of recent beachrock cemented foreshore sediment (St Barthelemy, West Indies)

Beachrock (Great Barrier Reef, Australia)

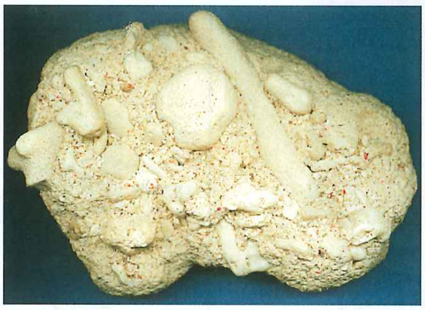

Recent cemented coral rubbles (Lady Elliot Island, Australia)

Pelecypod shell accumulation during storm (Noirmoutier Island)

Coral rubble beach (Wilson Island, Australia). Coral rubbles are accumulated during high-energy storm activity.

Detail of gastropod accumulation (Urgonian limestone - Vercors)

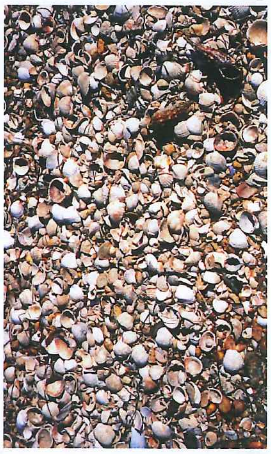

Storm accumulation of shells (Noirmoutier island)

Plate 28

Meniscus cement in Holocene eolianite (Yucatan, Mexico) Bar scale 200μ

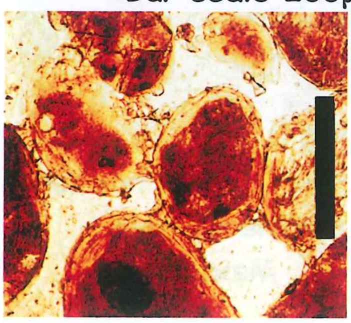

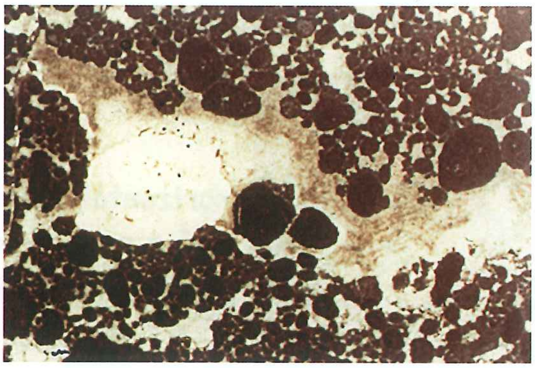

Microstalactitic cement (= asymetric cement) in fossil beachrock (Urgonian limestone - Vercors)

Facies F11 - Subaerial exposure: Soil - Caliche

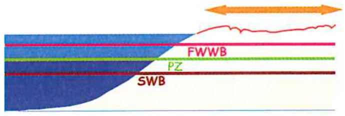

Plate 29

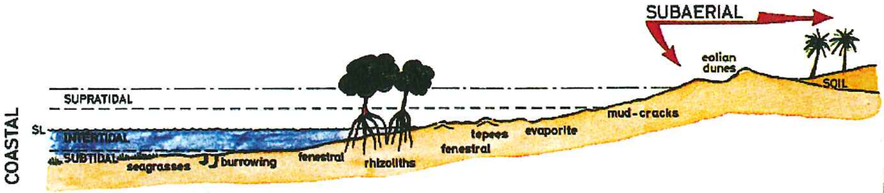

Schematic cross-section of coastal exposure surface (Esteban & Klappa, 1983)

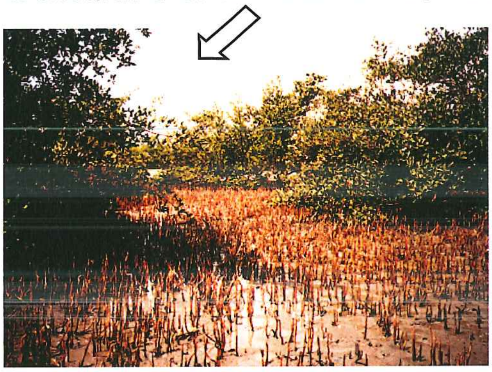

Mangrove and pencil roots (Martinique, West Indies)

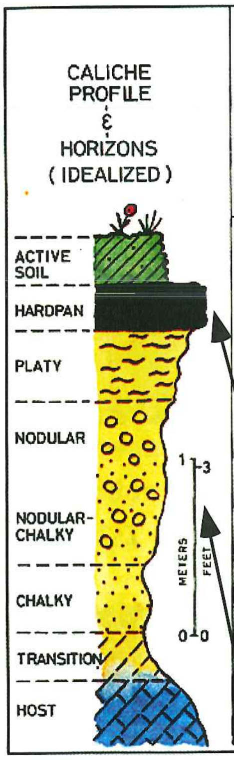

Idealized caliche profile (Esteban & Klappa, 1983)

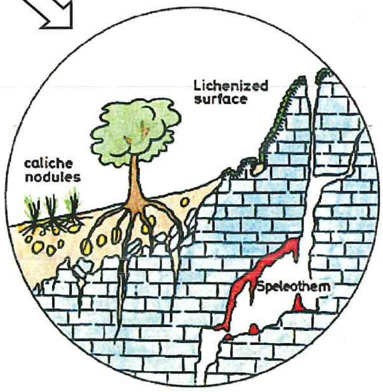

Caliche facies (Esteban & Klappa, 1983)

Root molds on top Miocene limestone (Mallorca, Spain)

Laminar caliche hardpan (Pliocene, Florida)

Root molds in Berriasian limestone (Jura)

Nodular caliche horizon (Eocene Chiapas - Mexico)

Horizontal section of a root mold (Berriasian, Jura)

Vertical section of a root mold showing various infilling

Facies F11 - Subaerial exposure - Karst

If subaerial exposure surfaces are exposed long enough, surfaces represent a diagenetic environment rather than a depositional one.

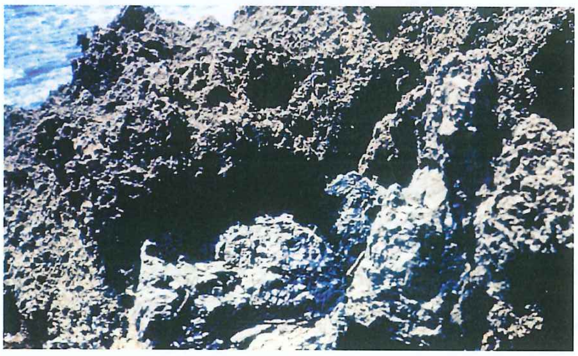

Littoral karst (St. Domingo, West Indies)

Fossil karst and terra rossa (Pleistocene, Mexico)

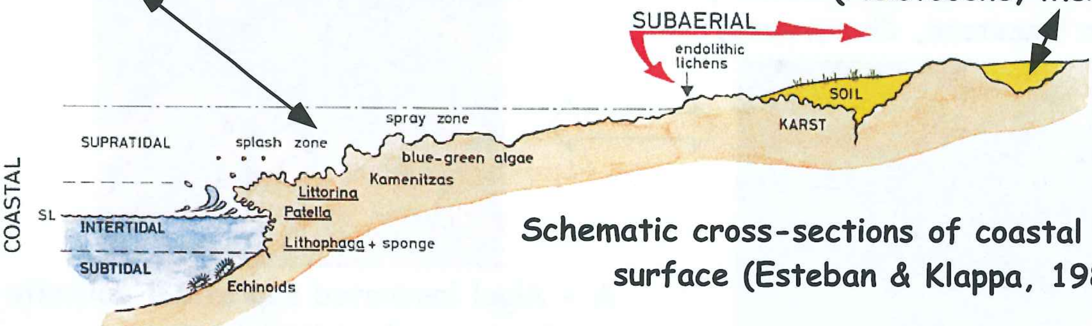

Schematic cross-sections of coastal exposure surface (Esteban & Klappa, 1983)

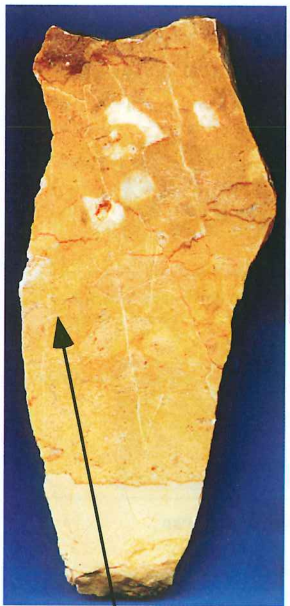

Early dissolution of the aragonite part of the rudist shell. Voids are filled with a red dolomitized micrite - Vercors

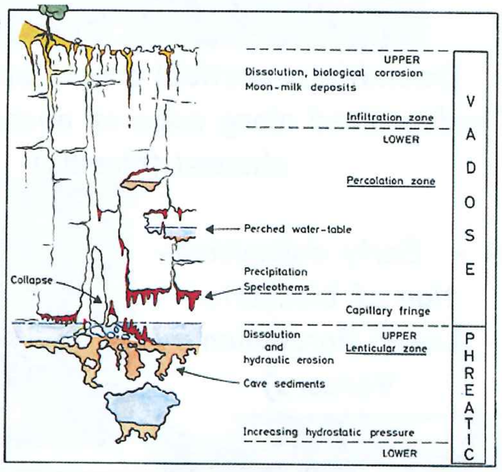

Idealized authigenic karst profile (Esteban & Klappa, 1983)

Fossil microcaves from littoral karst filled by dolomitized sediment - Gorges du Nant - Vercors

Fossil microcaves and laminated sediment - Early Aptian - Vercors

Plate 30

Fossil speleothem in lower Aptian microcave - Vercors

Early diagenesis: dolomitization - dedolomitization

Plate 31

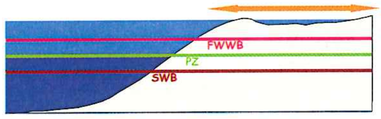

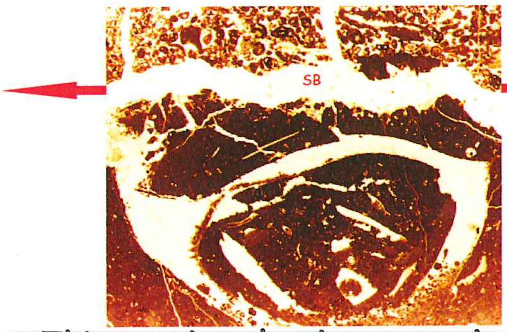

Thin section showing an ancient dissolution surface (= SB A1). Void in pelycipod shell created by dissolution is filled with sediment lying above the sequence boundary (Urgonian limestone, Chartreuse)

Humid climate, late HST to LST

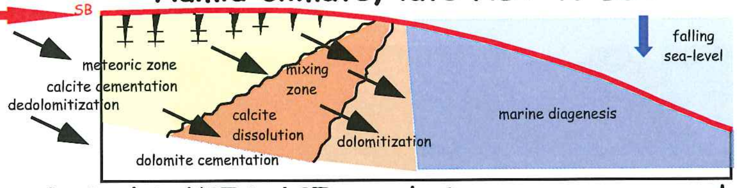

During late HST to LST groundwater zones move seaward dolomitization followed by meteoric diagenesis

Models for dolomitization showing migration of waters during lowering of sea-level (Purser, Tucker & Zenger, 1994)

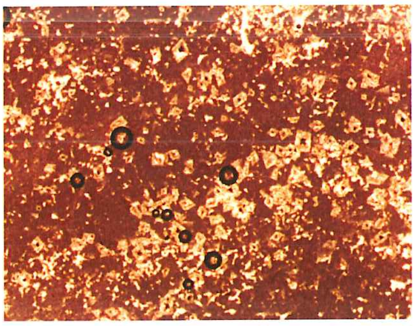

A - Algal laminated supratidal dolomite - early dolomitization (Urgonian limestone, Vercors)

Dolomitic supratidal crusts eroded and redeposited along edge of abandoned tidal channel (Florida)

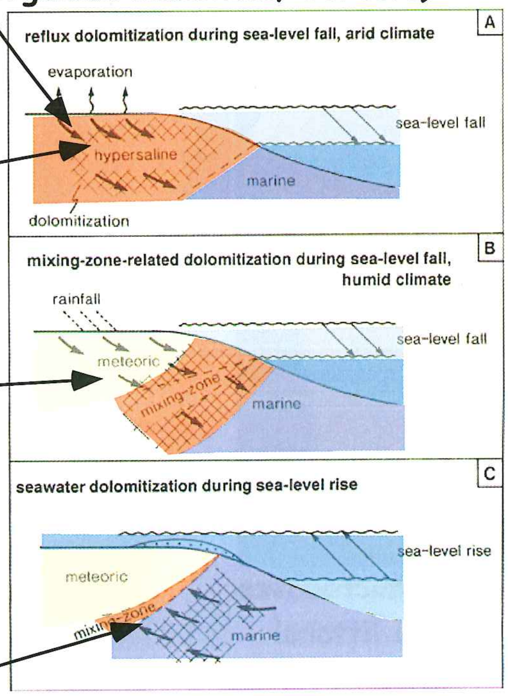

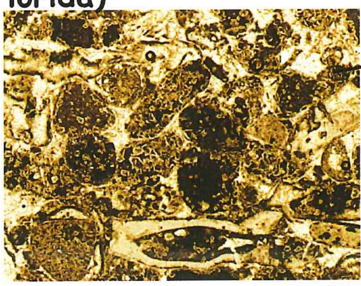

A - Early dolomitization of bioclasts (Lower Barremian, Vercors)

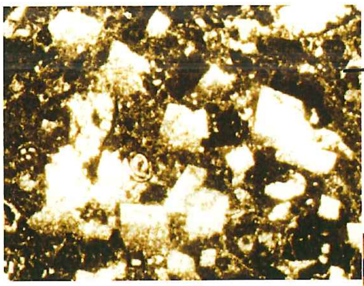

B - Dedolomitization (Urgonian limestone, Vercors)

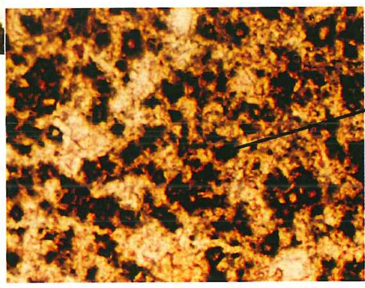

C - Secondary dolomitization following rising of sea-level (Urgonian limestone, Vercors)

Models for dolomitization induced by relative changes in sea-level (Purser, Tucker & Zenger, 1994)

Transgressive facies

Plate 32

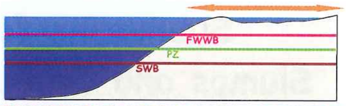

Shoaling- upward parasequence beginning with an erosive base which is overlain by reworked bioclastic sand - Lower Aptian TST in Urgonian limestone, Vercors

Lag with bored, worn and incrusted clasts can exist at the base of TST

Bioturbated various lithologies can be observed at the base of TST - Berriasian - La Chambotte, Jura

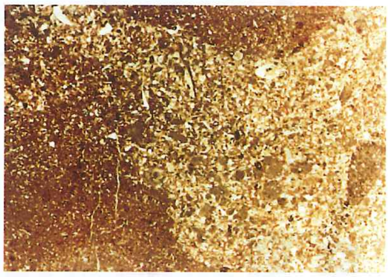

Bioturbation mixing two facies showing more than 50% reworked micritized grains.
Berriasian - La Chambotte

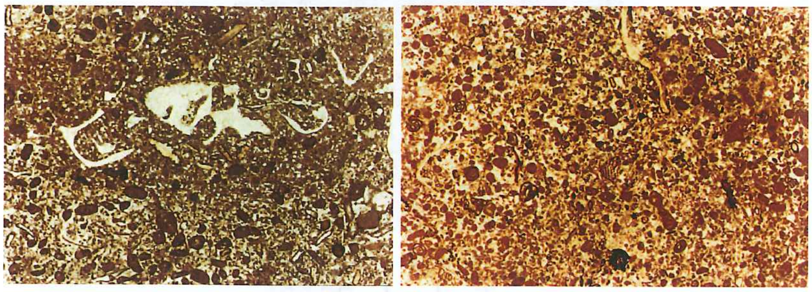

Bimodal grainstone with fine-medium grained bioclasts and larger fossil fragments associated to oxidized-micritized fossil grains (Urgonian limestone, Nant, Vercors)

Present day hard gound Long Island, Bahamas

Facies in TST: lower Aptian nodular bedding in Orbitolina wackestone, Vercors

Hardground is common in TST (Persian gulf)

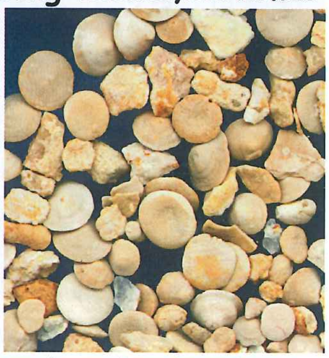

Isolated orbitolines "Couches inférieures à Orbitolines"-Vercors (early Aptian)

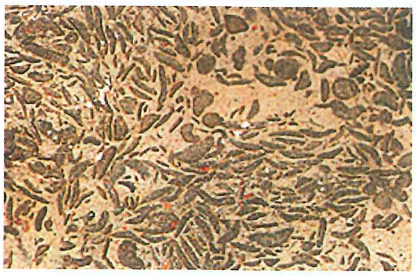

Orbitolina packstone (Mexico - Albian)

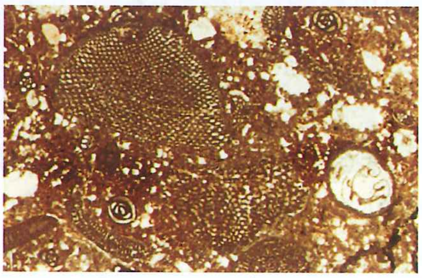

Lower Aptian wackestone with abundant orbitolines and green algae (TST Vercors)

Submarine fans
Slumps and debris flows

Plate 33

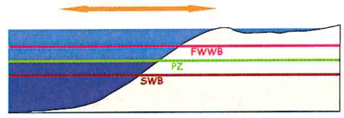

Barremian slump scar
Col de Menée - Vercors

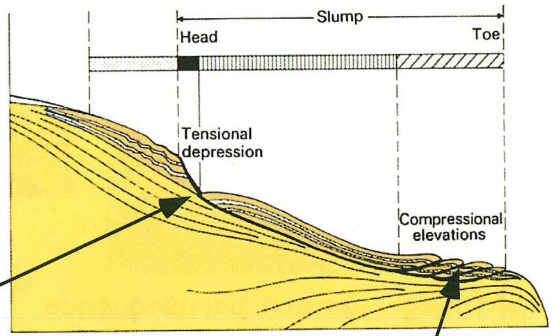

Cross section of a large submarine slump (from Lewis, 1971)

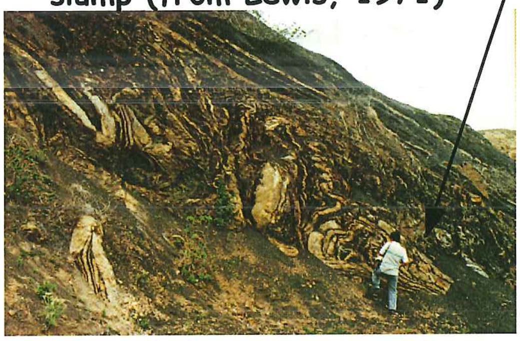

Miocene slump -Ecuador (from Jaillard, 2003)

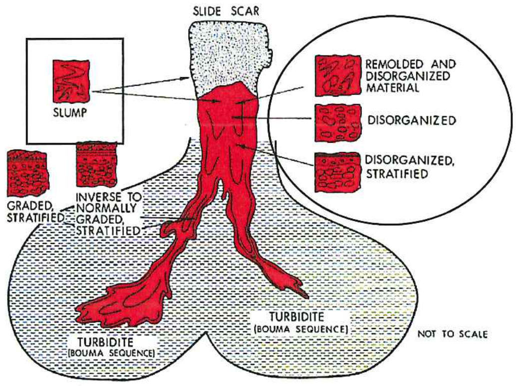

Sediment gravity flow model (from Krause and Oldershaw, 1979)

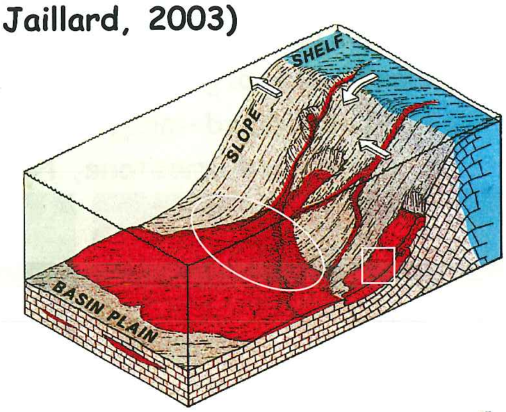

Model of interpreted shelf-slope-basin plain transition. Slope is incised by numerous gullies and a submarine fan develops at base of slope and basin plain (from Cook and Egbert, 1981)

Barremian debris flow with large limestone clasts interbedded with black marls (Col de La Chaudière, Drôme)

Texture of a middle Devonian debris flow deposit - circle 2cm (from Cook, 1983)

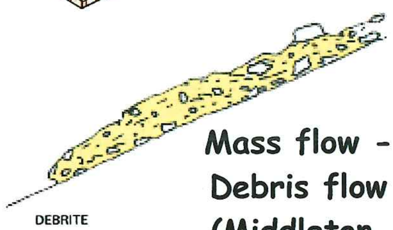

Mass flow - Debris flow (Middleton, 1969)

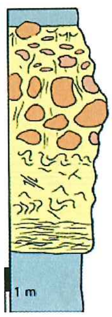

Idealized sequence of debris flow (Reading, 1986)

Submarine fans
Overbank deposits, Turbidites, Grain flows

Plate 34

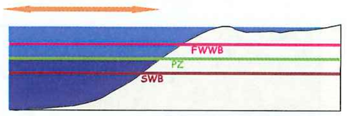

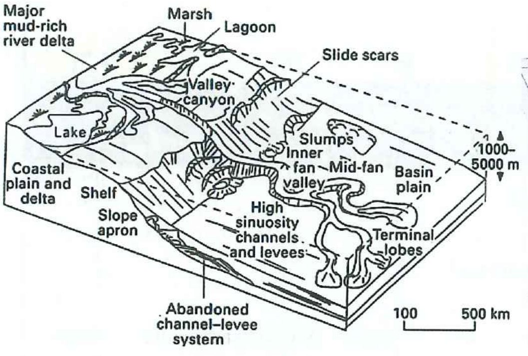

Depositional model for mud-rich submarine fan showing channel and levee system (Reading, 1996)

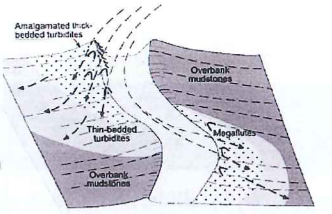

Channel and overbank mudstones (Walker and Martinsen, 2003)

Barremian fine-grained laminated limestone interpreted as overbank deposit (Col de Menée, Vercors)

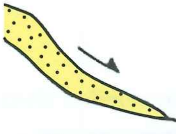

Grain flow (Reading, 1978)

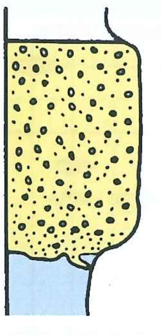

Idealized grain flow sequence showing injection structures (Cook and Mullins, 1983)

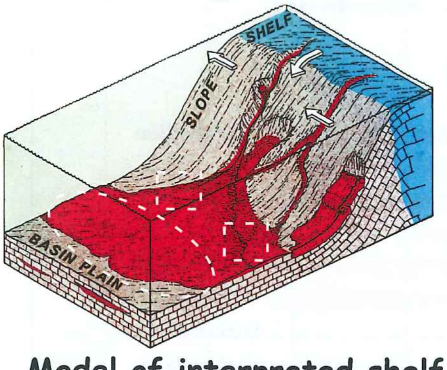

Model of interpreted shelf-slope-basin plain transition. Fan develops at base of slope and basin plain (from Cook and Egbert, 1981)

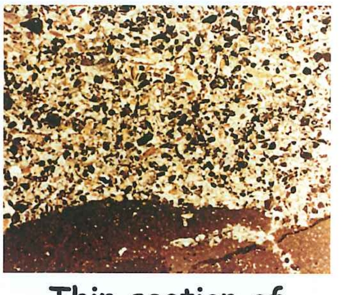

Thin section of Barremian grainflow showing injections (col de Menée, Vercors)

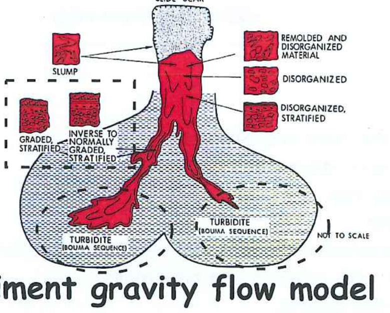

Sediment gravity flow model (from Krause and Oldershaw, 1979)

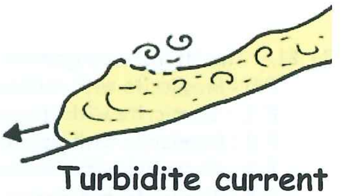

Turbidite current (Reading, 1978)

Upper parallel laminations and convolute laminations (top of turbidite) Miocene - Peru (Jaillard, 2003)

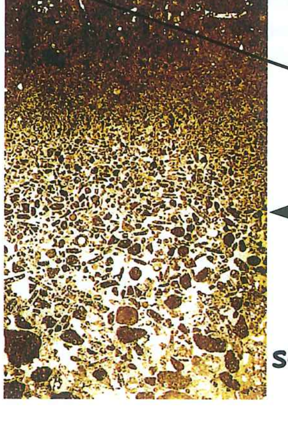

Thin section showing normally graded turbidite (basal part of turbidite)

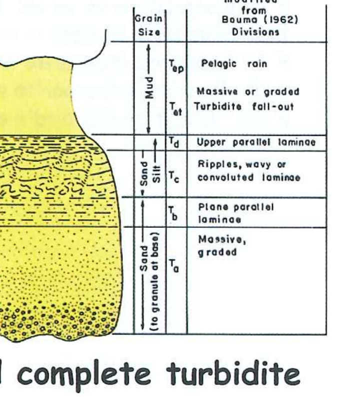

Idealized complete turbidite sequence (Howell and Normark, 1982)

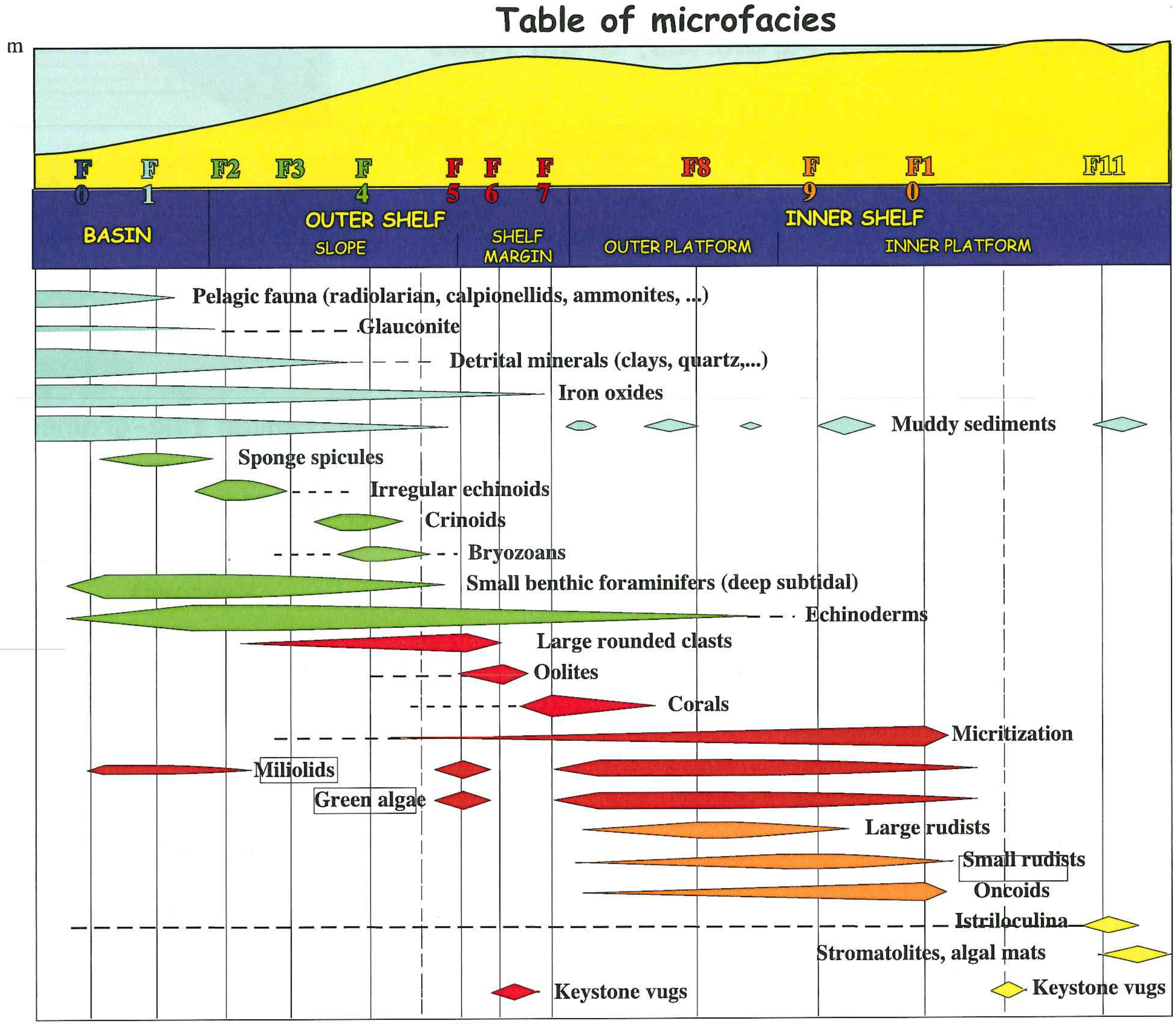

Fig. 21.- The lateral arrangement of the main microfacies.

F 0 : Biomicrite with radiolaria and calpionelids.
F 1 : Biomicrite with sponge spicules.
F 2 : Biomicrite with Spatangidae.
F 3 : Biosparite with rounded echinoderm debris and small foraminifera.
F 4 : Biomicrite and biosparites with crinoids and bryozoans.
F 5 : Biosparite with large rounded debris.
F 6 : Oosparite.
F 7 : Biosparite with corals; Boundstones.
F 8 : Biomicrite-biosparite with large foraminifera, sometimes accompagned by large-sized rudists.
F 9 : Biomicrite-biosparite with Miliolidae and rudists.
F 10 : Biomicrite-biosparite with oncolites and *bacinella*.
F 11 : Micrites with bird's eyes; emersion facies.

Diagenesis in carbonate rocks: Relations with sequence boundaries in a sequence stratigraphic framework.

Elisabeth Carrio-Schaffhauser

In carbonate platforms, the diagenesis is particularly complex beneath sequence boundaries according to the chemical properties of the carbonate minerals. Sequence boundaries are related to major unconformities due to regional uplift and/or 3rd order sea level and correspond to long-lived subaerial exposure. Diagenesis related to sequence boundaries could extend one to tens of meters down. Importance and duration of long term sea level falls induce distinctive diagenetic inprints and porosity type and distribution which can be distinguished from those developed during short term sea level falls. Size and property of reservoirs should be associated to magnitude of sea level fluctuations (eustasy), climate (environment), tectonics (tectonic subsidence, uplift and fracture joints) and time.

During very low sea level periods, subaerial diagenesis can also affect the top of the prograding sequences of the lowstand systems tracts (fig. 22), so inducing reservoir properties mainly by solution and dolomitisation (Tucker, 1990 and Moore, 2001).

Many examples are showing here in well-studied surface exposures from the Lower Cretaceous platform of the Southeastern France: the Urgonian platform from Vercors, France.

Among them, four type of reservoirs will be presented in this book.

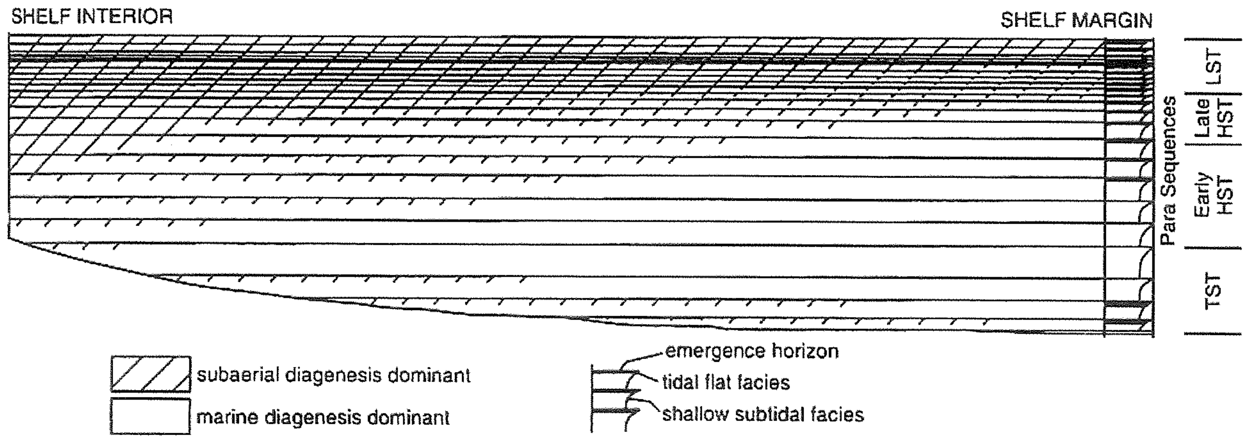

FIG. 22.- *General scheme showing lateral and vertical diagenetic evolution affecting the parasequences of the differents systems tracts in a carbonate platform. Subaerial diagenesis mainly concerns the late HST, the sequence boundaries and the prograding part of the LST (Moore, 2001).*

1.– Sequence boundary SbB4 (Gorges du Nant, Vercors and Pic de l'Oeillette, Chartreuse)

This sequence boundary is associated with an early karstification, dolomitization and dedolomitization processes (Plate 35). A thick, dolomitized interval (up to 7 m) is developed (mixed water dolomitization) above an unit of fine-grained grainstones with keystone vugs (beach record). Interconnected microcavities (mm to cm in size) of Barremian age with bedded infillings are observed in the dolomitized matrix.

Karstification, however, developped later in response to major drops of sea level during the Cenomanian and Turonian (due to the ante-Senonian folding). The resultant cavities are meter high and have a stratigraphic pattern along the sequence boundary. The cavity-filling deposits consists of white, fine grain sand with silicified bryozans and a few foraminifers of late Turonian-early Senonian age and red clays. This type of reservoir is a secondary reservoir. If it is associated with sequence boundary SbB4 in the inner part of the platform, it originated later during the Cenomanian to Turonian fluctuations in sea-level. In the Vercors massif, the ante-Senonian folding is responsable to a major emersion during the early Turonian.

In the Chartreuse massif, the same sequence boundary shows differents marks according to the fact that it developes in a differents carbonate facies. In the Pic de l'Oeillette site, emersion affects an oolitic grainstone (Plate 36) and is attested by paleosoils marked by root molds with pedogenetic calcite and dolomitization associated to organic matter. So, we can observed the developement of vuggy and moldic porosity affecting cements and oolitic cortex. As in the Gorges du Nant, karstic cavities developed later on this particular level.

2.– Sequence boundary SbB5 (Gorges du Nant, Vercors)

An early dissolution of low magnesium tests of foraminifers (mostly miliolids and orbitolinids) occurs below this sequence boundary. This dissolution was subsequent to the very early diagenesis that produced both the early dissolution of aragonite tests and the calcite replacement. In Chartreuse where this type of reservoir is well developed (Plate 37), calcitized tests of former aragonitic taxa (trocholines, dasycladal algae) are well preserved and never display voids. In contrast, miliolid tests are very often totally dissolved and filled by asphalt. This latter type of dissolution seems associated with a vegetal cover and the early production of humic acid. We have observed that green marls which are generally associated with a vegetal cover have been found in small cavities at the top of parasequences.

The reservoir has a stratigraphic pattern and the porosity is responsible for the very porous limestone that sometimes is transformed of powdery limestone.

3.– Sequence boundary SbA1 (Gorges du Nant and Balcon des Ecouges, Vercors)

Two particular porous levels appear beneath the SbA1 emersive sequence boundary with green marls and calcretes. Two to three meters thick, they display a chalky facies inducing a high porosity, up to 16%. This non-selective porosity concerns the cements as well the bioclasts or the micritic grains (Plate 38). These two levels are also marked by sharp variations of the $d^{18}O$ and the $d^{13}C$. In spite of the lack of classic meteoric features as meniscus or microstalagtitic cements, we can propose the hypothesis of a local floating meteoric water lens in an hydrologic setting of an island. During this period, active tectonic of tilted blocks seems to create in the Vercors an archipelago of islands along the top of the blocks. The tropical climate can induce the presence of meteoric floating lens that can range in size from less than 5 m to over 15 m, as in the Bahamas (Budd, 1984). So, dissolution of metastable carbonate components of the vadose zone leads input from high CO_2 soil gases and undersatured waters.

4.– Sequence boundary SbA2 (Les Rimets incised valley and the Achard syncline, Vercors)

The rate of sea-level changes and the duration of stillstands at each sea-level position control both the distribution and the type of karst facies. At the beginning of sea-level fall, carbonates are early and partly cemented, hence a superficial epikarst can develop small sized centimetre to decimetre microcaves resulting either from marine bioerosion (gastropods, bivalves, blue-green algae...) or early meteoric dissolution-enlarged, pre-existing porosity (shell molds, root molds, bioturbations, fractures...). These primary microcaves will be enlarged by the development of karstification. Nevertheless a few of them can be preserved and record later changes in sea level as well in complex cavity fills as phases of dissolution and cementation. The process is available only for isolated centimetre scale microcaves if the same sequence boundary is used later as "intraformational unconformity", which controlled the development of vertically and laterally extensive karst porosity such as caves, caverns and dissolution enlarged fractures and faults.

This method was successfully applied on several Jurassic and Cretaceous microcave fills. The most significant example corresponds to 5 to 7 cm size microcaves that developed on the top of lower Aptian carbonate platform of Vercors massif (France) and then were episodically and partially filled up to Late Albian. It allows us to characterise up to 30 various diagenetic phases extended on 15 MY, showing up to 4 fall and rise of sea levels attested by paleontologic, sedimentologic and diagenetic data.

After the deposition of the last shallow-water carbonates of the Urgonian platform, successive sea level falls induced a karst development whose only small-sized cavities and fissures are still preserved. So appears a succession of cavity-filling deposits separated by erosion surfaces, evidences of 4 sea-level fall and rise cycles (Plate 39).

The first fall in sea level, linked to the earliest karstification, is early Aptian in age (Bedoulian), induced the emergence of the top of the cretaceous platform and produced incised valleys like the Rimets in Vercors Massif whose the depth implies that there was at least 50 to 60 m fall in sea level. The first transgression corresponds to the Upper orbitolina marls (*Palorbitolina*) at the top of the early Aptian. The second sea-level fall probably occurred during Late Aptian and is attested by the presence of green marls. The second transgression occurred during Gargasian (Late Aptian), but was only recently identified on outcrop (the Jarrands section). It is recognised by a brown, brachiopod-bryozoan wackestone-packestone and called "First Lumachelle." So, during a long time, these "Lumachelle" infilling was the only witness of the Gargasian deposits on the Urgonian surface. The third fall in sea level is stratigraphically located at the Gargasian – Clansayesian boundary, near the top of Aptian, caracterized by new karstification processes and followed by the third transgression deposits represented by the "Second Lumachelle", crinoid-bryozoan packstone-grainstone rich in glauconite and quartz. Two specific levels of sanstone and pure crinoid grainstone described in the Jarrands section are well preserved in these microkarstic caves. The last cycle of sea level change is associated with the major fluctuations in sea level that occurred during the Cenomanian to Turonian. The sea level fall is attested by the presence of a vegetal cover (root molds and pedogenetic calcite *Microcodium*). This Albian - Turonian event is probably tectonic in origin and linked with the ante-Senonian folding. The further transgression is revealed by the presence of small foraminifers (Discorbids) trapped in the voids formed by roots.

5.– Reservoirs developed during lowstand systems tracts (LST) periods

After Tucker, 1990, subaerial diagenesis responsible of many resrvoir development in carbonate rocks affects mainly the upper parts of the platform interior sequences deposited during the 3rd order sea level cycle. During the sea level fall, parasequences of the late HST and sequences boundaries are concerned by this subaerial solution. But, parasequences of the LST may be severely affected by chemical modifications due to emersion, so showing development of reservoir properties.

At the Fontaine des Prêtres, Vallon de Combau, South of the Vercors massif, we can observed this type of reservoir with development of dolomitization, major porosity, emersion being attested by the presence of stalatitic cements (Plate 40).

Selected references

BUDD, D.A. (1984).– Freshwater diagenesis of Holocene ooid sands, Schooner Cays, Bahamas. Dissertation, The University of Texas/Austin, Texas, 491 p.

MOORE, C.H. (2001).– Carbonate reservoirs – Porosity evolution and diagenesis in a sequence stratigraphic framework, Developments in Sedimentology, 55, Elsevier, 444 p.

TUCKER, M. E. & WRIGHT, V.P. (1990). Carbonate Sedimentology. Oxford, Blackwell Scientific Publications, 482 p

SbB4 Sequence boundary - The Gorges du Nan
An example of early karstification and mixing zone

Hurghada, Red Sea

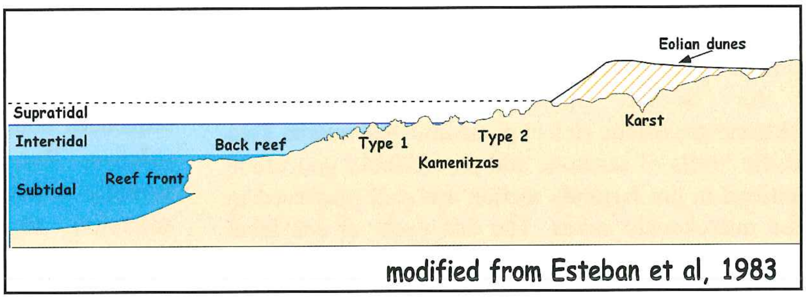

modified from Esteban et al, 1983

Plate 35

Subaerial exposure surfaces can occur on shallow marine carbonate platform. But, only sequence boundaries associated to wet climate, long enough time exposure and significant fall of sea level promote no-deposition, commonly erosion and diagenetic processes originating karst facies.

The rate of sea-level changes and the duration of stillstands at each sea-level position control both the distribution and the type of karst facies. At the beginning of sea-level fall, carbonates are early and partly cemented, hence a superficial epikarst can develop small sized centimetre to decimetre microcaves. These microcavities result either from marine bioerosion (gastropods, bivalves, blue-green algae,Ö) or early meteoric dissolution-enlarged, pre-existing porosity (shell molds, root molds, bioturbations, fractures,Ö). These primary microcaves will be enlarged by the development of karstification.

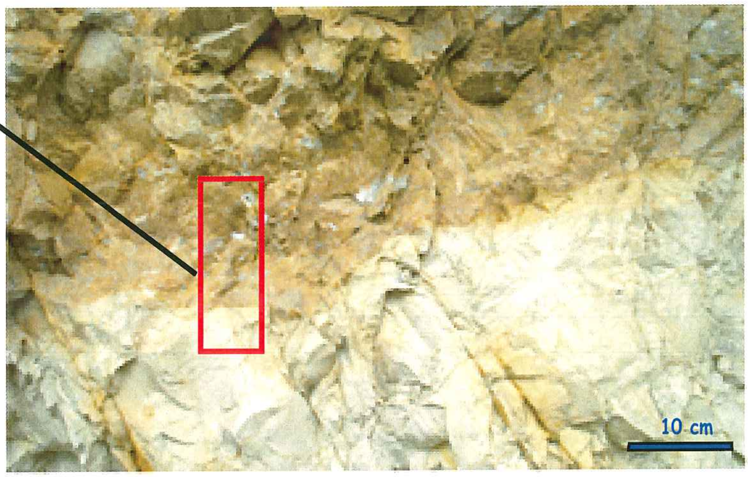

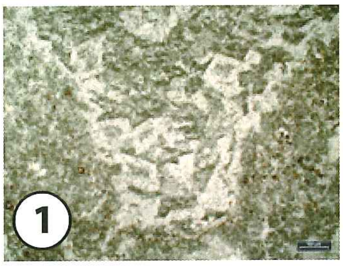

Microcave infilling

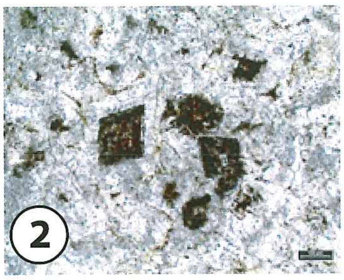

Ankerite development

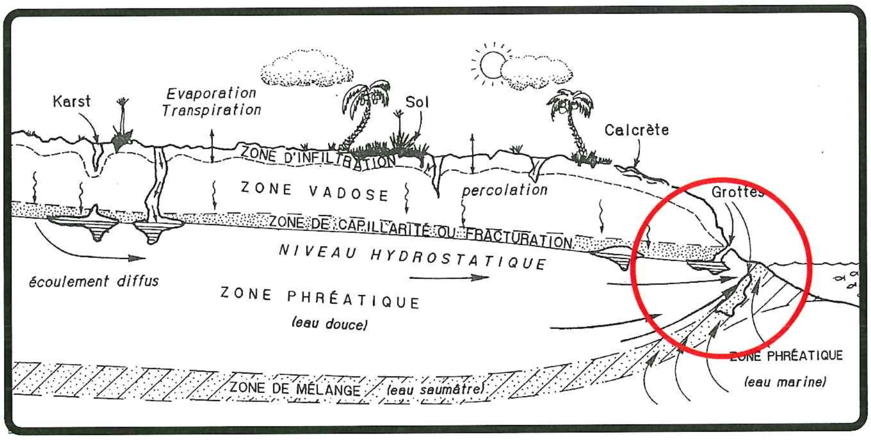

Relations Karstification / Mixing zone

Plate 36 SbB4 Sequence boundary - The Pic de l'Oeillette (Chartreuse massif) Development of vuggy and moldic porosity

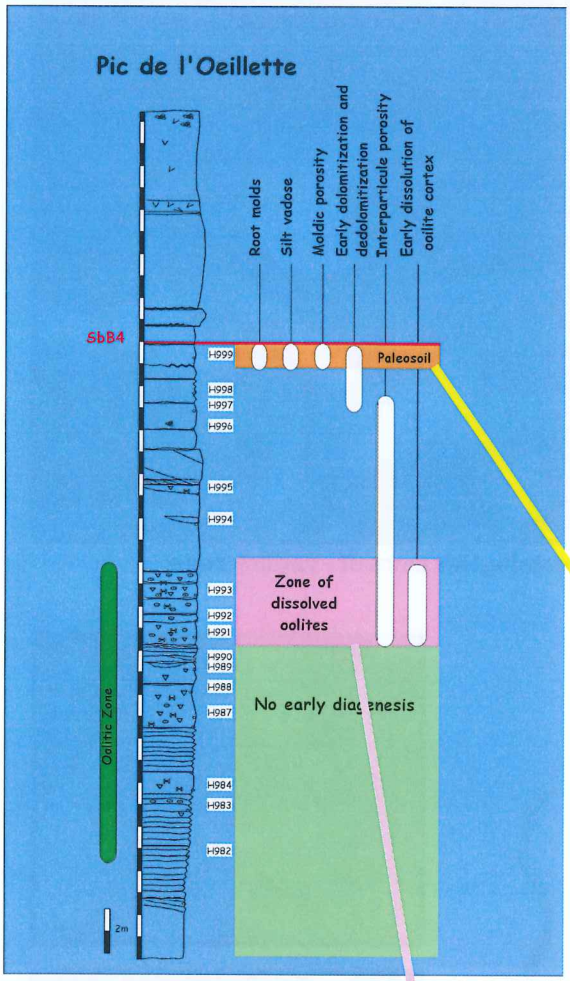

Pic de l'Oeillette, Chartreuse

Fronts of dolomitisation

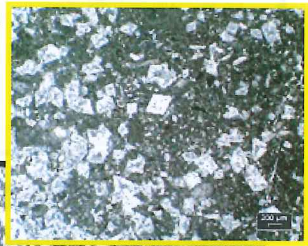

Paleosoil and root molds

Pedogenetic calcite

Cement and oolite solution

SEM view of the leached oolitic carbonate

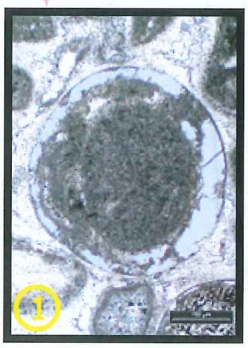

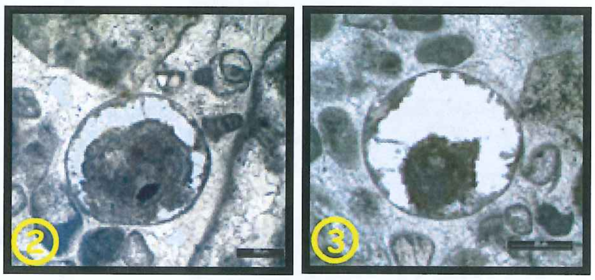

Successive stages of oolite solution

Plate 37 SbB5 Sequence boundary - Gorges du Nan
Development of moldic selective porosity

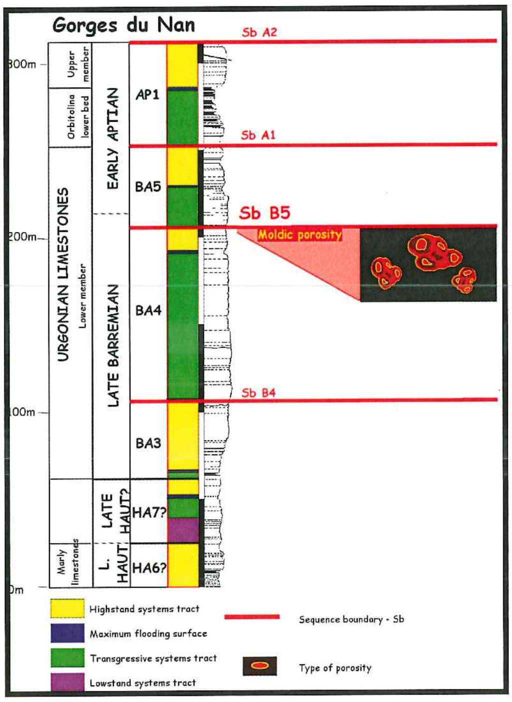

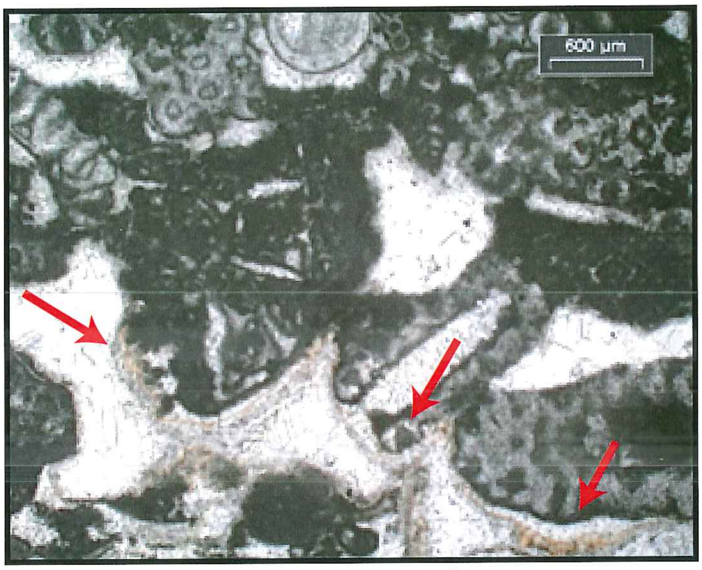

Microstalagtitic cement - Vadose zone

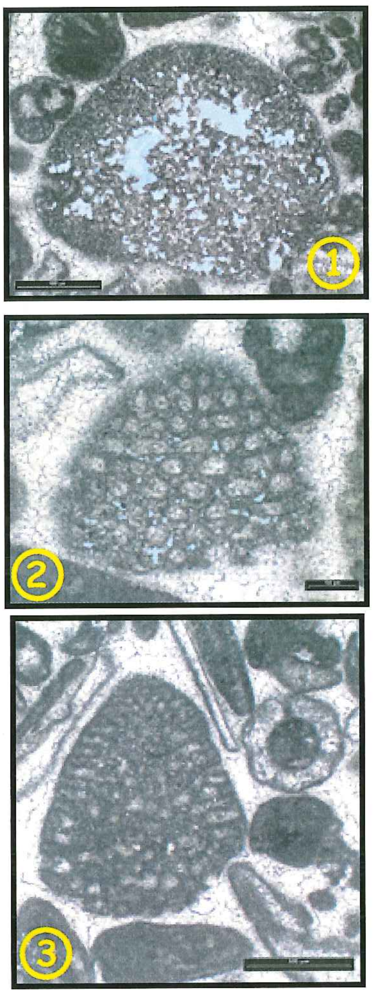

Moldic porosity in Orbitolina

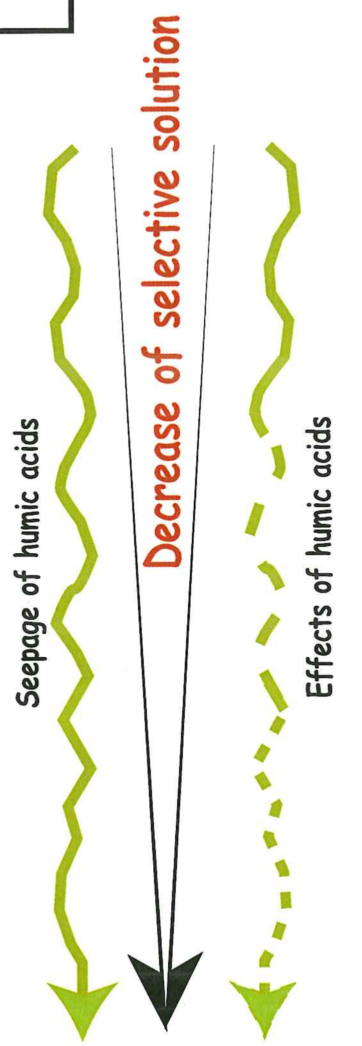

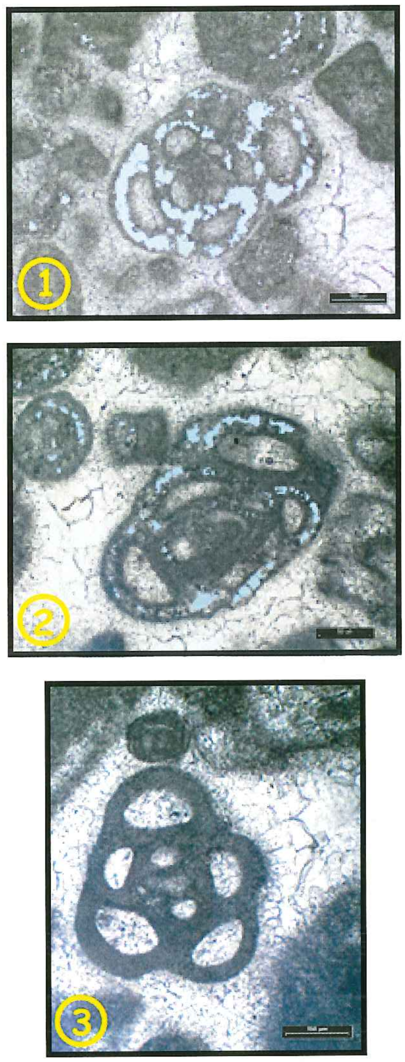

Moldic porosity in miliolide tests

SbA1 Sequence boundary - Balcon des Ecouges
Development of high porosity levels

Beneath the SbA1 sequence boundary appear two particular porous levels that could be associated to vadose zones developed in an hydrologic setting of island according to the sedimentologic, diagenetic, isotopic data.

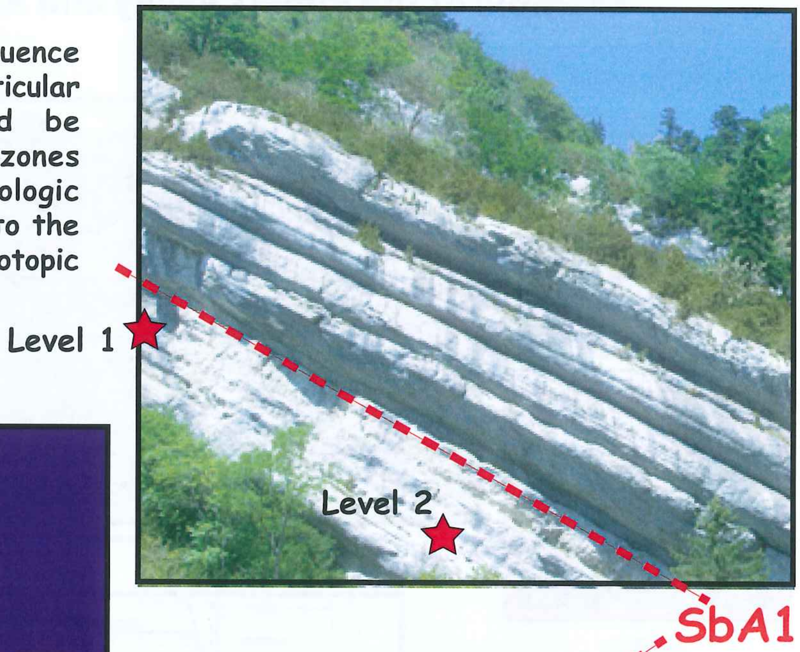

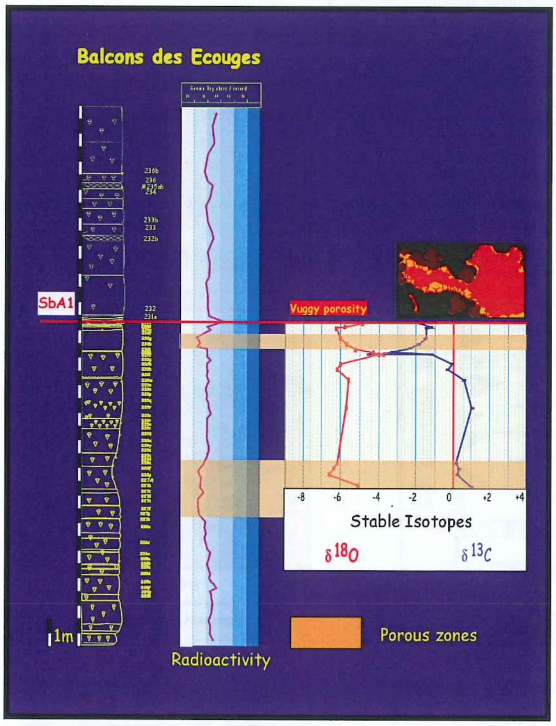

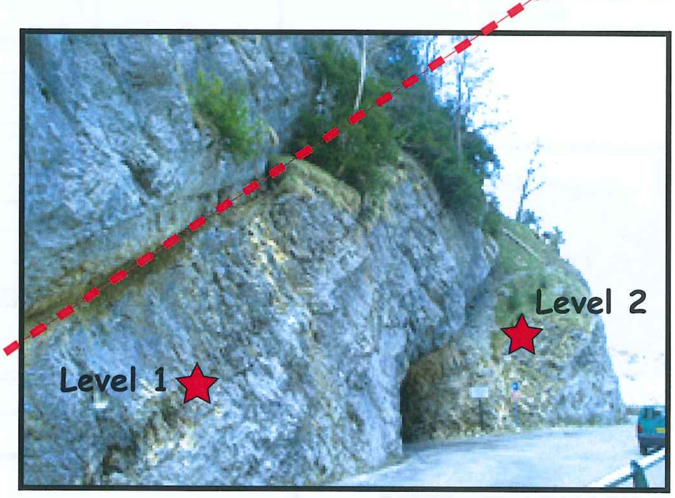

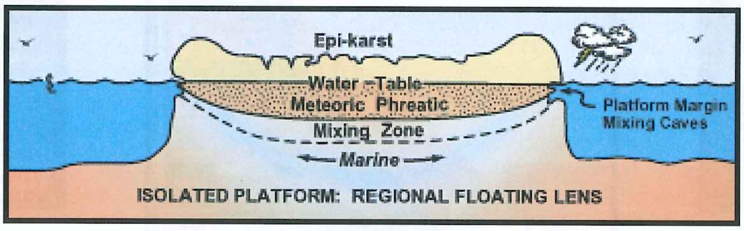

from Moore, 2001

Plate 38

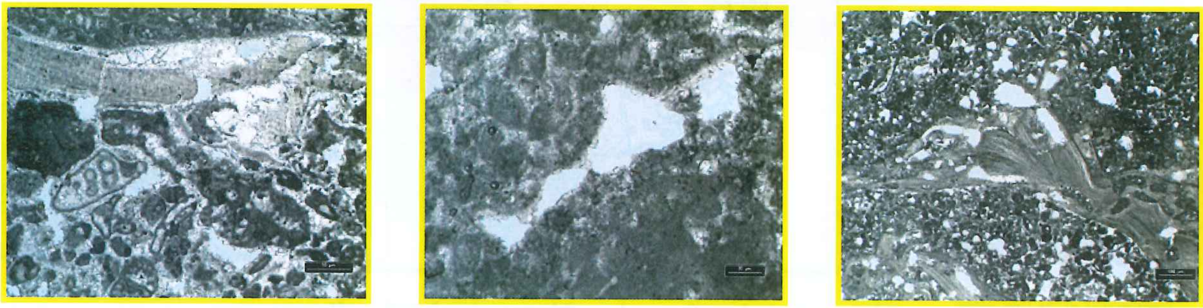

Moldic and vuggy porosity developed in specific levels possibly associated to vadose zones

Plate 39

Karstic microcaves fills: A tool for study of relative sea level changes Example of the Rimets valley and Achard syncline

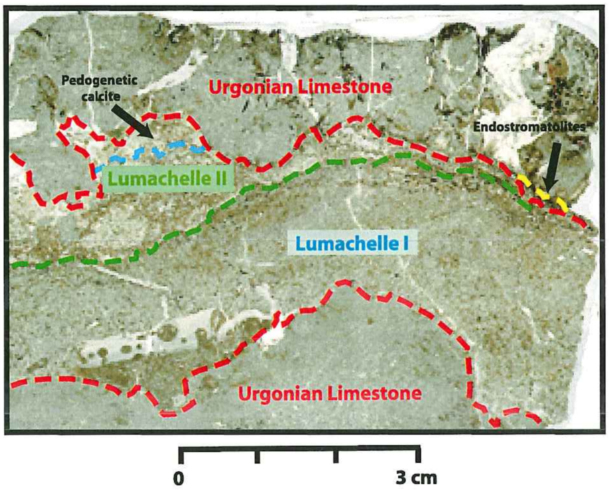

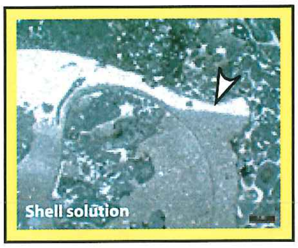

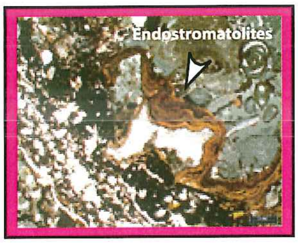

STAGE 1:
Early Aptian
sea-level fall

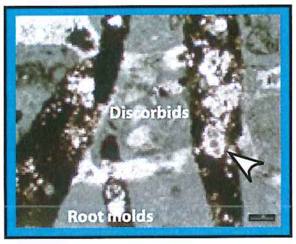

STAGE 8:
Last transgression

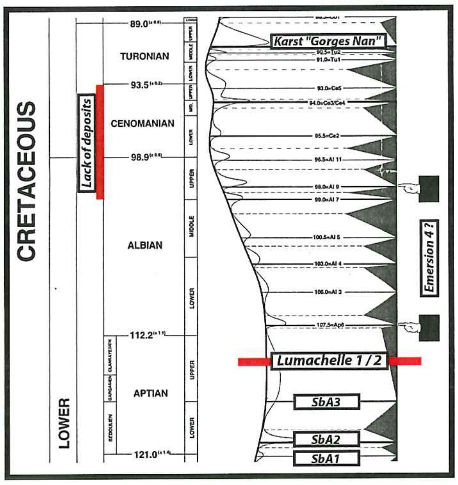

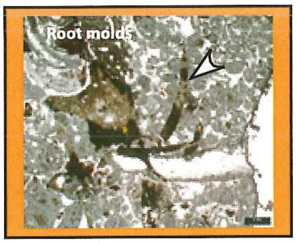

STAGE 7:
Sea-level falls during
Cenomanian to Turonian

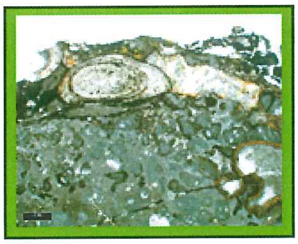

STAGE 2:
Transgression at the
top of early Aptian

STAGE 3:
Sea-level fall at the Late Aptian

STAGE 6:
Transgression at the Clansayesian

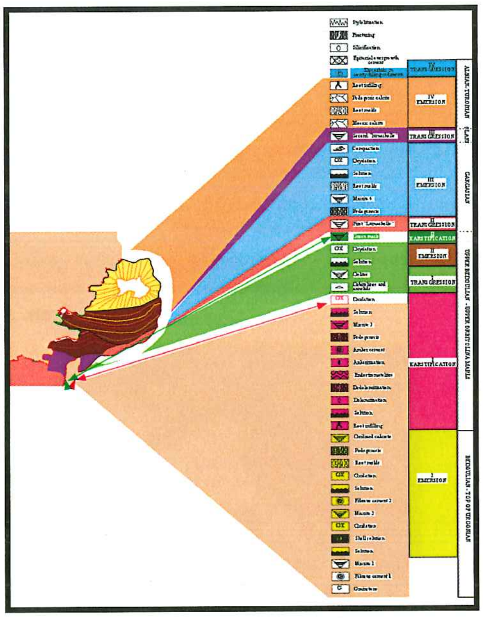

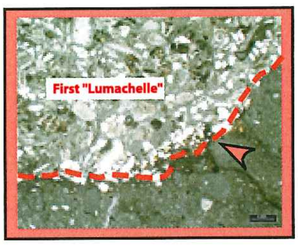

STAGE 4:
Transgression at the Late Aptian

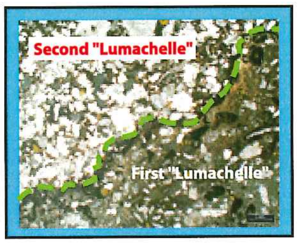

STAGE 5:
Sea-level fall near the top of Aptian

Diagenetic log from Les Rimets incised valley

Plate 40

Solution and dolomitisation during lowstand systems stracts Example of La Fontaine des Prêtres

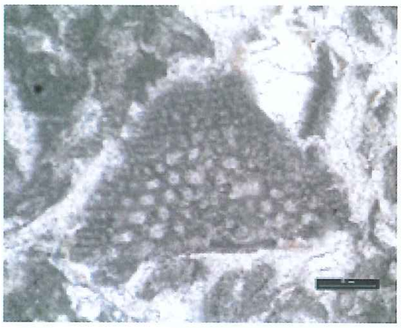

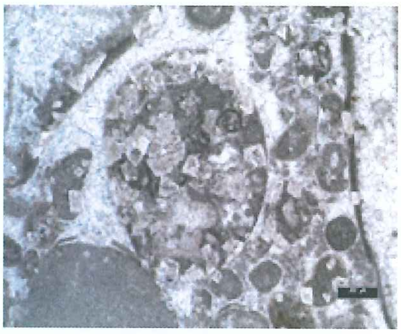

Dolomitization in mixing zone

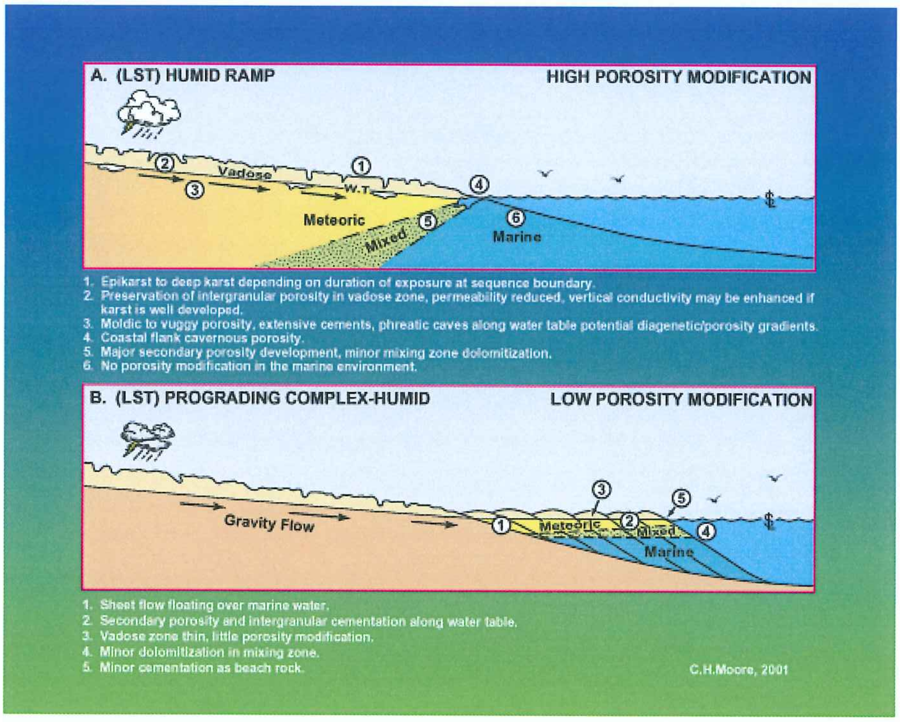

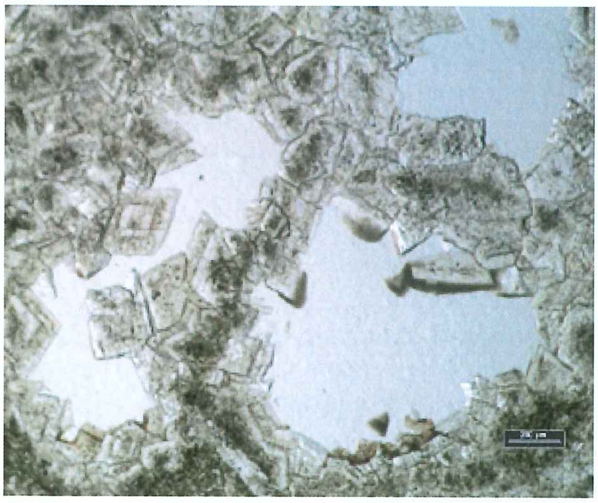

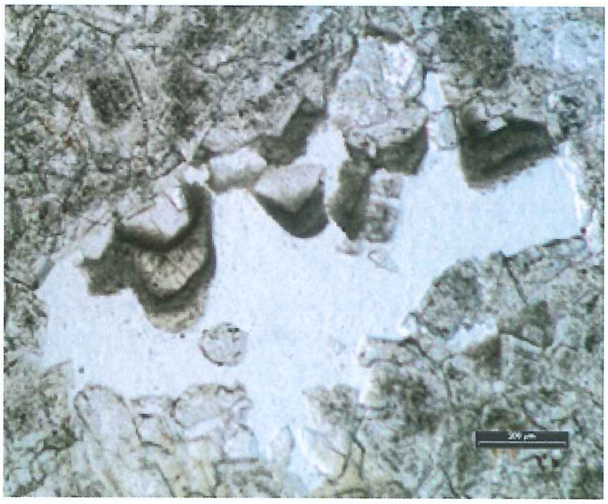

Dolomitization, solution and microstalactitic cements

Day 1

The Hauterivian - Barremian of the Western Swiss Jura around Neuchâtel

Alexis Godet, Marie-Caroline Blanc-Aletru, Stéphane Bodin, Thierry Adatte and Karl B. Föllmi

1.– Introduction: the formations from the early Cretaceous of the western Swiss Jura

1.1. Developments in the historical definition

In 1874, Renevier introduced the Hauterivian stage in the vicinity of Neuchâtel so as to re-establish the Neocomian of Thurmann (1836). Renevier's definition is clearly displayed in the local lithostratigraphy. The newly formed Hauterivian stage it comprised of the following units, from base to top (fig. 24):

The "Marne jaune de Morteau à *Ammonites astierianus*" (synonyms: Marnes à Astieria, Astieria-mergel, Astieriaschicht), which consists of 20-30 cm of yellow clayey marls, restricted only to the vicinity of Neuchâtel. Further from Neuchâtel, the Marnes à Astiera is sometimes replaced by a condensed bed which always marks the transition between the underlying Calcaire Roux (Valanginian) and the Marne bleue d'Hauterive.

The "Marne d'Hauterive à *Ammonites radiatus*" (synonyms: Marne bleue, Marne d'Hauterive) was deposited under open marine sedimentation. This formation can reach more than 20 m, contains several glauconitic-rich layers (e.g. the Cressier section located 15 km east of Neuchâtel). and is rich in ammonites and brachiopods. In the Cressier section, Busnardo and Thieuloy (1989) recognized *Teschenites* sp., *Acanhtodiscus pseudoradiatus*, *Acanthodiscus radiatus*, *Acanthodiscus* sp. ind., *Leopoldia leopoldina*, *Leopoldia* sp. ind., *Leopoldia levigata*, *Saynella neocomiensis* and *Saynella clypeiformis;* this assemblage may imply that the Marne bleue corresponds to the *radiatus* zone (fig. 25); even if the finding of one *Crioceras* belonging to the *loryi* group (Schardt, 1907 in Busnardo and Thieuloy, 1989), and of a *S. clypeiformis* at the top of the Cressier section would indicate that this formation developed until the *Crioceratites loryi* zone (Busnardo and Thieuloy, 1989).

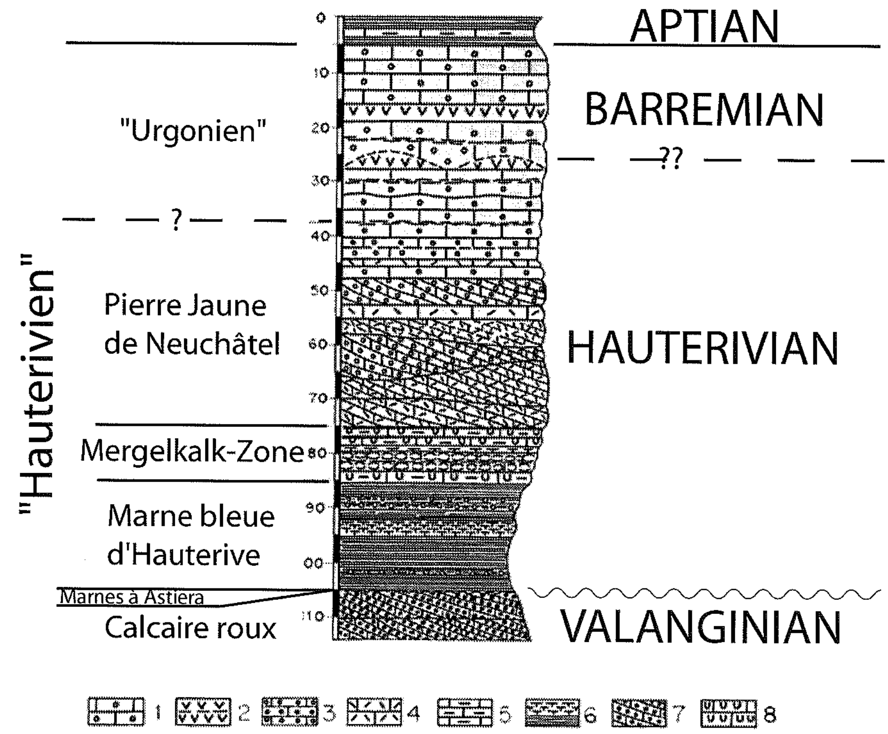

Fig. 24.- Historical succession around Neuchâtel. The local lithostratigraphic units and the ages are reported on the left and the right, respectively (after Remane, 1989). Lithologies : 1, pelsparites; 2, coral limestones (bioshermes or biostromes); 3, oosparites; 4, biosparites; 5, marly limestones; 6,calcareous marls and marls; 7, ferrugineous oolites; 8, burrows.

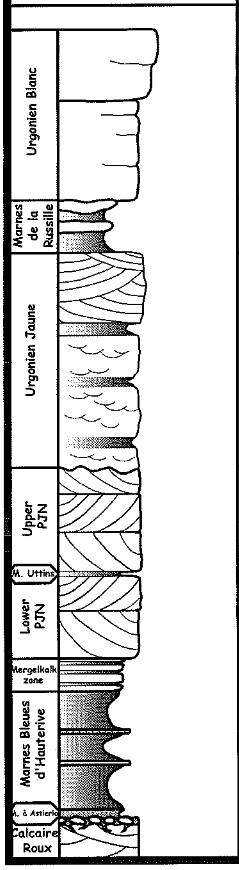

Formations	Mean Thickness	Lithology	Biostratigraphy (main faunas) after Rémane et al.(1989), Blanc-Aletru (1995) and this work
Urgonien Blanc	10 to 55 m	Oomicrite to oobiomicrite with builder organisms (rudists, stromatoporoids), orbitolinids and dasycladacae.	**Rudists:** *Agriopleura* sp., *Requiena renevieri.* **Dasycladacae:** *Suppiluliumella* gr. *verae* (Sokac) *corbarica, Falsolikanella* aff. *danilovae* (Radoicic), *Pseudoactinoporella fragilis.* **Orbitolinids:** *Paleodictyoconus cuvillieri, Paracoskinolina* sp., *Praedictyorbitolina carthusianna* (among others). **Echinoids:**
Marnes de la Russille	2 m	Orange to yellowish marls intercalated with limestones rich in stromatoporoids and corals	**Echinoids:** *Goniopygus* sp. *(?)*
Urgonien Jaune	30 m	Grainstones with oolites, extraclasts, large bryozoans debris and crinoids. Whereas no current beddings are noted at the bottom of the Urgonien Jaune, its upper part is characterized by well-sorted oolites grainstones with current beddings and even planar bedding organised into thinning-upward parasequences.	**Echinoids:** *Orthopsis* aff *repellini (?)*
Upper PJN	40 m	Orange to yellow oolitic grainstones rich in bryozoans and crinoids debris, with well-marked current bedding. Some marly intervals are clearly enriched in glauconite.	**Ammonites:** *Lyticoceras* sp. ind.
M. Uttins	< 1m	Orange clayey marls rich in glauconite over a hardgroung with burrows and oysters.	**Ammonites:** *Lyticoceras nodosoplicatum.*
Lower PJN	25m	Orange to yellow oolitic grainstones rich in bryozoans and crinoids debris, with well-marked current bedding. Silex are common.	
Mergelkalk zone	< 5 m	Yellowish, more or less marly limestones (wackestones and grainstones with current beddings) with thin marly intercalations.	**Ammonites:** *Leopoldia* sp. ind., *Cymatoceras pseudoelegans*
Marnes Bleues d'Hauterive	30 m	Dark calcareous marls with several glauconite-rich layers, resulting of an open marine sedimentation. Ammonites and brachiopods are easily found.	**Ammonites:** *Teschnites* sp., *Acanthodiscus* sp. ind., *A. pseudoradiatus, A. radiatus, Leopoldia* sp. ind., *L. leopoldina, L. levigata, Saynella neocomiensis* and *S. clypeiformis*
A. à Astieria	< 1m	Yellow condensed marly interval, rich in ammonites.	**Ammonites:** *Ammonites astieria, Olcostephanus atherstoni, Dichotomites gr. bidichotomoides.*
Calcaire Roux		Current-bedded, ferrugeneous grainstone which becomes nodular upward.	

Fig. 25.- Synthetic profile of the early Cretaceous formations around Neuchâtel (not to scale). Facies and significant faunas are described.

The Mergelkalkzone (synonym: zone marno-calcaire) is the transition between the Marne Bleue and the Pierre Jaune de Neuchâtel, which is the last formation of the Hauterivian of Renevier (1874).

The "Pierre Jaune de Neuchâtel" consists of an oolitic grainstone, sometimes enriched in bioclasts and characterized by oblique stratifications. The Pierre Jaune de Neuchâtel is divided into two parts by the "**Marnes d'Uttins**". This is a thin marly interval rich in glauconite; ammonites indicate an early Hauterivian age for the Marnes d'Uttins (*Lyticoceras nodosoplicatum* zone).

Above these units, the **Marnes de la Russille** divides the Urgonian limestones into two parts. The lower part is represented by the **Urgonien Jaune**, an oolitic – bioclastic yellow grainstone alternating with marly intervals.In the Marnes de la Russille, the first cnidarians occur.

Finally, the **Urgonien Blanc** is the last formation of the succession. It consists of white oolitic grainstones to slightly recrystallized white limestones and rudists. Some stromatoporoids or corals can also be found.

Whereas the age of the formations under the Marnes d'Uttins is well constrained by ammonite biostratigraphy, the lack of such fossils in the upper Pierre Jaune de Neuchâtel and the Urgonian limestones is problematic (fig. 25). In 1901 some controversy arose when Baumberger replaced the lithostratigraphic term "Urgonien" by the stage name Barremian, without any biostratigraphic clues for such an age. So, in the stratigraphic scheme of Baumberger (1901), the upper Pierre Jaune de Neuchâtel should belong to the late Hauterivian, and the Urgonien Jaune and the Urgonien Blanc to the Barremian.

1.2. Recent developments

A study by Remane *et al.* (1989) tried to resolve the questions relating to dating and of the continuity of the historical succession defined around Neuchâtel by Renevier (1874). To do this they studied all the faunas but also the mineralogy and the sequence stratigraphy, in order to try to correlate the western Swiss Jura with the meridional Jura. However, it seems that no consensus could emerge. Two main schools of thought appeared. Based on sequence stratigraphy and orbitolinids biostratigraphy, the conclusions of these two sides are the following (fig. 26):

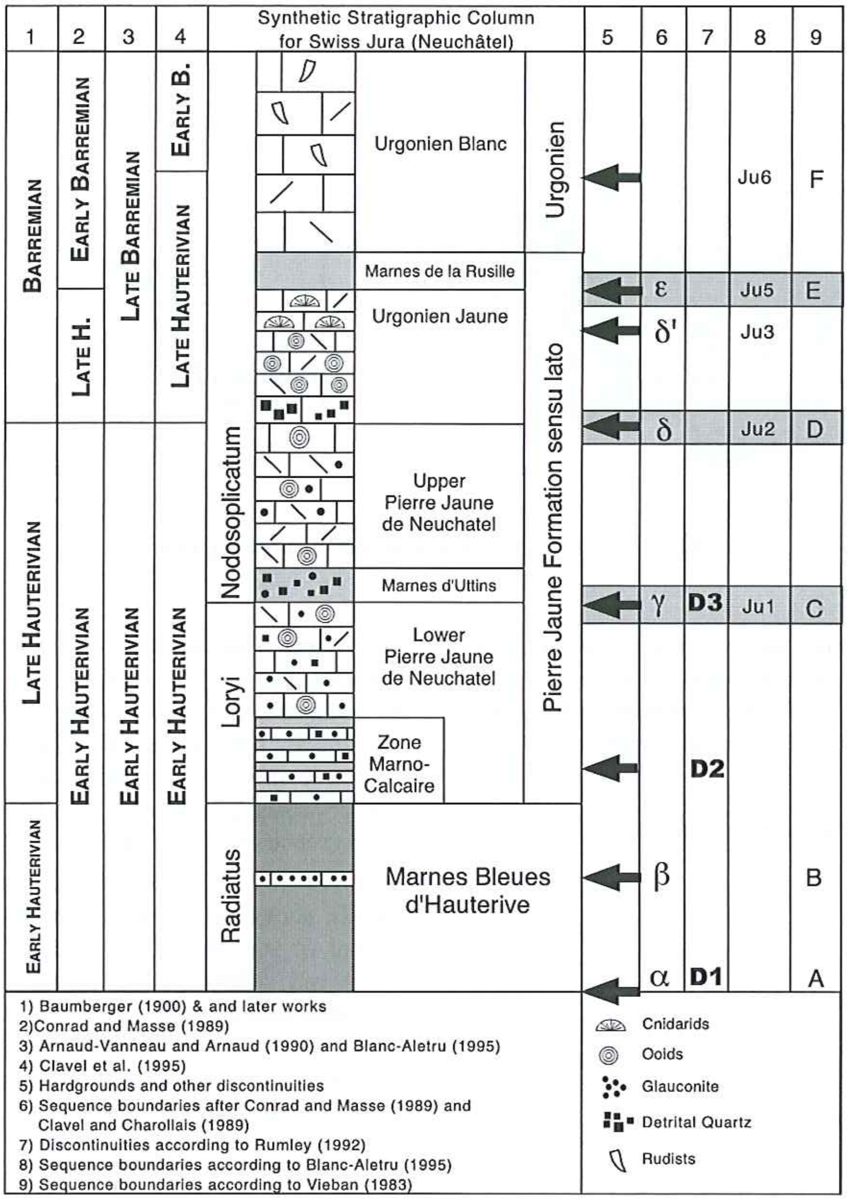

Fig. 26.- Synthetic stratigraphic column for the western Swiss Jura. The different proposed ages are reported on the left, as well as the main discontinuities (on the right) according to different authors (after van de Schootbrugge, 2001).

1. Arnaud-Vanneau and Arnaud (1990) proposed that a significant hiatus, located at the top of the Pierre Jaune de Neuchâtel, implies a late Barremian age for both the Urgonien Jaune and the Urgonien Blanc. From their point of view, the Urgonian limestones may have been deposited simultaneously from the Vercors to the vicinity of Neuchâtel, from the maximum flooding surface (mfs) B3 (*Gerhardtia sartousiana* ammonite zone).

2. On the other hand, Clavel *et al.* (1995) proposed that the sedimentation was continuous from the Pierre Jaune de Neuchâtel up to the Urgonien Blanc. Thus, the Urgonien Jaune would belong to the late Hauterivian and the Hauterivian – Barremian boundary may fall within the Urgonien Blanc.

During this first day of excursion, we will compare the historical succession around Neuchâtel between two sections:

At the Gorges de l'Areuse section (fig. 27), we will observe how the sediments from the Pierre Jaune de Neuchâtel are arranged in shallowing upward parasequences. We will also discuss the evolution of clay minerals, in particular kaolinite. We will also see how difficult it is to separate the Pierre Jaune de Neuchâtel from the overlying Urgonien Jaune.

At the Eclépens section (Holcim quarry of La Sarraz, canton of Vaud), the succession is more complete and developed than at the Gorges de l'Areuse; this will allow us to examine the Urgonien Blanc formation. Moreover, we will discuss of the sequence stratigraphic evolution (based on microfacies analysis) and on the

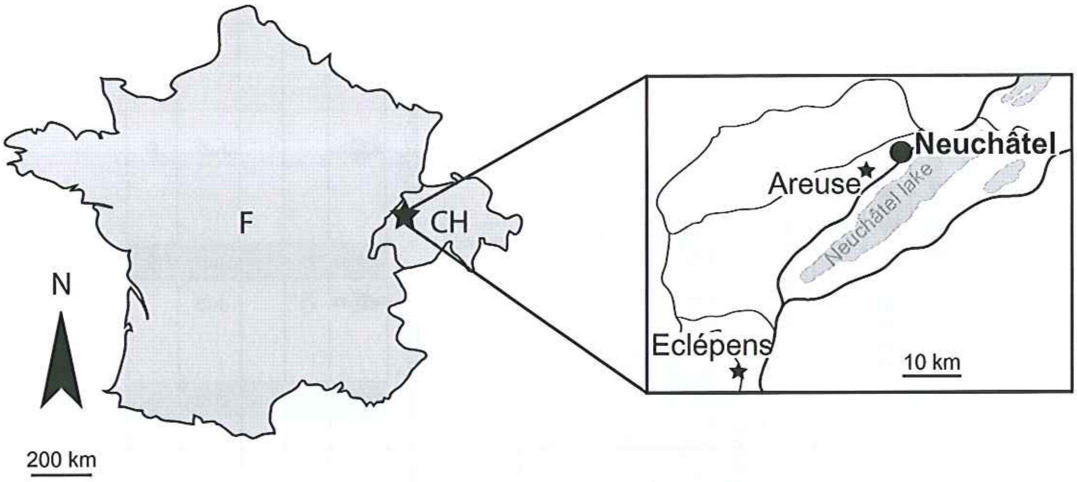

Fig. 27.- Location of the Areuse and Eclépens sections.

clay mineral evolution. We will finally discuss the age of the Urgonien Jaune and Urgonien Blanc, in view of kaolinite correlation, strontium isotopes stratigraphy, radiochronology and sequence stratigraphy.

2.– First stop: Gorges de l'Areuse

2.1. Location

The Gorges de l'Areuse section is located in the village of Boudry, approximately 10 km to the southwest of Neuchâtel (fig. 27). The section follows the southern edge of the River Areuse beginning at the end of a pedestrian tunnel entering the Val-de-Travers.

2.2. Previous works

The section at the Gorges de l'Areuse, also named the Boudry section, was first studied by Zweidler (1985), then by Rumley in 1993. Finally, Blanc-Aletru in 1995 conducted a high-resolution study of the biostratigraphy (mainly orbitolinids), the mineralogy and the microfacies (fig. 28) of the Boudry section.

2.2.1. Description of the section at Boudry

Blanc-Aletru divided the section of Boudry into three main parts.

From the base to the discontinuity "A": this part of the section is composed of oobiopelsparites with much crinoids and bryozoans debris. The amount of quartz, glauconite and iron oxides varies, as do the rocks textures, which range from packstone to grainstone. In "E" and "D", Blanc-Aletru pointed out the presence of perforated surfaces. Unfortunately, Blanc-Aletru did not exactly locate the boundary between the Pierre Jaune de Neuchâtel and the Urgonien Jaune.

Between the discontinuities "A" and "Y": from the discontinuity "A" upward, a major change in the sedimentation occurred as mudstones rich in corals remains and other bioclasts replace the oolitic grainstones. This facies is associated to the Marnes de la Russille. Blanc-Aletru attributed the discontinuity "A" to a major sequence boundary (Ju3 in her sequence stratigraphy scheme), and she observed the presence of bioclastic infill with orbitolinids in "X". Dissolution features observed under "Y" led Blanc-Aletru to deduce the presence of a major sequence boundary (Ju5).

From "Y" to the top: the last part of the section is mainly composed of oobiosparites rich in fragments typical of the internal part of the platform, such as micritised debris and bioclasts. The presence of important intergranular dissolution features, vadose silts and of oxidation could be the consequence of a final sequence boundary occurring at 35 m depth (Ju6 ? after Blanc-Aletru).

2.2.2. Microfacies and sequence stratigraphy of the Boudry section

Based on the presence or absence of micrite, on the type of clasts or lithoclats observed in thin section, Arnaud-Vanneau (1980) defined twelve microfacies (from F0 to F11), which are distributed from pelagic settings to supratidal environments. In the Western Swiss Jura, Blanc-Aletru (1995) recognized the following microfacies (Plate 41):

FT: biomicrite with spicules of sponges and cnidarians. FT microfacies were deposited in calm environments, under the wave base. When present, the corals can be encrusted by bryozoans or other faunas, such as foraminifera. Iron nodules are recognized in thin section.

F3: biopelsparite with crinoidal remains and small foraminifera deposited in deep environments of the outer platform.

F4: biosparite and biomicrite with crinoids and bryzoans. Whereas such facies are rare on the extern slope of standard platform, they are relatively common on drowned platforms.

F5: biosparite with big subspherical remains. They characterize infralittoral domains with constant hydrodynamism, but also circalittoral regions where the deposits are the results of storm currents.

F6: oosparite. Oolitic deposits are found in shallow water environments where tidal currents are dominant.

F7: biosparites and biomicrites with cnidarians and corals build-up. Such microfacies are characteristic of the platform border, and can be deposited in infralittoral domains with low hydrodynamism where the build-up are preserved, or in high-energy infralittoral environments. In this later case, the F7 microfacies would correspond to the breaking-up of reefs.

F8: biosparites and biomicrites with big foraminifera and big rudists. These facies were deposited in relatively calm environments where sand, muddy sand or mud can settle.

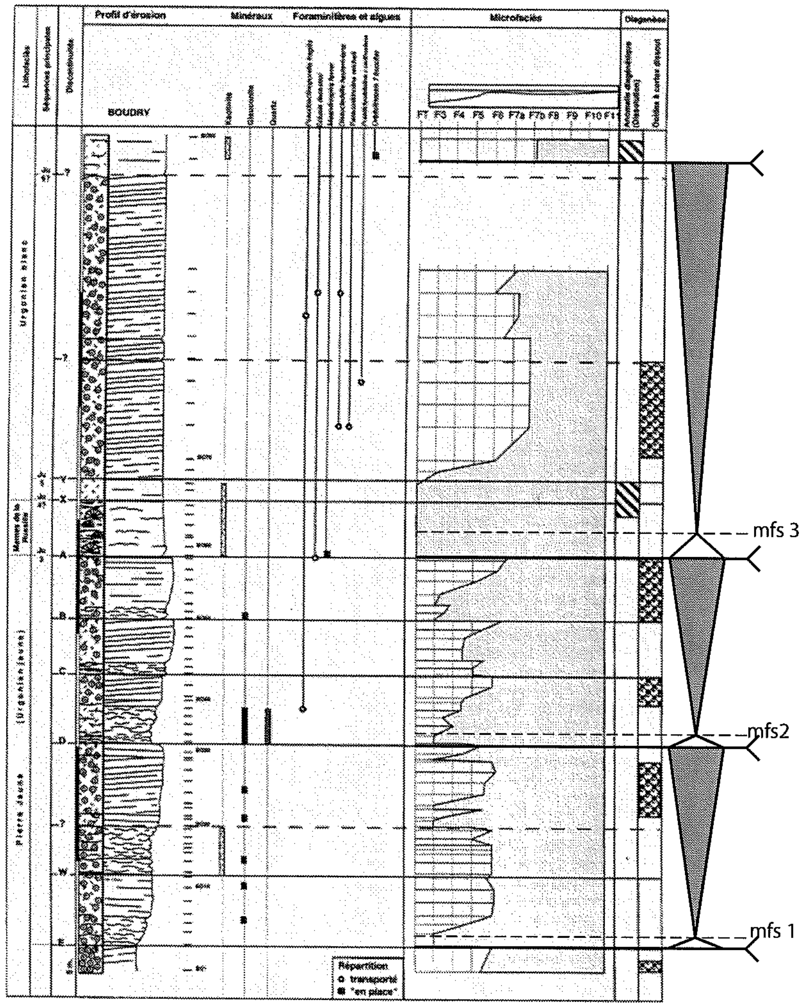

Fig. 28.- Profile, repartition of microfossils and microfacies of the Boudry section (after Blanc-Alétru, 1995). From the microfacies curve a sequence stratigraphic scheme is proposed.

The Boudry section can be split into three 3rd order sequences, each of them being delimited by two sequence boundaries:

The discontinuities "E" and "D" are both characterized by perforations. Morover, F6 microfacies with oomoldic porosity were observed by Blanc-Aletru, so these surface are interpreted as sequence boundaries. Just above "E", the microfacies curve displays a sharp shift toward FT microfacies, which may correspond to a maximum flooding surface (mfs 1). Consequently, the first meter above "E" and the interval between the mfs 1 and "D" may reflect a transgressive system tract (TST) and a highstand system tract (HST), respectively.

The microfacies curve indicates a next sequence boundary may be located at the base of the Marnes de la Russille (Ju3 after Blanc-Aletru). This is labelled as the "D" discontinuity. Both perforations and dissolution of the oolites cortex are recovered in Ju3. Regarding the microfacies curve, FT microfacies are observed in a marly interval just after "D"; they are interpreted as a mfs 2. So, the same scheme than between "E" and "D" is recognized, with a TST from "D" to the mfs 2 and a HST from the mfs 2 to the Ju3. However, high frequency microfacies variations observed in this interval may correspond to parasequences and consequently are not discussed in this paragraph (see paragraph 2.3.2.).

Finally, FT microfacies are again present at 5 meters just above Ju3; consequently, the Marnes de la Russille are interpreted as a mfs 3. Then, microfacies shift toward F6/F7 in the Urgonien Blanc. At the top of the section, clues for the presence of the sequence boundary are noted by Blanc-Aletru (see paragraph 2.2.1.). Consequently, a TST is defined between Ju3 and the mfs 3 whereas the end of the section may reflect a HST.

2.2.3. Mineralogy of the Boudry section

In the Boudry section (fig. 29), the main clay minerals of the <2μm fraction are smectite, irregular illite smectite mixed-layers, mica, chlorite, kaolinite and pyrophyllite. Small amounts of quartz and goethite are also present.

Mica is present all along the section, whereas the smectite and kaolinite have an antagonistic behaviour. Smectite is present in the 7 first meters of the section, between 12 and 14 m and in the Marnes de la Russille.

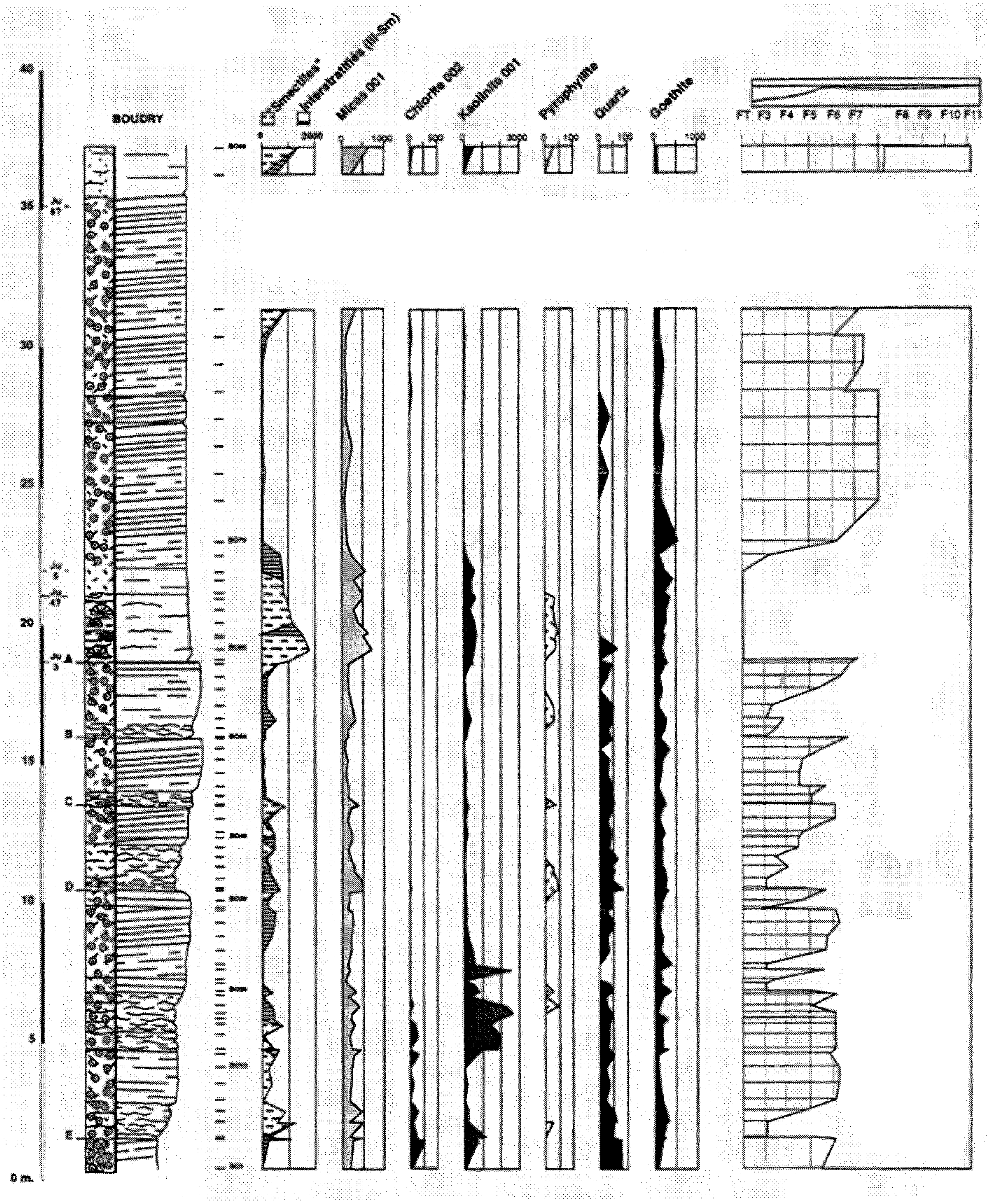

Fig. 29.- XRD results for the < 2 µm fraction of the Boudry section (after Blanc-Alétru, 1995), expressed in cps; the microfacies curve is reported on the right.

Plate 41.- Micrographs of the microfacies recognized in the studied sections (scale bar: 1 mm). (a) FT: biomicrite with spicules of sponges and cnidarians; (b) F3: biopelsparite with crinoidal remains and small foraminifera; (c) F4: biosparite and biomicrite with crinoids and bryzoans; (d) F5 bioparite with large subspherical bioclasts; (e) F6: oosparite (note the presence of oomoldic porosity on this picture; sample ECII 50, Eclépens); (f) F7: biosparites and biomicrites with cnidarians and corals build-up; (g and h) F8: biosparites and biomicrites with large foraminifera and large rudists.

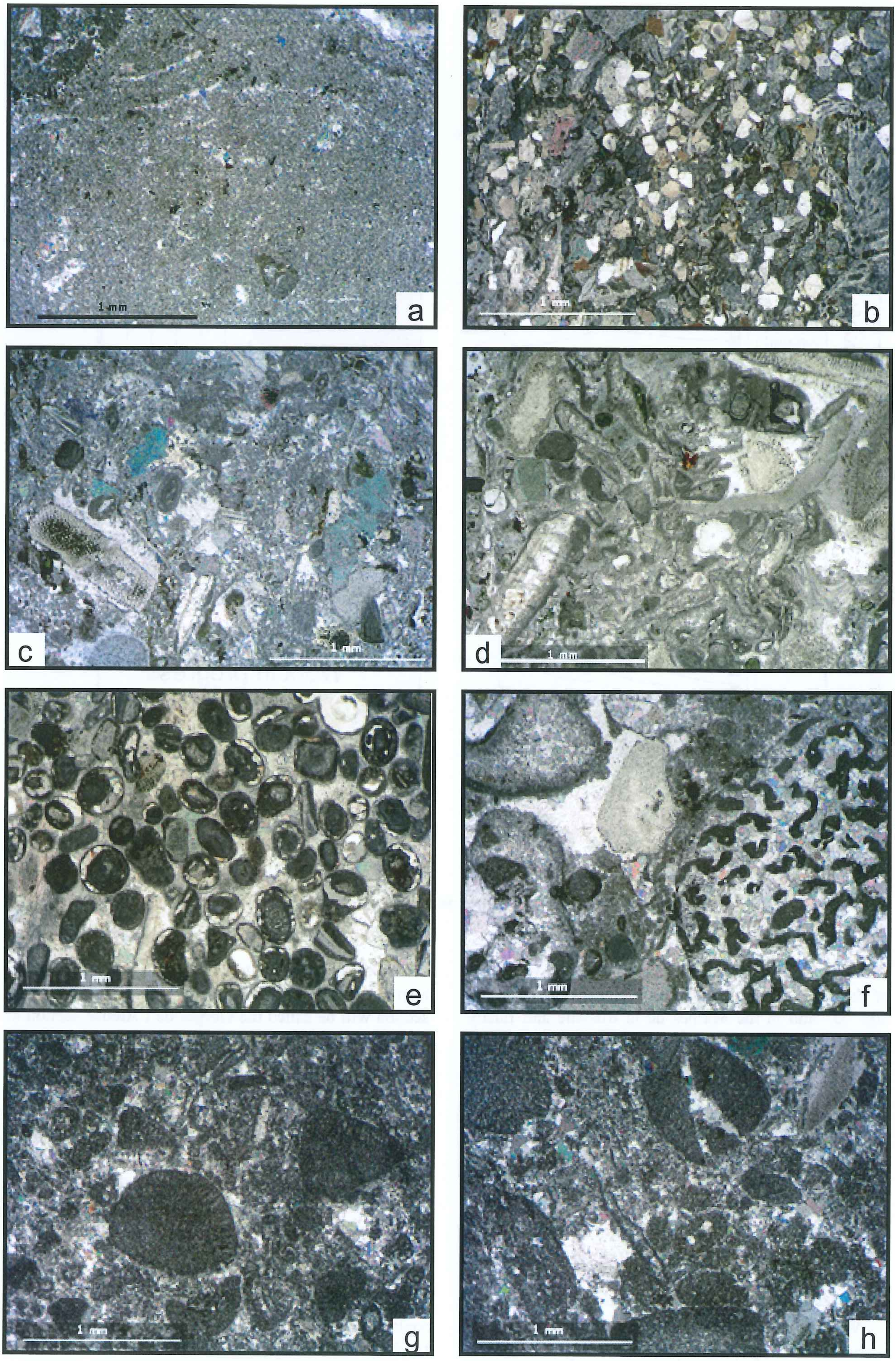
1 mm
a
1 mm
b
c
1 mm
d
1 mm
1 mm
e
1 mm
f
1 mm
g
1 mm
h

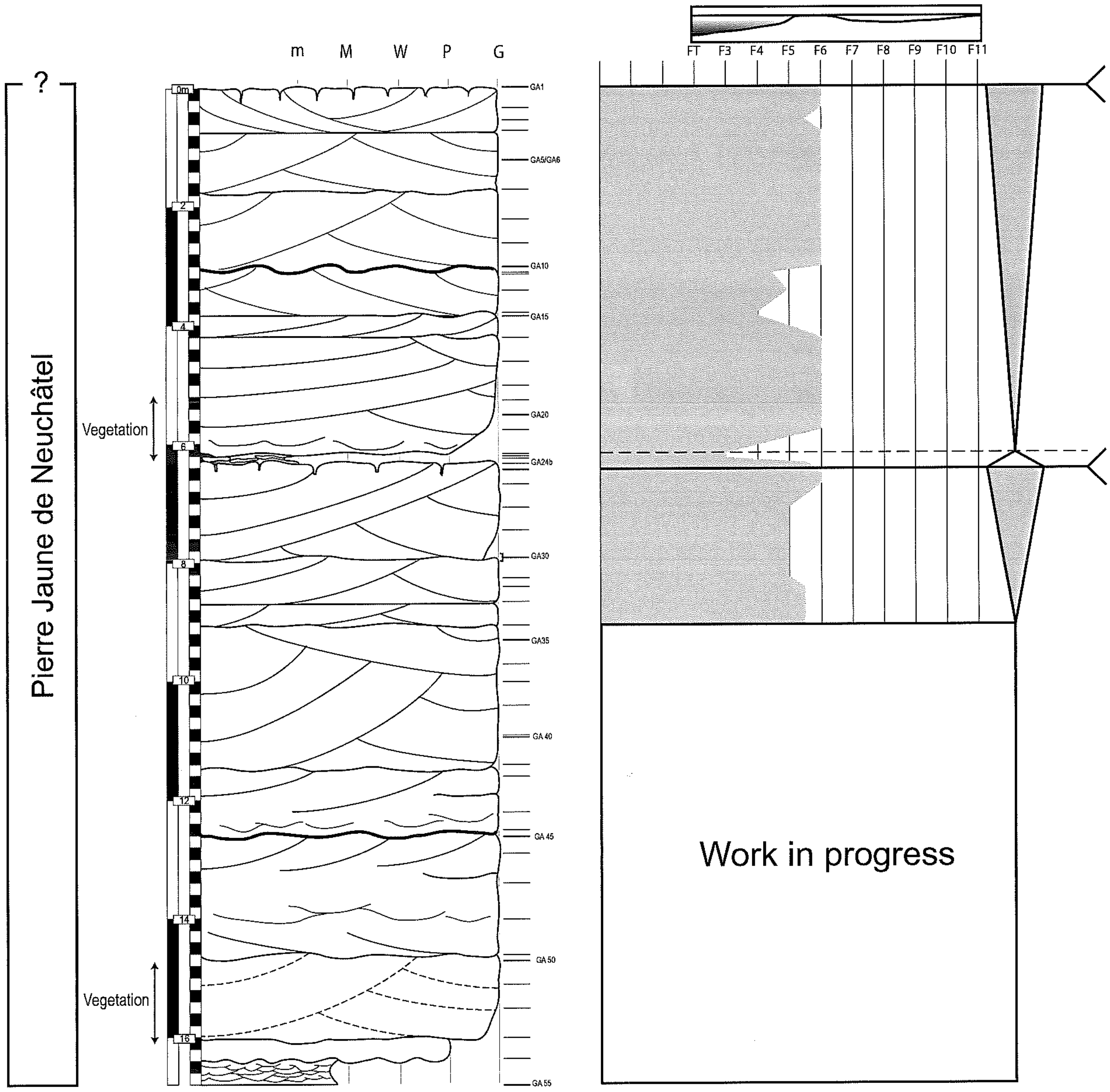

Fig. 30.- Microfacies evolution for the Gorges de l'Areuse section (base of the Boudry section).

On the contrary, the kaolinite is present in the whole part of the section, with significant increases between "E" and "D" and in the Marnes de la Russille and finally decreases in the Urgonien Blanc.

2.3. The Pierre Jaune de Neuchâtel – Urgonien Jaune transition

As shown by Zweidler (1985) and by Blanc-Aletru (1995), the transition between the Pierre Jaune de Neuchâtel and the Urgonien Jaune is often difficult to recognize in the field, as the facies of both formations are very similar. In the Boudry section, several perforated and erosive surfaces were described in the Pierre Jaune de Neuchâtel by these authors.

We propose a high-resolution study on a 16 m thick section and to try to define the boundary between the Pierre Jaune de Neuchâtel and the Urgonien Jaune with respect to sequence stratigraphy and mineralogy. This section will be called the Gorges de l'Areuse section in the following paragraphs.

2.3.1 Description of the section

The major part of the Gorges de l'Areuse section is composed of oolitic grainstones organised in beds with cross stratifications, which are usually easily recognizable (fig. 30). In the top of the section, the good quality of the outcrop allows the definition of a basic model.

At 6.40 m, an erosive surface with burrows is described, the laminations of the lower bank displaying toplap features. On this surface, which may corresponds to the discontinuity "ER" of Blanc-Aletru (1995), a

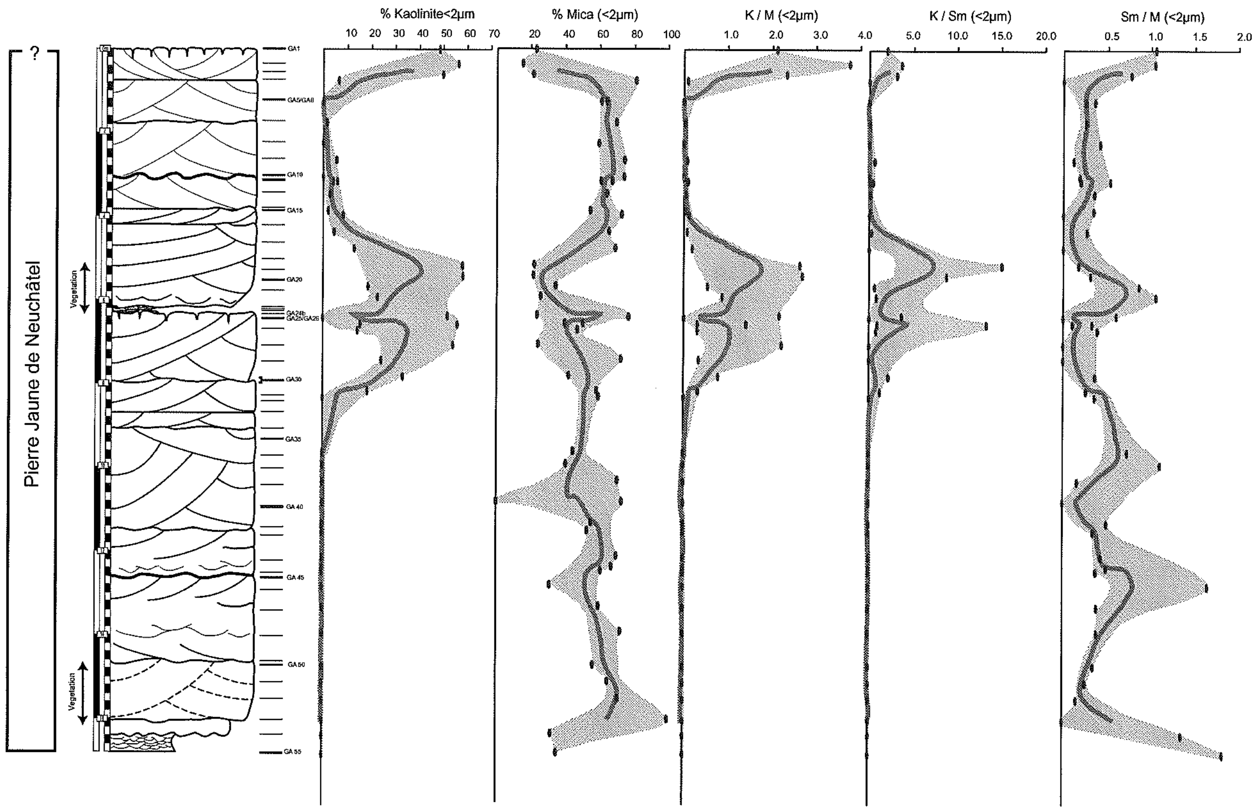

Fig. 31.- XRD results for the < 2 µm fraction of the Gorges de l'Areuse section, expressed in relative percents or in cps ratio.

marly interval (about 10 cm) contains some bioclastic pebbles. At 6 m depth, clues for channels were found. Upwards, oolithic banks are present in the following 3 meters. At 3 m depth, a very thin clay layer (less than 5 cm) separates a grainstone with oolites, crinoids, glauconite and some burrows (sample GA 11) from a packestone-grainstones with oolites and bioclastes (sample GA10). Above this, 3 meters of oolitic grainstones are exposed. Finally, a major discontinuity is observed at the top of that part of the section. This erosive surface is perforated erosive overlaid by a conglomerate with a marly matrix.

This kind of succession is repeated in the bottom of the section almost two times, with marly or clayey intervals more or less well-expressed. The section ends in a little depression, where the last bank of oolitic grainstone with cross stratifications surmounts a 50 cm thick interval of marl.

2.3.2. Microfacies and sequence stratigraphy

Thirty six thin sections were analysed in order to determine the main microfacies that occurred in the upper part of the Gorges de l'Areuse section. The results are shown on the figure 30. The microfacies range from the F3 to the F6 microfacies (Plate 41) of Arnaud-Vanneau (1980).

From the determination of the microfacies, a sequence stratigraphical interpretation can be proposed, from base to top.

– From 9.10 m (GA 34) to 6.40 m (GA 25): the evolution of the microfacies is shallowing upward, from F5 to F6. At 6.50 m, the erosive and perforated surface marks a parasequence boundary. In thin section, some oolites cortexes show traces of dissolution (oomoldic porosity). This interval corresponds to a highstand deposits.

– From 6.50 m to 6.20 m (GA 22): the F3 microfacies dominates, implying the presence of a flooding surface. This interval corresponds to transgressive deposits.

– From 6.20 m to 3.10 m (GA 10 / GA 11): here again, the evolution of the microfacies is shallowing upward, and thin section from the sample GA11 displays dissolution features and recristallisation characteristic of a parasequence boundary. This interval corresponds to highstand deposits.

– From 3.10 m to the top (GA1): except the very thin clay layer described between GA10 and GA11, the microfacies display a general shallowing upward evolution. As previously said (see 2.2), the top of the section is characterized by an erosive and perforated surface, which is interpreted as a parasequence boundary whereas the clay level at 3.10 m could represent a flooding surface. So, the last 3 m of the section represents a complete parasequence with a small interval of transgressive deposits and plurimetric thick highstand deposits.

2.3.3. *Mineralogy*

The composition of the clay mineral assemblage was determined by X-ray diffractometry on a Scintag XDS 2000 at the Institute of Geology, University of Neuchâtel. The samples were decarbonated by hydrochloric acid digestion using the method described by Kübler (1987). Air-dried (<2µm and 2-16µm fractions) preparations were analysed, as well as glycol saturated preparations (<2µm) in order to determine swelling minerals. Here we present the most important results of the <2µm fraction (fig. 31).

Mica, kaolinite, smectite, illite-smectite mixed-layers and chlorite were recognized, as well as quartz, pyrite, goethite, potassic feldspar and Na-plagioclase. The kaolinite is not present in the first 8 m of the section and appears abruptly just below the erosive contact observed at 8m (GA30). Then, the kaolinite curve displays a maximum between 4 and 8 meters depth, with a negative peak corresponding to the marly interval at 6 m depth (GA24). Upwards, the section is rather characterized by low contents of kaolinite, the uppermost part excepted, which shows a rapid increase in kaolinite values.

This striking behaviour of the kaolinite is also pointed out by the kaolinite / mica and kaolinite / smectite ratios curves, that show the same maximum between 6 and 8 meters whereas these ratios are close to zero is the rest of the section. Finally, the low values of the smectite / mica ratio (< 1) leads us to conclude that the mica is the main mineral of the clay assemblage, more particularly in the lower part of the section. The kaolinite appearance near the top of the Pierre Jaune is correlatable event over a large area (see section 4.3).

The clay minerals evolution reflects a drastic change between a climate with well-marked seasons, characterized by dominance of the smectite, toward intertropical conditions under kaolinite is produced (see paragraph 3.2.3. for more details).

3–. SECOND STOP: ECLÉPENS (HOLCIM QUARRY)

3.1. Location

The section of Eclépens crops out in the cement quarry of la Sarraz exploited by Holcim, at 60 km SW of Neuchâtel (fig.27). Due to the industrial exploitation of the quarry, the outcrop is very fresh and of a good quality.

3.2. The Pierre Jaune de Neuchâtel – Urgonien Blanc succession at Eclépens

3.2.1. *Description of the section*

The Eclépens section is composed of two sub-sections, each measuring more than 50 m. Combining these two parts, the composite section reaches 92 m in thickness (fig. 32).

The base of the section is situated in the lowermost part of the quarry and begins with 8 m of oolitic grainstones with some flintstones nodules or lenses. At 8 m a glauconitic hardground with oysters and burrows is surmounted by a yellow to reddish marly layer rich in glauconite and with some brachiopods (20 cm), and by a 15 cm thick layer of black marls with bivalves (Panopées); this interval is thought to be an equivalent of the Marnes d'Uttins, but ammonite findings are needed to confirm this hypothesis.

Above the black marls, there is a 2 meters thick black packestone to grainstone rich in bivalves and brachiopods. Above, oolitic sedimentation begins again, with relatively well-marked oblique stratification. This type of facies is attributed to the upper (?) Pierre Jaune de Neuchâtel. At 37 m depth, the glauconite content increases as well as the presence of marly intervals between the oolitic banks. This interval (between the samples ECII53 and ECII58) is also characterized by the presence of some kind of channels within the oolitic packestone banks. Then, the clay content seems to decrease rapidly, and at 40 m depth, the facies are similar to that recognized in the lower part of the section. Some changes occur at 45 m depth (ECII72) with the appearance of a black and massive bank, similar to the one described above the "Marnes d'Uttins equivalent". About 5 meters of bioclastic packestone to grainstone with oolites and glauconite alternating with marly intervals separate this black level from a second one which marks the end of the first part of the Eclépens section, and which can be used to correlate the two studied parts of the quarry. After Blanc-Aletru (1995), the base of this second black bank is erosive, and thus interpreted as a sequence boundary (Ju2 in Blanc-Aletru, 1995).

The upper part of the Eclépens quarry was studied by Blanc-Aletru in 1995; in particular, the repartition of the microfaunas is shown in figure 33. She proposed a threefold division:

– From 50 to 71 m: oolitic facies characteristic of the Pierre Jaune de Neuchâtel are recognized, but they may belong to the Urgonien Jaune. Effectively, the transition between the Pierre Jaune de Neuchâtel and the Urgonien Jaune is sometimes hard to recognized on macroscopic samples. At 71 m, Blanc-Aletru (1995) remarked the presence of dissolution in the cortex of the oolites and of an erosive surface, interpreted as a sequence boundary (Ju3 after Blanc-Aletru, 1995).

– From 71 to 83 m, Blanc-Aletru described three subsets:

– From 71 to 76 m, some mudstones to wackestones with corals fragments, transported foraminifera (with some orbitolinids) and algae, calcareous sponges.

– From 76 to 80 m, a transition from bio-ooclastic facies at the base to oolitic grainstones with dissolution of the cortex at the top which would be the consequence of a major discontinuity (Ju5 in Blanc-Aletru, 1995).

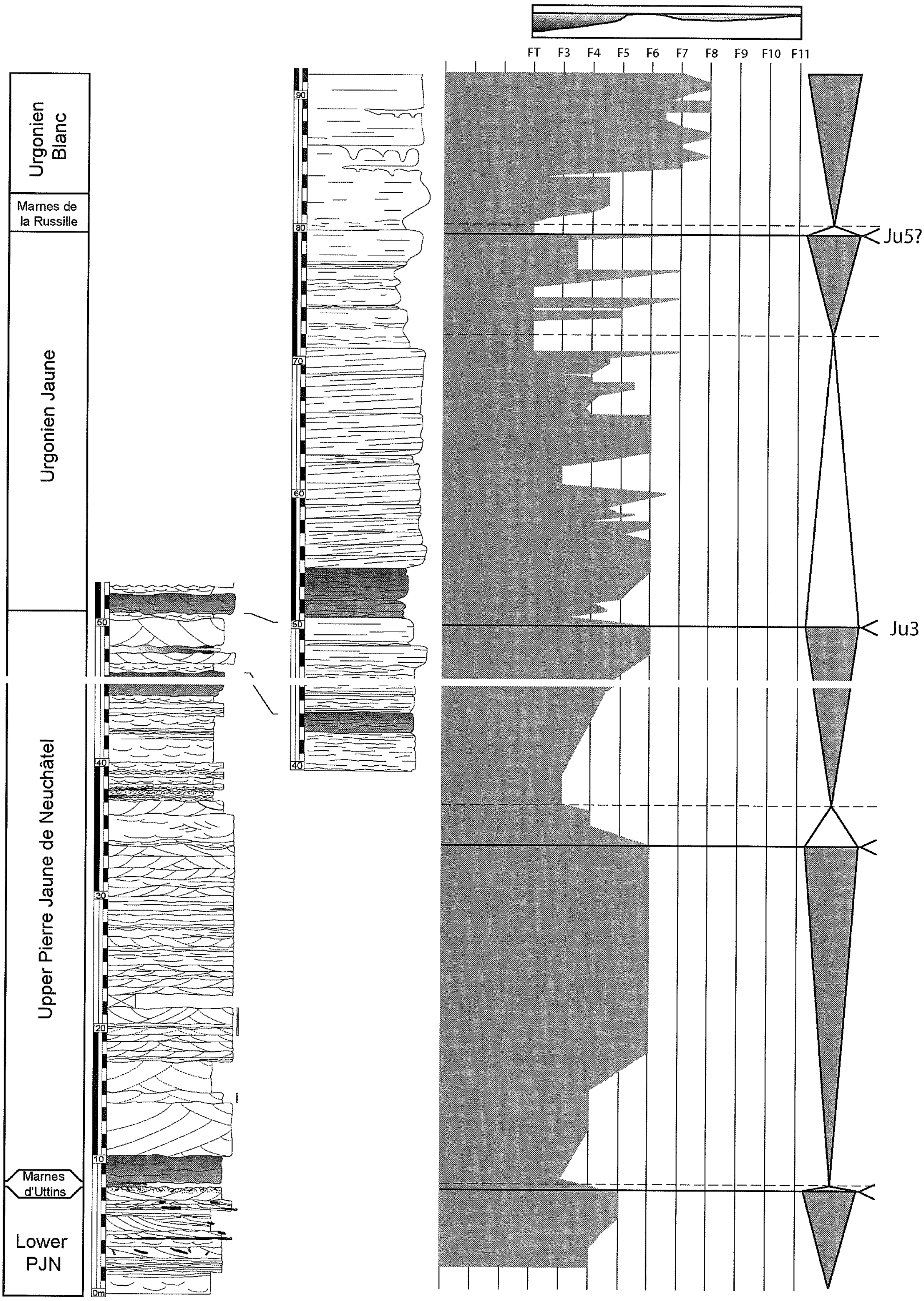

Fig. 32.- Microfacies and sequence stratigraphy interpretation of the Eclépens section. The upper part (on the right) is after Blanc-Aletru (1995; see figure 6 for more details) and the lower part (on the left) is from this study.

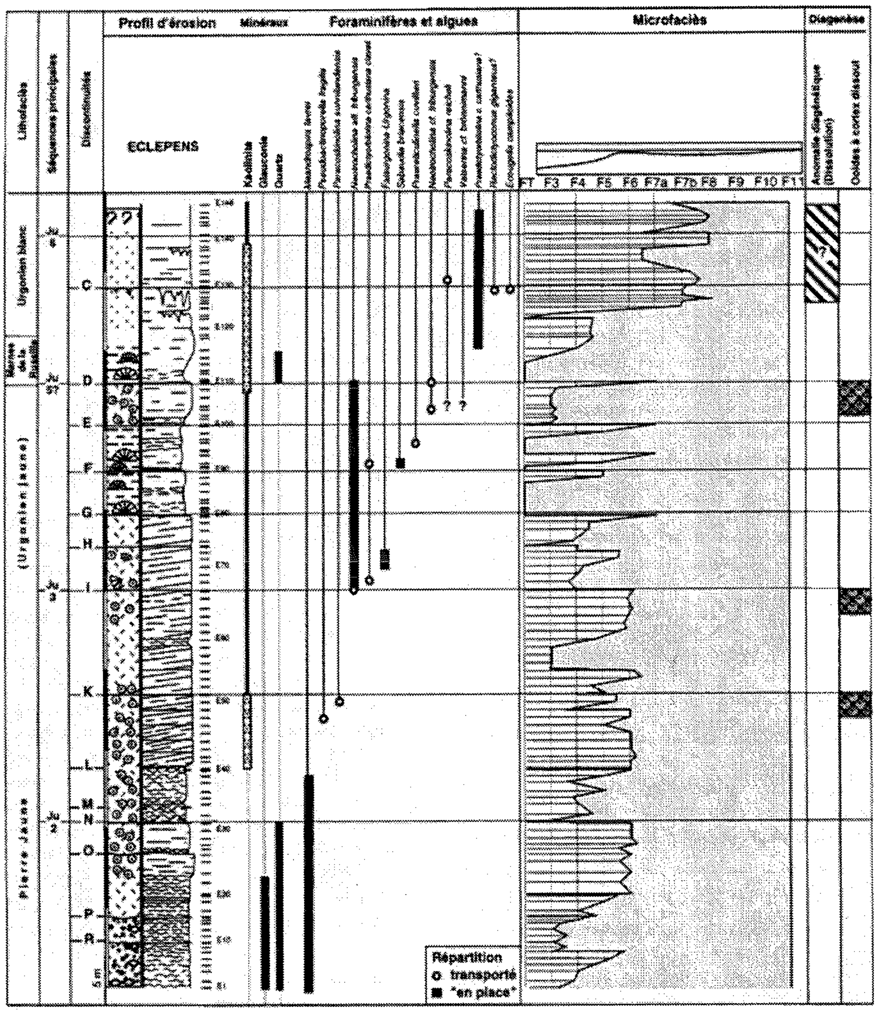

Fig. 33.- Profile, repartition of microfossils and microfacies of the upper part of the Eclépens section (after Blanc-Alétru, 1995).

– From 80 to 83 m, the facies is similar to the one described between 71 and 76 m. Blanc-Aletru (1995) attributed these deposits to the Marnes de la Russille.

– From 83 to 92 m (top of the section): the facies change from a wackestone to packestone rich in foraminifera, particularly in orbitolinids (between 83 and 90 m), toward a rudists-bearing facies (90 to 92 m). The presence of karsts is noted in this part of the section.

3.2.2. Microfacies and sequence stratigraphy

The microfacies recognized in thin sections from the Eclépens section are relatively similar to the ones described in the paragraph 2.3. The main difference is the appearance of microfacies typical of the internal part of the platform.

Based on the microfacies evolution a sequence stratigraphic scheme can be proposed. Only the 3rd order sequences are taken into consideration (fig. 32).

– From the base of the section to 8 m: the microfacies range from F4 to F5, describing a shallowing upward evolution and ending with a hardground with many glauconite and oysters, which may correspond to a sequence boundary. Thus, this interval is attributed to a highstand system tract (HST).

– From 8 to 8.4 m: F5 to F3. The marly interval, which is supposed to be an equivalent of the Marnes d'Uttins, may correspond to a maximum flooding surface (mfs), so this interval should be a transgressive system track (TST).

– From 8.4 to 34.5 m: the microfacies shift from F3 to F4 (at about 12 m), then rapidly from F4 to F6 (between 15.5 and 18 m). Then, F6 microfacies are recognized until 34.5 m. This shallowing upward evolution should correspond to a HST that lasts until a sequence boundary pointed out by erosive features such as reworking and channels.

– From 34.5 to 37.8 m: the evolution is deepening upward, from F6 to F3. Consequently, the marly and glauconitic layers previously described (paragraph 3.2) should correspond to a mfs and this interval to a TST.

– From 37.8 to 50 m: the microfacies evolve gently from F3 to F6 in a two steps fashion, with an acceleration of

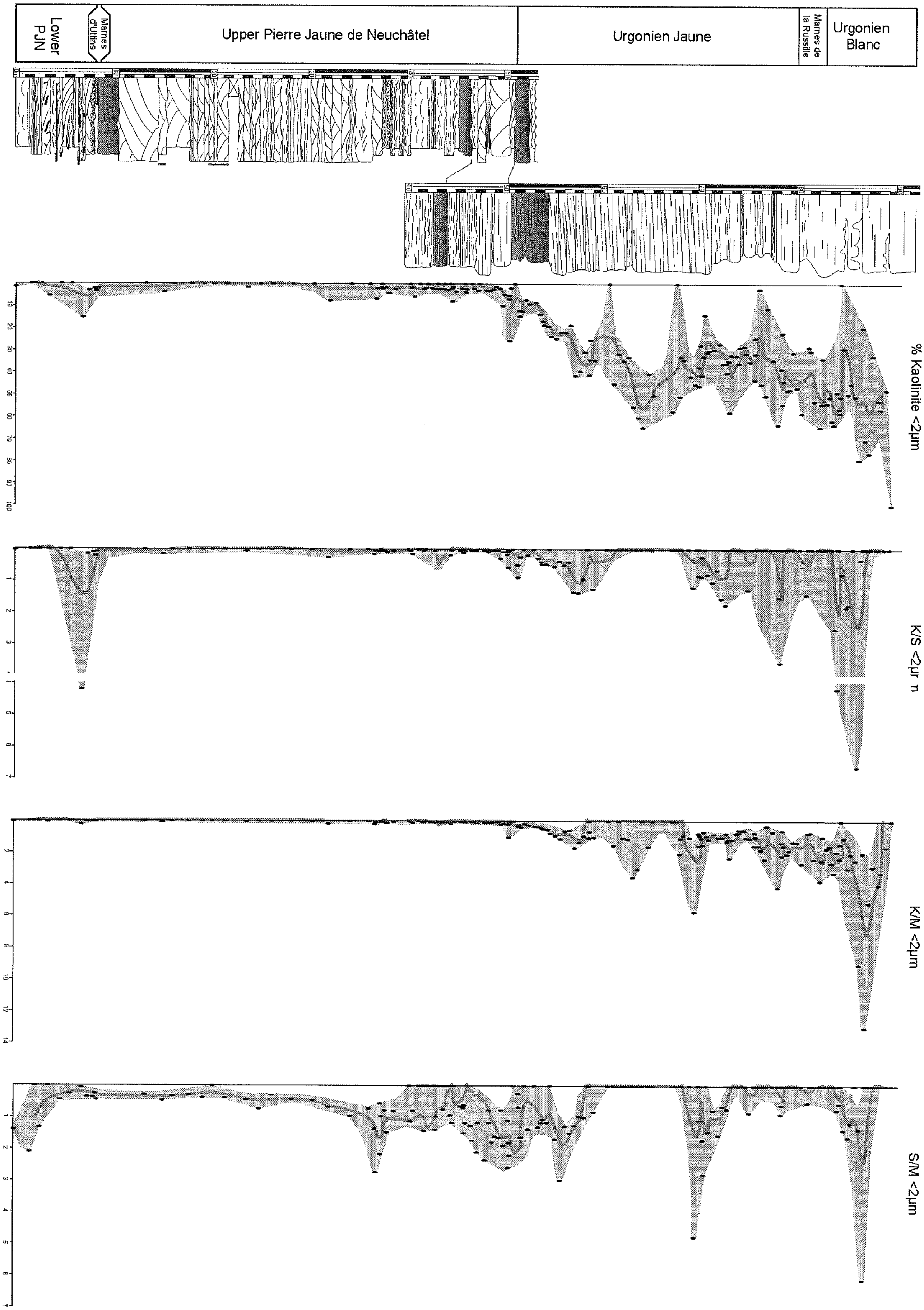

Fig. 34.- Kaolinite contents for the < 2 µm fraction for the Eclépens section (upper part after Blanc-Aletru, 1995) expressed in relative percents. Kaolinite / smectite, kaolinite / mica and smectite / mica ratios curves are also reported.

the evolution at approximately 45 m. This deepening upward progression may be related to a HST. At 50 m, reworking occurs, in particular pebbles with oysters were found. This surface is interpreted as a major sequence boundary (Ju2 in Blanc-Aletru, 1995).

– From 50 to 72.5 m: in detail, the microfacies curve displays high frequency changes from F3 to F7, but the general trend is a deepening upward evolution from F6 to FT microfacies. The high-frequency variations should be related to parasequence deposits. The FT microfacies should mark the mfs, and consequently this interval corresponds to a TST.

– From 72.5 to 80 m: the shallowing upward evolution of the microfacies curve led us to conclude to the presence of a HST, which ends with a sequence boundary marked by the dissolution of oolites cortex (Ju5 in Blanc-Aletru sequence stratigraphy scheme).

– From 80 to 83 m: the Marnes de la Russille display FT microfacies and correspond to a mfs. Thus, this small interval could be related to a TST.

– From 83 m to the top: the microfacies curve shows a general shallowing upward trend. At approximately 91.5 m, Blanc-Aletru described an emersive surface with microkarstification, which is interpreted as the sequence boundary Ju6. The presence of karsts in this part of the Urgonien Blanc supports this statement. This last part of the section should therefore correspond to a HST.

3.2.3. Mineralogy

At Eclépens, the <2µm clay minerals association is composed of mica, kaolinite, smectite, illite-smectite mixed-layers and chlorite, with mean values of 38, 22.6, 20.2, 14.9 and 4.2 %, respectively. Relative abundance of kaolinite, the kaolinite / smectite, kaolinite / mica and smectite / mica ratios are presented in figure34.

The entire Pierre Jaune de Neuchâtel is characterized by the absence of the kaolinite, whereas the smectite / mica ratio reaches values of about 1. Then, from 50 m upward, the kaolinite content increases, with values attaining almost 50% in the upper part of the section. In the same interval, the kaolinite / mica ratio is above 2, so the kaolinite is the dominant mineral of the clay mineral assemblage in the Urgonien Jaune and the Urgonien Blanc. This conclusion is also supported by kaolinite / smectite ratio with values above 2.

This rapid and drastic change in the main clay mineral type can be interpreted in terms of climate changes. Normally clay minerals are formed on continents and the type on clay being accumulated is dependent on the regional climate regime (principally on the rate of hydrolysis) and on the kind of rock that is being altered. The kaolinite is preferentially formed under hot and wet conditions, such under inter-tropical climate. On the other hand, smectite is generated under drier conditions, and its formation happens primarily under climate with well-marked seasons. So, it seems that between the time of deposition of the Pierre Jaune de Neuchâtel and of the Urgonien Jaune and Urgonien Blanc, the climate shifted from a relatively dry and seasonal climate, under which the mechanic erosion of land masses was predominant, toward inter-tropical conditions which favoured hydrolysis and thus the formation of kaolinite-rich soils. The later would enrich the oceanic sediments after erosion and transport to the basin.

4.– Dating the Urgonian Limestones from the Neuchâtel area

4.1. Strontium isotopes

During the early Cretaceous, the oceanic $^{87}Sr/^{86}Sr$ curve fluctuates. In particular, this curve shows a maximum at about 0.707455 in the late Hauterivian, then a minimum at 0.707450 in the earliest Barremian. The whole part of the Barremian is characterized by values higher than 0.707455, reaching two maxima (higher than 0.707550) in the end of the early Barremian and in the late Barremian. $^{87}Sr/^{86}Sr$ values then decrease rapidly in the latest Barremian and in the early Aptian (Jenkyns and Wilson, 1999; Veizer *et al.*, 1999; van de Schootbrugge, 2001). With these developments it seems possible to attribute an age to the Urgonian limestones.

Recently $^{87}Sr/^{86}Sr$ isotope work has been carried out at the University of Neuchâtel in order to refine our age estimates. $^{87}Sr/^{86}Sr$ was measured on brachiopods shells (rhynchonellids). The diagenetic state was controlled by both Scannig Electronic Microscope (SEM) analysis and by cathodoluminescence prospecting.

- Regardless of magnification, SEM images (fig. 35a) show the preservation of the primary lamellar structure of the secondary layer of the rhynchonellids shells, which is supposed to be less sensitive to diagenetic changes (e.g. Voigt *et al.*, 2003).
- The secondary layer of all analysed brachiopods was not luminescent (fig. 35b), revealing no mineralogical change.

From that we conclude that the diagenesis had little or no impact on the isotopic composition of the analysed shells.

The results of the $^{87}Sr/^{86}Sr$ analysis are shown in figure 35. Brachiopods from the Marne Bleue d'Hauterive and from Marnes d'Uttins display similar values to the ones obtained from the base and middle parts of the Hauterivian, respectively, which is in agreement with the dating obtained by ammonite biostratigraphy. Values from the Urgonien Jaune are comparable to the ones of the late Hauterivian or of the early Barremian. Finally, brachiopods from the Marnes de la Russile and from the top of the Urgonien Blanc give values typical for the Barremian, in particular one rhynchonellid from the Urgonien Blanc holds value of 0.707554 which is not recorded elsewhere other than in the late Barremian.

As a partial conclusion, even if there are still doubts on the age of the Urgonien Jaune, the Urgonien Blanc could be clearly attributed to the late Barremian.

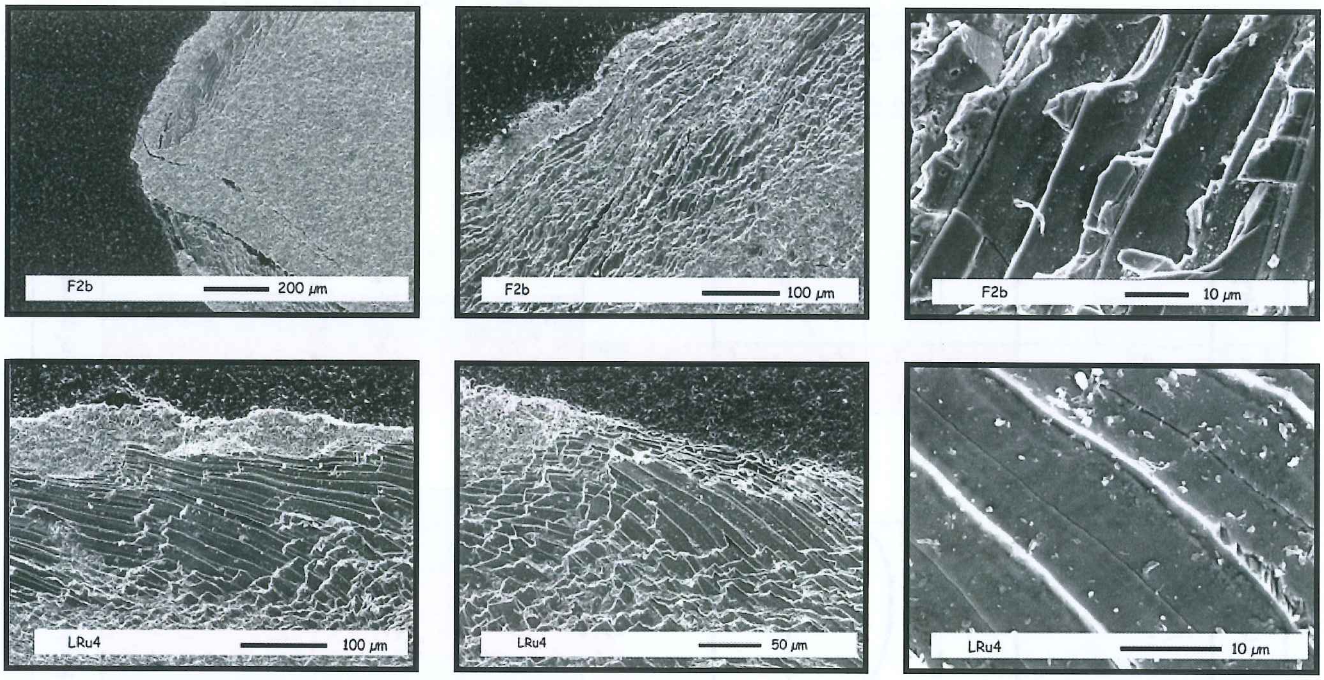

a

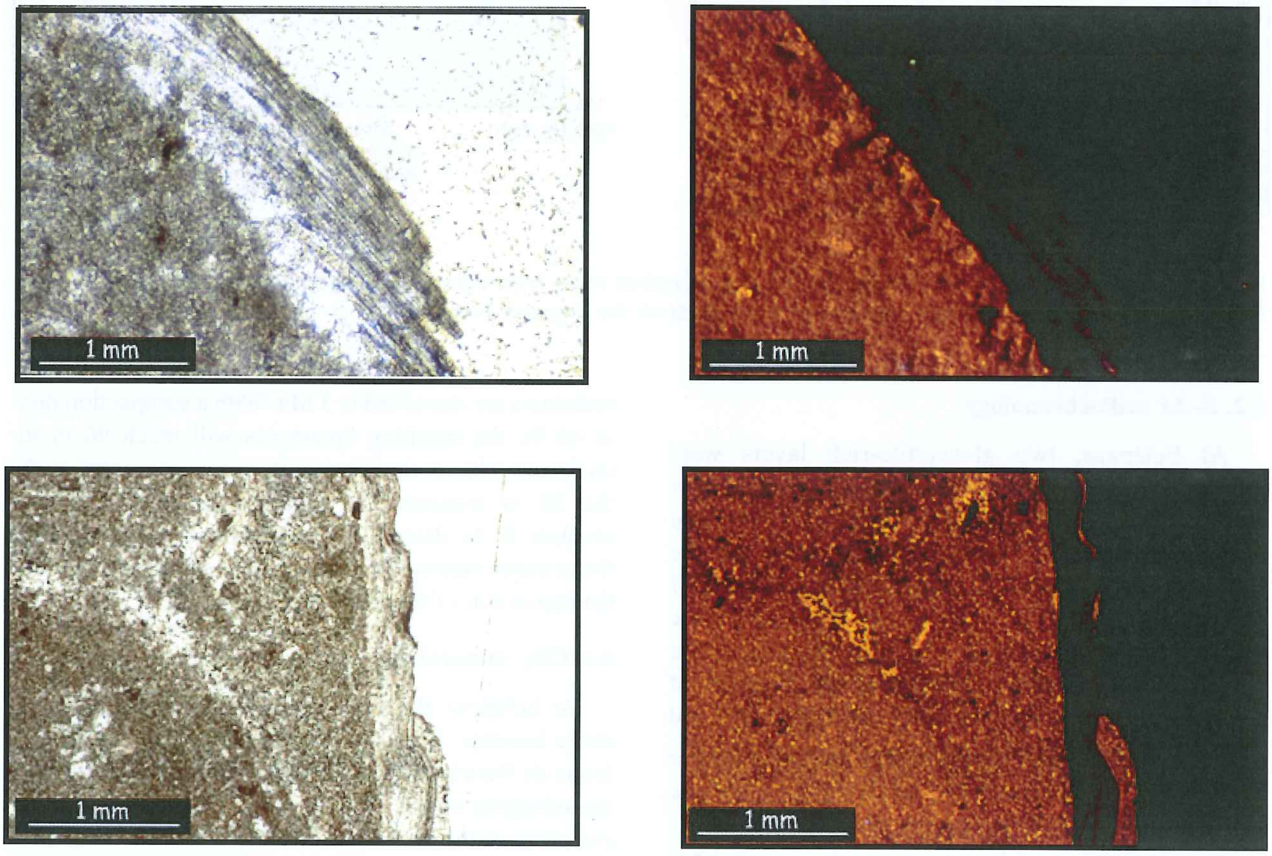

b

Fig. 35.- SEM (a) and cathodoluminescence (b) observations of rhynchonellids shells. In (a), the magnification increases to the right, revealing the good preservation of the lamellar structure of the secondary layer of the rhynchonellids shells. In (b), the micritic infill displays orange to brown colour whereas the non luminescence of the secondary layer testifies to the low diagenetic impact on the brachiopods shells.

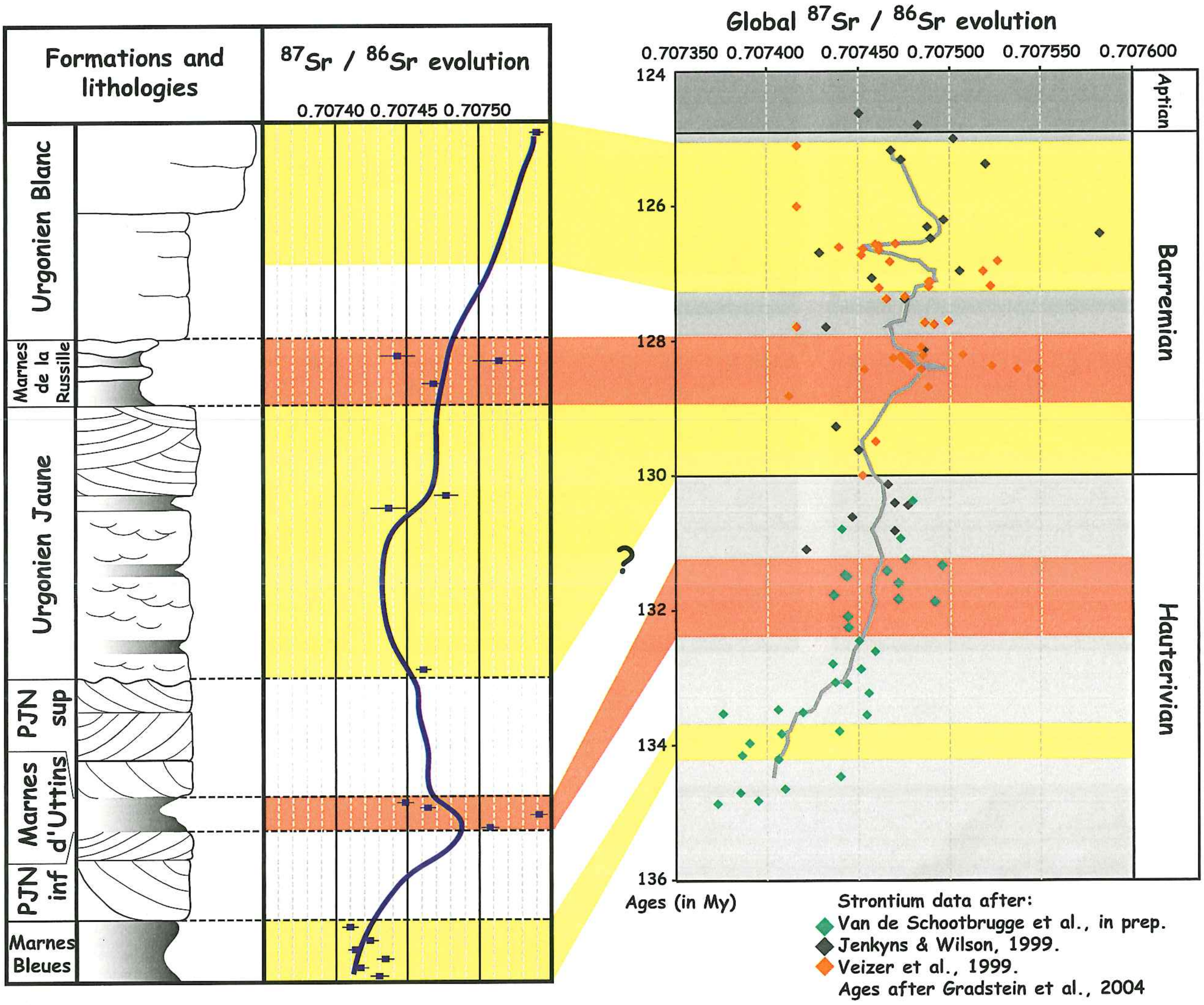

Fig. 36.- Comparison of the $^{87}Sr/^{86}Sr$ measured in rhynchonellids shells from the western Swiss Jura with the global oceanic $^{87}Sr/^{86}Sr$ curve. Note that doubts remains for brachiopods of the Urgonien Jaune.

4.2. K-Ar radiochronology

At Eclépens, two glauconite-rich layers were sampled in order to perform K-Ar dating. The first corresponds to the hardground rich in glauconite and oyster (sample ECII 21; cf. paragraph 3.2), and the second one to the glauconitic rich interval situated at 37 m (sample ECII 57). After hand separation, the glauconite grains were digested in an acid cocktail. The potassium content was measured at the Institute of Geology of the University of Neuchâtel by ICP-MS, and the ^{40}Ar was obtained on a VG1200 mass-spectrometer at the "Centre de Géochimie de la Surface" of the University of Strasbourg (France).

Even if XRD analyses of the glauconite revealed that they are relatively well evolved, K-Ar assign too young an age: ECII 21 is dated at 126.2 +/- 2.5 Ma and ECII 57 at 123.2 +/- 2.4 Ma, which are ages close to the Barremian–Aptian boundary (after Gradstein *et al.*, 2004).

On the other hand, if we assume a sedimentation rate of 5 cm.yr^{-1}, approximately 150 m of calcareous sediments are deposited in 3 Ma. With a compaction rate of 40 %, the resulting limestones will reach 90 m in thickness. This is therefore quite more, compared with the 30 m measured at Eclépens between the two absolute K-Ar dates. This inconsistency demonstrates that a major discontinuity occurred at some point during the deposition of these sediments.

4.3. Clay mineral correlation

At Eclépens, the evolution of the kaolinite shows a sharp increase from the boundary between the Pierre Jaune de Neuchâtel and the Urgonien Jaune upward. In the subalpine chains, Viéban (1983) described such an evolution in the Barterand section, where the kaolinite appears just after the discontinuity "D" which corresponds to the Hauterivian – Barremian boundary.

Recently, the mineralogy of the Angles section, the Barremian stratotype, was analysed, and surprisingly, in the <2μm fraction, the kaolinite appears gradually at the base of the *Balearites balearis* ammonite zone, and reaches amount of 40 to 70 % during the Barremian (see

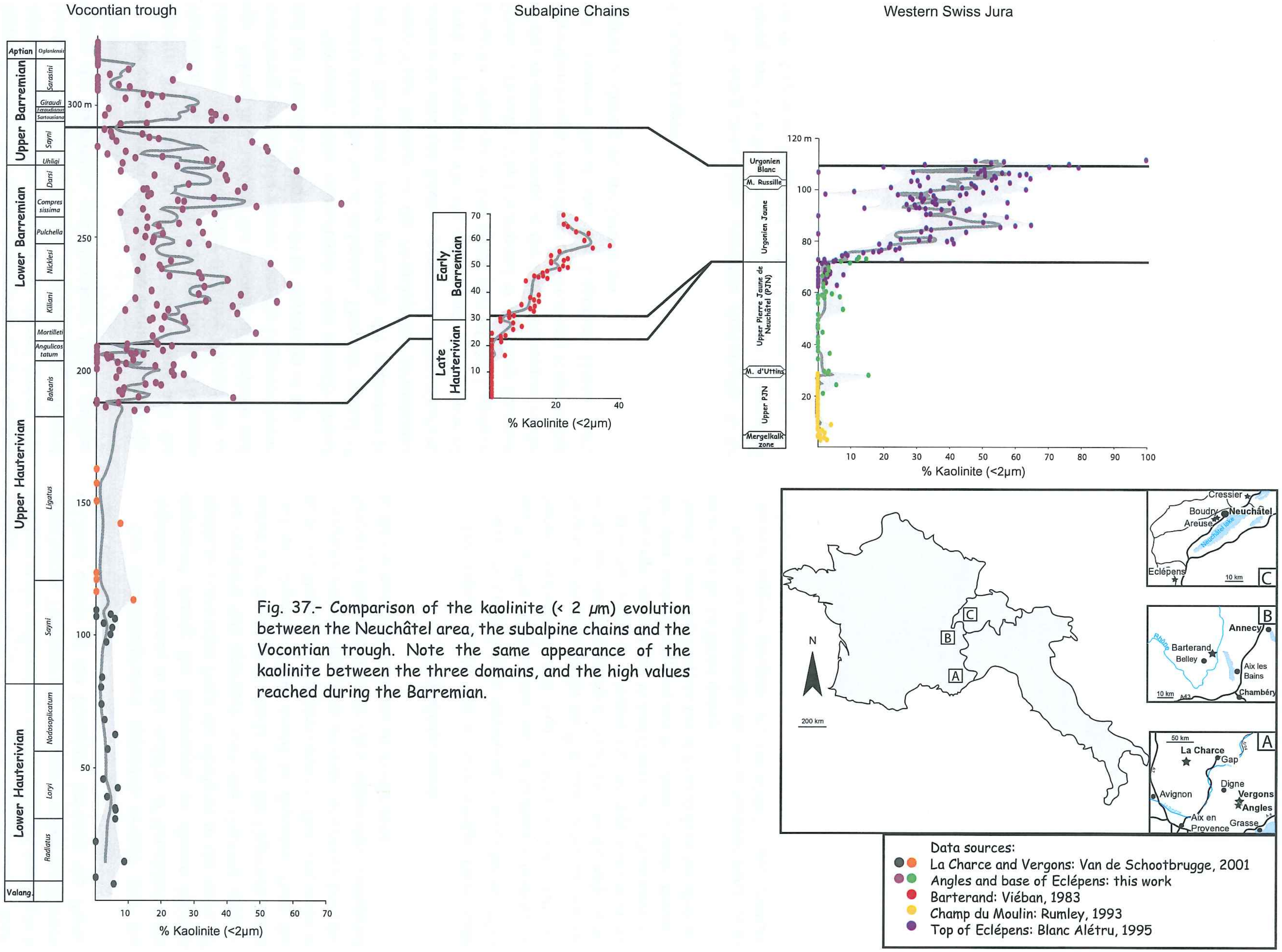

Fig. 37.- Comparison of the kaolinite (< 2 µm) evolution between the Neuchâtel area, the subalpine chains and the Vocontian trough. Note the same appearance of the kaolinite between the three domains, and the high values reached during the Barremian.

this volume, Day 4). Kaolinite content is compiled in figure 37, from the latest Valanginian to the earliest Aptian; whereas this mineral is absent during the Hauterivian, it becomes the dominant clay mineral during the Barremian, and disappears in the earliest Aptian.

The correlation of the kaolinite evolution, from the western Swiss Jura to the subalpine chains and the Vocontian Trough (fig. 37), indicates that the Urgonian limestones would be not older than late Hauterivian in age. Taking into account the amount of kaolinite and correlating comparable values, then the Urgonien Jaune and the Urgonien Blanc would be Barremian in age.

Moreover, some nannofossils were recently found directly above the Ju2 at Eclépens. They are typical of the late Barremian; more precisely the nannofossils assemblage belongs to the *Hemihoplites feraudianus* ammonite zone (de Kaenel, personnal communication; work in progress). On the other hand, the absence of kaolinite observed in the upper part of the Urgonien Blanc at Boudry may correspond to the sharp decrease of this mineral observed in the latest Barremian of the Vocontian trough. From these observations, it seems that the Urgonien Jaune and the Urgonien Blanc were deposited during the late Barremian.

5–. Conclusion

By using mineralogy, sequence stratigraphy, K-Ar dating and $^{87}Sr/^{86}Sr$ stratigraphy, ages can be assigned for the Urgonien Jaune and of the Urgonien Blanc.

Whereas the lower Pierre Jaune de Neuchâtel belongs undoubtedly to the early Hauterivian, at least one gap in the sedimentary record occurred, leading to a huge hiatus. This later can be located within the Marnes d'Uttins and/or at the boundary between the Pierre Jaune de Neuchâtel.

Our multidisciplinary approach reveals that the urgonian limestones in the vicinity of Neuchâtel were deposited during the Barremian, as shown by the kaolinite correlation from the platform to the basin. If we combine this approach with the $^{87}Sr/^{86}Sr$ measurements in brachiopods shells, then the Urgonien Jaune and the Urgonien Blanc would be deposited from the early–late Barremian transition onward. This conclusion is consistent with the age of the urgonian limestones from the Vercors or from the Helvetic Alps, where they correspond to the *Gerhardtia sartousiana* ammonite zone.

Acknowledgements

The authors would like to acknowledge Peter Stille (University Louis Pasteur, Strasbourg, France) for the ^{40}Ar and $^{87}Sr/^{86}Sr$ measurements, and Jan Kramers (University of Berne, Switzerland) and Viginie Matera (University of Neuchâtel, Switzerland) for the ^{40}K analysis.We are grateful to Haydon Mort (University of Neuchâtel) for the help on the field in the Gorges de l'Areuse and the improvement of the manuscript, and to André Villard (University of Neuchâtel) for the thin sections preparations.We thank Claude Brocard, André Caluori and François Girod from Holcim for allowing us to study the La Sarraz quarry.

Finally, we acknowledge the Swiss National Fund for its financial support (projects n°2100-067807/1 and 200020-105206/1).

Day 2

Urgonian deposits and Barremian-early Aptian sequence stratigraphy in the Vercors massif

Annie Arnaud-Vanneau, Hubert Arnaud, Elisabeth Carrio-Schaffhauser and Mohamed Chaker Raddadi

Purpose of the day.– This day is devoted to 1) the Barremian-Lower Aptian platform facies and sequence stratigraphy (Gorges du Nant section, Northern Vercors) and 2) the first approch of the Urgonian platform bank margin near the Col de Rousset (Southern Vercors) and in the Die area (Plateau de Glandasse, a famous panorama). Les Rimets incised valley will be visited only if weather is very rainy on the Southern Vercors.

Itinerary.– Grenoble, Cognin and Gorges du Nant section, Balcon des Ecouges, Rencurel syncline until the Col de Rousset, Die, Châtillon-en-Diois and les Nonières.

Berriasian-Valanginian bank margin. Overview of the Cluse de l'Isère near the Hotel

Near Veurey between Cognin and Grenoble, along the "Cluse (transverse valley) de l'Isère", the Berriasian-Valanginian bank margin is clearly visible, with well developped lowstand prograding wedges. This bank margin is more narrow and steep than that of the Urgonian platform, as exposed during day 3.

The Upper Jurassic Jura-Bas Dauphiné platform margin is located near the Bec de l'Echaillon. At this place, the series is made up of, from bottom to top :

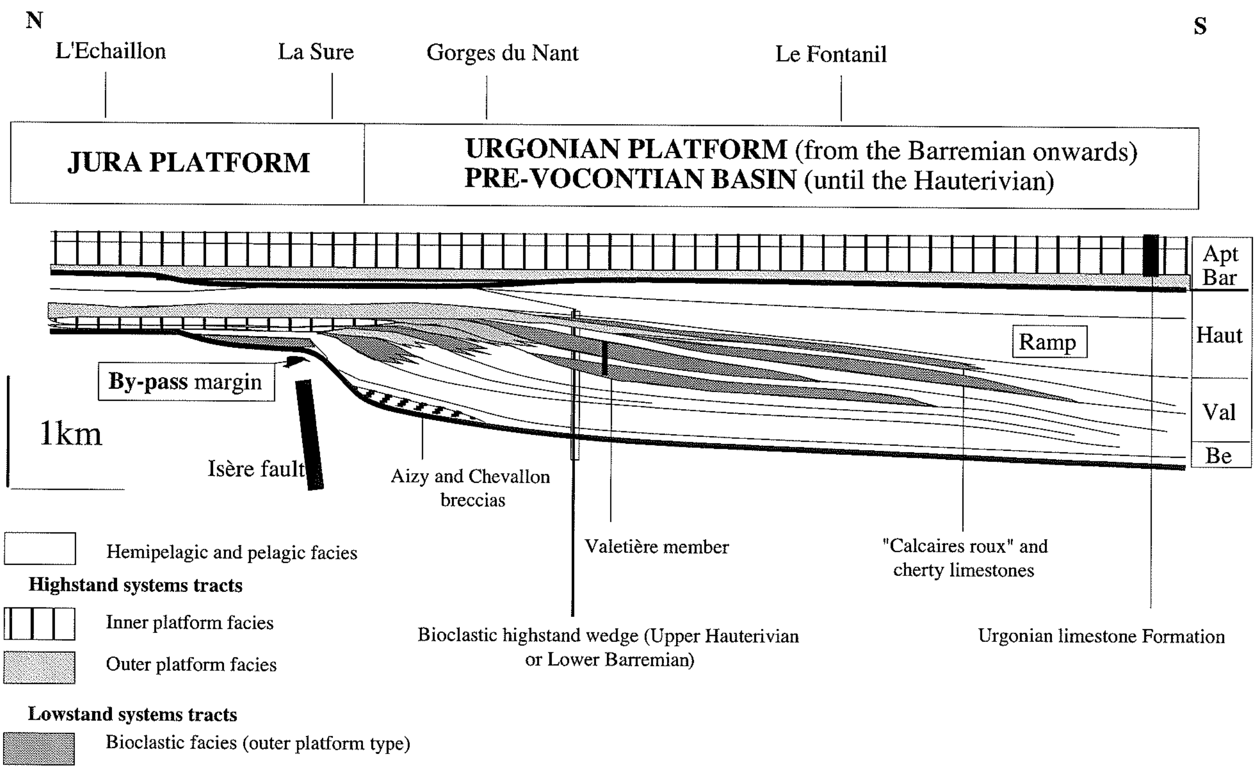

FIG. 38.- Section accross the edge of the Berriasian-Valanginian platform near Veurey.

– a first cliff made up of reefal limestones (Upper Jurassic reef),
– a transgressive marly level (basal Upper Berriasian),
– platform limestones of the Upper Berriasian and Lowermost Valanginian,
– Hauterivian marls and argillaceous limestones,
– the Urgonian limestones (inner platform facies).

Near Veurey-Le Fontanil (10 km North from Grenoble, near from our hotel), the Berriasian-Valanginian paleoslope shows (fig.):

1.– Basinal facies up to the upper part of the Upper Berriasian: *Calpionella*-bearing Tithonian limestones, Berriasian hemipelagic argillaceous sediments. These hemipelagic facies grade laterally to the North, on a less than 2 km distance, to platform facies (including facies with rudists at la Grande Sure).

2.– Lowstand wegdes at the Berriasian-Valanginian boundary (Valetière member, BE7 and VA1 sequences). Both of them disappear laterally to the North towards the platform edge, and display clinoforms and progradation of bioclastic facies to the South, towards the basin. The facies is a coarse-grained limestone with large foraminifers (*Pfenderina neocomiensis*) which laterally changes to argillaceous limestone containing few calpionellids. The presence of these both prisms implies :

– an important and rapid lowering of the relative sea level at the end of the Upper Berriasian (Cimmerian tectonically enhanced unconformity ?),
– a progressive rise of the sea level from the Berriasian-Valanginian limit.

3.– Vertical grading from a standard platform sedimentation up to a drowned platform sedimentation since the Upper Valanginian (which is generally missing on the Jura platform) and above all in the Hauterivian (important rise of the relative sea level).

4.– The Barremian (SbB1) tectonically enhanced unconformity which corresponds to a great drop of the relative sea level and emergence of the Jura-Bas Dauphiné platform. The overlying Urgonian limestone Formation show the sudden superposition of the Upper Barremian inner shelf facies above the Hauterivian hemipelagic marly limestones. Due to the tectonnically enhanced unconformity, no continuous progradation can be observed between Hauterivian and Upper Barremian, but a great paleogeographical change occurs: everywhere in the SE part of the Northern Subalpine Chains, the Urgonian limestone Fm. appears as the first platform body at the top of the basinal series of the Pre-vocontian trough.

Section within the Urgonian platform: Upper Barremian-Lower-Aptian of the Gorges du Nant

1.– Introduction

1.1. The Gorges du Nant section: general overview

Until the Valanginian, the Gorges du Nant section was located on the edge between the Jura-Bas Dauphiné platform and the Pre-vocontian basin. After the Late Hauterivian-Early Barremian crisis, the platform margin moved 60 kilometres southwards: the Gorges du Nant section was then located in the inner domain of the Urgonian platform.

The Gorges du Nant section is the best one of the Northern Vercors and could be considered as a school-type section. It is the reason why the *Parc régional du Vercors*.has protected this section.

From the bottom to the top, three main units are visible (the two first crop out along the river Nant while the last is well exposed long the road from Cognin-les-Gorges to Malleval).

1) Marls and marly limestone with *Toxaster* and bivalves (the so-called « couches à panopées »). The top of this thick level crop out along the Nant river, but all the marly Hauterivian series, more than 300 m thick, crop out in the St. Pierre-de Chérennes section, four kilometres south-east from the Gorges du Nant one. In the latter, marly limestone contain at the top *Crioceratites duvali* and *Spitidiscus ligatus* (Plate 41), two species that together characterized the *Plesiospitidiscus ligatus* zone, second of the Upper Hauterivian zones. Then this level is typical from the middle part of the Upper Hauterivian. In other points of the Northern Vercors, a few ammonites of the *Pseudothurmmannia angulicostata auct.*, of the uppermost Upper Hauterivian, have been collected so that it is clear that the top surface of the hauterivian marly limestones series was well-eroded before the deposition of the Urgonian limestones.

2) A 30 m thick bioclastic level which corresponds to a depositional sequence made of fine-grained wackestone-packstone to grainstone (facies F2 and F3). The maximum flooding surface is a more marly level with a large number of *Toxaster*. The basal sequence boundary is an irregular surface on which centimeter-scale quartzitic and calcareous pebbles occur. Until this day, this depositional sequence is undated. It corresponds perhaps to the HA7 or BA1 depositional sequence. The most interesting thing is that this sedimentary body does not exist everywhere in the

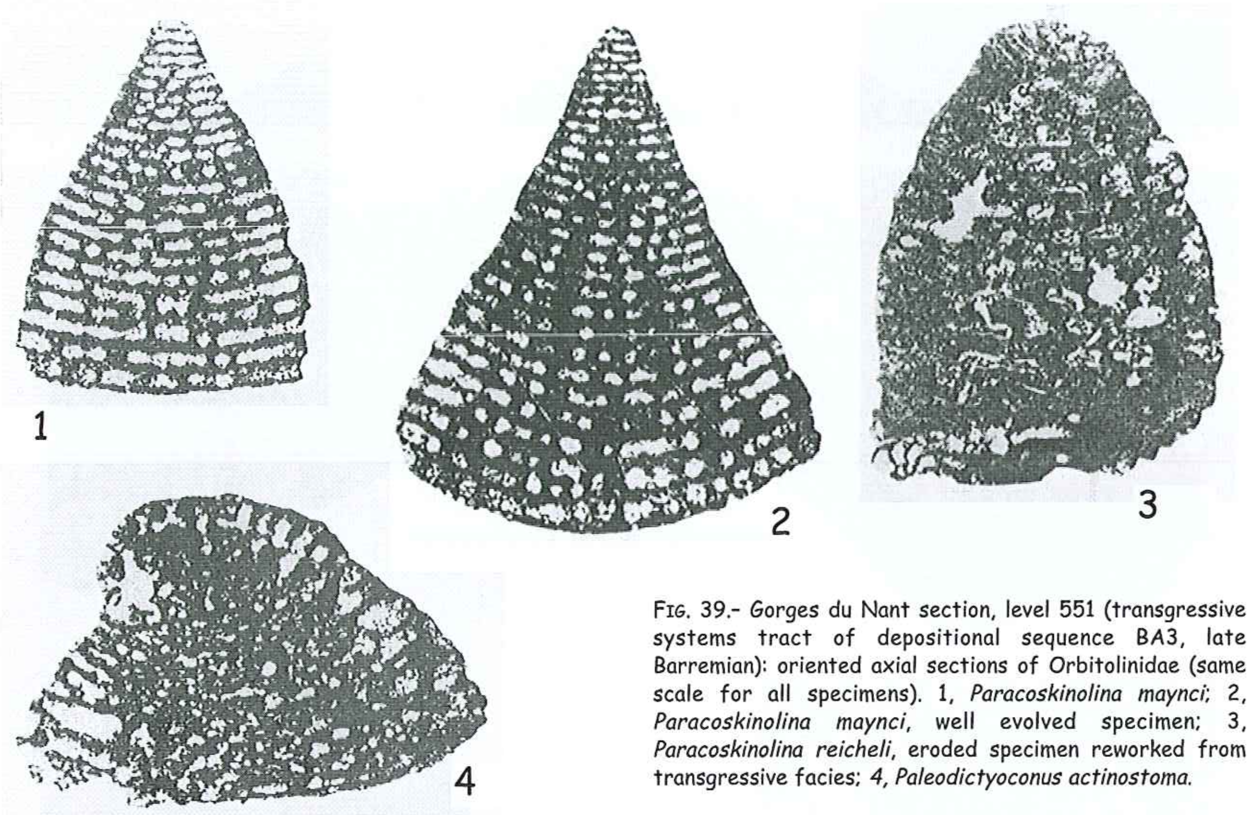

FIG. 39.- *Gorges du Nant section, level 551 (transgressive systems tract of depositional sequence BA3, late Barremian): oriented axial sections of Orbitolinidae (same scale for all specimens). 1, Paracoskinolina maynci; 2, Paracoskinolina maynci, well evolved specimen; 3, Paracoskinolina reicheli, eroded specimen reworked from transgressive facies; 4, Paleodictyoconus actinostoma.*

Northern Vercors (for example in the Balcon des Ecouges and Pas de Pré Coquet section, near the Gorges du Nant). The last parasequences of this unit are visible along the road.

3) The Urgonian limestone Fm. is well exposed along the road. It is a more than 300 m thick unit that xill be studied in detail during the field-trip.

According to the vertical facies distribution, four depositional sequences can be observed within the Urgonian limestones Fm., all of them characterized by well developed transgressive systems tracts and highstand prograding wedges. Lowstand systems tracts are missing.

These four depositional sequences (sequences BA3, BA4 and BA5 dated from Upper Barremian, AP1 dated from Lower Aptian) form massive cliffs (more than 300 meters thick) outcropping in the area of Grenoble and in the northern subalpine chains. This period of carbonate build up is associated with the early stages of an overall long-term transgression. The four sequences are mainly composed in this platform setting, of thick transgressive and highstand systems tracts, that overlay unconformably both the bioclastic limestones of the Glandasse limestones Fm. in the southern Vercors and the inner part of the Jura platform Pierre jaune de Neuchâtel Fm. (Jura) which had been emergent during the latest Hauterivian and early Barremian.

With the increasing rate of encroachment by coastal onlap during Lower Aptian time, the platform margin quickly evolves from overall aggradation to overall retrogradation. Thin deposits (Upper Aptian "Lumachelle" formation, Albian condensed section of the so-called "béton phosphaté", i.e. "phosphatic concrete") related to drowning unconformities overlay the previously deposited thick carbonates of the early transgression. This period of retrogradation also coincides with the maximum occurence of black shales in the basin (Bréheret and Delamette, 1988).

In carbonate platforms, sequence boundaries show early diagenesis processes, such as paleokarstification and early dolomitisation and dedolomitisation. The diagenesis is particularly complex beneath sequence boundaries which are surfaces that reflects erosion (dissolution) and early compaction; subsequently, cements are developed when the platform is again drowned (see E. Carrio-Schaffhauser, this volume).

Sea-level changes that occurred during Barremian to Aptian carbonate platform sedimentation are well represented beneath sequence boundaries by a succession of dissolution and cementation phases. Strangely, a porosity of variable preservation is also present beneath these surfaces, even if the origin of the porosity varies with the age of sequence boundary. Hence, each sequence boundary can be characterized regionally by its diagenetic sequence and type of porosity.

We will discuss the characteristics of the shelf members of these four sequences and how their stratal pattern evolves from the bottom upward with the overall increasing rate of relative sea level rise.

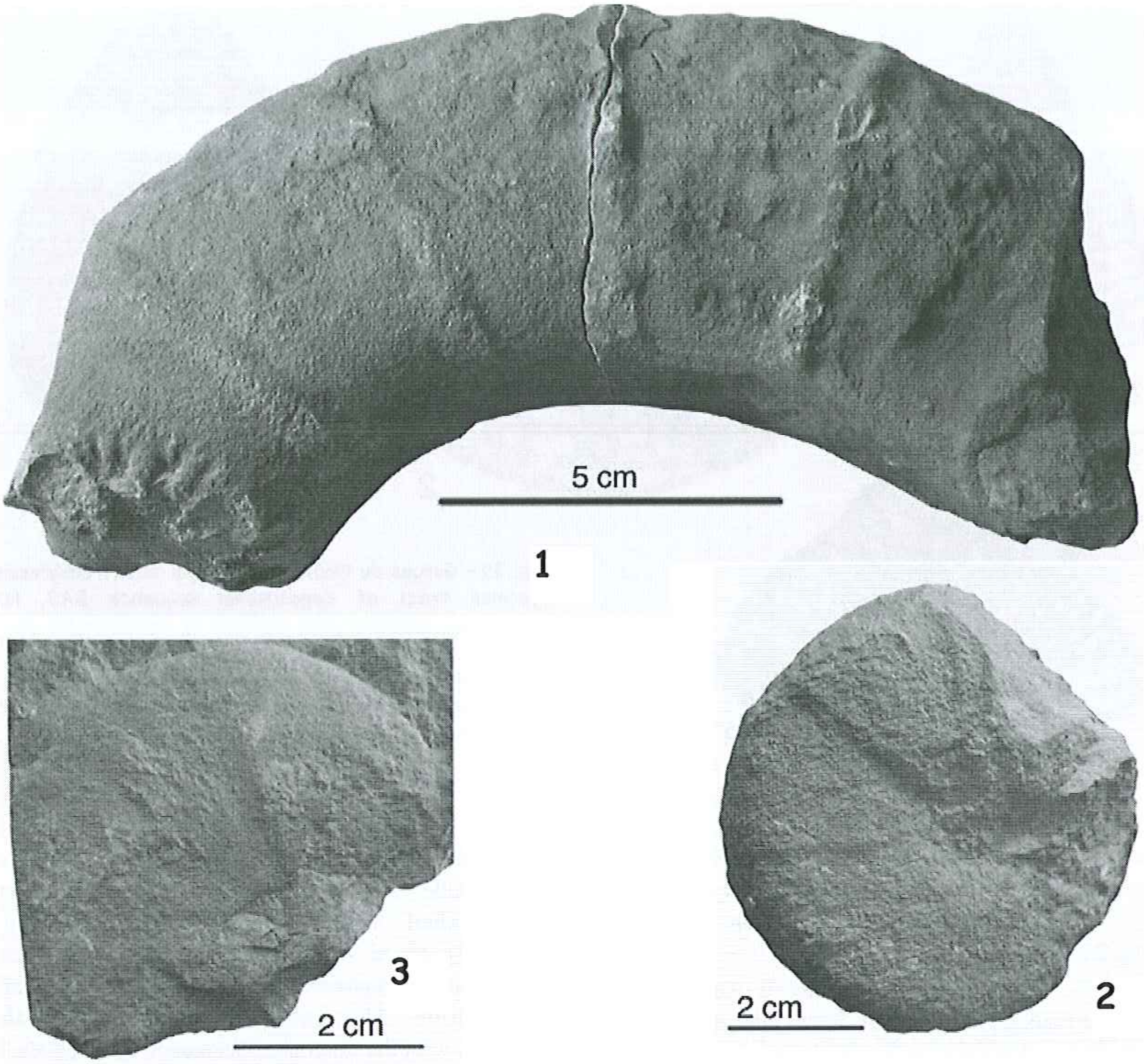

FIG. 40.- *Gorges du Nant*, section: ammonites collected on the upper part of the Hauterivian series (marly limestone with *Toxaster* and bivalves). 1, *Crioceratites* gr. *duvali*, just below sample 521, Arnaud-Vanneau (1980); 2, *Plesiospitidiscus ligatus*, sample 521, Arnaud-Vanneau (1980); 3, *Plesiospitidiscus ligatus*, just above sample 523.

2.– INTERPRETATION OF GAMMA-RAY LOGS IN CARBONATE PLATFORM

In well-logging, values of gamma-activity are measured by scintillometry. A conventional paradigm is to link high γ-activity to Potassium (K) and Thorium (Th) isotopes present in clays and to Uranium isotopes present either in detrital sediments (typically in zircon or monazite minerals) or to sediments rich in organic matter. In shallow-water carbonate platform, high γ-activities are interpreted in the same way. However, in a first γ-scintillometer survey of the *Gorges du Nant* section, we found inconsistencies between lithologies and their expected γ-responses: the highest radioactive beds do not correspond to high argillaceous or detrital limestones and marls, but to some low content argillaceous or "pure" limestones beds.

The aim of this study was to identify the radioactive isotopes associated to different types of carbonates, their localization, their abundance and their respective contribution to the total gamma response in order to propose a new method for the interpretation of gamma-ray logs in shallow-water carbonates.

This study was focused on two intervals:

- The first one corresponds to the Ba3 depositional sequence (Upper Barremian) which is composed essentially of limestones. We studied this sequence in the Vercors and Chartreuse subalpine massifs near Grenoble and in the Swiss Jura near Neuchâtel;
- The second one corresponds to the "Lower orbitolina beds" interval (lowermost Lower Aptian). We studied this interval in the Vercors and Chartreuse subalpines massifs near Grenoble, in Spain (Organya basin) and in central Tunisia near Kairouan.

In addition to the sedimentological, digenetic and isotopic studies of all these sections, we curried out detailed γ-scintillometry field surveys and performed analyses of selected samples from the *Gorges du Nant* (Vercors) and *Gorges du Frou* (Chartreuse) sections by low-level γ-spectrometry and ICP-MS. The results confirm the common idea that K and Th contents are associated to clays and detrital sediments. On the contrary, they show that Uranium contents does not follow the same behavior and are not associated to a specific lithology. In all the studied sections we noticed a good correlation between gamma-ray peaks and some key surfaces in sequence stratigraphy (sequence boundaries, maximum flooding surfaces and some parasequence boundaries). We noticed also a good correlation between uranium content peaks and the abundance of echinid fragments. In every analyzed samples, isotopes of the uranium decay series are by far the main source of gamma-activity. The contributions of K and of the Th decay series are negligible. Thus the interpretation of gamma-ray logs in shallow water carbonate platform should be revised: rather than a lithological index, it should be used to identify key surfaces in sequence stratigraphy in addition to other diagraphic tools.

3.– Description of the Urgonian limestones Fm

3.1. Depositional sequence BA3 (Upper Barremian)

3.1.1. Sequence boundary Sb B3

Below this sequence boundary, the hemipelagic facies and argillaceous limestones are mostly strongly dolomitized which is unusual in this type of marine facies. We refer this type of dolomitization to platform emersion and the subsequent first late Barremian marine transgression. This emersion and sequence boundary is not associated with any reservoir.

3.1.2. Depositional sequence BA3 (Upper Barremian)

Sequence BA3 forms the base of the Urgonian platform above the emergent surface related to the early Barremian exposure (Arnaud *et al.*, 1990).

The transgressive systems tract at the base is a few meters thick and displays lag deposits with thin pebbles onto the emersive surface, and from bottom upward fine-grained biosparite-grainstone with peloids and small foraminifers (F3 facies), and coarse, rounded skeletal debris grainstones with coral fragments (transgressive facies, Arnaud-Vanneau [1980]; Arnaud-Vanneau *et al.* [1987]).

The subsequent highstand systems tract evidences the first true Urgonian facies. In the Northern Vercors, it begins with high-energy grainstones (F3 facies) and ends with corals, bivalves, gastropods and spine of regular Echinoids (F7 facies) as well as, locally, the first wackestone-packstone beds with rudists and coral debris (F8 facies) and the first beachs (grainstone with keystone vugs) [Arnaud-Vanneau, 1980 ; Arnaud-Vanneau *et al.*, 1990]. At the top, the emergence related to the sequence boundary B4 is indicated by a discontinuity underlaid by a series of paleokarst cavities due to early dolomitization-dedolomitization and, in other sections, various types of emergent facies. The paleokarst cavities are now filled up with lateTuronian-early Senonian sediments (white sands with Bryozoans and red clays) that document the Turonian emersion.

3.2. Depositional sequence BA4 (Upper barremian)

3.2.1. Sequence boundary SbB4

The sequence boundary is associated with an early karstification, dolomitization and dedolomitization processes. A thick, dolomitized interval (up to 7 m) is developed (mixed water dolomitization) above a unit of fine-grained grainstones with keystone vugs (beach record). Interconnected microcavities (mm to cm in size) of Barremian age with bedded infillings are observed in the dolomitized matrix.

Karstification, however, developed later in response to major drops of sea-level during the Cenomanian and Turonian (due to the ante-Senonian folding). The resultant cavities are meter high and have a stratigraphic pattern along the sequence boundary. The cavity-filling deposits consist of white fine grain sand with silicified bryoza and a few foraminifers of Turonian-early Senonian age and red clays. This type of reservoir is a secondary reservoir. If it is associated with sequence boundary Sb B4 in the inner part of the platform and corresponds to later polyphazed evolution during the late Lower and early Upper Cretaceous fluctuations in sea level.

In the Vercors massif, the ante-Senonian folding, well-known in the Dévoluy massif, is responsible to a major emersion during the early Turonian.

3.2.2. Sequence BA4 (Upper Barremian)

The next transgressive systems tract in the same area of the Northern Vercors consists of innershelf shallowing upward parasequences. They "keep-up" over a thickness of more than 60 meters with the rising sea level and then "give-up" (25 meters) at the maximum flooding surface. Each parasequence consists of, from bottom up: wackestone-packstone with large rudists (F8 facies), packstone-grainstone or mudstone with small rudists and oncoids (F9 facies), wackestone with oncolites (F10 facies) and mudstone with small Miliolids (Istriloculina, F11 facies) associated with algal mats, bird's eyes, early dissolution and dolomitization, indicating the proximity of the emergent level at the end of each parasequence before the next flooding.

All these microfacies indicate the lagoonal nature of the depositional environments (shallow and restricted

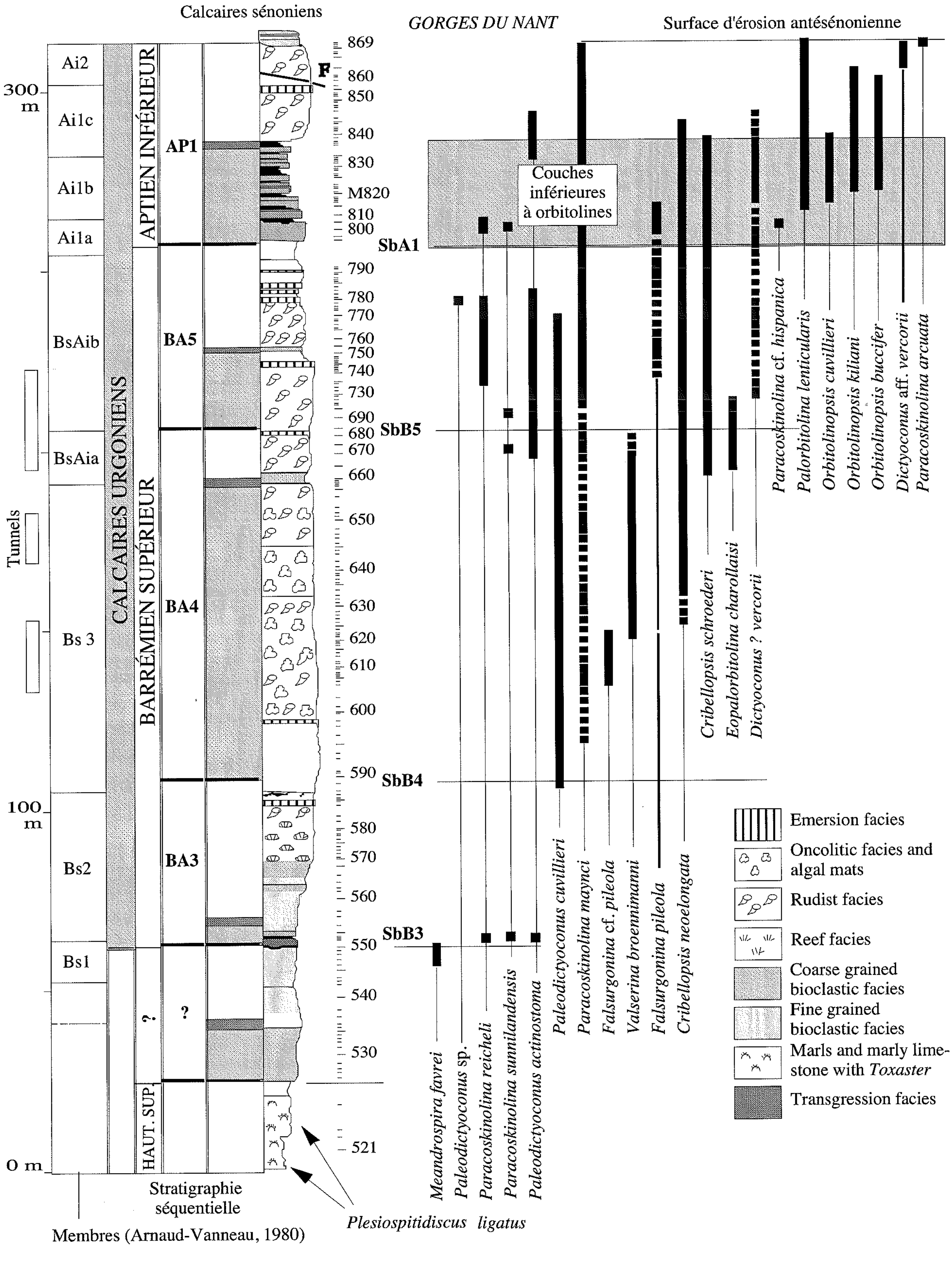

FIG. 41.- Distribution of Orbitolinidae and *Meandrospira favrei* in the Gorges du Nant section.

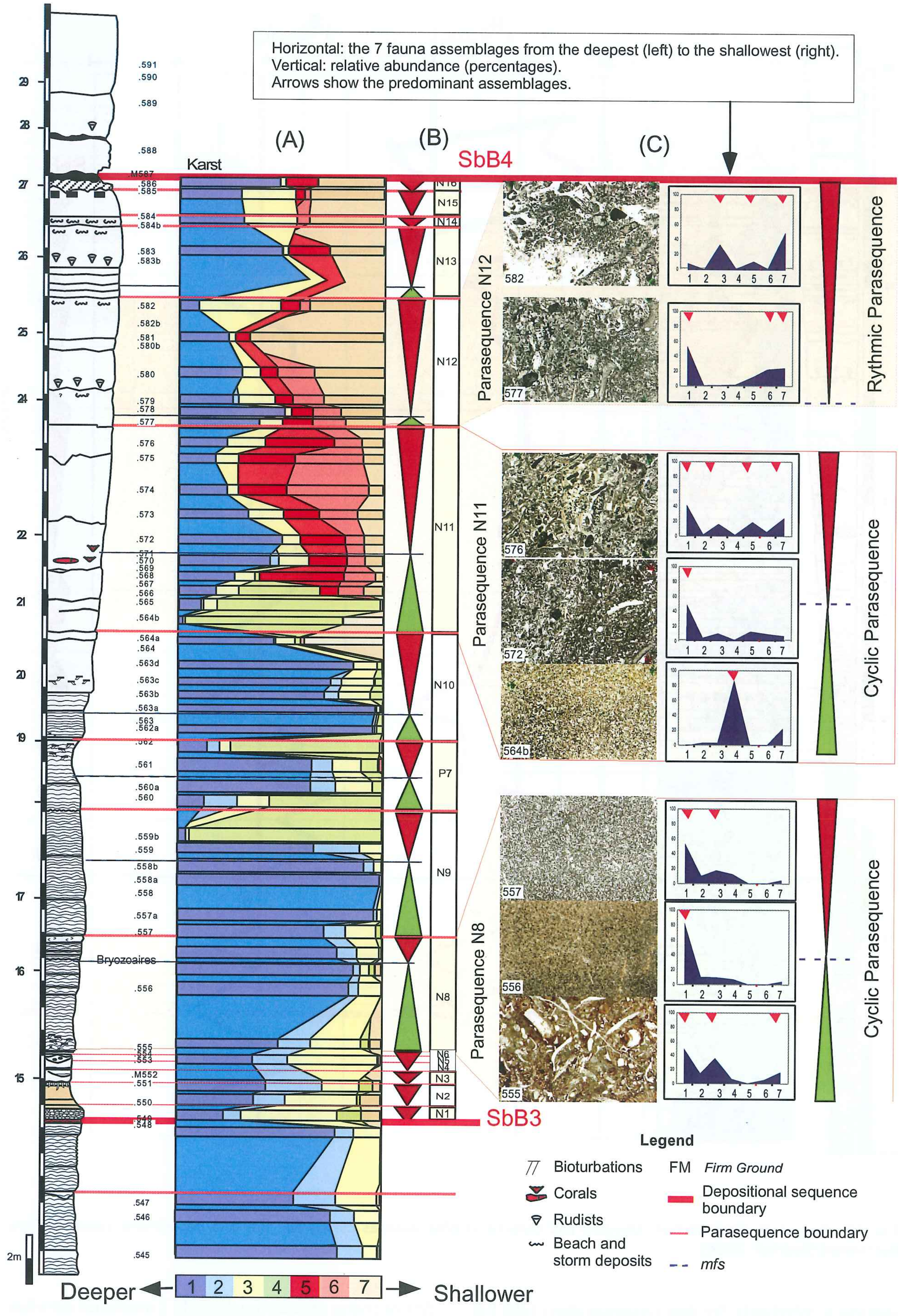

FIG. 42.- Gorges du Nant section: facies organization of parasequences belonging to depositional sequence BA3 (late Barremian) (Raddadi, 2004).

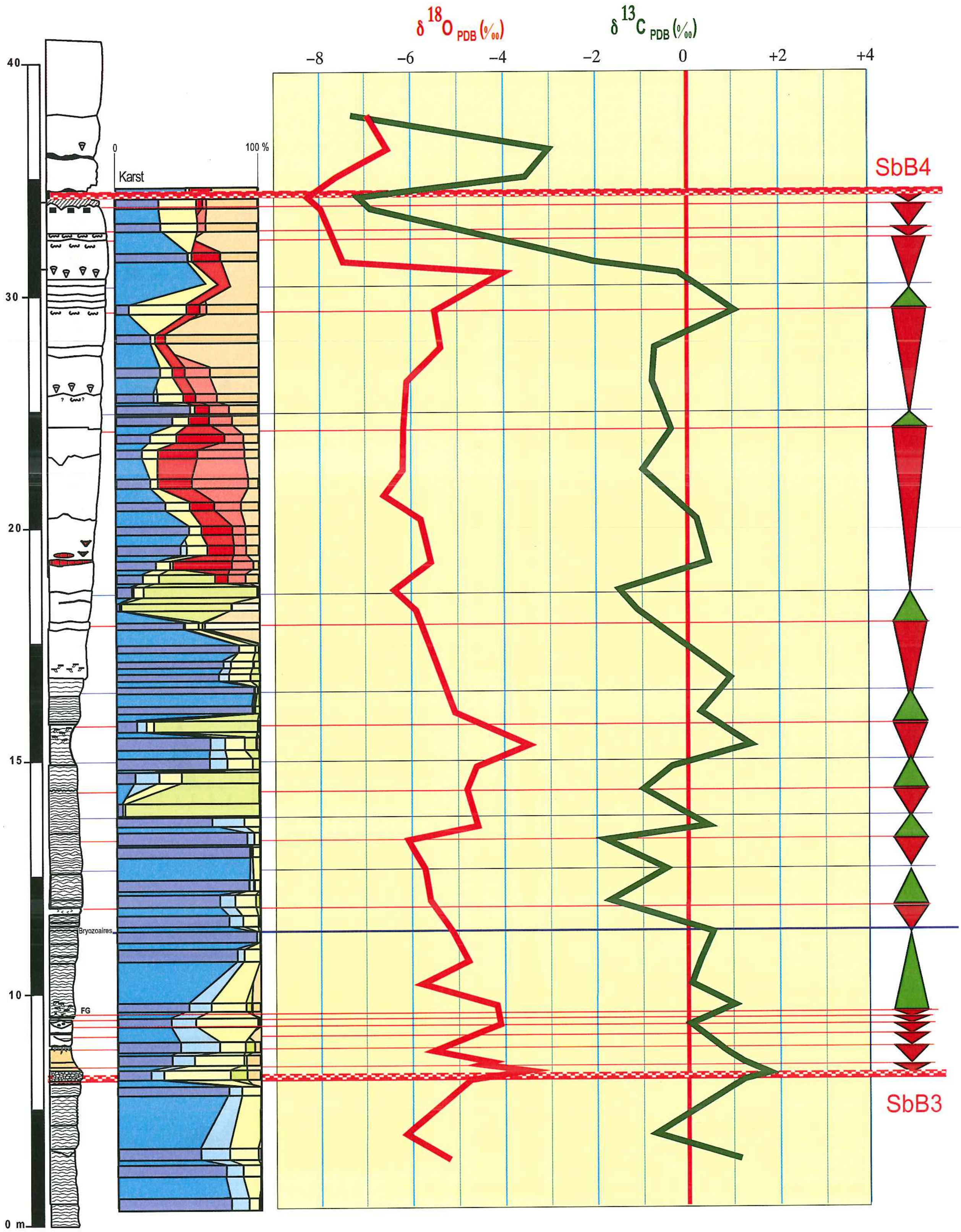

FIG. 43.- Gorges du Nant section: Oxygene and Carbone stables isotopes curves for the BA3 depositional sequence (late Barremian) (Raddadi, 2004).

subtidal to intertidal). We may recognize many tidal flat facies, especially muds deposited in quiet and protected areas with restricted conditions. We have not observed fine or coarse grained beach sands. Limestones are often dolomitized, especially those of facies F10 and F11.

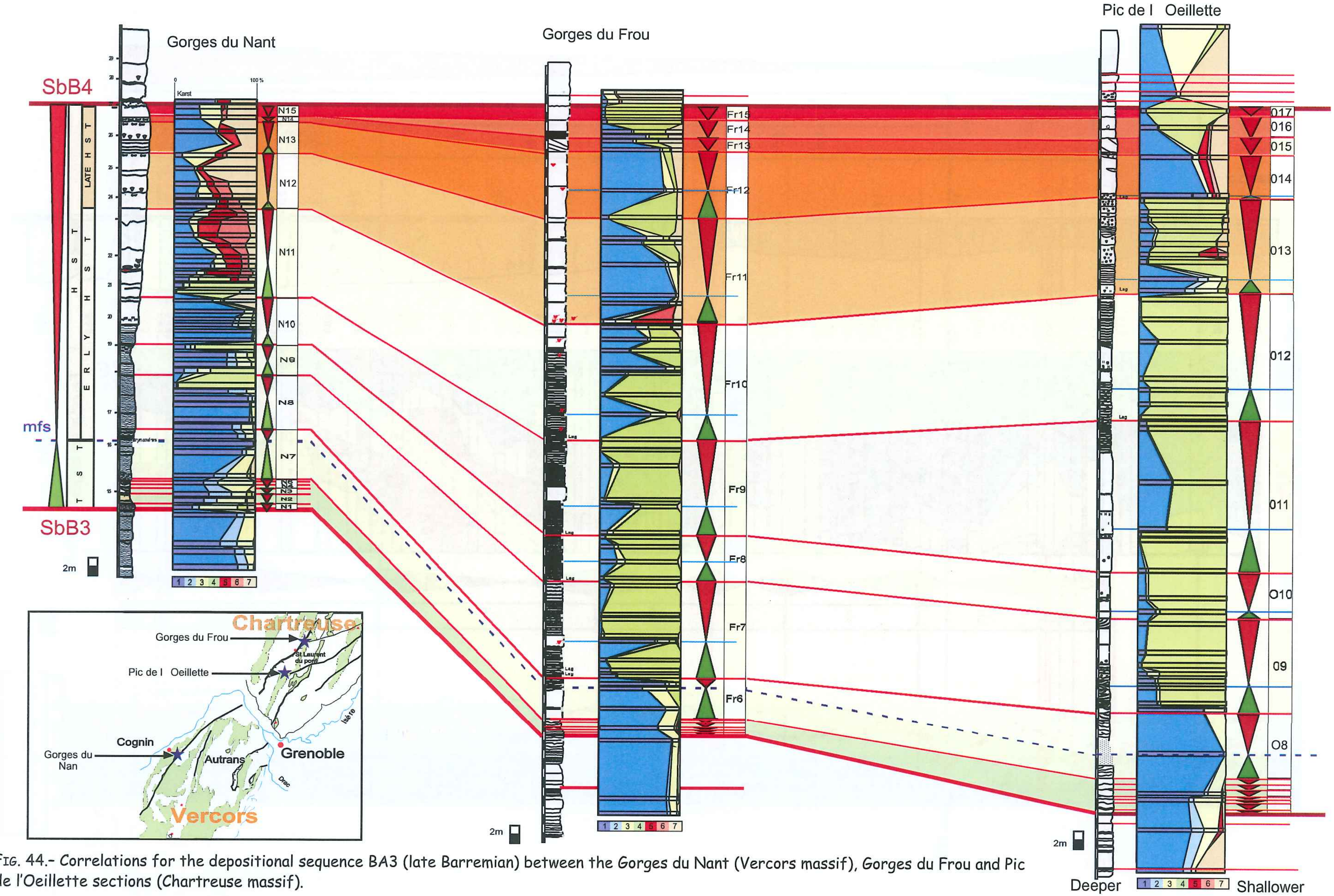

FIG. 44.- Correlations for the depositional sequence BA3 (late Barremian) between the Gorges du Nant (Vercors massif), Gorges du Frou and Pic de l'Oeillette sections (Chartreuse massif).

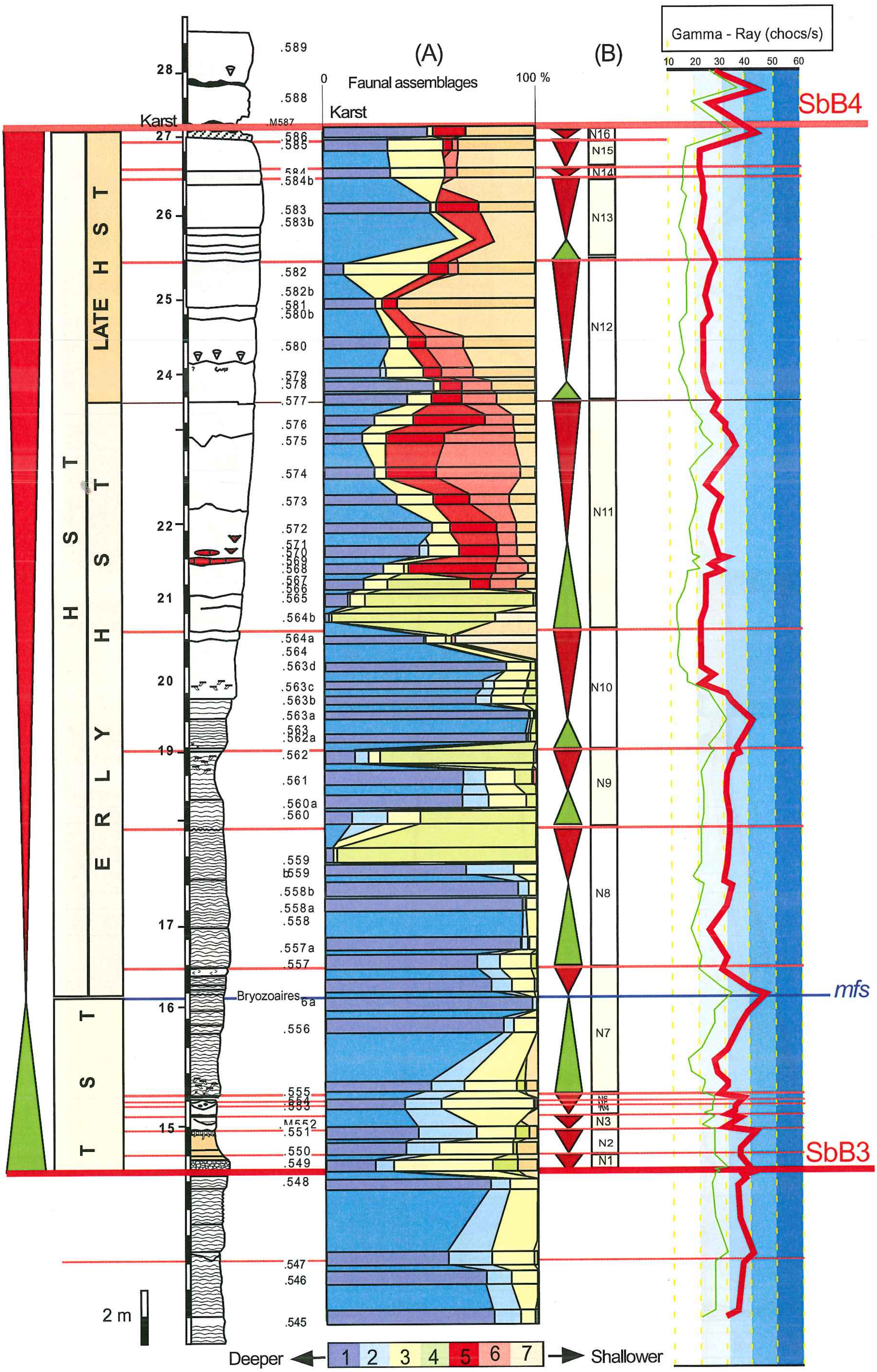

FIG. 45.- Evolution of the gamma radioactivity in the depositional sequence BA3 (late Barremian, Gorges du Nant section). The two curves have been obtained by two different scintillometers (Raddadi, 2004).

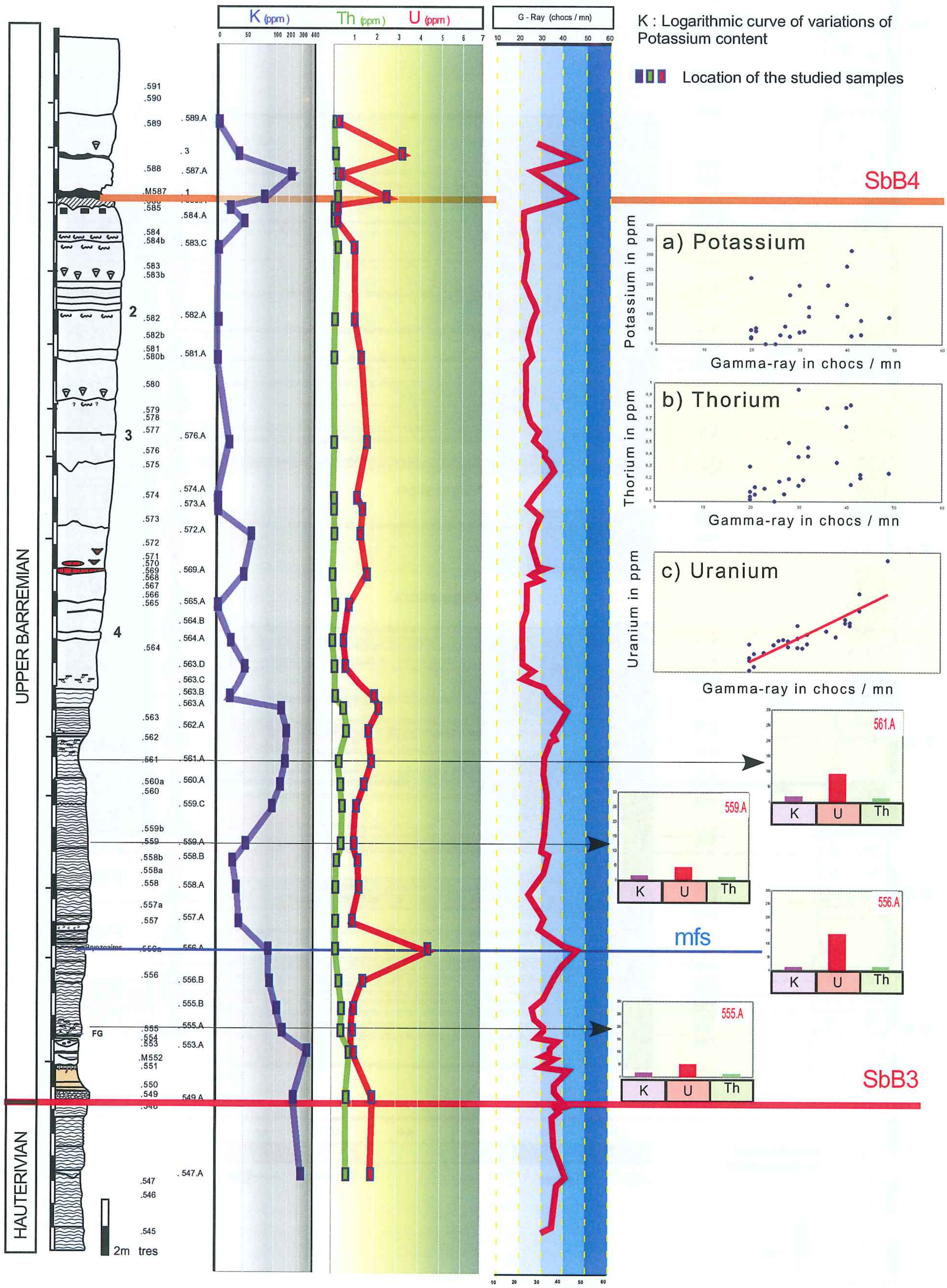

FIG. 46.- Gorges du Nant section, depositional sequence BA3 (late barremian) : correlations between potassium, thorium and uranium curves (ICP-MS analysis) and gamma-ray curve (field data obtainded with a scintillometer) (Raddadi, 2004).

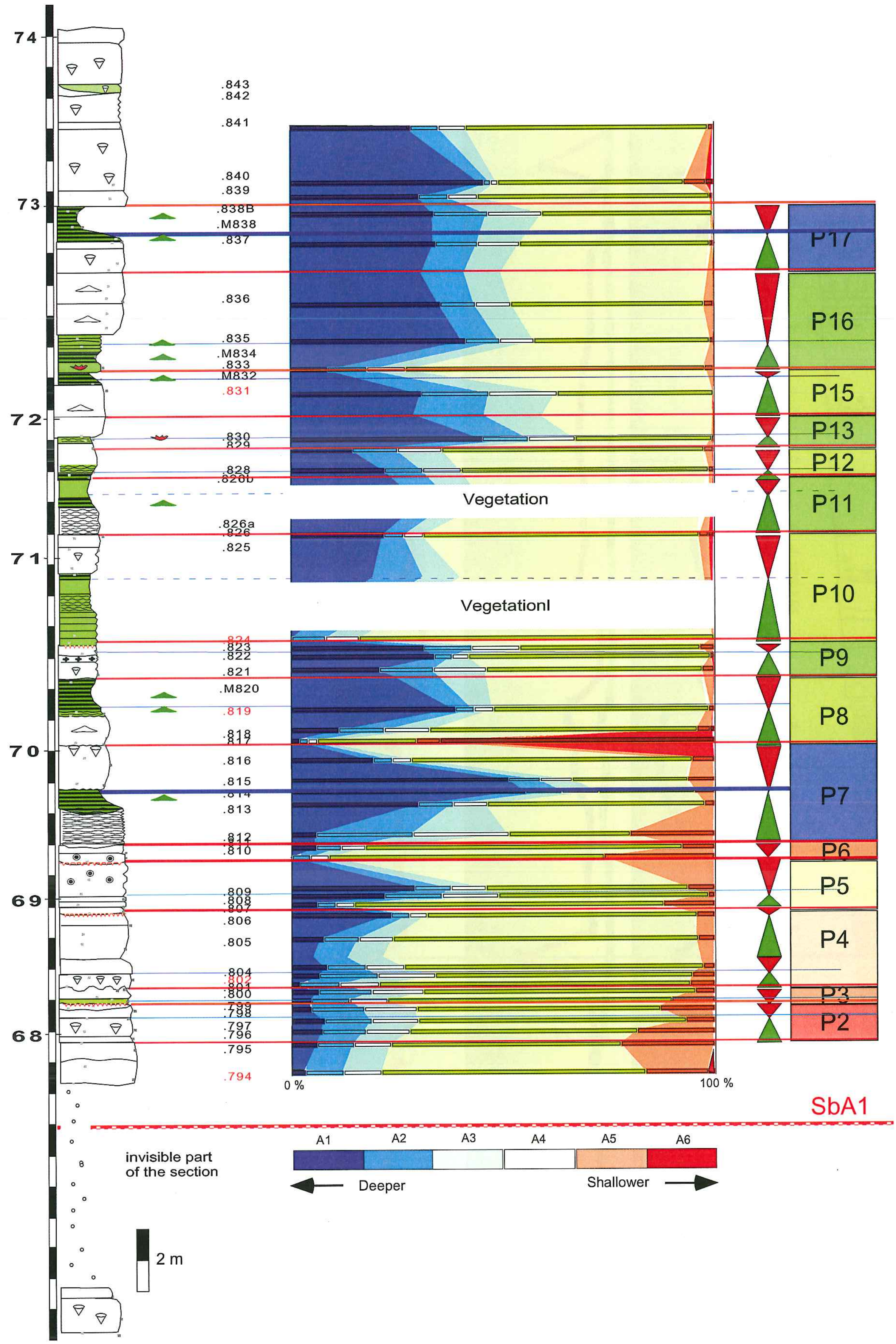

Fig. 47.- Gorges du Nant section: vertical evolution of the faunal assemblages and sequential analysis of the Lower orbitolina member (transgressive systems tract of the depositional sequence AP1, early Aptian) (Raddadi, 2004).

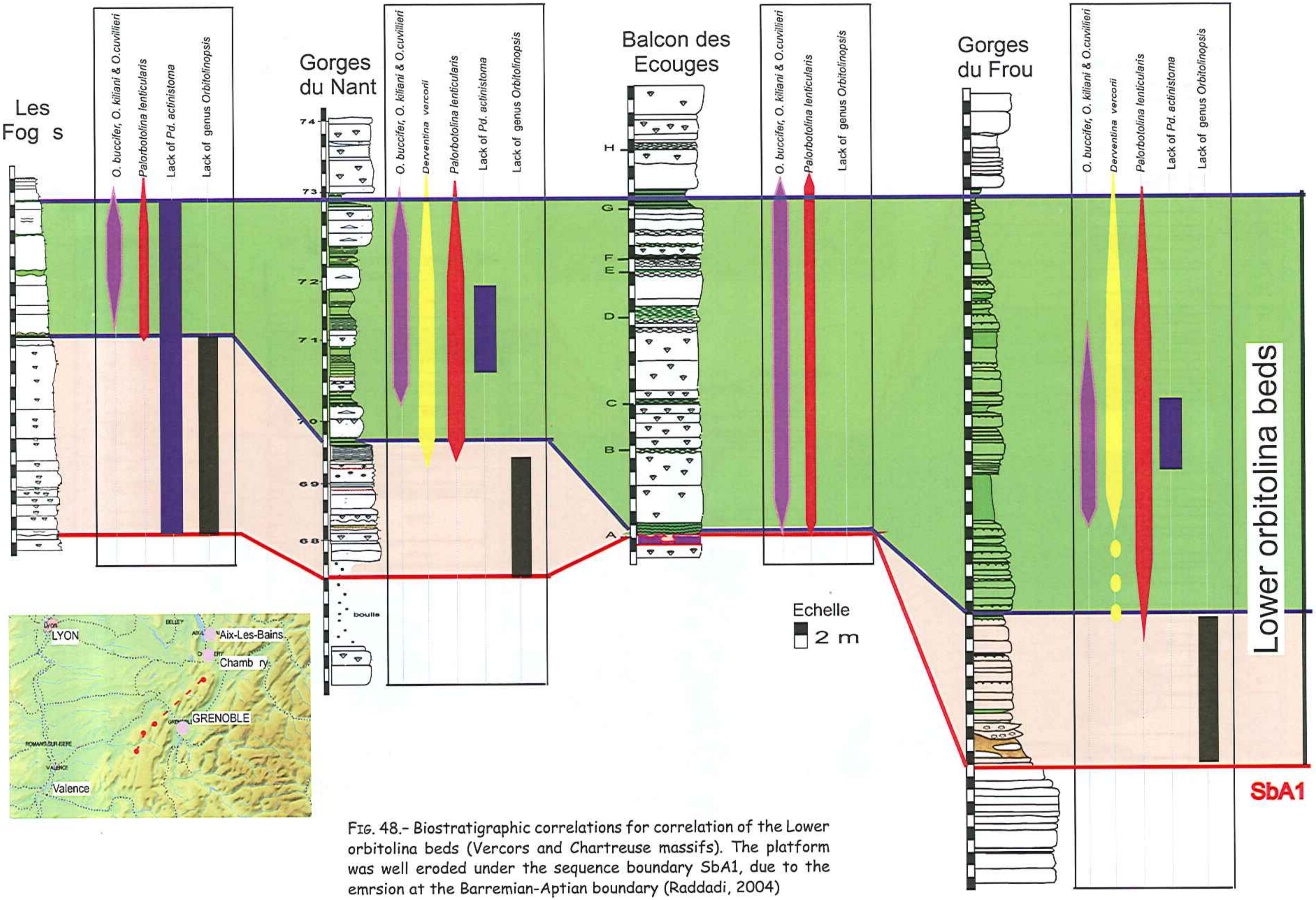

FIG. 48.- Biostratigraphic correlations for correlation of the Lower orbitolina beds (Vercors and Chartreuse massifs). The platform was well eroded under the sequence boundary SbA1, due to the emrsion at the Barremian-Aptian boundary (Raddadi, 2004)

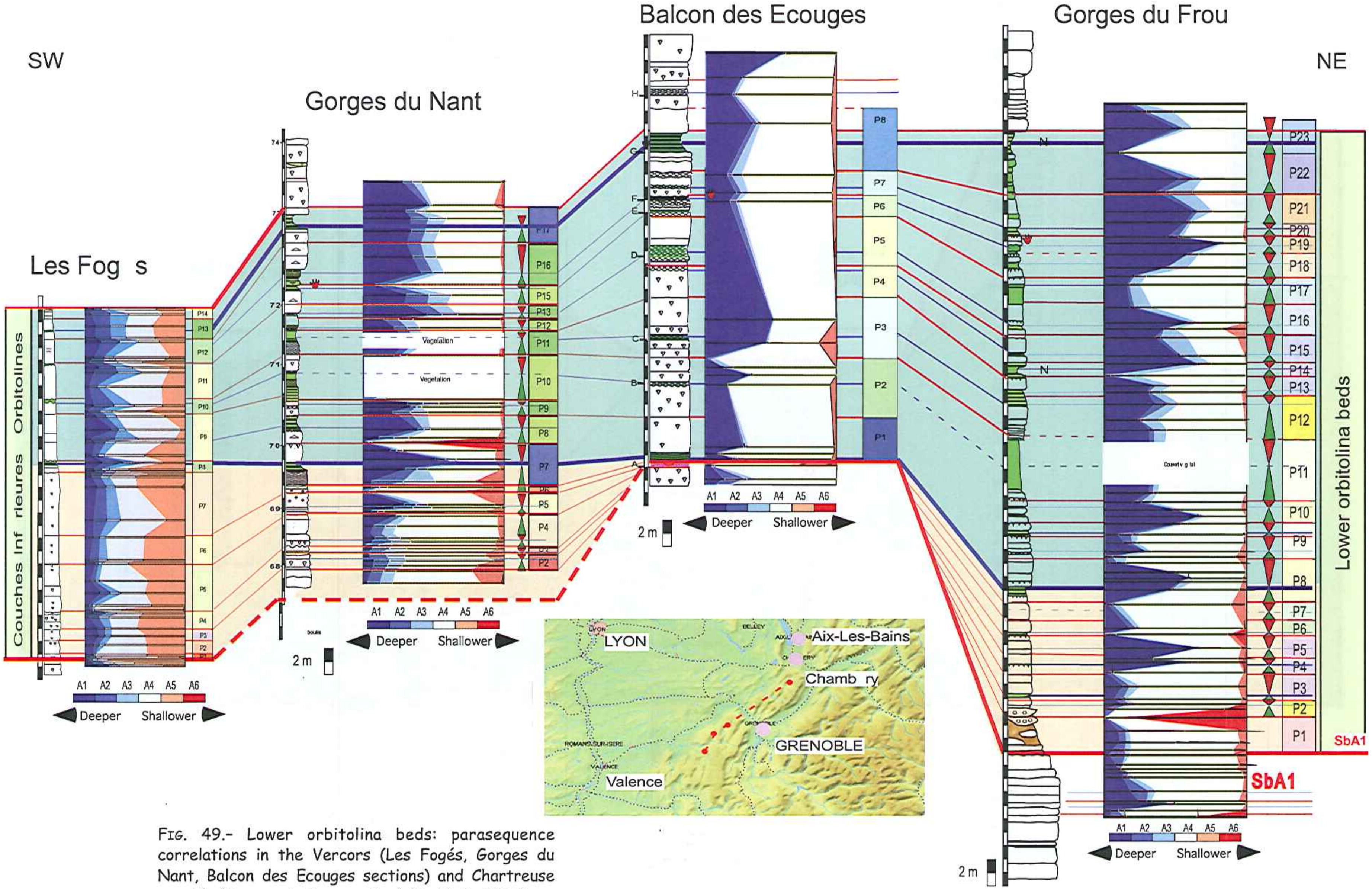

FIG. 49.- Lower orbitolina beds: parasequence correlations in the Vercors (Les Fogés, Gorges du Nant, Balcon des Ecouges sections) and Chartreuse massifs (Gorges du Frou section) (Raddadi, 2004).

There are very good correlations of the $\delta^{13}C$ curves between the Gorges du Nant section (Lower orbitolina beds) and the basal part of the La B doule section.

Correlations of $\delta^{18}O$ curves are also good, but there is a systematic difference ot 2 3 ‰.

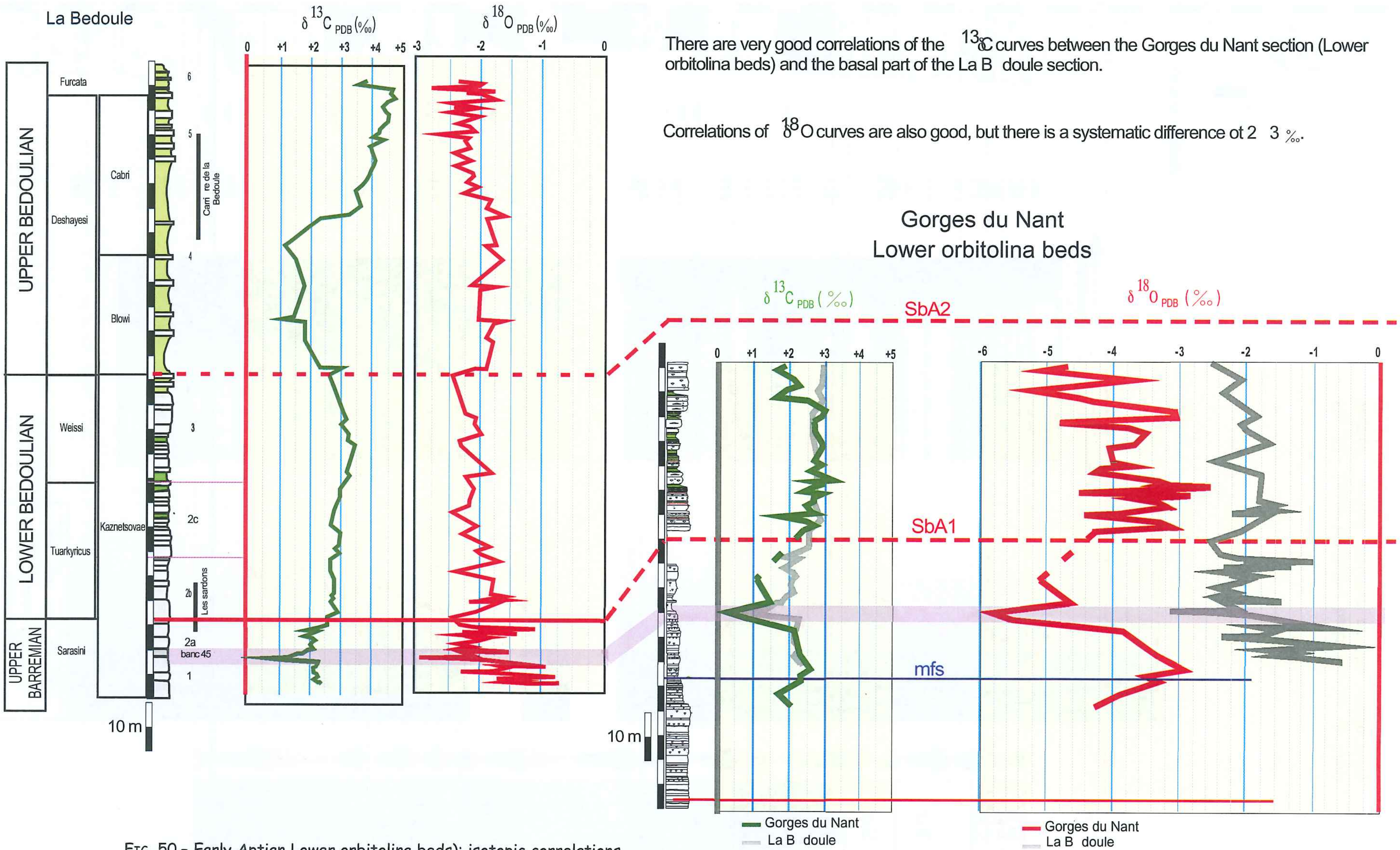

FIG. 50.- Early Aptian Lower orbitolina beds): isotopic correlations from the Gorges du Nant to La Bédoule sections (Raddadi, 2004).

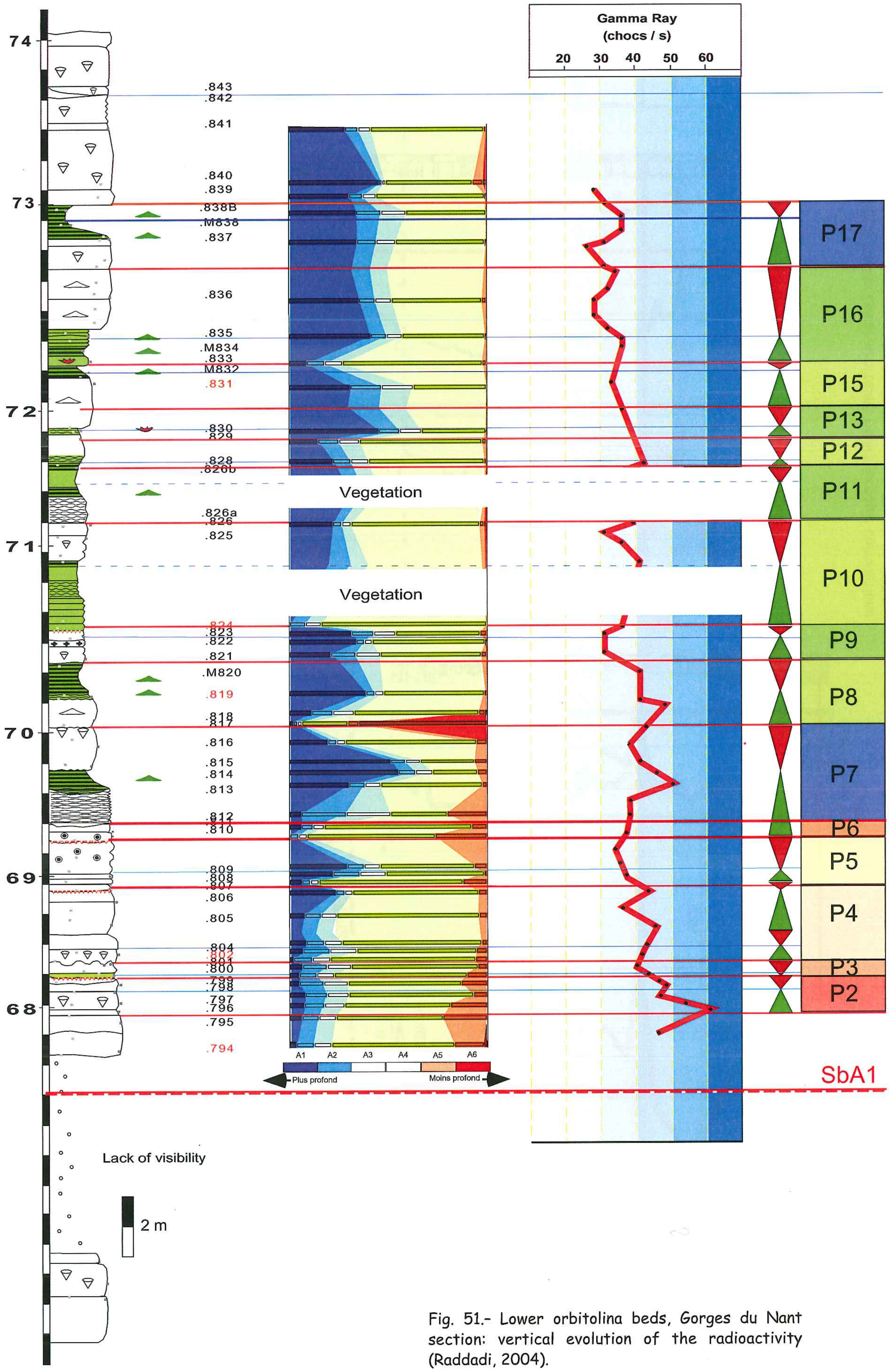

Fig. 51.- Lower orbitolina beds, Gorges du Nant section: vertical evolution of the radioactivity (Raddadi, 2004).

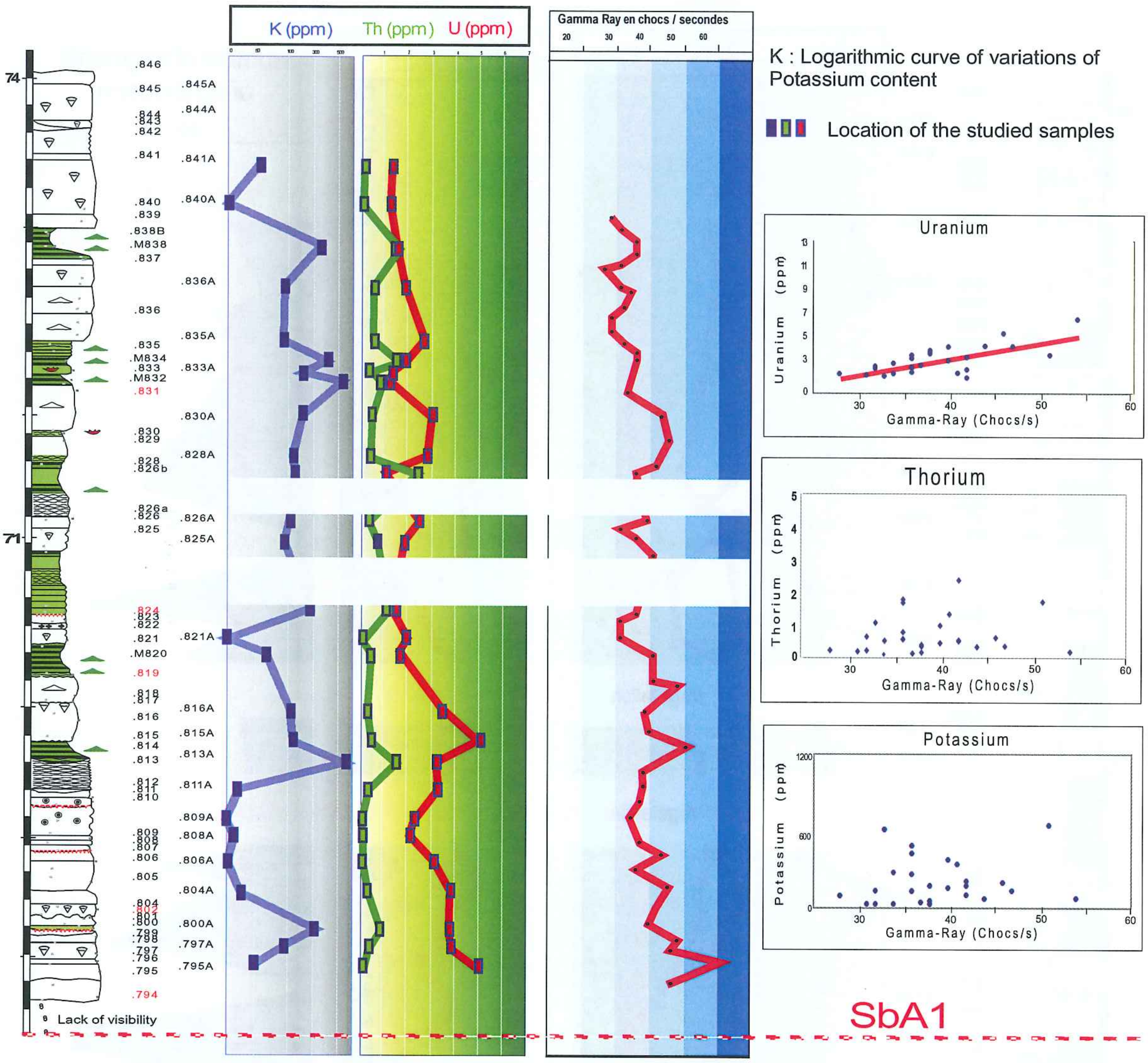

FIG. 52.- Gorges du Nant section, Lower orbitolina beds (depositional sequence AP1, early Lower Aptian): correlations between potassium, thorium and uranium curves (ICP-MS analysis) and gamma-ray curve (field data obtainded with a scintillometer) (Raddadi, 2004).

The maximum flooding surface is only indicated in this restricted lagoonal environment by a slight deepening (fine-grained biosparite grainstone, F3 facies). However, the slight deepening can be traced throughout the area of the Urgonian facies. On the outcrops, this maximum flooding surface can be easily picked, because it separates underlying massive limestones from overlying decimeter thick well-bedded limestones.

The following highstand systems tract shows the same type of shallowing upward parasequences. We can observe biosparite-grainstone with large isolated or colonial Rudists (*Agriopleura*) and a rich microfauna with abundant Orbitolinidae and Dasycladaceans (F8 facies). Parasequences are thicker than those of the underlying TST and show more open marine environment highlighted by the presence of *Agriopleura* rudists and several species of Orbitolinidae. Coarse-grained grainstone (storm deposits) are well developped with emergent surface (grainstone with microstalactitic cement). This highstand parasequence set is clearly thinning-up and capped by SbB5.

3.3. Depositional sequence BA5

3.3.1. Sequence boundary Sb B5

An early dissolution of low magnesium tests of foraminifers (mostly miliolids and orbitolinids) occurs below this sequence boundary. This dissolution was subsequent to the very early diagenesis that produced both the early dissolution of aragonite tests and the calcite replacement. In the Chartreuse massif, where this type of reservoir is well developed, calcitized tests of former aragonitic taxa (trocholines, dasycladal algae) are well preserved and never display voids. In contrast, miliolid tests are sometimes totally dissolved and filled by asphalt. This latter type of dissolution seems

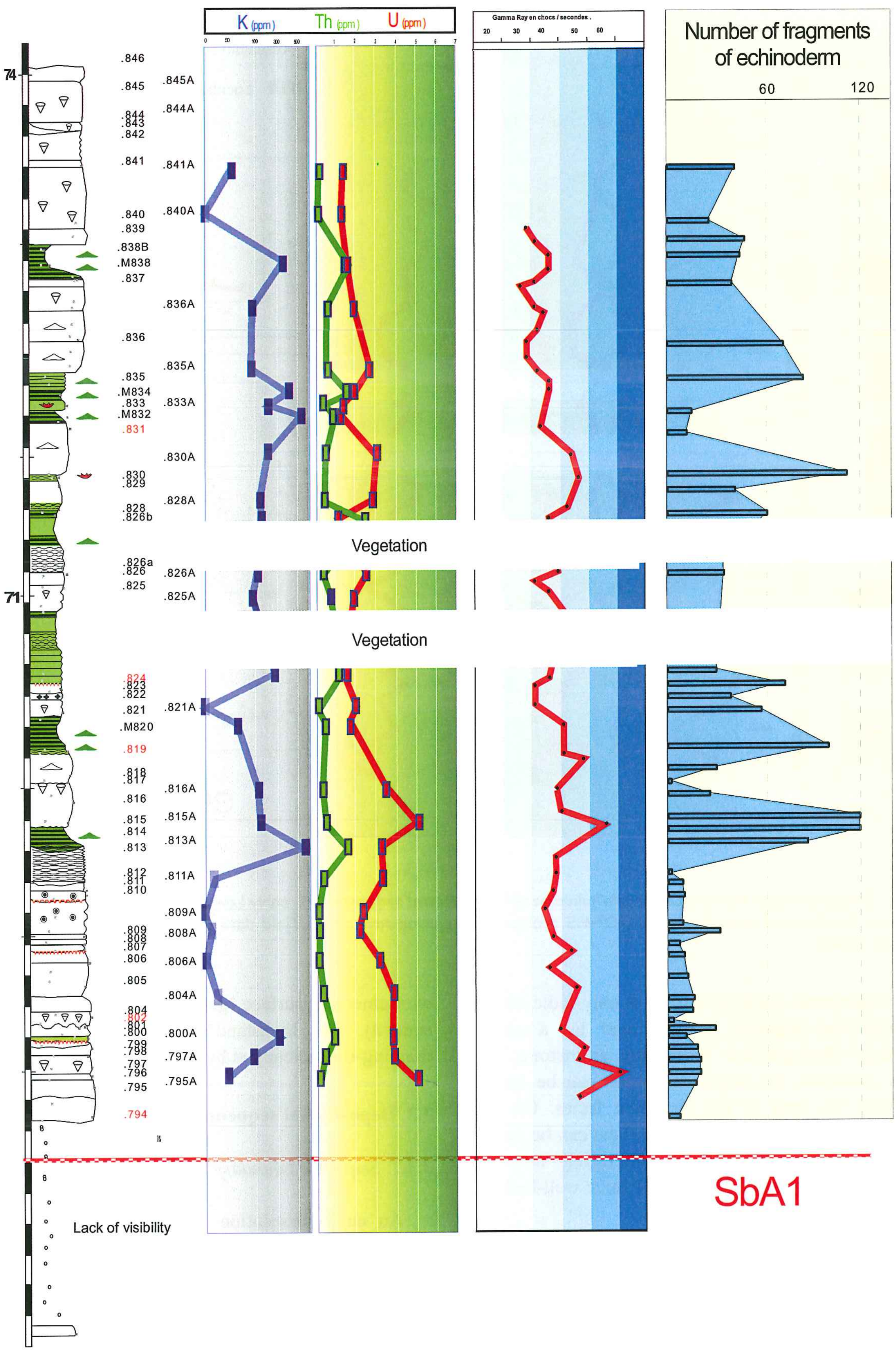

Fig. 53.- Gorges du Nant section, Lower orbitolina beds (depositional sequence AP1, early Lower Aptian): comparisons between potassium, thorium and uranium spectrums and the abundance of echinoderm fragments (Raddadi, 2004).

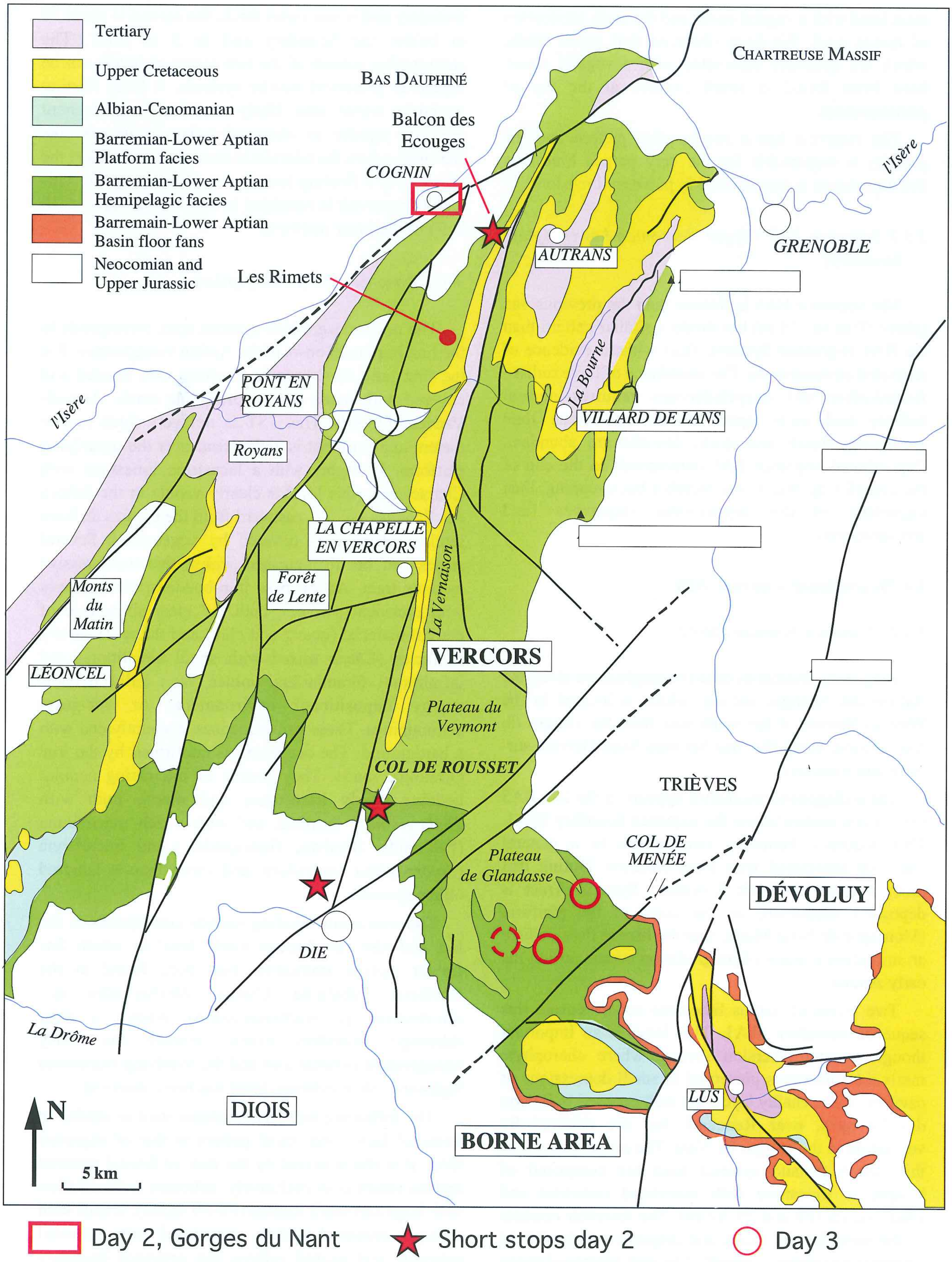

Fig. 54.- Geological simplified map from the Isère valley to the Buëch valley (Vercors, eastern Diois and wesrern Devoluy).

associated with a vegetal cover and the early production of humic acid. We have observed that green marls, which are generally associated with a vegetal cover, have been found in small cavities at the top of parasequences.

The reservoir has a stratigraphic pattern and the porosity is responsible for the very porous limestone that sometimes is transformed in powdery limestone.

3.3.2 Sequence BA5 (Upper Barremian-Lower Aptian boundary)

The sequence BA5 is thinner than the previous one (about 50 m vs 110 m) but shows a similar pattern than the BA4 Highstand Systems Tract without evidence of restricted environments. The abundance of large rudists, foraminifers and dasycladaceans requires normal salinity and more open marine conditions than previously. Beach and storm deposits are abundant. Depositional sequence BA5 corresponds to the end of the overall Urgonian lower member backstepping, then aggrading of the depositional sequences (and environments).

3.4. Depositional sequence AP1

3.4.1. Sequence boundary SbA1

Diagenetic anomalies could be emphasized along the Balcon des Ecouges section, which is located in the Western Vercors, 4 km south-east from the Gorges du nant section, along the road between Saint Gervais-sur-Isère and Rencurel.

These diagenetic anomalies appears in the late BA5 HST, a few meters below the sequence boundary SbA1. This sequence boundary corresponds to a general emersion associated with local erosions. During that time, a huge bioclastic Lowstand Systems Tract is deposited southward, on the slope of the platform (Montagne de Belle Motte, near the Menée Pass), where an important «jump» of progradation occurs during the early Aptian.

Two levels of porous limestone occur beneath this sequence boundary SbA1. This latter is an important though uneven emersion surface where charophyte marls are sometimes preserved in small depressions or cavities. These chalky layers are well exposed in Balcon des Ecouges, near Rencurel, but are covered by vegetation in the Gorges du Nant. The parasequences of this late highstand systems tract are composed of biosparitic limestone with micritized oncolites and small rudists (F8 and F9 facies). The reservoir consists of the same lagoon facies and displays a lack of final cementation (mosaic cement). The well preserved shape of the calcite crystals in the fringing rim cement and the lack of dissolution marks attest to the primary origin of this interparticle porosity (N = 16%). The upper porous level is located a few meters below the sequence boundary and is one meter thick; the second is about 10 m below the boundary and is 3 m thick. The stratigraphic pattern of the two reservoir levels can be related to preserved aquifer systems. A local floating meteoric water lens likely overlaid a permanent meteoric aquifer as observed today in islands like Bermuda where the rainfalls is strongly seasonal and the presence of a floating lens thus tends to be cyclic. This type of reservoir is restricted to small areas (around 10 km^2) of the inner platform.

3.4.2 Sequence AP1 (Lower Aptian)

The next transgressive systems tract corresponds to the first important onset of the Aptian transgression. For the first time the Urgonian platform was flooded and covered with marls (lower Orbitolina marls, Arnaud-Vanneau [1980]). This TST is not very thick (a few meters to 30 m), but is widespread over the underlying platform. It begins with a lacustrine limestone with Characaeans (this level is clearly visible in the Balcon des Ecouges section, eastward from the Gorges du Nant section where it is covered by vegetation). Several stages can be distinguished within this transgressive systems tract. At the base thin-bedded parasequences with erosional surfaces, both the great abundance of detrital material (quartz and clay) and the wide variety of facies (*Chara* mixed with small circalittoral and infralittoral foraminifers, oolites, etc.) indicate high-energy depositional environments or sea-grass communities. These parasequences frequently end with a hardground. The deepening is confirmed by the true Orbitolina marls. They consist of alternating nodular bedding marly limestones and marls, both with *Thalassinoides* burrows, and with a rich macrofauna (Echinoids, Bivalves, Gastropods...) and microfauna (*Palorbitolina lenticularis* and more than a hundred others species).

The maximum flooding surface corresponds to the last and also the thickest marly level in which few Lower Aptian ammonites had been found in the Northern Subalpine Chains (*Deshayesites* sp., *Ancyloceras* gr. *matheronianum*). Above, a clear lithologic boundary exists between the marly transgressive systems tract and the overlying calcareous highstand. No condensed level has been observed.

The following highstand systems tract is similar in terms of facies and stratal pattern to that of sequence BA5. It is characterized by the lack of detrital material and the return to an exclusively carbonate sedimentation with large and small Rudists (F8-F9 facies). It ends with a major erosional surface, associated with subaerial exposure and incised valleys: the sequence boundary AP2 (Arnaud-Vanneau *et al.*, 1990). This sequence boundary is not visible in the Gorges du Nant section, due to erosion below the Upper Turonian tectonically enhanced boundary.

4–. Different types of parasequences

4.1. Highstand systems tracts parasequences

Highstand systems tract parasequences correspond throughout to shallowing-upward sequences, the base of which are transgressive and discordant on the Hauterivian beds of varying ages. The first BA3 HST parasequence shows commonly a very clear-cut lithological boundary, easily seen on wire-line logs, between the Urgonian limestone formation and the marly limestone or marl of the underlying Hauterivian. The presence or absence of clay and detrital quartz usually allows the muddy limestones of the Hauterivian to be distinguished from the pure limestones of the late Barremian (Urgonian platform). These Urgonian platform initial sequences [Arnaud-Vanneau *et al.*, 1987] display, from the bottom upwards: 1) wackestone-packstone with small foraminifers, in decimetric wavy beds (Facies F2); 3) grainstone with bioclasts and/or oolites (Facies F3) above which there occur cross-bedded facies oolites in the Chartreuse and southern Jura (facies F6) and, in the northern Vercors, first coral reefs, and then, still farther towards the southeast, grainstone with corals debris (Facies F7). This sequence may end locally in the first wackestone-packstone beds with rudists (Facies F8).

Early Highstand systems tracts are characterized by the predominance of the first facies (Facies F3-F6) while late highstand prograding wedges show the great development of inner shelf facies (Facies F8). Towards the Urgonian platform bank margin, the sequence BA3 late highstand prograding wedge is well developped as in the Gorges du Nant section (with rudist facies). Towards the North, on the contrary, only early highstand exist, characterized by thick parasequences made of Facies F3 and F6 while inner shelf facies are unknown.

5.2. Transgressive systems tract parasequences

Early TST: basal transgressive systems tract parasequences has been clearly observed with a general aggradational then backstepping disposition (BA4 sequence, Gorges du Nant section).

Throughout the Jura and the Northern Subalpine Chains, inner platform facies are observed above the sequence boundary (for exemple sequence boundary B4). There are white, exclusively carbonate facies characterized by the micritization of bioclasts due to the activity of endolithic micro-organisms (Cyanophycae, bacteria, fungi) and by the presence of algal oncolites. These sequences are from 1 to 4 m thick. Always of the shallowing-upward type, they display from the bottom upwards: l) packstone with large and small rudists, large benthic foraminifers, Dasyclad algae, Miliolidae and locally, a few corals (Facies F8); 2) packstone-wackestone with small rudists and oncolites which are locally very common. Among the foraminifers, only Miliolidae are abundant (Facies F9 and F10). The sequence may end in two different ways. In one case, there is a grainstone of storm deposits made up of either oncolites, numerous rudist shells or coral fragments. In the other case, the top of the sequence is composed of a more restricted facies: first wackestone-mudstone with oncolites and then mudstone with restricted microfauna (l or 2 species of Miliolidae), bird's eyes or stromatolites (Facies F11).

This type of parasequence occurs only after an important emersion and lack of sedimentation followed by a slow rate of relative sea-level rise. We have to note, but without surprise, that the most restricted environment of the Urgonian platform are known only in the transgressive system tract of the sequence BA4.

Late TST: at the top of transgressive systems tracts (sequence BA4) or just above the sequence boundary (sequence AP1) the important rate of relative sea-level rise induces always the appearance of transgression facies [Arnaud-Vanneau, 1980]. Whatever the location or the stratigraphic level, transgressive facies always display four fundamental features:

1) Appearance or notable increase in clay, quartz and iron oxide content, resulting in a highly recognizable bluish, reddish or yellowish colour.
2) Rounded lithoclasts in a fine-grained sediment, or a mixture of bioclasts of different sizes or a mixture of two facies types.
3) Substantial reworking and mixing of fauna and flora: brackish-freshwater organisms (Characae) occur with deep subtidal marine organisms (small agglutinated foraminifers), or even pelagic organisms (ammonites).
4) Skeletal grains are commonly surrounded by a coating of iron oxides, locally cemented together in a ferruginous hard ground.

Transgressive facies are observed either directly on an emergence surface or at the top of a shallowing-upward sequence set characterized by the gradual vertical deepening of the environment from one parasequence to the next one. The interval between the transgressive facies and the maximum transgression level is usually taken up (late Barremian transgression in the southern Vercors, Lower orbitolina beds in the northern Vercors and the Chartreuse) by one or more shallowing-upward sequences made up of argillaceous facies rich in irregular echinoids, *Palorbitolina lenticularis* (opportunist species which invades all the platform during late transgressive systems tracts), benthic foraminifers and Dasyclad algae. The maximum transgression stage (mfs) generally corresponds to marls which, especially on the outer shelf, may include glauconitic beds that are locally rich in ammonites (likelihood of condensed sections).

5. Conclusion

To summarize, this section allows us to observe the installation and evolution of the Urgonian platform in the Dauphinois basin.

After an important depositional gap (at less 3 my are probably missing), and emergence and erosion of the former Berriasian-Valanginian slope, the rise of sea level led to new sediment deposits. The first deposits are composed of reworked former argillaceous sediments. The facies is similar to the previous sediment, and it is difficult to distinguish between *in situ* sediment and reworked sediments when pebbles are not visible.

Along the section, two types of systems tracts are present : transgressive systems tract and highstand systems tract. TST are composed of shallowing upward sequences with an erosive base in the early TST, and with more and more argillaceous sediments in the late TST. HST are mainly made up of rudist limestone. During the early HST, sequences are thick and, on the contrary, sequences are thin in the late HST. Prooves of emersion are well documented at the end of late HST sequences.

In relationship with sequences boundaries, many diagenetic anomalies exist: karstification, dolomitization, anomalies of posity. These anomalies are regionally important along the SbB4 and SbA1 where good reservoirs are known, with thicknesses up to 10 metres and porosity up to 16% (or details, see E. Carrio-Schaffhauser, this volume).

Les Rimets incised valley

This outcrop is located on the western side of the Rencurel syncline, near “Les Rimets” farm. It allows us to observe the end of the last Urgonian deposits and a fossilized “incised valley” which was used as tidal channel and later filled up by Orbitolina marls, so-called “Marnes à Orbitolines supérieures”. It will be visited only if weather is too bad in the Southern Vercors.

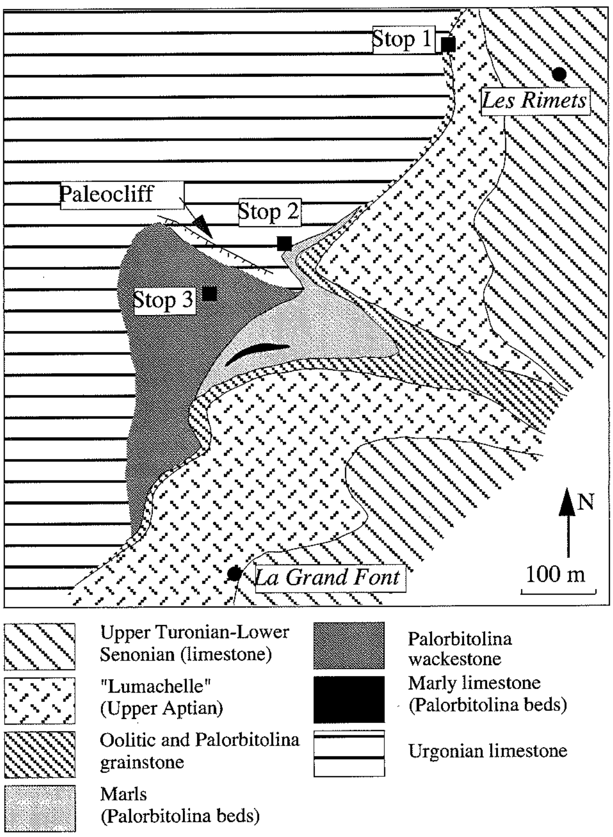

Fig. 55.- Schematic map of the Rimets incised valley showing location of main stops.

1.– End of the Urgonian platform

The emergence at the top of the sequence AP1 highstand systems tract is quite substantial. It is marked first of all by diagenetic changes in sediment at the top of the parasequences (shell dissolutions and vadose cementation), and then by distinct cavities of various forms and dimensions (Plate 39, p. 76). Some of these cavities are rootmolds while others, sometimes more than 1 m size, are karstic cavities. In both cases, they are filled first by limestone containing crinoid bioclasts, and then by *Palorbitolina* limestone similar to that of the upper Orbitolina beds.

Finally, large extensive depressions, tens of kilometers in length, hundreds of metres wide and tens of metres deep cut into the surface of the Urgonian platform.

During the transgression at the upper Lower Aptian (the french Bedoulian), these depressions served as tidal channels, and then they are filled up by «upper Orbitolina beds». The channels are very deep, especially downcurrent, at least 40m deep in the case of the Rochers de la Ferrière channel north of the Gorges de la Bourne (Arnaud, 1981). This depth would appear to be incompatible with a simple erosion by tidal currents since this region was affected by early lithification and by a probably small tidal range, given the death of intertidal facies in the Urgonian limestone. It therefore appears more likely that these valleys were cut in a continental environment. The maximum depth of the valleys implies that there was at least a 50 to 60 m fall in sea level. In this event, the shoreline must have dropped over the edge of the Urgonian platform, i.e. to the SE of the Northern Subalpine Chains.

2.– Sedimentation in the “incised valley”

At the end of this period, the rapid rise in sea level brought about the submergence of the area. The valleys

FIG. 56.- Overview of the Rimets cliff, corresponding to the northern side of a Lower Aptian incised valley. The cliff is incised in Urgonian limestone and covered by condensed sediments («hard ground»), then infilled by Orbitolina marls.

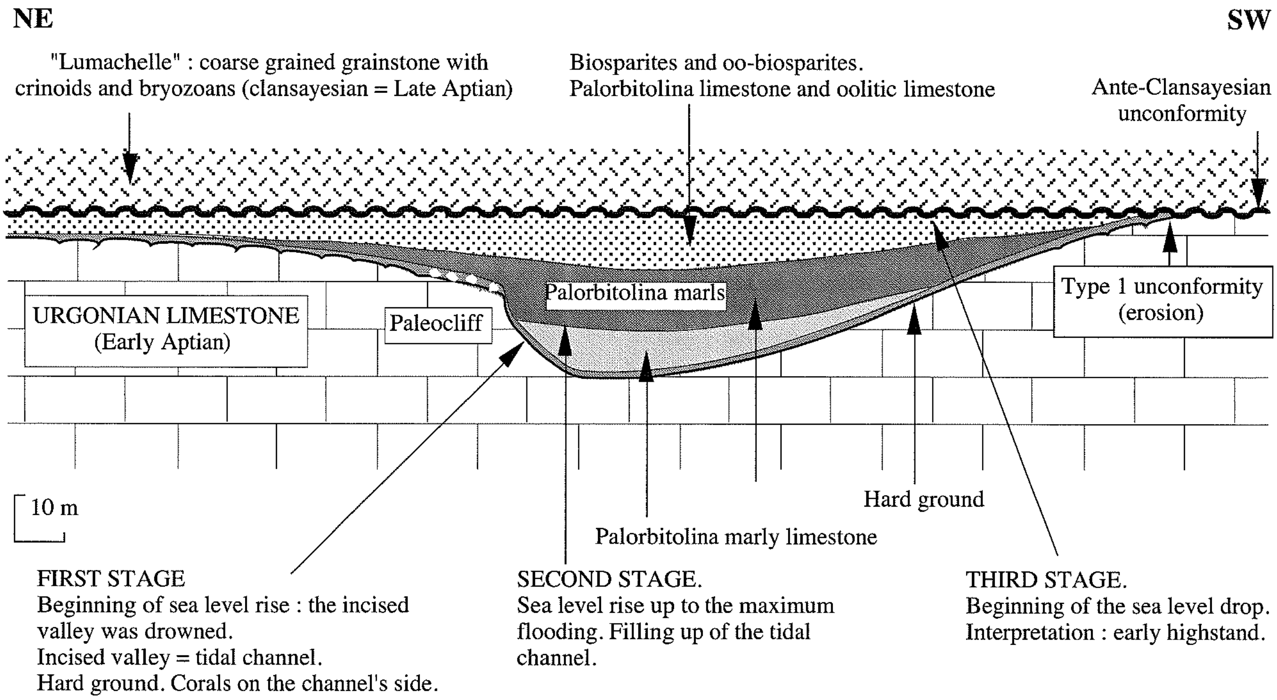

FIG. 57.- Schematic section through the incised valley of Les Rimets (Northern Vercors). This section shows : (1) the type 1 unconformity above the Urgonian limestone (which was eroded during the Early Aptian emersion); (2) the three main stages of infilling by the upper Orbitolina beds during the sea level rise of the upper part of the Early Aptian (the valley was then used as a tidal channel); and (3) the onlap arrangement of the different levels of the upper Orbitolina beds.

became first tidal channels, and they were then filled up by a variety of sediments making up the depositional sequence AP2 (parasequence Ai3, Arnaud-Vanneau, [1980]) at the top part of the Lower Aptian (*Deshayesites deshayesi* and *Tropaeum bowerbanki* ammonite Zones of Casey [1961]). The transgressive systems tract exists solely in the paleovalleys and on their edges, corresponding to upper Orbitolina beds. These marls are very rich in quartz, clay and heavy minerals, as is usually the case in transgressive environments.

One of these valleys found near Les Rimets farm (Northern Vercors), wich is remarkably well-preserved, shows three main stages of fill (Plate 39 and fig. 19).

1.– At the beginning of the platform drowning, the sea must have been fairly shallow. Tidal currents were rapid

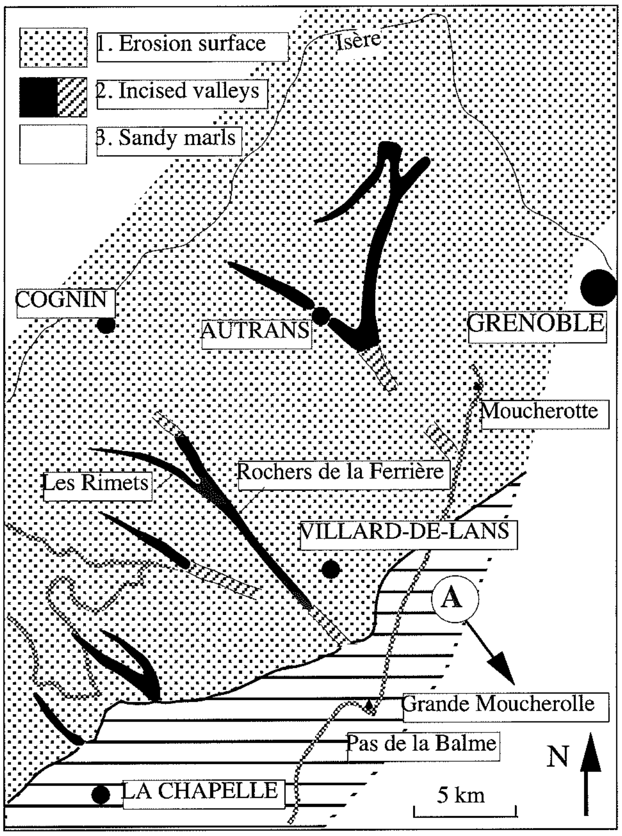

FIG. 58.- Schematic map of the Early Aptian incised valleys in the Northern Vercors. 1, erosion surface of the Urgonian limestone. 2, incised valleys with transgressive systems tracts of the upper part of the Early Aptian (upper Orbitolina beds). 3, glauconitic sandy marls which were deposited above the Urgonian platform during the upper Early Aptian. These marls may be considered as the lateral equivalent of the upper Orbitolina beds; they are observed only on the outer part of the previous inner-shelf of the Urgonian platform. A, direction of the platform margin.

and they were channelled by the valleys, in the same way as those presently observed on the Pelagian platform to the East of the Kerkennah islands (Tunisia, Burollet *et al.* [1979]). A condensed section covers the bottom and sides of this valley. It consists of a thin, iron rich centimetre to decimetre-thick level which was lithified early (numerous boring organisms). It locally contains numerous corals and large rudists on the edge of the valley.

2.– At the highest point of the sea-level rise, the currents were less strong, allowing the filling of the tidal channels by marls which are very rich in *Palorbitolina lenticularis*. The channel running through Les Rimets and continuing on the eastern edge of the Vercors (South of Villard-de-Lans) shows longitudinal zonation of the fill from the edge towards the inner platform. Seaward, the fill is coarse outer shelf type grainstone whereas the inner platform (Rochers de la Ferrière), this bioclastic limestone is overlain by *Palorbitolina* marls. Finally, farther to the NW, in Les Rimets, the multi-phased filling consists of several distinct layers of marls and marly *Palorbitolina* limestone resting against the slopes of the valley. These observations confirm the onlap arrangement of the various sedimentary bodies on the erosional surface, both longitudinally and transversely.

3.– The beginning of the sea-level fall corresponds to the accumulation in a subtidal, shallow marine environment of bioclastic (*Palorbitolina* grainstone) or oo-bioclastic sands, either on the previous transgressive systems tract or, laterally, directly upon the Urgonian limestone. This highstand deposit is dated as late Bedoulian (Lower Aptian) by ammonites. Highstand deposit is separated from the Upper Aptian bryozoan and crinoid grainstone (the so-called "Lumachelle") by sequence boundary SbA3.The complex late Aptian story isnow known by the study of small-size karstic cavities.

1) The first fall in sea-level probably occurred during the lowermost late Aptian (Gargasian). Again, there is karstification and the development of a vegetal cover as attested by the presence of small root molds and green marls covering the cavity walls.

2) The first late Aptian transgression is not identified on outcrop. It is recognized in paleocavities as a brown, brachiopod-bryozoan wackestone-packstone (first "Lumachelle"). Cavity-filling deposits are the only witness of the Gargasian on the Urgonian surface.

3) The second fall in sea-level is located stratigraphically at the Gargasian-Clansayesian boundary near the top of Aptian. Renewed solution and karstification at this time cut through the previous boundaries.

4) The second transgression is represented by the second "Lumachelle" deposits of the late Aptian (Clansayesian) which lie generally directly upon the Urgonian surface. This second Lumachelle facies is a crinoid-bryozoan packstone-grainstone rich in glauconite and quartz grains that fills the deeper fissures which probably developped during the last fall in sea-level.

5) The third fall in sea-level is associated with the major fluctuations in sea level that occured during the Cenomanian to Turonian.

The last aptian deposits are overlain by Albian very thin condensed section corresponding to phosphatic pelagic deposits with many Ammonites ("Béton Phosphaté").

3. PALAEOGEOGRAPHIC DISPOSITION

In the Vercors, numerous outcrops have made it possible to construct the network of paleovalleys. The valleys mostly run perpendicularly to the edge of the Urgonian platform. Their depth decreases rapidly towards the Northwest and they disappear within 20km, probably explaining their absence in subalpine massifs farther north.

At the end of the Bedoulian, a major transgressive pulse drowned the Urgonian platform, and this platform gradually disappeared.

The Southern Vercors: overview of the Glandasse Plateau section

1.– Overview of the Col du Rousset

Near the Col du Rousset pass, we have a spectacular overview on the Glandasse plateau and the global Lower Barremian lowstand in one hand, and the Lower and Upper Barremian hemipelagic succession of the Col du Rousset in the other hand.

1.1. Col de Rousset Hauterivian section

This section is located along the road to Col de Rousset. Our main interest will therefore go to the Upper Hauterivian - Lower Barremian transition beds in which three lithological units can be distinguished :

1) at the base (early *Subsaynella sayni* zone), a "member" in which marly beds and limestone beds are about the same thickness,

2) In the middle (late *Subsaynella sayni* zone and *Plesiospitidiscus ligatus* zone), a thick marly level containing several pyritaceous ammonite levels (maximum flooding surface),

3) at the top, a calcareous entity in which only the lower part of the *Pseudothurmmannia angulicostata* zone has been recognized.

1.2. Col de Rousset Barremian-Lower Aptian section

The pelagic limestone and marls of the Hauterivian are directly overtopped, without any transition (sequence boundary SbH7), by hemipelagic argillaceous limestones that have yeld at their base late *Pseudothurmmannia angulicostata* zone ammonites.

At the Hauterivian-Barremian boundary, the sequence boundary SbH7 corresponds to a sharp contact between Hauterivian pelagic succession with regular

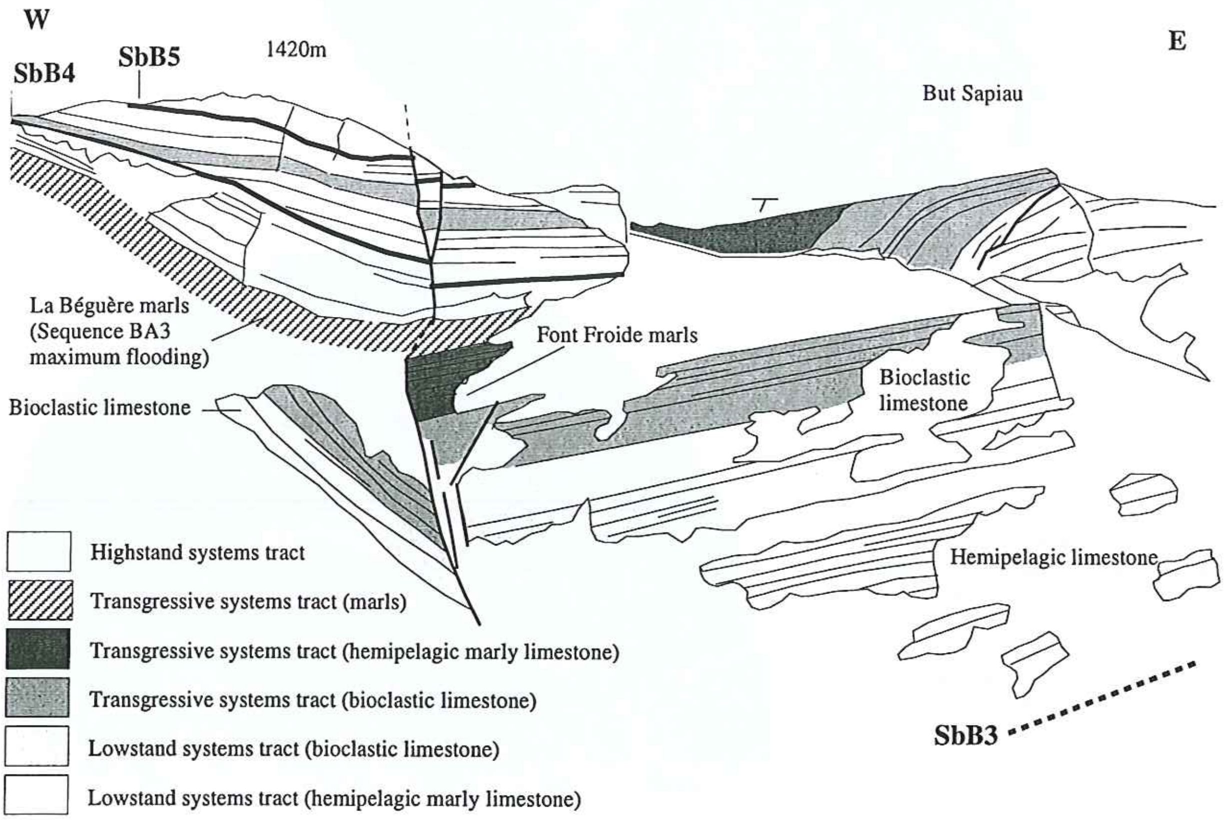

Fig. 59.- Panorama of the Col de Rousset (Urgonian limestone Formation and top of the Glandasse limestone Formation) : strattal pattern and sequence stratigraphy. Both formations correspond here to bioclastic limestone owing the location on the bank margin. It is the reason why the sequence BA4 and BA5 lowstand systems tracts (proximal parts) are clearly visible in the surrounding of the Col de Rousset.

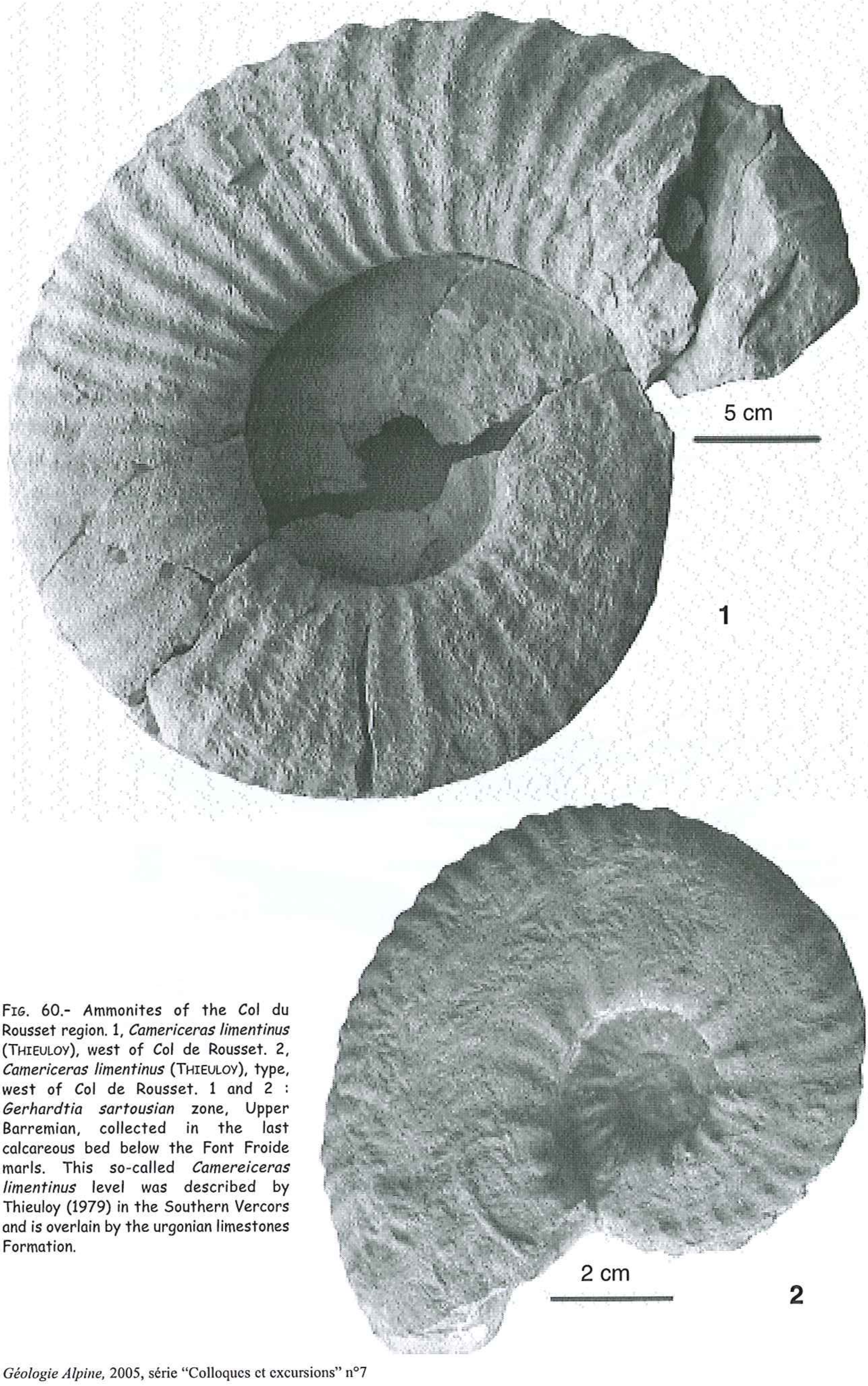

FIG. 60.- Ammonites of the Col du Rousset region. 1, *Camericeras limentinus* (THIEULOY), west of Col de Rousset. 2, *Camericeras limentinus* (THIEULOY), type, west of Col de Rousset. 1 and 2 : *Gerhardtia sartousian* zone, Upper Barremian, collected in the last calcareous bed below the Font Froide marls. This so-called *Camereiceras limentinus* level was described by Thieuloy (1979) in the Southern Vercors and is overlain by the urgonian limestones Formation.

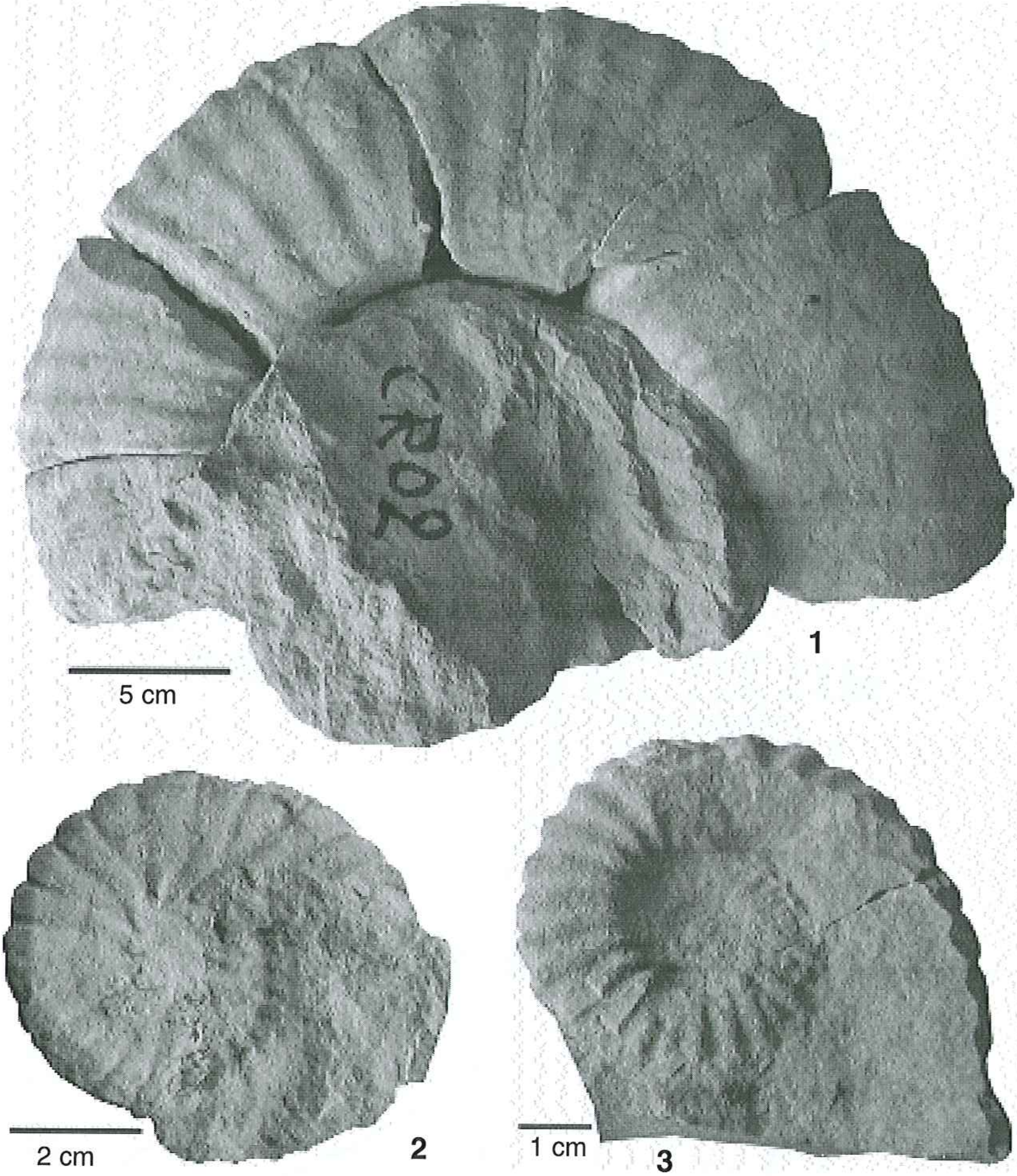

Fig. 61.- Ammonites of the Col du Rousset region. 1,*Camericeras limentinus* (THIEULOY), Col de Rousset road (= *Emericiceras* sp. or *Camereiceras* sp. *in* Arnaud *et al.*, 1998), *Gerhardtia sartousiana zone*, Upper Barremian. 2, *Gerhardtia sartousiana* (D'ORBIGNY), Col de Rousset road, *Gerhardtia sartousiana zone*, Upper Barremian. 3, *Hemihoplites soulieri* (MATHERON), east of Col de Rousset, between Font Froide marls and La Béguère marls, *Hemihoplites feraudianus* zone, Upper Barremian.

marl-argillaceous limestone alternations and uppermost Hauterivian- early Barremian hemipelagic limestone. This event (the so-called **"Barremian crisis"**), manifestations of which are perceptible from the top of the Hauterivian to theearly Barremian, is isochronous with :

1) an important drop of sea level, indicated by change of facies (pelagic to hemipelagic),

2) a sudden increase of the subsidence rate, explaining why we have here more than 1000 m thick Lower Barremian hemipelagic facies.

This break in sedimentation can be correlated with the Sb H7 tectonically enhanced unconformity, that we can see also in the Menée pass area.

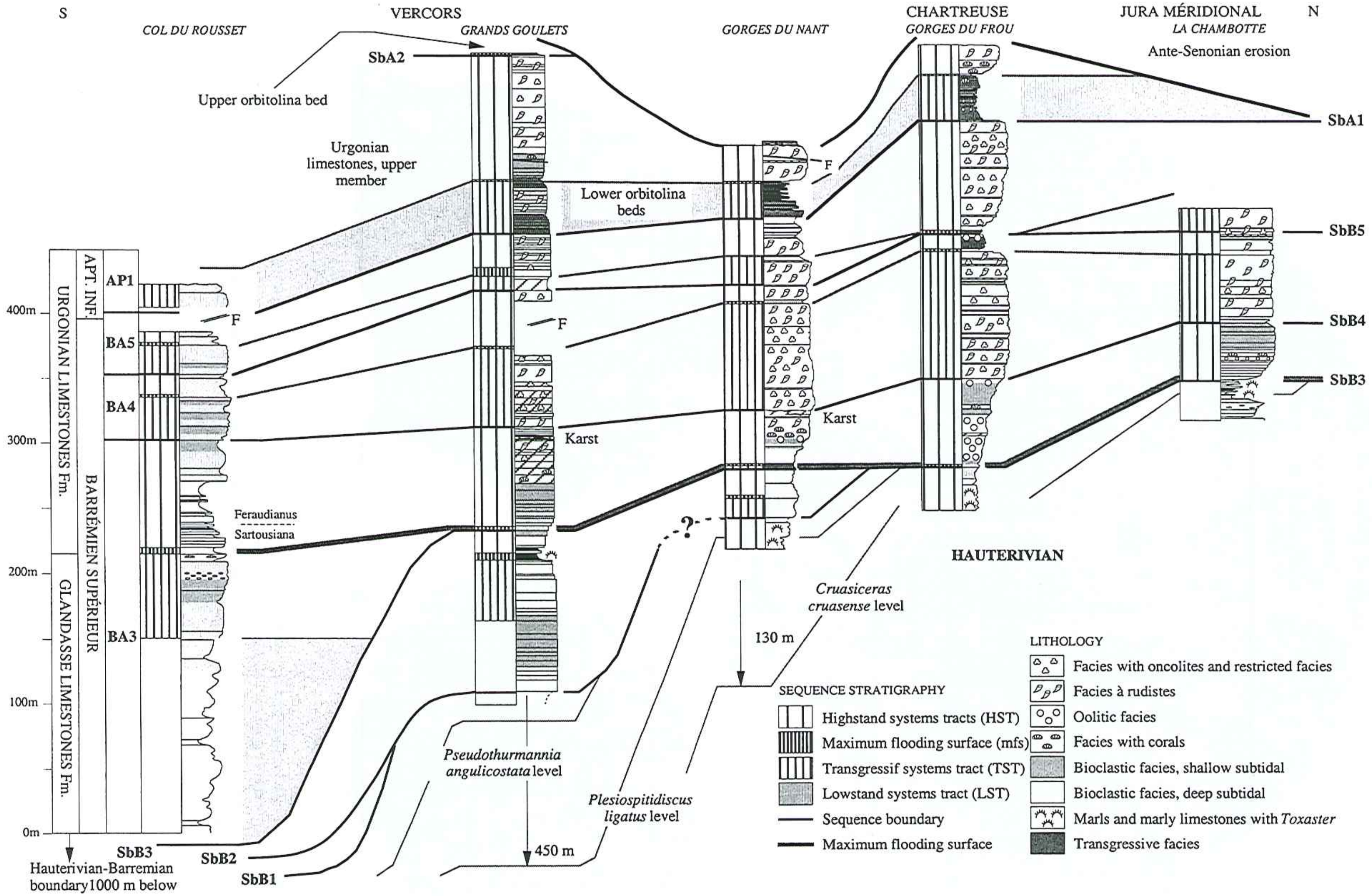

FIG. 62.- Correlations within the Urgonian limestones Fm. from the Southern Vercors (Col de Rousset section) to the Southern Jura (La Chambotte section). Note that depositional sequences BA1 and BA2 are visible only on the bank margin. The hauterivian series is truncated below SbB1 and SbB3 sequence boundaries as the last beds below SbB3 are older and older from the south to the north.

At the top of the Col du Rousset section and for the first time, the Urgonian limestone formation is clearly visible lying on a very thick barremian succession.

The sequences BA1 and BA2 are made of by several hundred meter thick hemipelagic marls and argillaceous limestones.

The sequence BA3 (fig. 77) starts with argillaceous hemipelagic limestone, followed by coarse grained bioclastic limestones and ends with the Font Froide marls corresponding to the late transgressive systems tract and aximum flooding surface where glauconite is abundant. This TST and the maximum flooding, contains several ammonites belonging to the *Gerhardtia sartousiana* zone (middle part of the late Barremian). The *Camereiceras limentinus* level, defined in this region of the Southern Vercors,corresponds to the lower part of the Font Froide marls and to the last underlaying calcareous beds. Above the Font Froide marls, ammonites of the *Hemifoplites feraudianus* zone occur. Along the Col de Rousset section, the first carbonate platform deposits belonging to the Urgonian limestones Fm. appear in the highstand systems tract of the depositional sequence BA3. Above, the syncline shows the top of the Urgonian limestone Fm. (BA4, BA5 and AP1 depositional sequences).

2.- Overview of the Western cliff of the Glandasse plateau

This stop give us the opportunity to observe the global Barremian lowstand systems tract of the southern Vercors. The geometry and succession of all sequences are clear (from the sequence BA1 HST to the sequence BA3 TST). The Glandasse plateau section is one of the more impressive (20 km long with a 2000 m thick Barremian) of the South-East France.

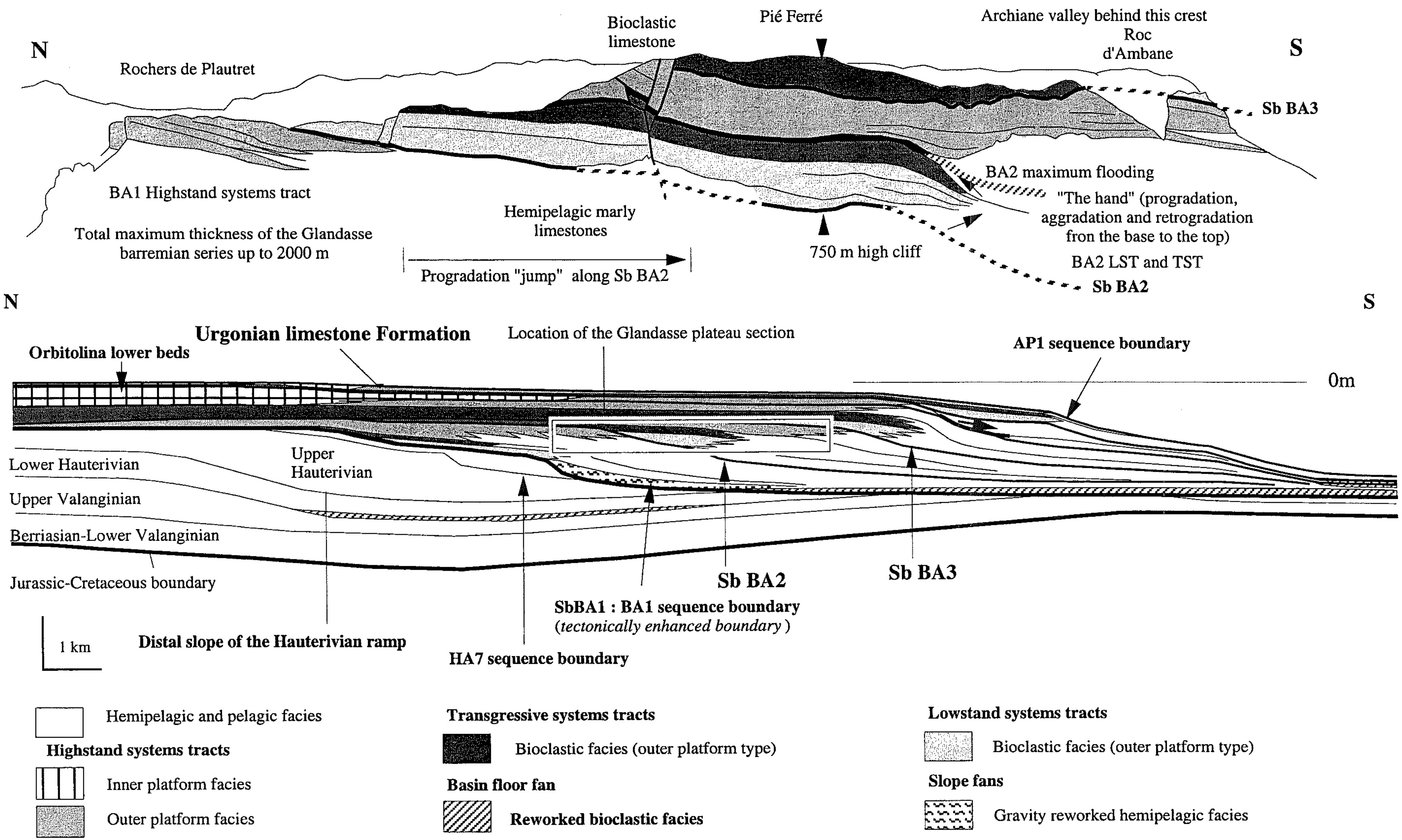

FIG. 63.- Overview of the western cliff of the Glandasse plateau. Platform to the left, Vocontian basin to the right. Four bioclastic units are observed from the North to the South. **The first one** (Rochers de Plautret) shows several more and more upwards prograding sequences, and corresponds to the Montagnette BA1 highstand prograding wedge. **The second one**, very thick, is made up of prograding, then retrograding sequences : it corresponds to the lower Archiane unit (BA2 lowstand prograding wedge and transgressive systems tract). **The third one** shows a succession of prograding sequences (below Roc d'Ambane); it corresponds to the BA2 highstand systems tract, here particularly developped, contrary to the Combau and Archiane sections. **The fourth one** is not clearly visible in this panorama, but corresponds, at the top of the Glandasse plateau, to the BA3 transgressive systems tract.

Day 3

Urgonian platform bank margin

Outer shelf Lowstand prograding facies in a ramp setting
Transition to the lower slope

Hubert Arnaud, Annie Arnaud-Vanneau and Elisabeth Carrio-Schaffhauser

Purpose of the days.– This day is devoted to (1) sequence stratigraphy at seismic scale of the Urgonian platform bank margin and (2) lateral change from bioclastic outer shelf facies to hemipelagic marly-limestone facies of the vocontian through.

Itinerary.– Les Nonières (hotel) - Bénevise- Vallon de Combau and return. Châtillon-en-Diois-Sisteron-Barrême-St. André-les-Alpes (hotel)

Three depositional sequences are visible along the Vallon de Combau section. All of them are characterized

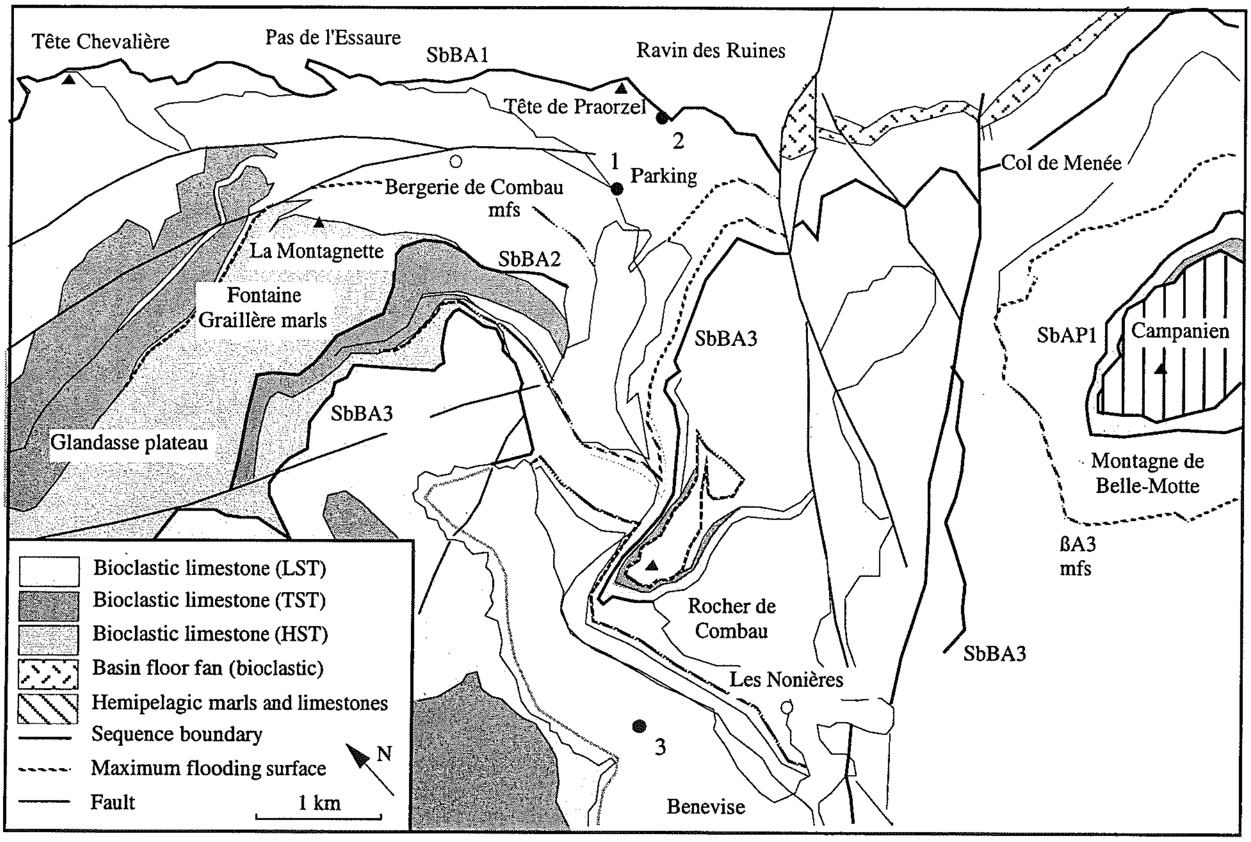

Fig. 64.- Schematic map of the Vallon de Combau showing location of stops: 1, Fontaine des Prêtres; 2, Tête de Praorzel; 3,Bénevise (panorama of the Rocher de Combau).

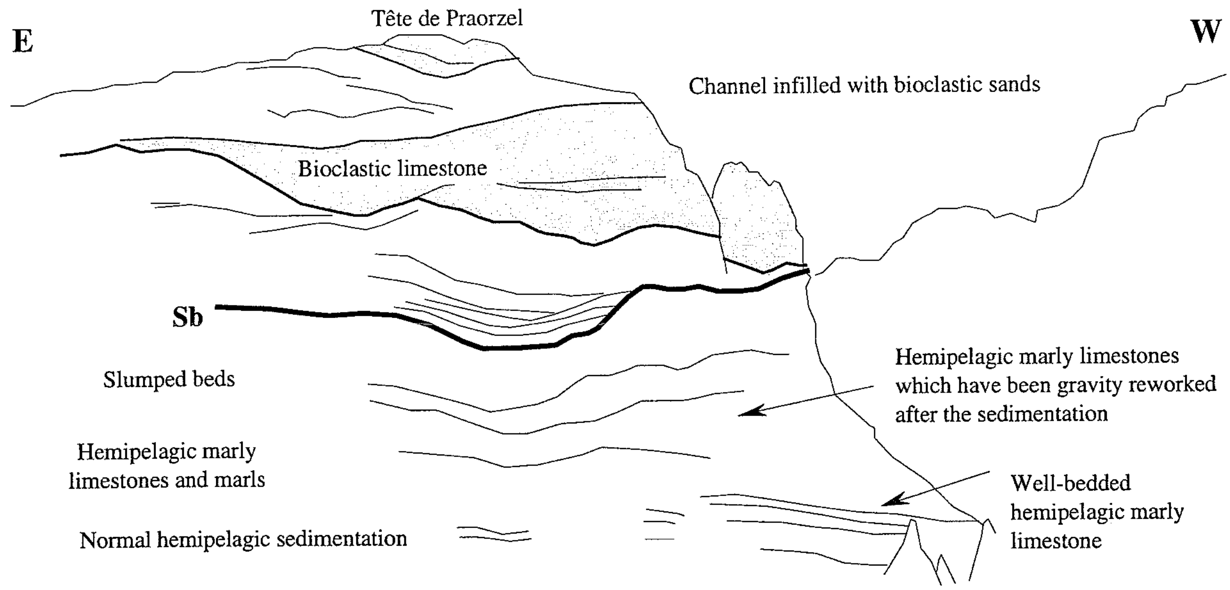

FIG. 65.- Overview of the Ravin des Ruines. The platform is to the right, the basin to the left. The B1 sequence boundary separates two groups : (1) below, well bedded hemipelagic argillaceous limestones and marls (Upper Hauterivian); (2) above, pelagic argillaceous limestones and marls with numerous ablation surfaces overlaid by onlapping beds. At the top, fine grained bioclastic limestones that originate from the platform edge (located at that time about three kilmometres in the North-East, near la Tête Chevalière, fig. 64). All these beds above the B1 sequence boundary are considered as a slope fan *sensu* Vail. Contrary to deep sea fans, slope fans are not the result of a piling up or coarse turbidites.

by their thicknesses (several hundred of meters) and their systems tracts, including thick lowstand wedges. Examples of parasequence sets and, perhaps, of stratal pattern are shown both for lowstand and highstand systems tracts.

From the Hauterivian-Barremian boundary (Barremian crisis) to the early Late Barremian, the sediments prograde towards the vocontian through and pinch out towards the emergent Jura-Bas Dauphiné platform. Upwards, the general backstepping, which corresponds to the Urgonian formation deposits (lower member), is clearly visible until the transgressive surface (TS) of the depositional sequence BA3 (Late Barremian). Then, the Urgonian limestones, that are well developped everywhere in the Dauphiné zone (Subalpine Chains), appears clearly as a general **transgressive formation.**

Slope fans can be observed near Menée pass (BA1 sequence) and Bénevise (BA2 sequence).

1.– Some more general data.

The field data presented in the Chichilianne-Glandasse area show that the unconformity that we followed at the base of the Urgonian cliff (**Gorges du Nant**) passes on basinward, along the Early Barremian paleoslope, to major surfaces of submarine erosion due to collapse features and canyons incisions.

We will emphasize the fact that these erosional surfaces are located in an area where the hemipelagic ramp is probably structurally steepened (Menée fault, Arnaud [1972 and 1981] and, perhaps, Cléry fault). The first one among these faults bound half grabens, ten to twelve km wide, that are comparable in size to those recognized on seismic profiles of passive margins of present-day oceans or in the external basement massifs between La Mure and Bourg d'Oisans.

These half grabens, however, are of Early Cretaceous age, and may be correlated with the so-called "Atlantic-Biscay rifting." Thus we can think that the location of the Early Barremian paleoslope is locally controled by this half graben. To the North it is a gently deeping hemipelagic ramp, whereas to the South it is a complex network of half-grabens and tilted blocks with a hemipelagic, then pelagic sedimentation. The Menée fault direction is NE-SW, and corresponds to the elongation of the major Jurassic tilted blocks known in the external zone of the Western Alps. Chichilianne (near the famous Mont Aiguille) is located in the thickest part of the half-graben. This one is filled up by mainly hemipelagic early Cretaceous sediments.

We have found evidence for two sequences boundaries (SbH7 et SbB1) in this slope setting, laterally to the early Barremian unconformity of the Northern Vercors. We consider these sequence boundaries as tectonically enhanced unconformities, because of the horizontal extent and magnitude of the erosion both along the slope and onto the emergent Jura platform. They appear on tectonic subsidence curves of this area as an uplift.

2.– SbB1 SEQUENCE BOUNDARY BETWEEN CHICHILIANNE AND THE MENÉE PASS

The distant examination do not allow to clearly separate the two erosional surfaces SbH7 and SbB1. They both coincide with the downcutting erosional truncation of a submarine canyon. SbB1 is particularly well documented. In some places, submarine erosion has removed several hundred of meters of late Hauterivian-early Barremian slope hemipelagic facies, cutting below the sequence boundary SbH7 (fig. 17).

The erosional surface of sequence boundary SbB1 is visible in outcrops for more than 10 km from the pre-existing slope-break (Mont Aiguille area) to the toe of the slope to the South-East (east from the Menée Pass). The SbB1 sequence boundary served as a sediment transport path accross the slope and is back-filled by onlap of hemipelagic shales, debris flows and turbidites within the base of the slope. It is downlapped by the toes of the overlying lowstand prograding complex in the upper slope area.

Within the basin, the SbB1 erosional surface passes into a conformable surface. The conformable area is characterized in outcrop sections by an abrupt change in the lithology at the sequence boundary. Highstand pelagic (or deep hemipelagic) shales of the underlying sequence are overlain by coarse-grained massive bioclastic limestones of the **basin floor fan** (Calcaires de Borne formation).

The HA7 sequence is different. The truncation below the sequence boundary HA7 extends into the basin, where both the Hauterivian and part of the Valanginian have been removed by erosion.

The erosion is well visible between the Menée pass and the Col de la Croix-Haute pass where the BA1 basin floor fan lies just over valanginian marls.

3.– RAVIN DES RUINES, CLOSE EXAMINATION OF SLOPE FAN DEPOSITS

Above the sequence boundary B1, we will see that carbonate slope fans may have a stratal pattern that is surprisingly similar to siliciclastic slope fans. They always pinch out by onlap onf the underlying sequence boundary. They are overlain by the basinal toes of clinoforms of the overlying prograding complex. The top of the slope fan is a downlap surface indicating sediment starvation and a place where a hardground may develop. It is called the top slope fan surface (Vail, 1987).

The slope fan of sequence BA1, along the slope surface, can be separated into an **upper slope fan** (Tête Chevalière area, in front of Chichilianne) and a **lower slope fan** (Tête de Praorzel-Ravin des Ruines area).

The upper slope fan (Tête Chevalière area) is characterized by fine-grained limestones composed of skeletal debris grainstones or packstones that onlap the canyon floor in a landward direction.

The lower slope fan (Tête de Praorzel-Ravin des Ruines) is deposited at the base of the erosional canyon and displays evidence of reworked material, such as large slide blocks, debris flows, chaotic slumps, coarse-grained turbidites, interbedded with hemipelagic shales. These reworked sediments fill in the irregular topography of the canyon floor, and fill in erosional distributary channels that cut into thick hemipelagic shales.

4.– MENÉE PASS ROAD : SEQUENCE BA1, UPPER PART OF THE BASIN FLOOR FAN

This outcrop is located 2 km basinward from the Ravin des Ruines. The erosional SbB1 sequence boundary cuts down into the early Upper Hauterivian made of deep hemipelagic marly limestone and marls.

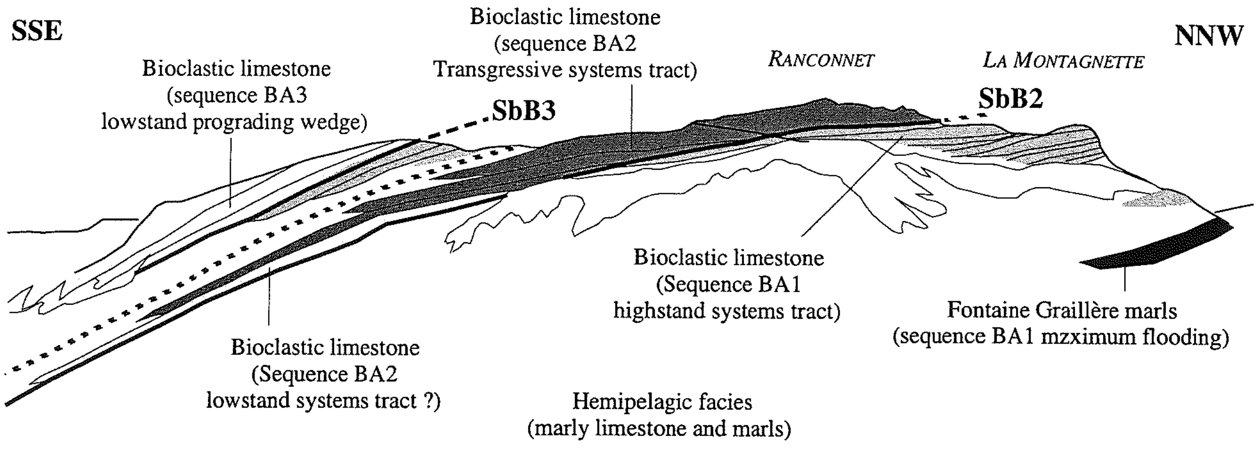

FIG. 66.- Overview of the eastern side of the Montagnette cliff showing BA2 and BA3 sequences. Sequence BA2 lowstand systems tract is not well developed, because sediments were probably reworked on the slope (source sediments for the sequence BA2 basin floor fan).

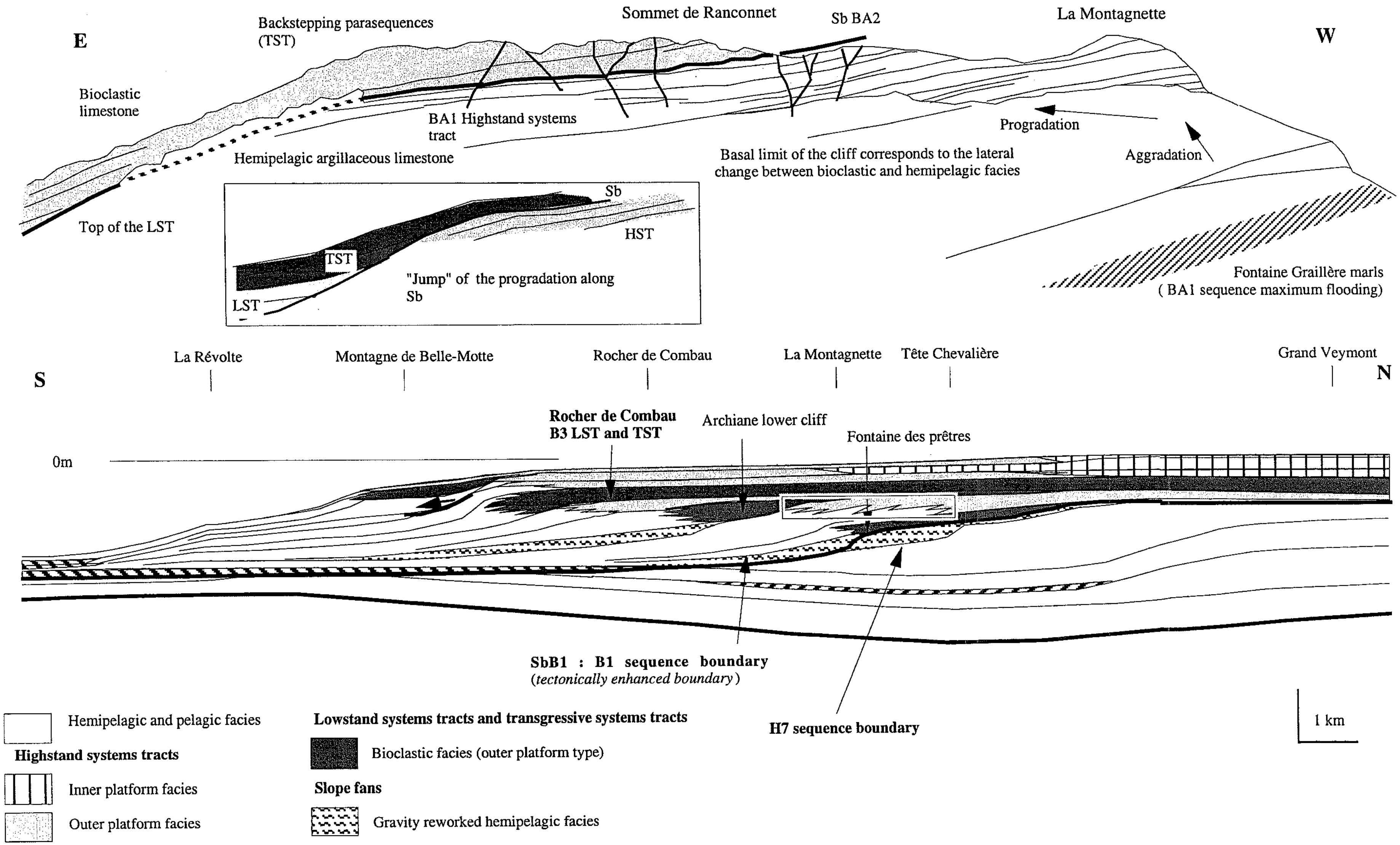

Fig. 67- Overview of La Montagnette seen from the shepherds house. The platform is to right.

The BA1 erosional surface is onlapped by coarse grained bioclastic turbidites. These reworked sediments fill in the irregular topography of the erosional surface and channel floors. They correspond to the upper part of the BA1 basin floor fan which develops basinward in the Borne-Glandage area (area more than 300 km^2, maximum thickness around 200 m). This basin floor fan is the more important of the Barremian-Lower Aptian series. In the Borne area and the Dévoluy basin floor fan are also known in sequences BA2, BA3 and AP1 and show a progradational trend along the slope-basin boundary.

5.– Platform-Basin transition in a shelf-break setting : BA1, BA2 and BA3 depositional Sequences

5.1. Tête de Praorzel

This stop allows the closed observation of the erosive sequence boundaries SbH7-B1 which were visible along the "Ravin des Ruines". They correspond to an abrupt change in lithology: highstand hemipelagic marls and marly-limestones are overlain by bioclastic limestones.

On the other side, the entire depositional sequence BA1 is well exposed from the sequence boundary BA1 to the highstand systems tract (top of the Montagnette cliff) . The following transgressive systems tract of the sequence BA2 is located at the toe of the last bioclastic Ba1 HST clinoforms and onlap on the sequence boundary BA2. Note that, in this point, the lowstand prograding wedge of the depositional sequence BA2 does not exist, probably due to the gravity reworking of sediments towards the basin.

5.2. Tête Chevalière

The hemipelagic shales are eroded by the sequence boundary SbB1. Above, the upper slope fan is characterized by fine grained limestone composed of skeletal grains (F2 and F3 facies). This limestone has a basal erosive surface. Incised surfaces, dislodged beds, synsedimentary gliding planes and channels are well exposed. The upper slope fan is overlaid by the first coarse grained bioclastic parasequences (F5 facies) of the BA1 lowstand prograding wedge.

5.3. Vallon de Combau, La Montagnette

At the bottom of the Combau valley, the parking place is located only at 1,5 km from Ravin des Ruines), but a bit more upstream on the Barremian slope. The Barremian beds comprise here two depositional sequences (BA1 and BA2).

The BA1 depositional sequence (Montagnette unit) begins with a lowstand prograding wedge. Its more prograding sequence shows a thinning out of the coarse grained bioclastic facies at the parking place (Fontaine des Prêtres). These coarse grained bioclastic beds (biosparites with Orbitolinidae, Dasycladacean algae, crinoids and numerous fragments of corals) are partially or completely dolomitized and display a very important secondary porosity (see E. Carrio-Schaffhauser, this volume). Above, the transgressive interval corresponds to a facies retrogradation along more than 3 km. The above mentioned bioclastic facies are overlaid by argillaceous limestones (Fontaine Graillère marls). The maximum flooding is capped up by the beds of the Montagnette cliff, entirely made up of coarse grained bioclastic limestones. The sequences are more and more prograding upwards and are separated by clinoforms. The whole is therefore interpreted as a *highstand prograding wedge.*

The BA2 depositional sequence. The top of the highstand wedge of the Montagnette is marked by an erosional surface above which the BA2 sequence begins with rather massive bioclastic limestones. The limit of the latter towards the basin is clearly prograding with respect to that of the upper parasequence of the underlying highstand prograding wedge. These limestones of the lower part of BA2 sequence show a backstepping disposition so that they could be interpreted as a transgressive systems tract. These bioclastic parasequences are overlain by the argillaceous limestones of the so-called Fontaine Colombette marls (*maximum flooding* of sequence BA2).

The facies can be easily observed in this area. Several points have to be emphasized.

(1) Two families of facies only are present, viz. on the one hand the more or less argillaceous hemipelagic F1 facies (micrites with sponge spicules), on the other hand coarse grained F5 bioclastic facies (biosparites with Orbitolinids, Dasycladacean algae, large benthic fomarimifera and numerous fragments of infralittoral or circalittoral fossils).

(2) *The transition from one facies to the other is particularly rapid,* both vertically and laterally. **Erosional surfaces** between the hemipelagic facies and the underlying bioclastic ones are frequently observed. This could be linked with the presence of **storm-transported sediments.** Upstream, the very coarse grained, badly sorted bioclastic facies grade laterally within a few hundred metres to better sorted facies, then sometimes to oolithic facies. The role of hydrodynamics, especially of the waves, is very important so that the stormweather wave base might have been only a few metres below or above the limit between bioclastic and hemipelagic facies.

(3) In detail, great facies differences exist in terms of precise location within the depositional sequence. This point has to be more studies, but from now it seems clear that :

– the more badly sorted bioclastic facies and the erosional surfaces occur above all basinward,

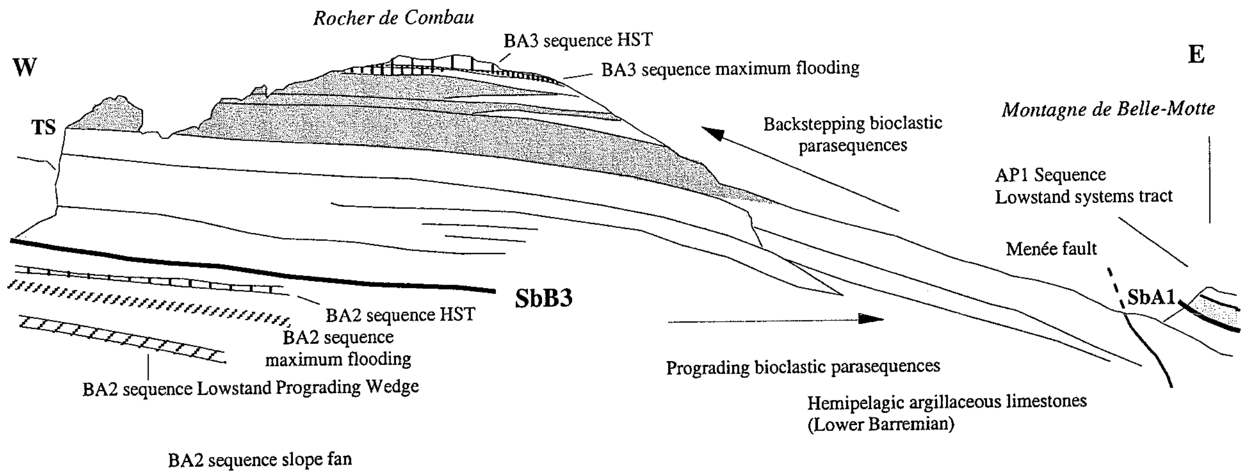

FIG. 68.- Overview of the Rocher de Combau. A carbonate body at the edge of the platform. The platform lies to the left, the vocontian basin to the right.

– the more fine grained facies, sometimes better sorted, and above all rich in various fossils occur above all landward, in highstand systems tracts.

– the first rudists facies may occur locally landward in the upper parasequences of the highstand wedges,

– the oolithic facies are particularly developped in the late transgressive systems tracts and early highstand systems tracts.

On this margin, two main types of shallowing upward sequences grouped together in parasequence sets can be observed in all the depositional sequences.

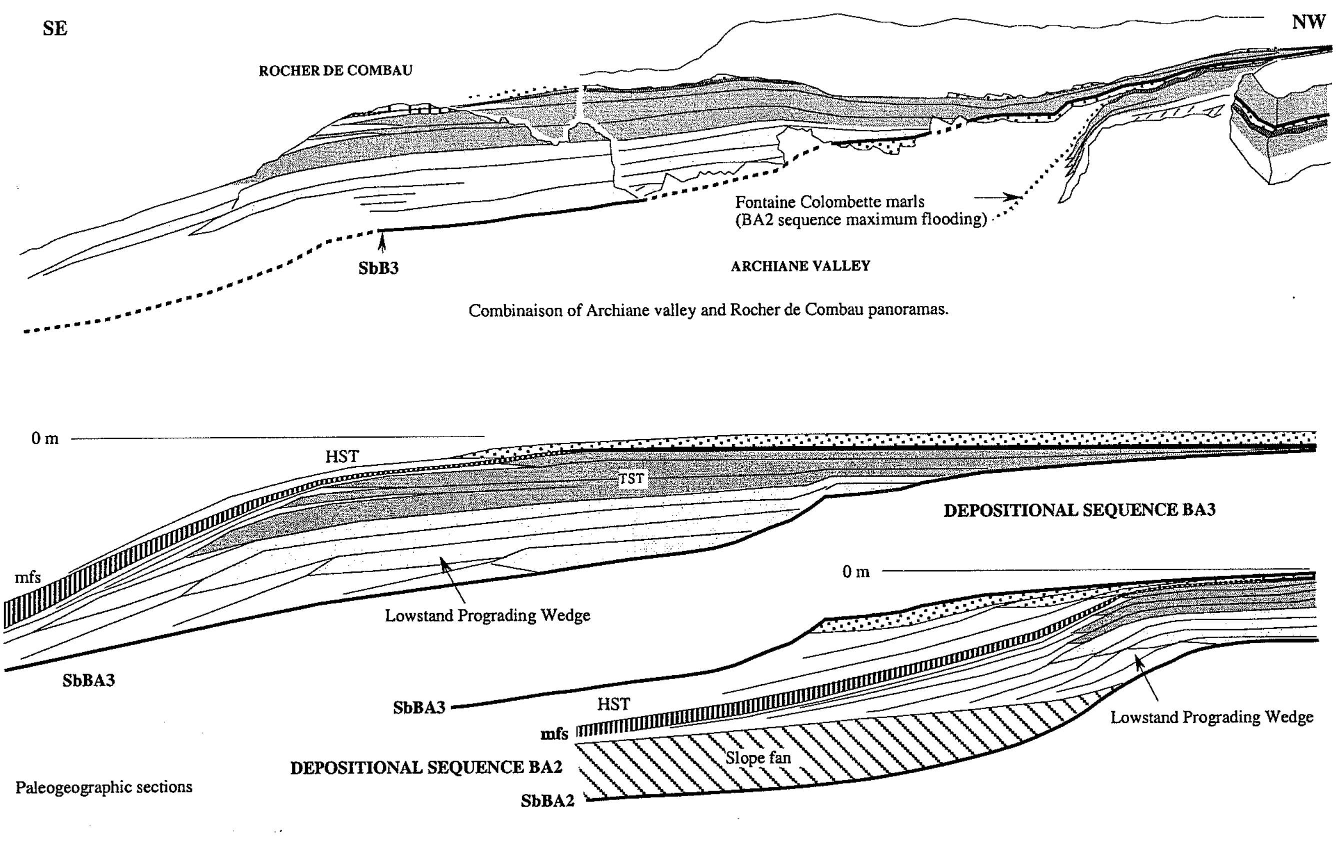

FIG. 69.- Reconstitution of the sedimentary geometries in the southern Glandasse plateau (Archiane valley and Rocher de Combau).

The first ones are thin and correspond to sequences present at the toe of the bioclastic clinoforms. They take place where bioclastic facies laterally change to hemipelagic facies. They are arranged in the following order above the hemipelagic facies : 1) fairly argillaceous wackestone with debris of circalittoral organisms ("ball-shaped" bryozoans, crinoids); 2) poorly sorted packstone-grainstone with little or no clay and dominant circalittoral squeletal grains.

The second ones correspond to sequences of clinoform. They are more complete and finish with 3) grainstone with coarse or very coarse debris (corals, large foraminifers, Dasycladacae algae) arranged in well-sorted millimetric beds, alternately fine or coarse (influence of the waves in foreshore environments); 4) oolitic grainstone with cross bedding. This top level is locally overtopped by small patch reefs. The nature and vertical distribution of bioclasts suggests a variation in environments which were circalittoral at the base and infralittoral at the top. The sedimentological features indicate deposition above fairweather wave base.

5.4. Rocher de Combau : Geometry of lowstand wedges and of transgressive systems tracts on a plaform edge

The Rocher de Combau is a thick cliff of coarse grained bioclastic limestones (well sorted biosparites with numerous Orbitolinidae, benthic foraminifers, metazoans and Dasycladacean algae, Facies F5) that overlays argillaceous limestones and hemipelagic marls (Facies F1). The limit between the Lower and the Upper Barremian is probably very near to the sequence boundary SbB3, according to the sequence stratigraphy correlation with the Angles section (stratotype for the Barremian). Four points will be emphasized :

(1) the Rocher de Combau bioclastic limestones rest upon a very clear sequence boundary (SbB3),

(2) the facies transition between coarse grained bioclastic limestones and argillaceous hemipelagic limestones is particularly rapid, as we can observe all along the barremian bank margin,

(3) the Rocher de Combau bioclastic unit shows the following stratal pattern : prograding at the base, then retrograding at the top. The proposed interpretation consists in a **lowstand prograding wedge overlaid by a transgressive systems tract,**

(4) at the top of the transgressive systems tract, hemipelagic facies (argillaceous limestones, then marls of the maximum flooding of the sequence BA3) rest upon coarse grained bioclastic facies. At the top, the hisgstand systems tract is represented by cherty limestones. The overlaying late Barremian deposits correspond to hemipelagic facies which is interpreted as the general backstepping of the carbonate sedimentation on the urgonian platform.

5.5. Overview onto the eastern and western sides of the Archiane Valley

This famous panorama will be visited only if heavy clouds cover the northern part of the Glandasse Plateau.

The Archiane valley cuts accross the Barremian platform-bank margin and displays a continuous outcrop exposure of the shelf-slope transition.

The following points are visible from distant examination, on both sides of the Archiane valley :

– the stratal pattern and facies changes inside BA2 lowstand prograding wedge,

– the aggrading and then backstepping BA2 transgressive systems tract,

– the downlap surface and the thin prograding BA2 highstand systems tract (landward, the top of this HST sonsist of a rudist bed with fresh water dissolutions),

– the thick prograding BA3 lowstand prograding wedge and its correlative pinching out towards the bank margin,

– the BA3 transgressive surface and facies changes throughout BA3 transgressive systems tract,

– the BA3 highstand systems tract.

These large overview provide very nice examples at seismic scales of lowstand prograding complex (depositional sequences BA2 and BA3).

Depositional sequence BA2. The top of the lowest outcropping prograding complex at the offlap break is the maximum progradation of bioclastic facies towards the basin for the BA2 sequence. Its thickness ranges up to 150 m and progradation may extent over a few km. The foreset beds of BA2 LPW in the bottom of the Archiane valley dip southward with an angle reaching 20°. In the proximal areas, each parasequence commonly consists of coarse-grained bioclastic limestones, with poorly sorted skeletal fragments packstone-grainstone at the base and well sorted grainstone at the top. In a basinward direction, foreset beds prograde southward along the foreslope to grey hemipelagic marly limestones and marls. Large slump scars are common in the area of the mudstone slope.

The offlap pattern of this lowstand prograding complex evolves from oblique in the early stage of the progradation to oblique aggradational in the latest stage.

Depositional sequence BA3. The top of the lowest outcropping prograding complex at the offlap break (lowstand prograding wedge of BA3 sequence) is the maximum progradation of bioclastic facies towards the basin for the BA3 sequence and all the Barremian series. Its thickness ranges up to 250-300 m and progradation may extent over 5 km.

Lowstand prograding complexes are composed of progradational to aggradational parasequence sets (the offlap pattern of the prograding clinoforms evolves within each LPW from oblique to aggradational). They are characterized by oblique clinoforms with toplap terminations within each of the parasequences.

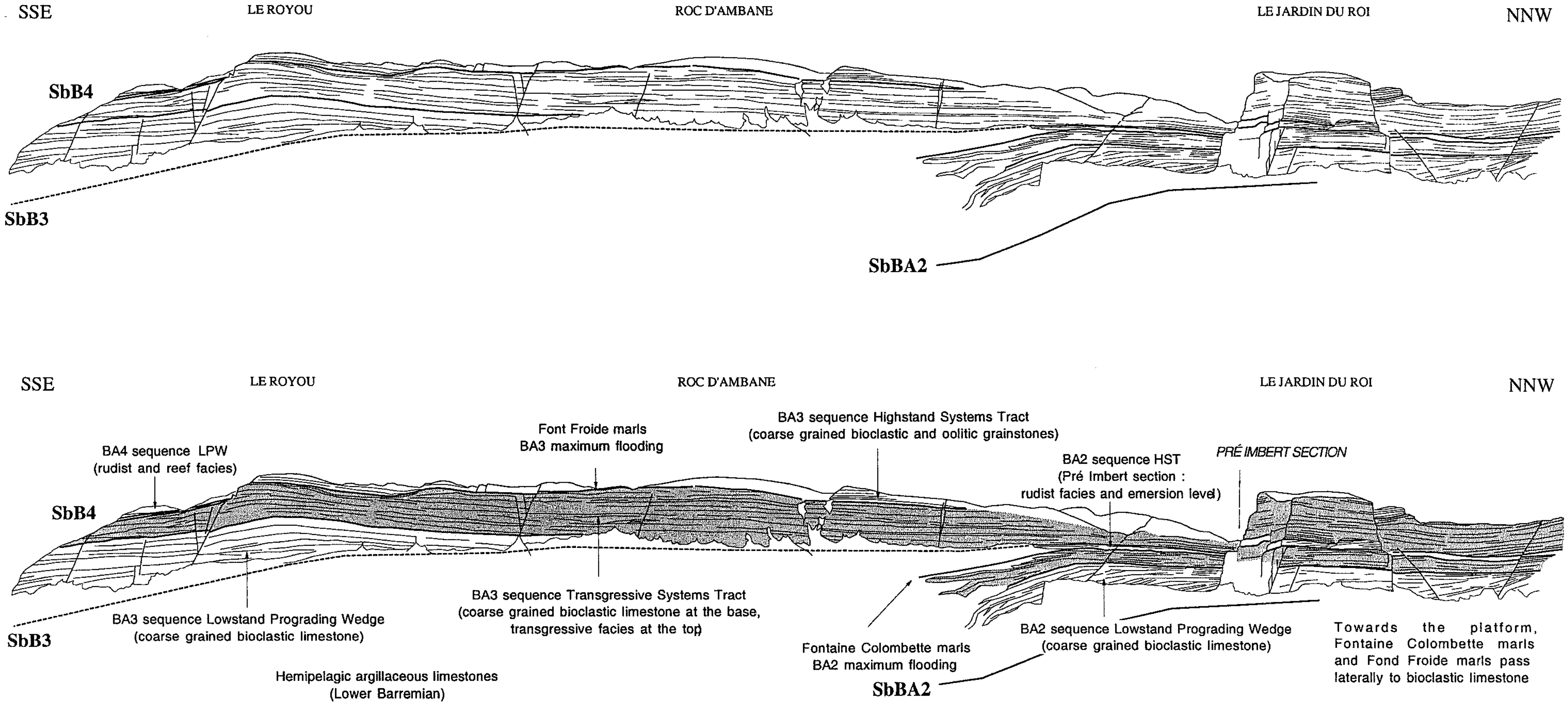

Fig. 70.- Overview of the Archiane cliff (Southeast cliff) : stratal pattern and sequence stratigraphy interpretation. Platform to the right, vocontian basin to the left. The lower Archiane unit, with its prograding then retrograding sequences, is the equivalent of the upper part of the Montagnette cliff (BA2 sequence Lowstand prograding wedge and Transgressive systems tract). Above, the Fontaine Colombette marls correspond to the maximum flooding of sequence BA3. The limestones of the upper Archiane cliff are the same as those of the Rocher de Combau (Base of the Upper Barremian, BA3 sequence Lowstand prograding wedge overlaid by Transgressive systems tract). They disappear laterally towards the North-East, i.e. towards the edge of the platform. They are overlaid by the transgressive systems tract of the Upper Barremian BA3 sequence.

Sequence BA3 provides an excellent example at the seismic scale of a lowstand prograding complex. It is composed of thick aggradational offlaps (200-300 m thick), deposited over the shallow marine limestones of the underlying sequence (HST BA2). It displays a "catch up" sigmoidal progradational geometry, where the concordant shallowing-upward parasequences of the shelf change basinward at the outer slope to thicker bioclastic wedges. These wedges made up of rounded, coarse-grained skeletal-debris grainstone dip gently basinward.

Towards the basin, the aggradational offlap pattern grades into a parallel pattern composed of well-bedded limestones and hemipelagic marly limestone and marls.

Towards the platform, the BA3 lowstand prograding wedge is only a few km NW from the offlap break of the underlying BA2 HST). The thickness and lateral extent of the bioclastic sediments deposited over the shelf is such that within the shelf-margin systems tract a very large accomodation space is required.

The BA3 transgressive surface and the *overlying transgressive systems tract* overlay the previous BA3 lowstand prograding wedge. The top of thelowstand complex of sequence BA3 is a flat erosional surface, called the transgressive surface, clearly visible as well in the Archiane valley as in the Rocher de Combau.

At the shelf margin, the BA3 transgressive systems tract is composed of thick backstepping parasequences of outer shelf facies. Each parasequence displays a flooding surface and shallows upward to bioclastic limestones. The parasequences and especially their marly basal part thicken upward to the flooding surface. The last of them is overlained by transgressive marls (Tussac marls = Font Froide marls). These marls indicate that this part of the platform was temporarily drowned ("give-up"), because of the rapid relative rise of sea level that exceeds the growth potential of the carbonate ecosystem. The Font Froide marls are dated by numerous ammonites of the Late Barremian *Gerhardtia sartousiana* zone. The HST, well developped from Glandasse Plateau to the Col de Rousset region, is made of coarse-grained bioclatic facies (F5 facies) with oolitic grainstones and patch-reefs. During the Barremian-Lower Aptian time, BA3 sequence late highstand and early TST correspond to the maximum abundance period of corals from the Southern Vercors to the Swiss Jura. This fact could be interpreted as a good tool for the interpretation of Barremian carbonate platform deposits.

6.– Conclusion

The Southern edge of the Urgonian platform is particularly interesting during Upper Barremian-Lower Aptian times for four main reasons.

1.– The thicknesses of the deposits are exceptionally high with respect to those of the Grenoble area. This results from accelerated subsidence rates after the Barremian crisis.

2.– During the transgressive interval of the top of the Upper Barremian, **facies backstepping occurs everywhere** in the South Vercors and around the Glandasse plateau. It is precisely the time when **the relative rise of sea-level gave birth to the flooding of the Jura-Bas Dauphiné platform, to the spread of the transgressive marly levels onto the inner platform, and to the appearance in this area of inner shelf sedimentation** with rudists (Urgonian limestones formation, lower member). At the same time, the edge of the platform was starved, characterized by absence or poor development of coarse grained bioclastic facies. Consequently, basin floor fan are missing in the basin, as other gravity reworked sediments (turbidites). **There are no bioclastic reworked deposits coeval with Urgonian limestone, lower member.**

3.– The Barremian-Aptian boundary is characterised by a **rapid fall of the relative sea level and by the individualization of a large lowstand wedge,** which is well visible below the Montagne de Bellemotte. This bioclastic lowstand wedge is separated from the Upper Barremian platform carbonates, by marly levels, locally several hundred metres thick. Therefore, there is no regular facies progradation on the edge of the platform, but, on the contrary :

– a retrogradation or at the best a stagnation of the facies limits during the Upper Barremian,

– a progradation in Aptian times, that results only from the presence of a lowstand wedge linked with an important fall of the relative sea level, coeval with the appearance of a large system of incised valleys in the Northern Vercors (and also fresh water cementation just below the sequence boundary SbA1, for example in the Balcon des Ecouges section).

(4) The period which is characterized by a maximum development of the platform carbonate facies on a regional scale (Urgonian limestones, lower member) globally corresponds to a predominantly marly, basinward thinning sedimentation on the edge of this platform. At the same time sandy bioclastic turbidites are absent or poorly developped in all the basin around.

DAY 4

THE VOCONTIAN TROUGH SERIES: THE BARREMIAN STRATOTYPE (ANGLES SECTION)

Thierry Adatte, Hubert Arnaud, Stéphane Bodin, Karl B. Föllmi, Alexis Godet and Jean Vermeulen

Purpose of the day.– This day is devoted to the Angles section, which is the Barremian stratotype. This section is a part of one of the most complete one of the vocontian trough, from Lias which crops out along the Castillon lake, to the Upper Cretaceous (and Eocene) at the top of the Pic de Chamatte mountain. Due to new data obtained these last years, this famous section appears now as a reference, not only for all study concerning the Barremian but also for correlation at regional scale.

Itinerary.– St. André-les-Alpes is only a few kilometres far from the Angles section. After the short study of the section we have to return to Neuchâtel, which is a long trip through the vocontian trough, the Northern subalpine chains and the Jura. The main road that we take, pass through the cities of Sisteron, Grenoble, Genève and the Col de la Croix-Haute pass. From Angles to Sisteron this road corresponds to the so-called "route Napoléon."

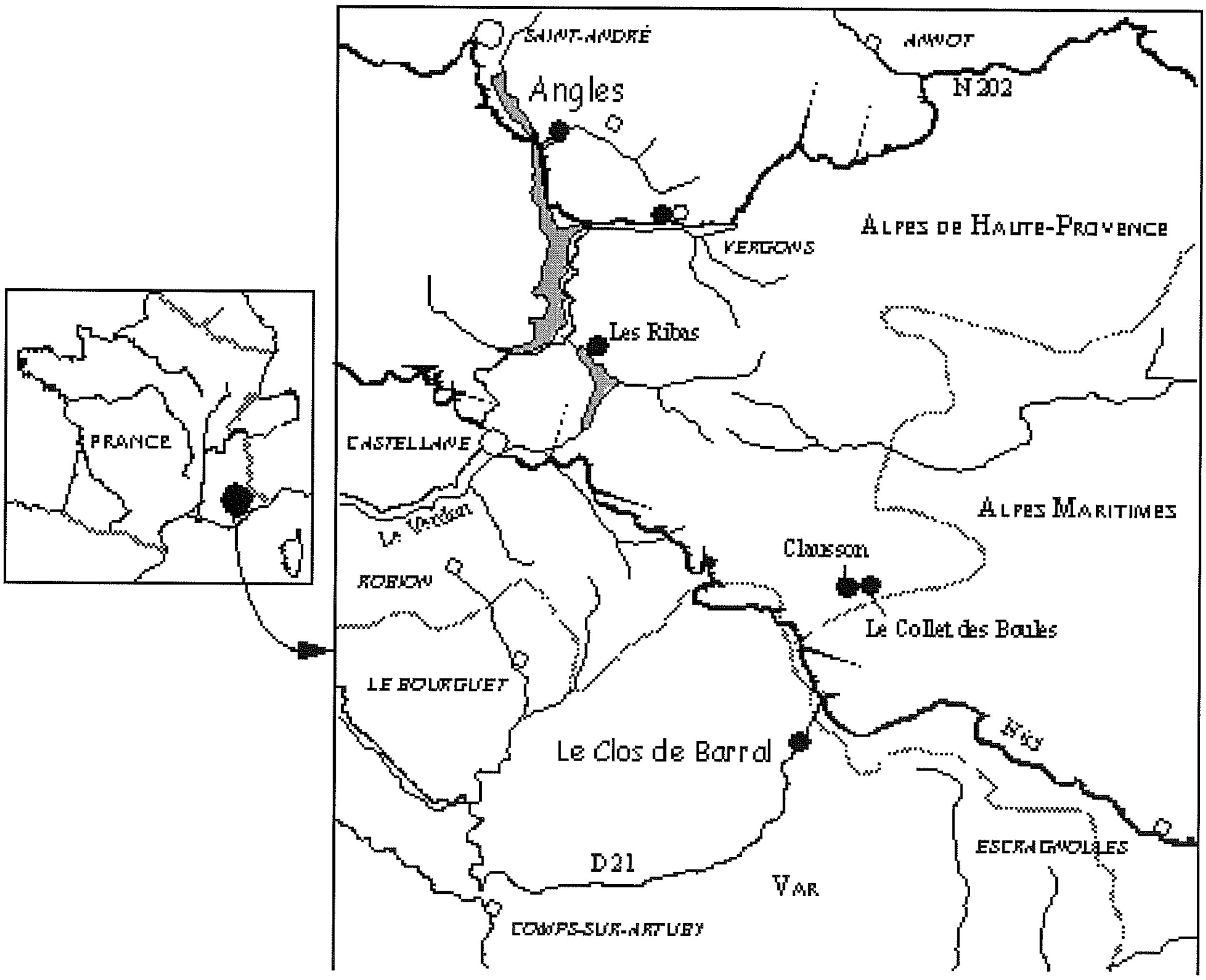

Fig.71.- Schematic map of the Barrême-Castellane region.

Palaeoceanographic and palaeoclimatic changes of the northern tethyan realm during the Hauterivian - Barremian: New insight from the Angles section (SE France)

Stéphane Bodin, Alexis Godet, Thierry Adatte and Karl B. Föllmi

1–. Introduction

The Hauterivian – Barremian is a time of major palaeoceanographic and palaeoceanographic changes. For example, during the latest Hauterivian, an oceanic anoxic event occurs and is recorded by the Faraoni level (e.g. Cecca *et al.*, 1994). During the late Barremian, the onset of the Urgonian platform marks the installation of oligotrophic conditions along the northern tethyan realm.

In order to better understand these palaeoceanographic and palaeoclimatic changes during the Hauterivian–Barremian of the northern tethyan realm, we have analyzed the Angles section in term of its mineralogy and geochemistry. In particular, we have focused on clay mineral assemblage changes for the mineralogical part of this study and on redox-sensitive trace elements, phosphorus and stable isotope ratio variations for the geochemical part.

Mineralogical assemblage changes recorded in both carbonates and marls are a fruitful proxy to assess palaeoclimatic changes. Indeed, by the way of total rock analyses, it is possible to quantify the detrital contribution at the time of its deposition and by the way of clay fraction analyses, it is possible to obtain information on the palaeoclimatic conditions. Indeed, the clay fraction in the whole rock is mainly formed on the continent in soils in function of the climate and is thereafter transported into the sea.

In complement of mineralogy, geochemical analyses give us information on the palaeoceanographic conditions. Thus, the redox-sensitive trace elements are a fruitful proxy to the palaeoredox conditions prevailing in the past oceans, whereas phosphorus gives information on nutrient level and stable isotopes are useful to understand palaeotemperature changes (for the oxygen stable isotopes) and carbon cycle (for the carbon isotopes).

2.– Methods

2.1. Mineralogy

X-ray diffraction allows the identification and the quantification of the different minerals which compose the sample. Two kinds of analysis are achievable. On the one hand, whole-rock analysis are performed in order to determine the major minerals of the rocks, and in a second time this approach permits to trace detritic influences. On the other hand, analysis on decarbonated samples help to determine the nature of the insoluble residue that is mainly composed of clay minerals in pelagic rocks; this method was applied to the fractions <2µm. The samples were prepared following the procedure of Kübler (1987) and analyzed by X-ray diffractometer (SCINTAG XRD 2000 Diffractometer). The precise methods for both whole-rock and insoluble residue analysis are described in Adatte *et al.* (1996).

2.2. Redox-sensitive trace elements

ICP-MS analyses were performed on bulk rock samples from the limestone intervals for all three sections. The samples were sawed in order to eliminate the altered parts and the veins of the rock. Then, powders were obtained using a mechanic agate crusher. A portion of approximately 250 mg was transferred into a digestion vessel (PTFE) and 10 ml of concentrated nitric acid (suprapur, Merck) were added. The sample was digested in a microwave oven (MSL-Ethos plus, Milestone) using the heating program recommended by the EPA 3051 method. After cooling, the resulting solution was filtered (0.45 µm) and diluted to 100 ml with ultrapure water. Solubilization percentages determined after filtration were about 91.3 ± 2.6 % of initial sample weight.

A second dilution (1/20) was then performed prior to analysis. To correct for matrix-induced ion signal variation and instrumental drift, rhodium was used as the internal standard. The element concentrations of the acid digests were determined by ICP-MS (ELAN 6100, Perkin Elmer) using a semi-quantitative mode (Totalquant).

2.3. Phosphorus

Total phosphorus analyses were performed on bulk rock samples from the limestone intervals for all four sections. The samples were sawed in order to eliminate the altered parts and the veins of the rock. Then, powders were obtained using an agate crusher. Around 100 mg of powder were mixed with 1 ml of MgNO3 and left to dry in an oven at 45°C for 2 hours. The samples were then ashed in a furnace at 550°C during two hours. After cooling, 10 ml of 1N HCl were added and placed under constant shaking for 14 hours. The solutions were filtrated with a 63µm filter, diluted ten times, and analyzed using the ascorbic acid method of Eaton *et al.* (1995). For this process, the solution was mixed with ammonium molybdate and potassium antimonyl tartrate, which in an acid medium react with orthophosphate to form phosphomolybdic acid. This acid is reduced with ascorbic acid to form an intense blue color. The intensity of the blue color is determined with a photospectrometer (Perkin Elmer UV/Vis Photospectrometer Lambda 10). The concentration of PO4 in mg/L is obtained by calibration with known standard solutions. Individual samples were measured three times and precision was better than 5%. Replicate analyses of samples have a precision better than 10%.

In order to avoid problems of condensation, we decided to calculate phosphorus accumulation rates (PAR). The PAR is expressed in mg of P per cm2 per kyr. This is a multiplication of the concentration in P (mg/g), the density (g/cm3), and the sedimentation rate (cm/kyr). As all the samples are pelagic or hemi-pelagic mudstones, the density was assumed to be constant and equal to 2.5 g/cm3 for all analyzed samples.

To obtain sedimentation rates, we need an age model. This one was obtained by a cyclostratigraphic approach. Indeed, following the study of Giraud *et al.* (1995) in the late Hauterivian (angulicostata zone) sediment of Vergons, we considered that each limestone-marl couplet represents a duration of 20 kyr. We estimated as such an average sedimentation rate for the successions of sediments that correspond to the time envelopes of complete ammonite zones (Vermeulen, 2002). It appears that in the Angles section, the *G. sartousiana* and the *H. feraudianus* zones are not complete due to the presence of hiati and/or condensed sediments (Delanoy, 1997; Vermeulen, 2002; see also Wissler *et al.*, 2002). For the sediments attributed to these two ammonite zones, we decided to use the time envelopes for the corresponding sedimentary intervals from the Saut-du-Loup section, which is situated in the same area (close to Barrême) and appears to be more complete (Vermeulen, 1980).

2.4. Stable isotopes

The samples were analyzed at the stable isotope laboratory of the Department of Mineralogy and Geochemistry at the University of Karlsruhe, Germany, using an Optima (Micromass, UK) ratio mass spectrometer equipped with an online carbonate preparation line (MultiCarb) with separate vials for each sample. Subsequent replicate sample analyses for ?13C were within 0.05 to 0.06‰ and for ?18O ranged from 0.06 to 0.12‰.

3.– Results

3.1. Mineralogy

At Angles, whole-rock analysis reveal the presence of five major minerals (fig. 1): the calcite, the phyllosilicates (clay minerals and micas), the quartz, the Na-plagioclase (albite) and the potassic feldspar (microcline), with mean values of 68.35, 8.85, 5.81, 0.5 and 0.25 %, respectively. Some phyllosilicates, the organic matter and some badly crystallised minerals (such as pyrite and goethite) can not be quantified; this unquantified component represents an average of 16.12 % of the whole-rock.

At first sight, the calcite shows no huge variations, except in the *B. balearis* and *S. angulicostatum* zones, and in the *H. uhligi* and in the *H. sayni* zones on the other hand, where decreases of 15 to 20 % are observed. The quartz decreases slightly from the base of the section up to the *N. pulchella* zone; then, it increases up to the Aptian. The evolution of the phyllosilicates is comparable to the one of the quartz, with a rapid increase in the bancs just before the Faraoni level (at 24.50 m depth). Finally, the evolution of the plagioclases and the feldspars are broadly stable, expect peaks located just below the Faraoni level, in the early Barremian (*A. kiliani* and *K. nicklesi* zones) and in the late Barremian (from the *K. compressissima* zone upward). A detritism index (DI) is calculated by dividing the percent of calcite by the percent of quartz plus the percent of phyllosilicates. High values of the DI reflect therefore low detritic flux.

In the <2µm fraction (fig. 2), the smectite, the kaolinite, the mica, the chlorite and the mixed-layers were identified, with mean relative abundances of 21, 19, 44, 7 and 10 %, respectively. The evolution of the kaolinite/mica, kaolinite/mica and smectite/mica ratios points out the predominance of the kaolinite on both the smectite and the mica. In particular, the kaolinite amount reaches 25 % of the clay mineral content in the part II in both fractions, whereas this mineral disappears in the early Aptian. A remarkable negative shift can be distinguished within the early late Barremian (*H. uhligi* and *H. sayni* zone). On the contrary, the smectite is the most abundant mineral in part I and especially in part III where the smectite reaches a maximum of about 80 % in the *M. sarasini* zone (<2µm fraction). Then, in the <2µm fraction, the evolution of the mica is rather stable, except a plateau in the *K. compressissima* zone that shifts the values from 45 to 35 %. The evolution of the mixed-layers and of the chlorite is rather comparable: small variations of second-order are superimposed to a uniform general trend.

3.2. Redox-sensitive trace elements

Interesting results were obtain for Zn, As, V, Mo and U (fig. 3). Except for the vanadium which present high frequency fluctuations, the other four elements have a similar behavior. Indeed, all along the Angles section, with the exception of two peculiar level (Faraoni level equivalent and *H. feraudianus* ammonite zone), the values are very low. In the beds equivalent to the Faraoni level we can distinguish a huge enrichment of the five elements (420.8, 6.3, 8.9, 4.9 and 2.1 ppm respectively). In the *H. feraudianus* ammonite zone, a clear enrichment of U and a small enrichment of Zn, As and V can be distinguished too.

3.3. Phosphorus

For the Angles section, PAR values vary between 0.57 and 1.96 mg/cm2/kyr, with an average value of 1.08 mg/cm2/kyr (Fig. 4). After a more or less constant trend in sediments attributed to the B. balearis zone (mean value of 1.28 mg/cm2/kyr), a first decrease is observed in sediments of the *S. angulicostatum* zone, and a minimum in PAR values is reached within the Faraoni level (0.57 mg/cm2/kyr). Higher up in the section, the trend in PAR values increases again up to the sediments of the latest *K. nicklesi* zone. A small positive shift is observed in sediments of the middle *A. kiliani* zone. In sediments from the *N. pulchella* to the *C. darsi* zones, the values are firstly rapidly decreasing, and then more or less constant with a positive shift in sediments dating from the beginning of the *K. compressissima* zone. In the following, the PAR values are increasing up to the end of the *C. darsi* zone. Finally, in the sediments near the top of the section dated as late Barremian – earliest Aptian, the long-term trend appears more or less constant (around 0.98 mg/cm2/kyr) despite some high-frequency fluctuations (especially in sediments of the *G. sartousiana – H. feraudianus* zones).

3.4. Stable isotopes

The $\delta^{13}C$ curve (fig. 4) displays a slight increase for sediments belonging to the *B. balearis* and *S. angulicostatum* zones (from 1 to 1.4‰); the data corresponding to the Faraoni equivalent display an acceleration of the general increase before a stabilization of the signal. Sediments attributed to the *P. mortilleti* and *A. kiliani* zones show a decreasing trend of 0.2‰. Overlying sediments characteristic for the *K. nicklesi, N. pulchella,* and *K. compressissima* zones display an irregular evolution in $\delta^{13}C$. Sediments attributed to the *C. darsi* zone show an increase in $\delta^{13}C$ values from 1.3 to 1.8‰, whereas sediments from the *H. uhligi* to *G. sartousiana* zones display more stable and slightly increasing values. The $\delta^{13}C$ curve shows an increase for sediments of the *H. feraudianus* zone, followed by a decrease from 2.25 to 1.75‰ for sediments belonging to the *I. giraudi* and *M. sarasini* zones. The $\delta^{13}C$ trend increases again to 2.25‰ in sediments of the *D. oglanlensis* zone, thereby marking a minimum in sediments right at the Barremian – Aptian boundary.

The evolution of the $\delta^{18}O$ curve is more variable (fig. 4), with a double negative peak from –3 to –4.15‰ near the base of the measured section. Then, the$\delta^{18}O$ record slowly increases in sediments belonging to the latest Hauterivian and remains rather stable for sediments from the remainder of the Hauterivian and the lower part of the early Barremian. In sediments attributed to the upper part of the early Barremian and the lower part of the late Barremian, the trend in $\delta^{18}O$ is negative, and a minimal value of about –4.15‰ is reached in sediments of the *H. sayni* zone. The subsequent positive trend in $\delta^{18}O$ values lasts until the base of the *I. giraudi* zone, where the $\delta^{18}O$ curve reaches a value of –2.75‰. The uppermost part of the $\delta^{18}O$ curve displays a decrease toward the lowest values of the measured section (–4.18‰).

4. Discussion

4.1. Mineralogy

For the whole rock analysis, it appears that the main feature is the evolution of the detritism index, which can be divided into three parts:

I. From the base of the section to the Faraoni level (*S. angulicostatum–P. mortilleti* boundary), the DI is low.

II. From the Faraoni level to the *H. feraudianus* zone (around 109 meters), the values of the DI increase sharply.

III. From 109 m to the top of the section, the DI decreases to values comparable to the first part of the curve.

It appears thus than the detritic contributions from the continent were lower from the Faraoni level to the *H. feraudianus* zone than in the lower and upper part of the section.

In the clay mineral fraction, the most striking feature is the predominance of the kaolinite in comparison to the smectite in the great part of the Barremian of Angles. Kaolinite is formed under humid and wet climate on continental soils. This may reveal a climatic change in the northern tethyan realm, from a well-contrasted (mostly arid) season climate (during the *B. balearis* zone) to a humid and warm climate (such as an intertropical climate) from the *P. mortilleti* to the *H. feraudianus* zone. In the early late Barremian, this humid climate is however marked by a slow return to more arid climate. The intertropical climate ended within the *I. giraudi* zone with the return of a dryer climate, as revealed by the disappearance of kaolinite. The rise of the DI, linked to the diminution of the quartz part and especially the feldspar part of the whole rock, could thus be explained by more hydrolysis on land, linked to more humid climate.

An other interesting point of clay mineral analysis is the presence of interstratified Illite/Smectite that underline a well developed diagenetic history of the Angles section. The latter may be link to the overthrust of the "nappe de Digne". This observation has to be taken into account, knowing that diagenetic processes easily affect the $\delta^{18}O$ signal.

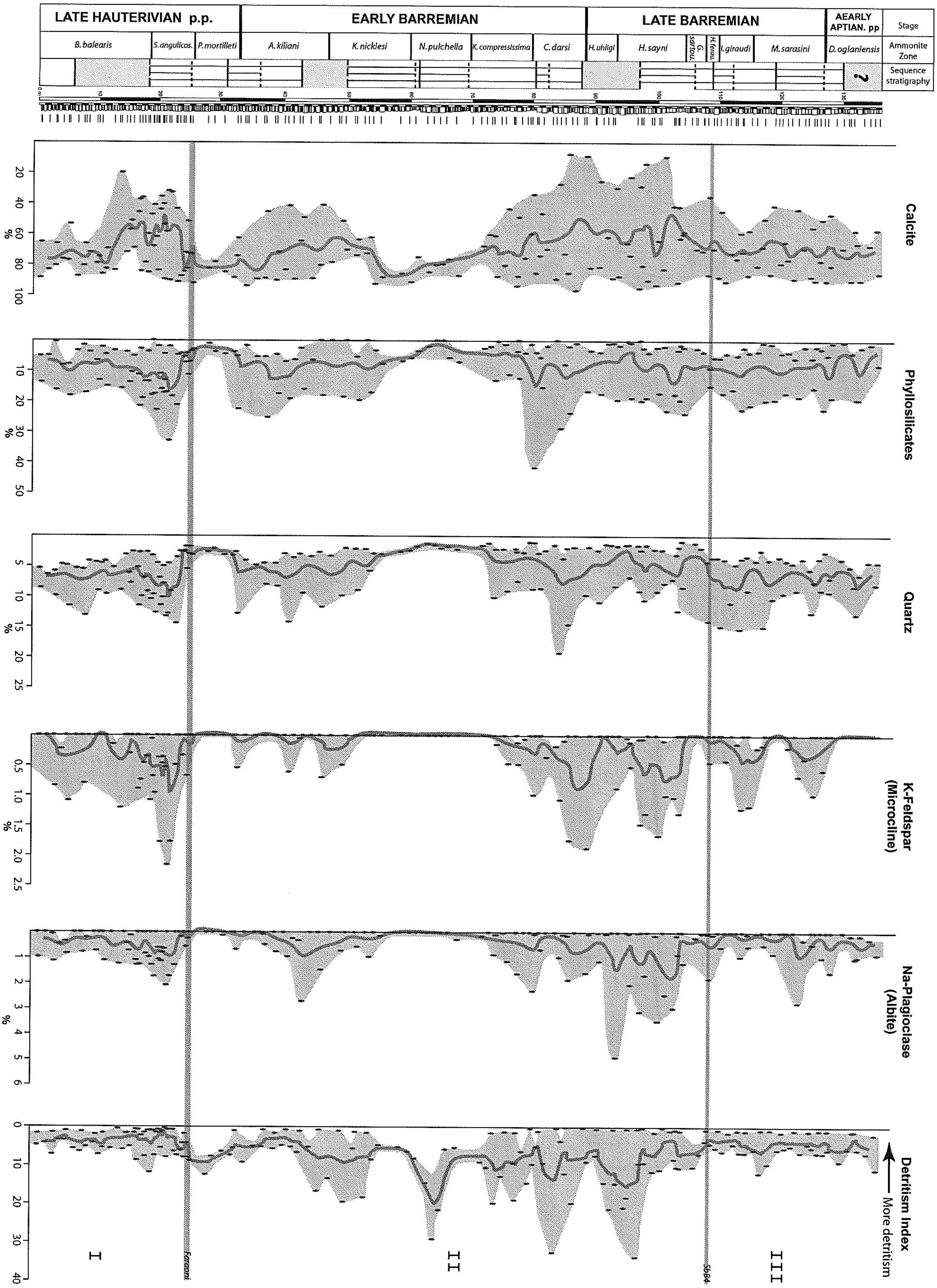

FIG. 72.- Whole-rock mineralogy results of the Angles section.

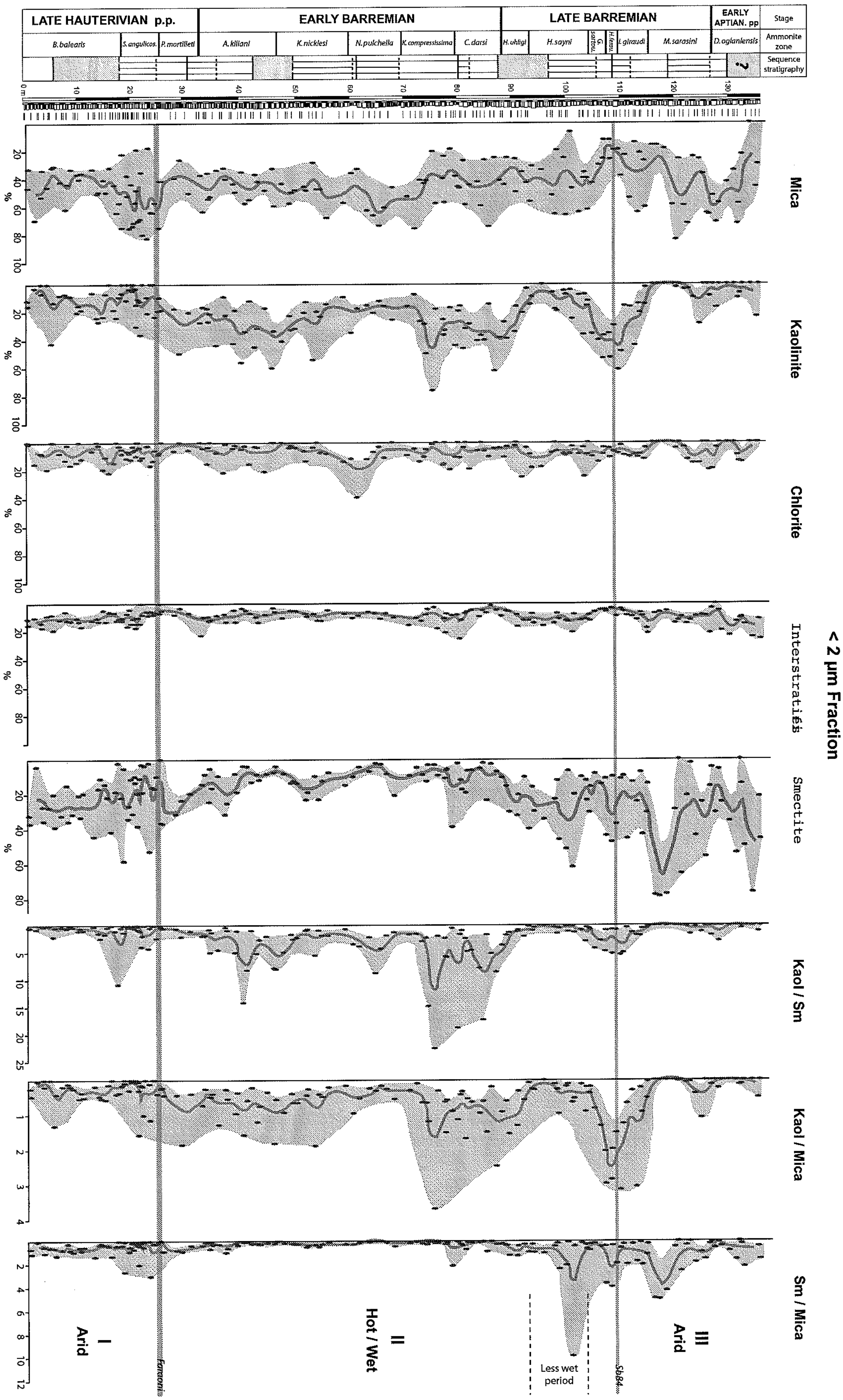

FIG. 73.- <2µm insoluble residue results of the Angles section.

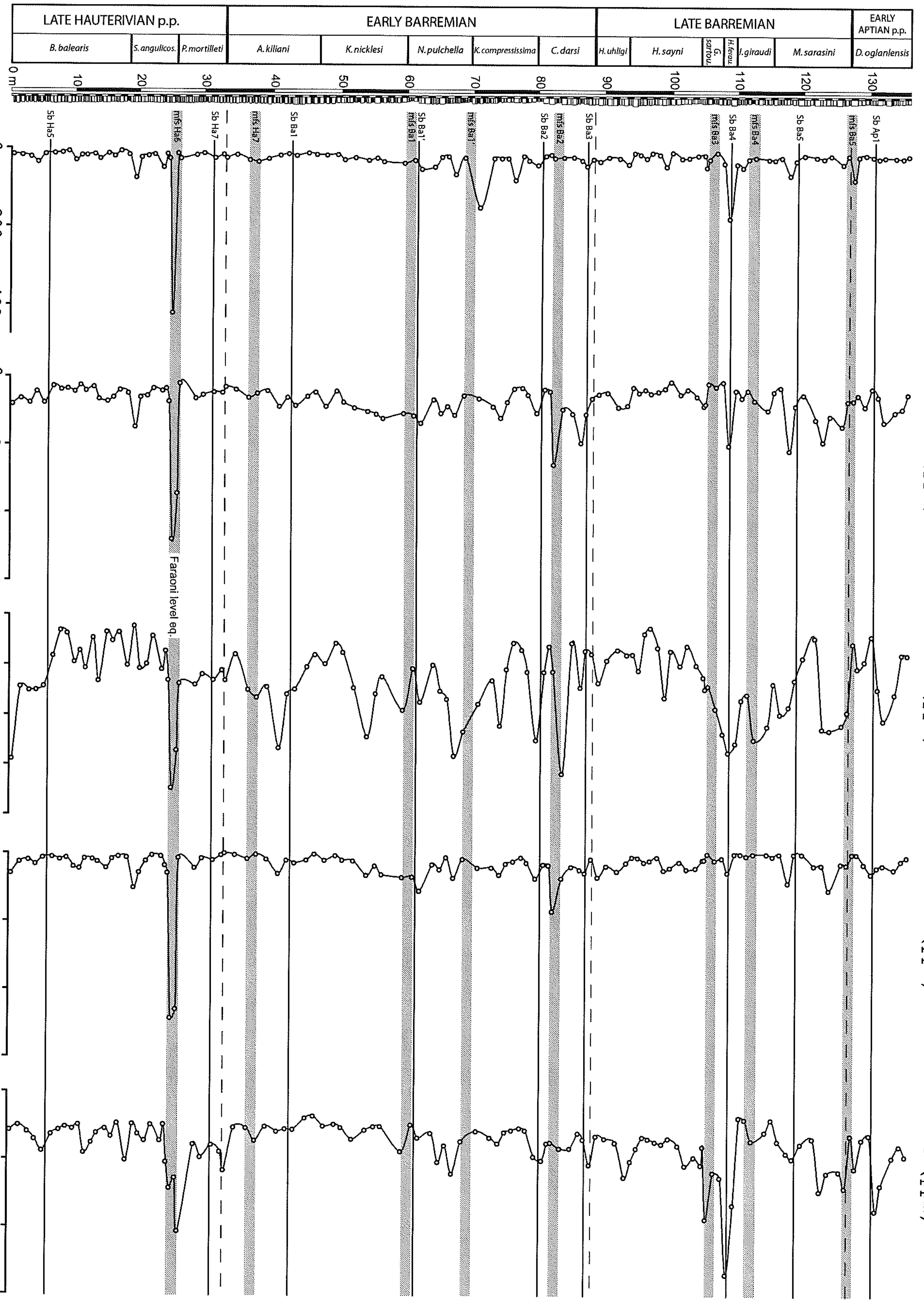

FIG. 74.- Zn, As, V, Mo and U results (in ppm) for the Angles section. The grey bands underline the maximum flooding zone.

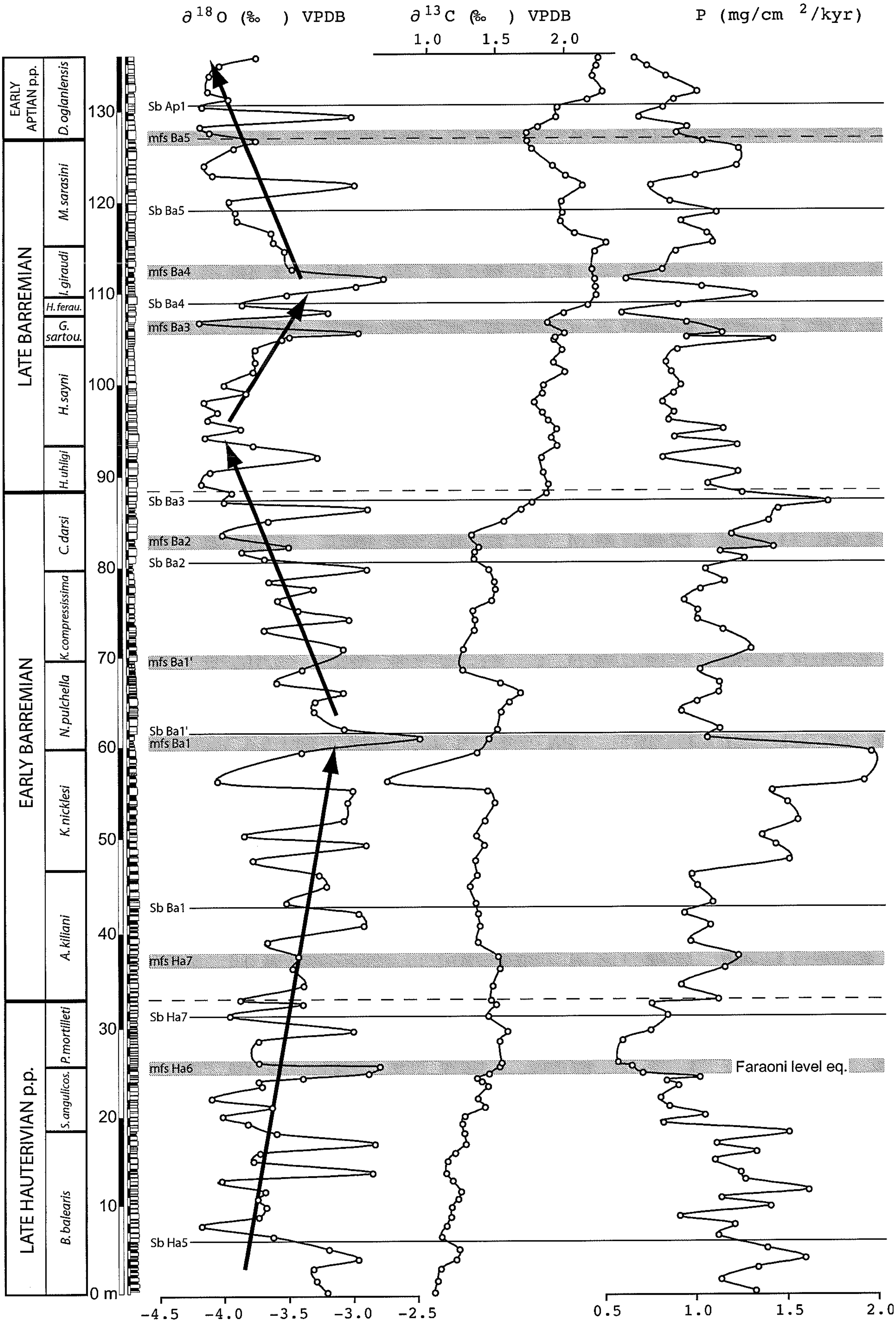

FIG. 75.- d18O, d13C (in ‰ VPDB) and P (in mg/cm2/kyr) results for the Angles section. The grey bands underline the maximum flooding zone.

4.2. Redox-sensitive trace elements

Enrichment of redox-sensitive trace elements is well known to be a good marker of bottom water anoxia (e.g. Algeo *et al.*, 2004). In the Angles section, the first enrichment situated within the beds AN 52 to AN 55 (that are equivalent in time of the Faraoni level) argue for anoxic bottom water at that time and thus support the fact that these beds are the equivalent of the Faraoni level. They provide another tools to identify this level, that is not obviously marked in the Angles section (contrary to the Italian sections). The second enrichment, within the *H. feraudianus* zone, may mark another level of anoxic bottom water. This anoxia is for the moment not recognized in other part of the tethyan realm and could then be a local anoxia. It could also explain the observed condensation of this part of the Angles section (cf. Delanoy, 1997; Vermeulen, 2002; see also Wissler *et al.*, 2002).

4.3. Phosphorus

The flux of dissolved, bio-available, P into the ocean is mainly controlled by continental runoff and atmospheric transport (e.g. Föllmi, 1996; Delaney, 1998). The removal of bio-available P from the ocean reservoir is given by the difference between the rate of P sedimentation and its return flux from the sedimentary reservoir. The transfer of bio-available P into the sedimentary reservoir occurs either by sedimentation of organic matter bound P, P adsorbed on clay particles and Fe- and Mn-oxyhydroxides, P in fish debris, or by direct (microbial?) precipitation of dissolved inorganic P (e.g., Ruttenberg, 1993; Filippelli and Delaney, 1996; Föllmi, 1996). Early diagenetic regeneration of P and its removal from the sediments is an important process (Broecker and Peng, 1982; Colman and Holland, 2000). The efficiency of P storage in the sedimentary reservoir is redox dependent and P regeneration becomes more important in oxygen-depleted bottom waters (Ingall and Jahnke, 1994; Van Cappellen and Ingall, 1996; Colman and Holland, 2000). The redox-sensitive capacity of P storage in the sedimentary reservoir may result in a positive feedback mechanism between water-column anoxia, enhanced benthic phosphorus regeneration, and increased marine productivity (Ingall and Jahnke, 1994; Van Cappellen and Ingall, 1996; Colman and Holland, 2000).

The rate of P accumulation integrated over larger areas and time scales exceeding the actual residence time of P (approximately 10 kyr; Ruttenberg, 1993; Filippelli and Delaney, 1996; Colman and Holland, 2000) is therefore driven by two main processes: (1) the combined river and atmospheric input of P, which is linked to the rates of continental weathering, erosion, and runoff; and (2) the degree of bottom-water oxygenation. As such, an increase in PAR indicates either an increase in the intensity of continental weathering and erosion rate, for example induced by a more humid climate and/or an increase in bottom-water oxygenation. On the other hand, a decrease in PAR indicates either a decrease in continental weathering rates, related for example to a change to a drier climate, or a spread of dysaerobic to anoxic bottom-waters, or the combined effect of both processes.

In the Angles section, the clear identification of anoxic level allows us to assess the oxygenation of bottom water and then to good understand the variation of the PAR. Thus, the first minimum in PAR, which is situated within the Faraoni level, may be the result of the Faraoni anoxia. The beginning of this decrease is coeval with the Ha6 trangressive surface, what may underline here a link between the anoxia and sea level changes (the Faraoni anoxia being coeval with the Ha6 maximum flooding surface). During the early Barremian, the general high PAR values may argue for important nutrient input into the northern tethyan realm. During the late Barremian and the earliest Aptian, the average PAR values is low compared to the late Hauterivian – early Barremian, indicating low input of nutrient into the northern tethyan realm. In the *H. feraudianus* zone, the local anoxia revealed by redox-sensitive trace elements is underlined by a small negative shift of the PAR value.

Moreover, it appears that almost every maximum in PAR values are related to a maximum flooding surface (mfs), except for of the Faraoni level and the mfs Ba4, which are characterized by a minimum in PAR values. Interestingly, the sea-level lowstands are not characterized by high PAR values. These observations correlate well with the observations of Föllmi (1995) who noted a positive correlation between sea level and phosphorus burial during greenhouse climates. The Barremian sediments of the Angles section underline then the clear difference in the nutrient cycle between greenhouse and icehouse conditions. Indeed, during icehouse period, nutrient inputs are stronger during sea level lowstand than during highstand.

4.4. Stable isotopes

The $\delta^{18}O$ curve interpretation is difficult due to the high frequency oscillation, which is probably due to diagenetic overprint. However, the general trend could suggest that during the early Barremian, the sea surface temperatures may have been lower than during the late Hauterivian and the early late Barremian. A second episode of colder sea surface temperature may also have occurred during the middle late Barremian. These interpretations are however submitted to controversies, due to the diagenetic history of this section that could have altered the $\delta^{18}O$ signal (cf. the mineralogy chapter). However, the same trend can be found in many other tethyan sections (Godet *et al.*, submitted), what allows us to think that, despite a diagenetic overprint, the long-term trend is valuable.

The $\delta^{13}C$ signal is a much more robust signal. In the Angles section, the $\delta^{13}C$ curve is comparable to other late Hauterivian – Barremian tethyan curves, what allows us to be confident with these data.

Contrary to other OAE, the Faraoni level is not underlined by a huge positive shift of $\delta^{13}C$, but rather by a small long-term increase, reaching its maximum within the Faraoni level. In a classical interpretation of $\delta^{13}C$ curve, this may indicate that the primary productivity and organic matter preservation is not very enhanced during this episode. During the late Barremian, the positive shift of the$\delta^{13}C$ curve is difficult to explain. Indeed, this time is not characterized by organic matter preservation, but rather by well-developed carbonate production (the Urgonian facies). At alternative explanation could be given by carbonate factory changes associated with palaeoceanographic changes (see Godet *et al.*, submitted).

Another interesting point of the $\delta^{13}C$ curve is the negative shift characterizing the Barremian – Aptian boundary. The same shift is observed in other sections of the northern tethyan realm (e.g. Erba *et al.*, 1999) and is thus a chemostratigraphic marker of this boundary.

5.– Conclusions

The palaeoclimatic and palaeoceanographic changes of the western tethyan realm, as recorded by the Angles section, could be resumed in a threefold history.

1. **During the early late Hauterivian**, the Angles section is characterized by a well-contrasted season and medium nutrient input.

2. **During the latest Hauterivian**, high nutrient input, along with the installation of a humid climate may have contributed to the initiation of the Faraoni anoxia. All along the early Barremian, this humid climate reaches its maxima and may be responsible of very high nutrient input into the Tethyan Sea. The possible cooling of sea surface water at that time could reflect enhanced upwelling or stronger Tethyan – Boreal realm connections.

3. **During the late Barremian and the earliest Aptian**, as indicated by the progressive disappearance of the Kaolinite, the climate becomes more and more arid. It is accompanied by a diminution in nutrient input and the initiation of oligotrophic conditions. These changes are mirrored in proximal settings by the installation of the photozoan Urgonian platform.

Selected references

ADATTE T., STINNESBECK W. & KELLER G. (1996).– Lithostratigraphic and mineralogic correlations of near K/T boundary clastic sediments in northeastern Mexico: Implications for origin and nature of deposition. *In*: G. Ryder, D. Fastovsky and S. Gartner (Editors), The Cretaceous-Tertiary Event and Other Catastrophes in Earth History. Geological Society of America, Special Paper 307, Boulder, Colorado, 211-226.

ALGEO T.J. & MAYNARD J.B. (2004).– Trace-element behavior and redox facies in core shales of Upper Pennsylvanian Kansas-type cyclothems. *Chemical Geology*, **206** (3-4), 289-318.

BROECKER W.S. & PENG T.-H. (1982).– Tracers in the sea. Lamont-Doherty Geological Observatory, Columbia University, Palisades, New-York, Eldigio Press, 690 pp.

CECCA F., MARINI A., PALLINI G., BAUDIN F. & BEGOUEN V. (1994).– A guide-level of the uppermost Hauterivian (Lower Cretaceous) in the pelagic succession of Umbria-Marche Apennines (Central Italy): the Faraoni Level. *Riv. Ital. Paleontol. Stratigr.*, **99**, 551-568.

COLMAN A.S. & HOLLAND H.D. (2000).– The global diagenetic flux of phosphorus from marine sediments to the oceans; redox sensitivity and the control of atmospheric oxygen levels. *In*: C.R. Glenn, L. Prévôt-Lucas & J. Lucas (Editors), Marine authigenesis; from global to microbial. *SEPM Special Publication* n° **66**, 53-75.

DELANEY M.L. (1998).– Phosphorus accumulation in marine sediments and the oceanic phosphorus cycle. *Global Biogeochemical Cycles*, **12** (4), 563-572.

DELANOY G. (1997).– Biostratigraphie des faunes d'ammonites à la limite Barrémien-Aptien dans la région d'Angles-Barrême-Castellane. ***Ann. Mus. Hist. Nat. Nice***, Nice, **XII**, 1-270.

EATON A.D., CLESCERI L.S. & GREENBERG A.E. (1995).– Standard methods for the examination of water and wastewater, 19th edition.

ERBA E., CHANNELL J.E.T., CLAPS M., JONES C.E., LARSON R.L., OPDYKE B., PREMOLI-SILVA I., RIVA A., SALVINI G. & TORRICELI S. (1999).– Integrated stratigraphy of the Cismon APTICORE (Southern Alps, Italy): A "reference section" for the Barremian-Aptian interval at low latitudes. *Journal of Foraminiferal Research*, **29** (4), 371-391.

FILIPPELLI G.M. & LOIS DELANEY M. (1996).– Phosphorus geochemistry of equatorial Pacific sediments. *Geochimica et Cosmochimica Acta*, **60** (9), 1479-1495.

FÖLLMI K.B. (1995).– 160 m.y. record of marine sedimentary phosphorus burial: Coupling of climate and continental weathering under greenhouse and icehouse conditions. *Geology*, **23**, 859-862.

FÖLLMI K.B. (1996).– The phosphorus cycle, phosphogenesis and marine phosphate-rich deposits. ***Earth-Science Reviews***, **40** (1-2), 55-124.

GIRAUD F., BEAUFORT L. & COTILLON P. (1995).– Contrôle astronomique de la sédimentation carbonatée dans le Crétacé inférieur du Bassin vocontien (SE France). *Bull. Soc. géol. France*, **166** (4), 409-421.

GODET A., BODIN S., FÖLLMI K.B., VERMEULEN J., GARDIN S., FIET N., ADATTE T., BERNER Z., STÜBEN D. & VAN DE SCHOOTBRUGGE B. Evolution of the marine stable carbon-isotope record during the early Cretaceous: A focus on the late Hauterivian and Barremian in the Tethyan realm. Submitted in *Earth and Planetary Science Letters*.

INGALL E. & JAHNKE R. (1994).– Evidence for enhanced phosphorus regeneration from marine sediments overlain by oxygen depleted waters. *Geochimica et Cosmochimica Acta*, **58** (11), 2571-2575.

KÜBLER B. (1987).– Cristallinité de l'illite: méthodes normalisées de préparation, méthode normalisée de mesure, méthode automatique normalisée de mesure. *Cahiers de l'Institut de Géologie, Université de Neuchâtel*, Suisse, Série ADX n°2.

RUTTENBERG K.C. (1993).– Reassessment of the oceanic residence time of phosphorus. *Chemical Geology*, **107** (3-4): 405-409.

VAN CAPPELLEN P. & INGALL E.D. (1996. Redox stabilization of the atmosphere and oceans by phosphorus-limited marine productivity. *Science*, **271**, 493-496.

VERMEULEN J. (1980).– Etude de la famille des Pulchelliidae, révision de trois espèces types du Barrémien du Sud-Est de la France, Thèse de Doctorat de Spécialité, Nice, 101 pp.

VERMEULEN J. (2002).– Etude stratigraphique et paléontologique de la famille des Pulchelliidae (ammonoidea, Ammonitina, Endemocerataceae). *Géologie alpine*, Mém. H.S. **42**, Grenoble, France, 333 pp.

WISSLER L., WEISSERT H., MASSE J.-P. & BULOT L.G. (2002).– Chemostratigraphic correlation of Barremian and lower Aptian ammonite zones and magnetic reversals. *International Journal of Earth sciences (Geol. Rundsch.)*, **91**, 272-279.

Boundaries, ammonite fauna and main subdivisions of the stratotype of the Barremian

Jean Vermeulen

The stratotype of the Barremian, is situated along the secondary road n° 33, near the village of Angles, France. Its easy access, its continuous outcrop and its numerous fossils, mostly ammonites, were the main reasoning for its appointment as stratotype (Busnardo, 1965b, p. 162).

The boundaries of the stratotypical Barremian

1–. The HauterivianN-Barremian boundary

Concerning the ammonites fauna, the disappearance of the family CRIOCERATITIDAE is the most important event; it is situated near the Hauterivian-Barremian boundary, in the lower part of the last hauterivian Zone of *Prieuriceras picteti*.This event is not taken in consideration to define the Hauterivian-Barremian boundary because, in biostratigraphy, only the appearances of new taxa are used to define the limits of stages and zones.

Except the genus *Avramidiscus*, all the ammonites genera present at the base of the Barremian appear in the upper Hauterivian, in different levels, from the Zone of *Subsaynella sayni* to the Zone of *Prieuriceras picteti.*

The base of the stratotypical Barremian is defined by the appearance of *Avramidiscus kiliani* which is the index-species of the lowest zone of the Barremian (Vermeulen, 2002).

Remarks: some authors have proposed to place the Hauterivian-Barremian boundary at the base of the Zone of *Balearites catulloi* (ex *Pseudothurmannia catulloi* = Zone of *Balearites mortilleti sensu* Vermeulen, 2004). Their arguments are now either obsolete or erroneous.

A team managed by the author of this work is now working in the SE France in order to make clear the evolution of the ammonites fauna in the uppermost Hauterivian and in the lowest part of the Barremian.

2.– The Barremian-Aptian boundary

The top of the Barremian is consequently defined by the appearance of the index-species of the lowest zone of Aptian, *Deshayesites oglanlensis*, not yet collected in the stratotypical section. Delanoy (1998, p. 231) collected this species at the base of the "thick bundle" in the section of Méouilles, near Saint-André-les-Alpes ; therefore, awaiting new data, the base of the Aptian is still placed, in the stratotypical section, at the base of the bed n° 201/041 which corresponds at the base of the "thick bundle", despite the fact that the first specimen of the genus *Deshayesites* was until now collected in the bed n° 206/041.

Outline of the evolution and the classification of Mediterranean barremian ammonites

Precise collections of several thousands of specimens allow to give an outline of the phylogenesis of mediterranean barremian ammonites and to build the foundations of a new phylogenetical classification. Some phylogenetical diagrams were previously proposed (Vermeulen, 2000; 2001a; 2002) ; new data concerning them are given herein.

The phylogenetical classification of barremian ammonites implies to divide up the order AMMONOIDEA ZITTEL, 1884 into four suborders, AMMONITINA HYATT, 1889, ANCYLOCERATINA WIEDMANN, 1966, PROTANCYLOCERATINA VERMEULEN, 2005, this work, PHYLLOCERATINA ARKELL, 1950, and LYTOCERATINA HYATT, 1889.

1.– Suborder Ammonitina Hyatt, 1889

The AMMONITINA of the mediterranean Barremian are classified into the two superfamilies, DESMOCERATACEAE ZITTEL, 1895 and ENDEMOCERATACEAE SCHINDEWOLF, 1966 *nom. transl.*

1.1. Desmocerataceae Zittel, 1895

The genus *Plesiospitidiscus* BREISTROFFER, 1947, derives from SPITIDISCINAE VERMEULEN & THIEULOY, 1999 ; it appears in the Lower Hauterivian. This genus marks the appearance of DESMOCERATACEAE ZITTEL,

		ZONES	SUB-ZONES	HORIZONS	S.H.A., S.H.M.A. and S.H.D
UPPER BARREMIAN	5	*Pseudocrioceras waagenoides*			S.H.A. non encore décelée dans le stratotype
	4	*Martelites sarasini*			177 S.H.M.A. *Leptoceratoides puzosianum* 176.2 S.H.A. *Martelites sarasini*
		Imerites giraudi		*Heteroceras emerici* *Imerites giraudi*	171 *S.H.A. Heteroceras emerici* 170 S.H.M.A. *Argvethites* sp. 168 S.H.A. *Imerites giraudi*
	3	*Hemihoplites feraudianus*		*Pseudoshasticrio. magnini* *Hemihoplites feraudianus*	166 S.H.M.A. ? *Pseudoshasticrio. magnini* 164.2 S.H.A. *Hemihoplites feraudianus*
		Gerhardtia sartousiana	*Gerhardtia provincialis* *Gerhardtia sartousiana*		162 S.H.A. *Gerhardtia provincialis* 160.1 S.H.A.? *Gerhardtia sartousiana*
		Heinzia sayni			151.2 S.H.A. *Barrancyloceras alpinum* 147.2 S.H.A. *Heinzia sayni*
		Holcodiscus uhligi			144 S.H.A. *Barrancyloceras* gr. *barremense* 140 S.H.A. *Holcodiscus uhligi*
LOWER BARREMIAN	2	*Coronites darsi*		*Macroscaphites tirolensis*	134 S.H.A. *Macroscaphites tirolensis* 125 S.H.A. *Coronites darsi*
		Kotetishvilia compressissima	*Subtorcapella defayi* *Kotet. compressissima*	*Met. fallax et Met. nodosus*	120 S.H.A. *Subtorcapella defayi* 116 S.H.M.A. *Kotetishvilia compressissima* 112.5 S.H.A. *Kotetishvilia compressissima*
		Nicklesia pulchella			109.4 S.H.D. *Honnoratia thiollierei* 109.1 S.H.A. *Nicklesia pulchella*
	1	*Kotetishvilia nicklesi*			105 S.H.D. *Hamulina astieri* 96 S.H.D. *Anahamulina davidsoni* 94 S.H.A. *Kotetishvilia nicklesi*
		Avramidiscus kiliani	*Psilotissotia colombiana* *Psilotissotia mazuca* *Avramidiscus kiliani*		89 S.H.A. *Psilotissotia colombiana* 75 S.H.A. *Psilotissotia mazuca* 72 S.H.A. *Avramidiscus kiliani*
UP. HAUTERIVIEN *p. p.*		*Prieuriceras picteti*			64.1 S.H.A. *Prieuriceras picteti*
		Balearites mortilleti			54.1 S.H.A. *Balearites mortilleti*
		Parathurmannia ohmi			43 S.H.A. *Parathurmannia ohmi*
		Pseudothurmannia seitzi			35 S.H.A. *Pseudothurmannia seitzi*

Fig. 76.- Biostratigraphy of the uppermost Hauterivian and of the stratotypical Barremian (Angles section, SE France).

1895, and also the appearance of the family BARREMITIDAE BRESKOVSKI, 1977 *nom. transl.*

About that time the family HOLCODISCIDAE SPATH, 1923 appears, with the genus *Abrytusites* NIKOLOV & BRESKOVSKI, 1969. The family SILESITIDAE Hyatt, 1900 appears in the Lower Barremian, in the lower part of the Zone of *Nicklesia pulchella*.

The family PUZOSIIDAE SPATH, 1922 *nom. transl.* VERMEULEN, 2005, this work, is only represented, in the uppermost Barremian, by the genus *Pseudohaploceras* HYATT, 1900.

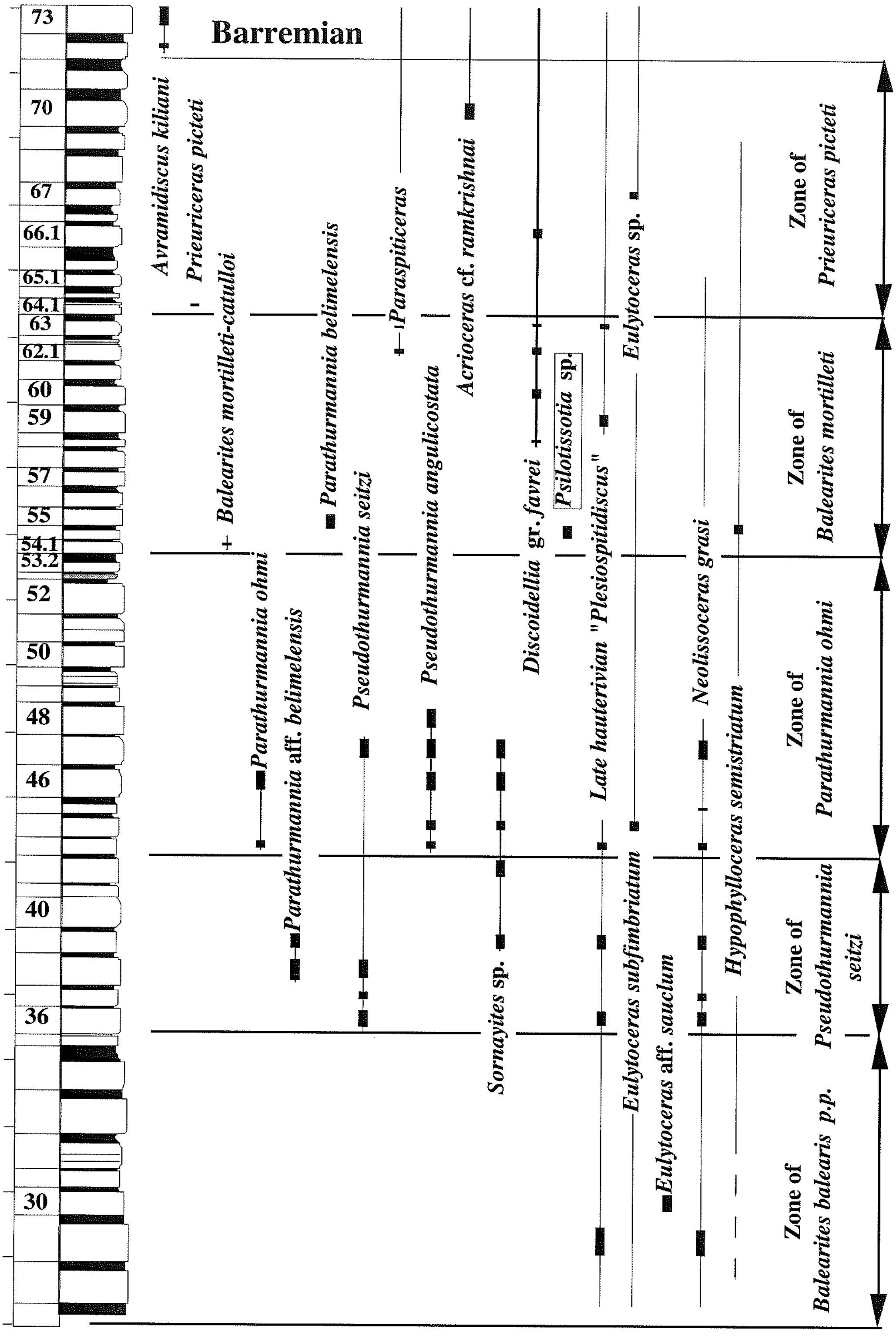

FIG. 77.- Ammonite ranges (been examined) in the uppermost Hauterivian (Angles, Alpes de Haute-Provence, section n° 341).

1.1.1. BARREMITIDAE BRESKOVSKI, *1977*, ***nom. transl.***

The typical species of *Barremites* KILIAN 1913 appear in the lower Barremian, in the Zone of *Kotetishvilia nicklesi*. The precise origin of this genus must be investigated from the species of the uppermost Hauterivian, derived from *Plesiospitidiscus* BREISTROFFER, 1947.

The following genera appear successively:

– *Plesiospitidiscus* BREISTROFFER, 1947, Lower Hauterivian, probably in the Zone of *Crioceratites loryi*;

– *Taveraidiscus* VERMEULEN & THIEULOY, 1999, upper Hauterivian, Zone of *Prieuriceras picteti* (Vermeulen, 2004);

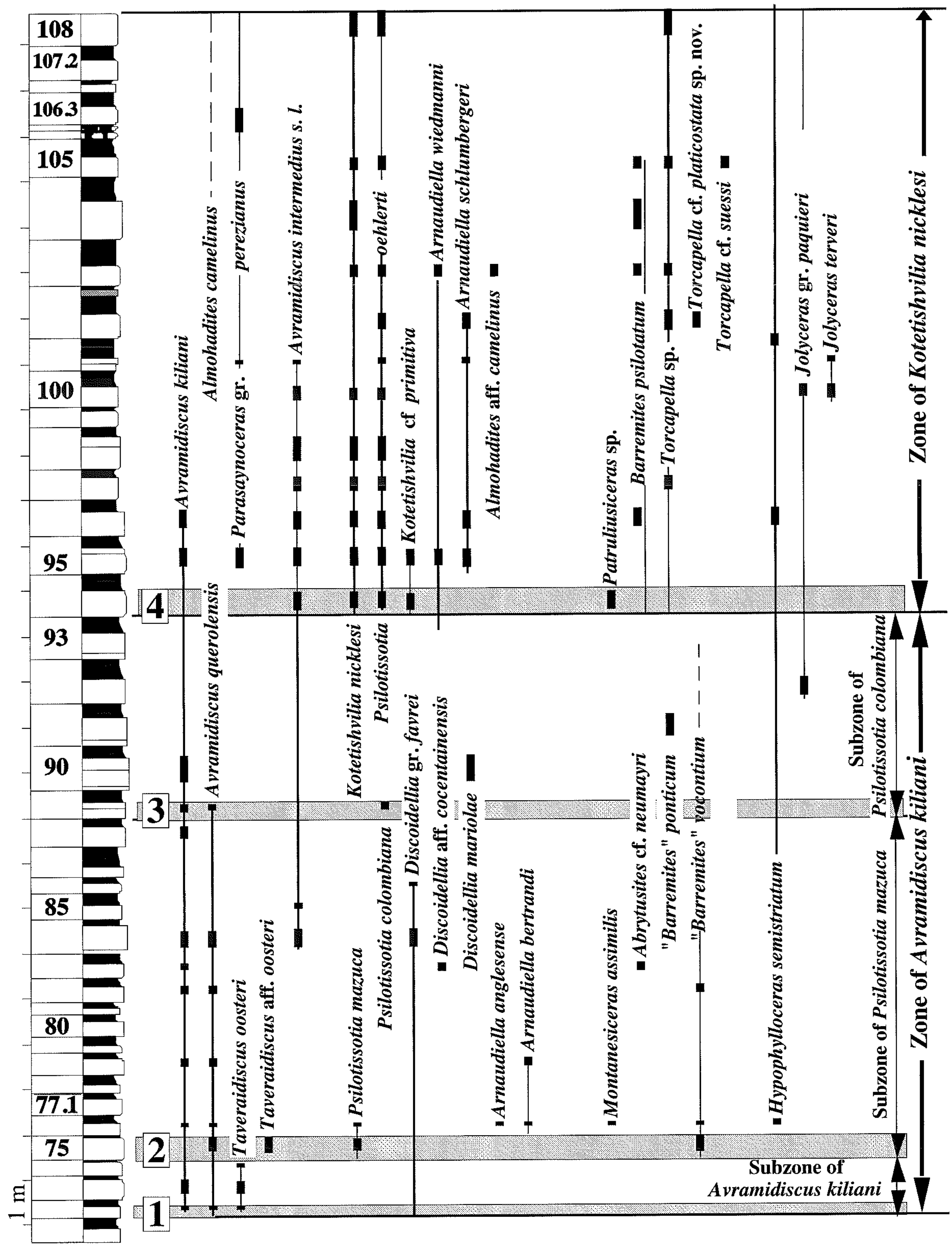

FIG. 78.- AMMONITINA and PHYLLOCERATINA ranges, Barremian 1, Zones of *Avramidiscus kiliani* and of *Kotetishvilia niklesi*, section n° 041, Stratotype of Angles. 1, Horizon-strata (AHS) of *Avramidiscus kiliani*; 2, Horizon-strata (AHS) of *Psilotissotia mazuca*; 3, Horizon-strata (AHS) of *Psilotissotia colombiana*; 4, Horizon-strata (AHS) of *Kotetishvilia nicklesi*.

– *Torcapella* BUSNARDO, 1970, uppermost Hauterivian according to Company (oral information) or Zone of *Avramidiscus kiliani* according to my own collections;
– *Puezalpella* DIMITROVA 1967, Zone of *Avramidiscus kiliani*;
– *Barremites* KILIAN 1913, typical forms, Zone of *Kotetishvilia nicklesi*;
– *Davidiceras* VERMEULEN, 2003, Zone of *Kotetishvilia nicklesi*;

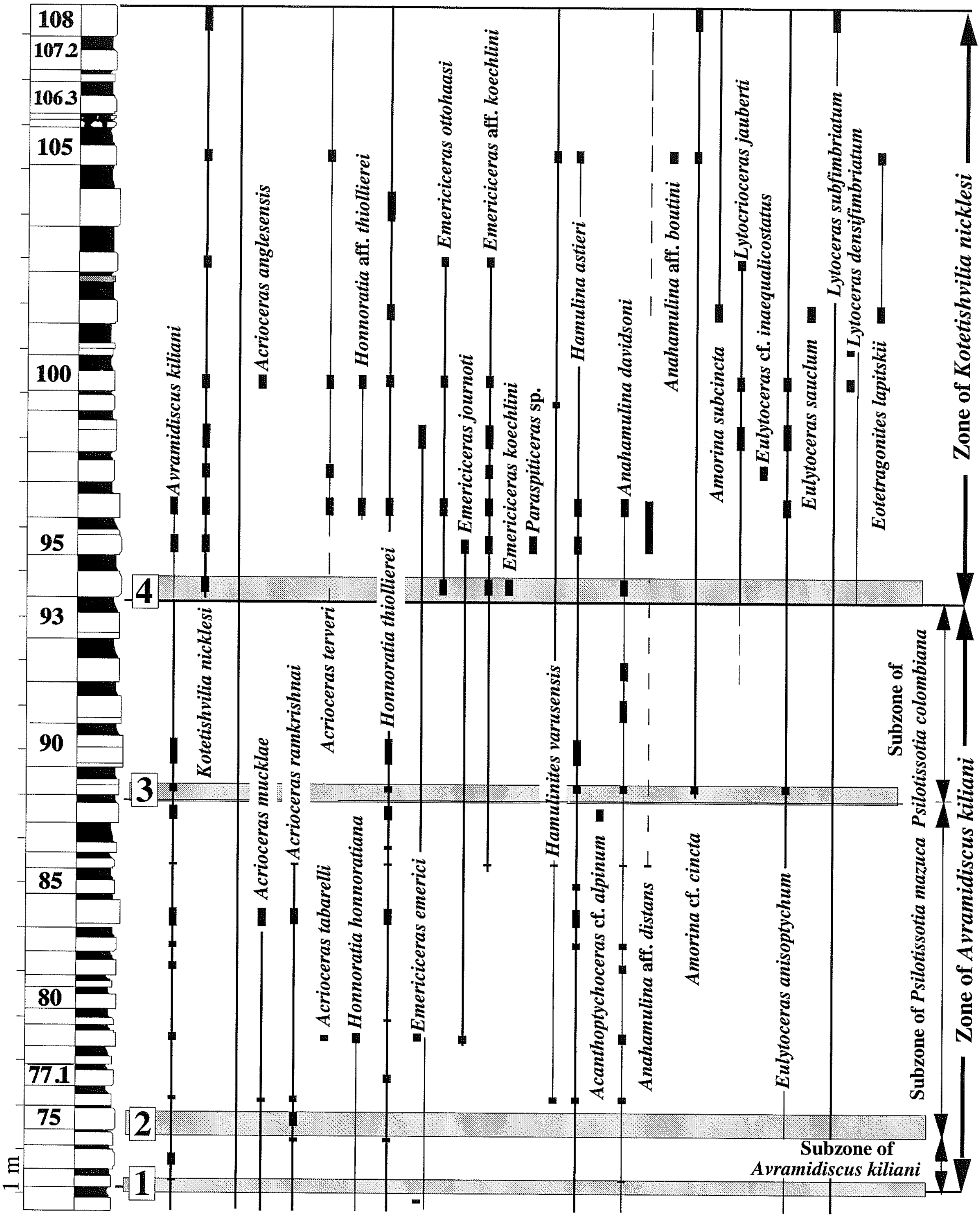

FIG. 79.- ANCYLOCERATINA and LYTOCERATINA ranges, Barremian 1, Zones of *Avramidiscus kiliani* and of *Kotetishvilia niklesi*, section n° 041, Stratotype of Angles. 1, Horizon-strata (AHS) of *Avramidiscus kiliani*; 2, Horizon-strata (AHS) of *Psilotissotia mazuca*; 3, Horizon-strata (AHS) of *Psilotissotia colombiana*; 4, Horizon-strata (AHS) of *Kotetishvilia nicklesi*.

– *Montanesiceras* BRESKOVSKI, 1977, senior synonym of *Kostovites Breskovski*, 1977, of *Trimontioniceras* BRESKOVSKI, 1977 and of *Nikolovites Breskovski*, 1977,Zone of *Kotetishvilia compressissima* ;

– *Subtorcapella* VERMEULEN, 1980, Zone of *Kotetishvilia compressissima*;

– *Pseudovaldedorsella* CECCA *et al.*, 1998, typical forms, Zone of *Kotetishvilia compressissima*;

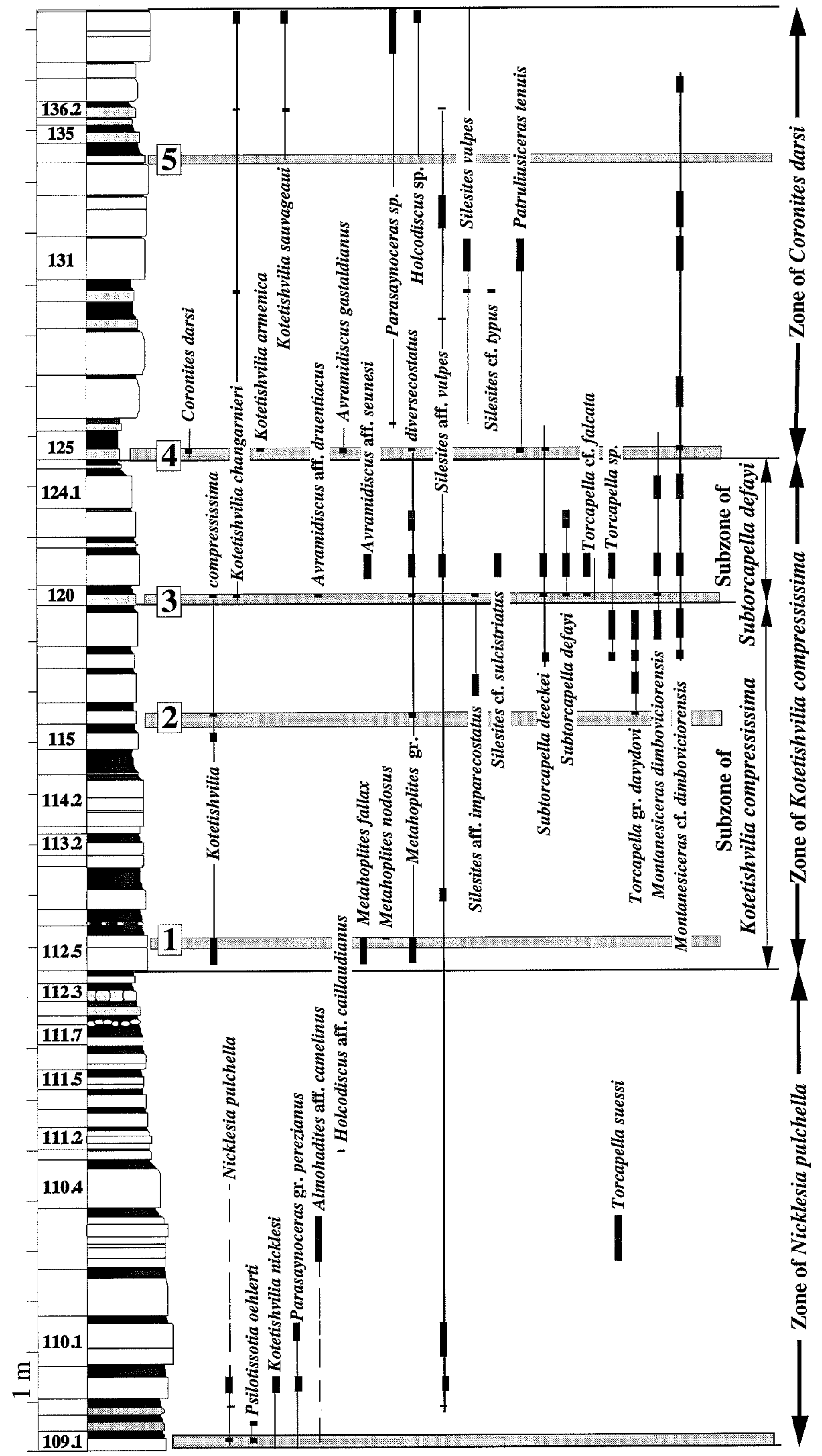

FIG. 80.- AMMONITINA ranges, Barremian 2, Zones of *Nicklesia pulchella*, of *Kotetishvilia compressissima* and of *Coronites darsi*, section n° 041, stratotype of Angles. 1, Horizon-strata (AHS) of *Nicklesia pulchella*; 2, Horizon-strata (AHS) of *Metahoplites fallax* and of *Metahoplites nodosus*; 3, Horizon-strata (MFHS) of *Kotetishvilia compressissima*; 4, Horizon-strata (AHS) of *Subtorcapella defayi*; 5, Horizon-strata (AHS) of *Coronites darsi*; 6, Horizon-strata (AHS) of *Macroscaaphites tirolensis*.

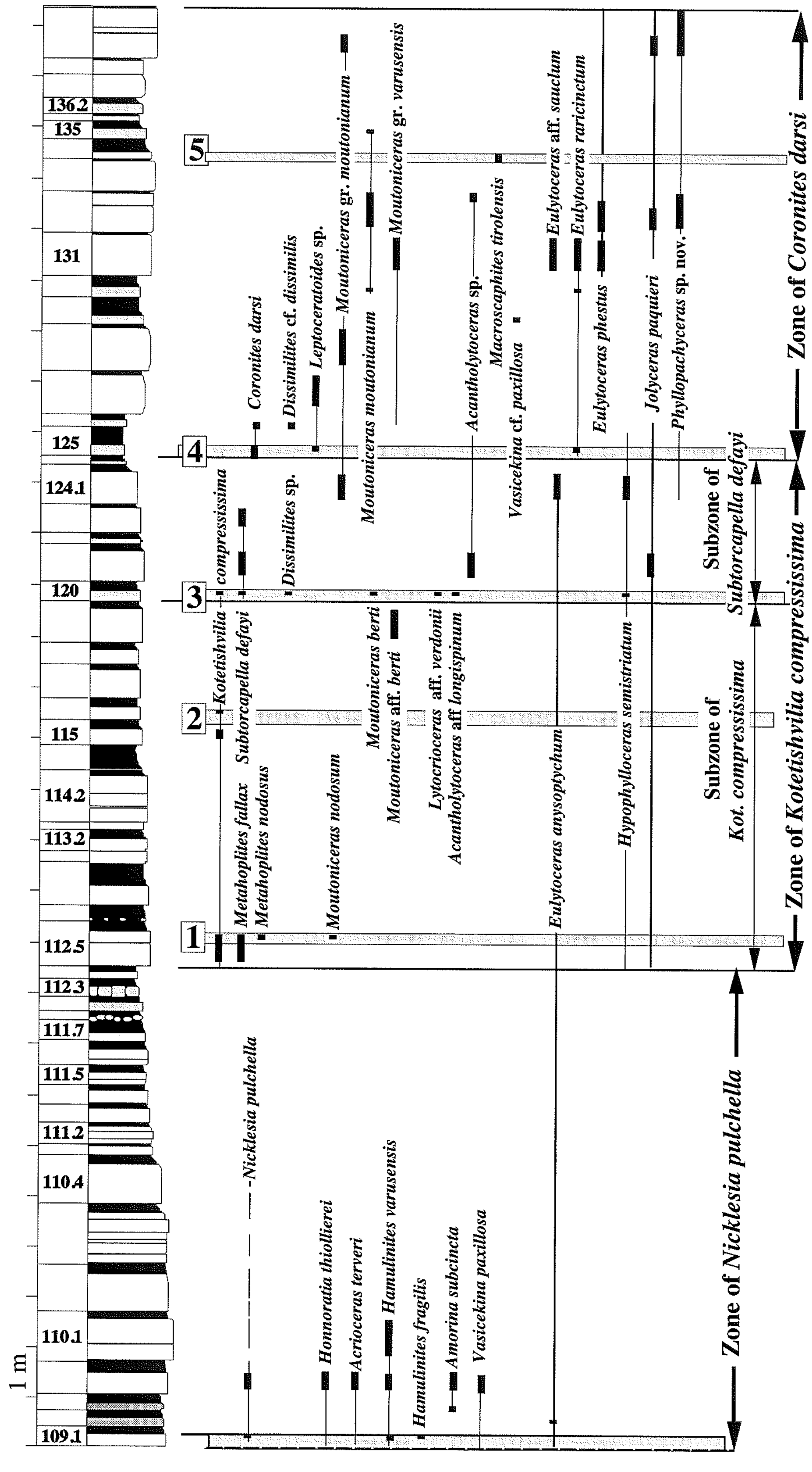

FIG. 81.- PROTANCYLOCERATINA, ANCYLOCERATINA, LYTOCERATINA and PHYLLOCERATINA RANGES, Barremian 2, Zones of *Nicklesia pulchella*, of *Kotetishvilia compressissima* and of *Coronites darsi*, section n° 041, stratotype of Angles. 1, Horizon-strata (AHS) of *Nicklesia pulchella*; 2, Horizon-strata (AHS) of *Metahoplites fallax* and of *Metahoplites nodosus*; 3, Horizon-strata (MFHS) of *Kotetishvilia compressissima*; 4, Horizon-strata (AHS) of *Subtorcapella defayi*; 5, Horizon-strata (AHS) of *Coronites darsi*; 6, Horizon-strata (AHS) of *Macroscaphites tirolensis*.

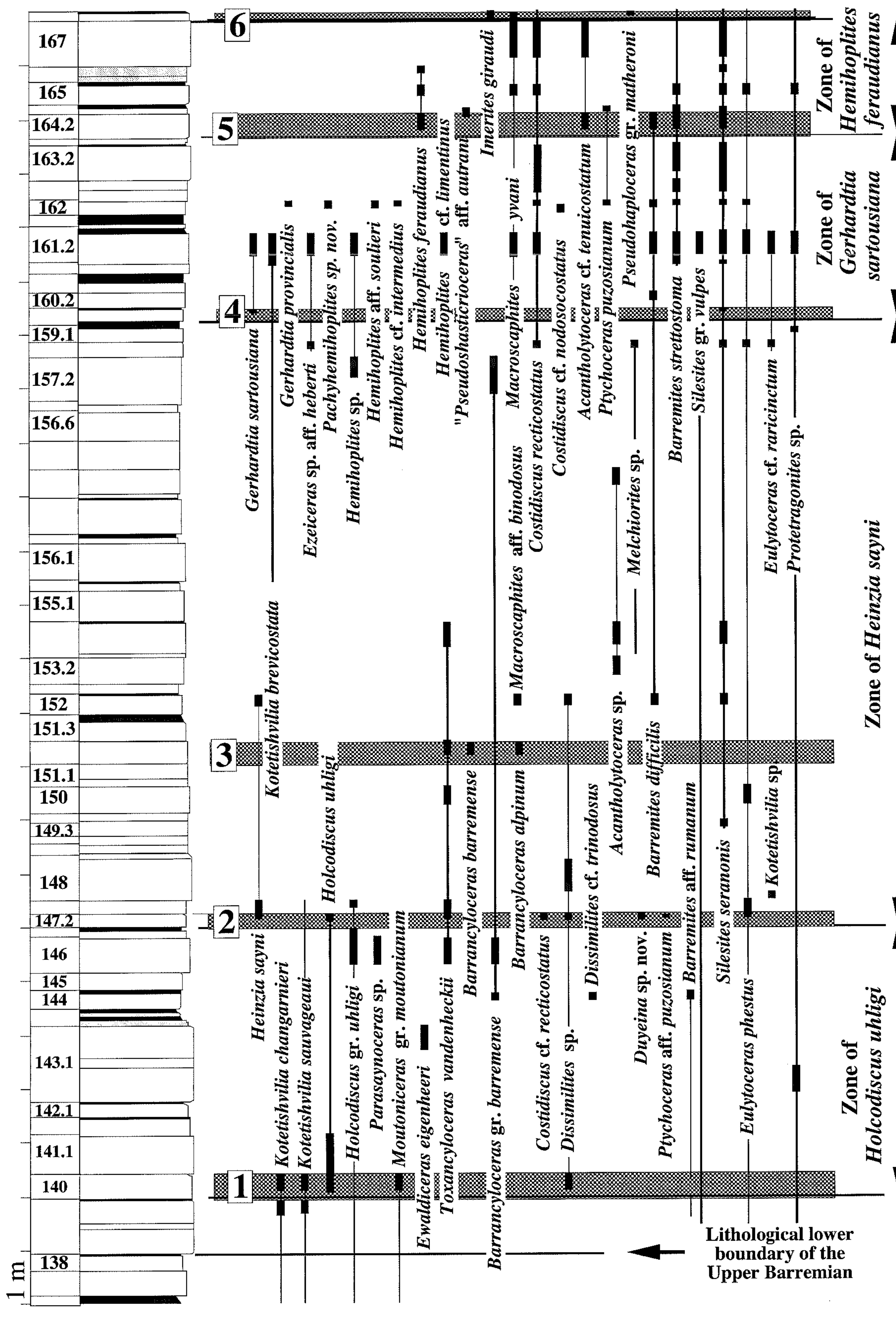

FIG. 82.- Ammonite ranges, Barremian 3, Zones of *Holcodiscus uhligi*, *Heinzia sayni*, *Gerhardtia sartousiana* and *Hemihoplites feraudianus*, section n° 041, stratotype of Angles. 1, Horizon-strata (AHS) of *Holcodiscus uhligi*; 2, Horizon-strata (AHS) of *Heinzia sayni*; 3, Horizon-strata (AHS) of *Barrancyloceras barremense*; 4, Horizon-strata (AHS) of *Gerhardtia sartousiana*; 5, Horizon-strata (AHS) of *Hemihoplites feraudianus*; 6, Horizon-strata (AHS) of *Imerites giraudi*.

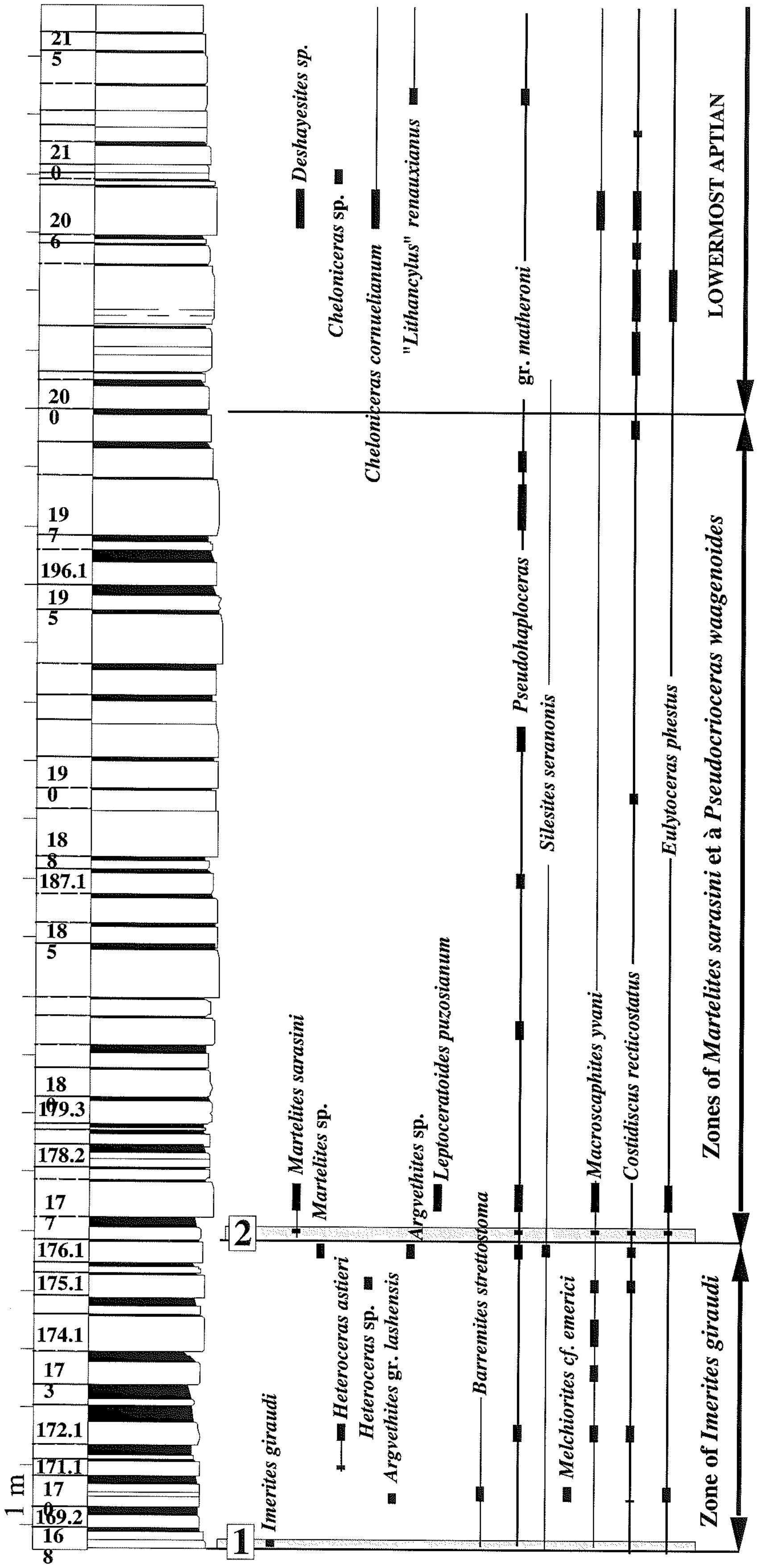

Fig. 83.- Ammonite ranges, Barremian 4 and 5, Zones of *Imerites giraudi*, *Martellites sarasini* and ? *Pseudocrioceras waagenoides*, and in the basal part of the Aptian, section n° 041, srtatotype of Angles. 1, Horizon-strata (AHS) of *Imerites giraudi*; 2, Horizon-strata (AHS) of *Martellites sarasini*.

– *Melchiorites* SPATH, 1923, senior synonym of *Cassidoiceras* DIMITROVA, 1967, Zone of *Heinzia sayni*;

This family still needs more work in order to establish a precise phylogenetical evolution.

1.1.2. *HOLCODISCIDAE SPATH, 1923*

As supposed by Hoedemaeker (1995), *Abrytusites* NIKOLOV & BRESKOVSKI, 1969, is the ancestor of the HOLCODISCIDAE SPATH, 1923 and therefore it must be classified into this family.

The appearance of *Avramidiscus kiliani* (PAQUIER, 1900) marks the lower boundary of the Barremian. This index-species is contemporary with *Avramidiscus querolensis* (BUSNARDO, 1957).

The ultimate species of *Avramidiscus* VERMEULEN, 1996, *Avramidiscus fallacior* COQUAND *in* MATHERON, 1878, disappears in the Zone of *Coronites darsi*

Parasaynoceras BREISTROFFER, 1947 derives from *Avramidiscus kiliani* (PAQUIER, 1900) at the base of the Zone of *Kotetishvilia nicklesi*; it disappears in the upper Barremian, in the Zone of *Heinzia sayni.*

Almohadites WIEDMANN, 1966 and *Astieridiscus* KILIAN, 1910 derive from *Parasaynoceras* BREISTROFFER, 1947; they appear respectively near the top of the Zone of *Kotetishvilia nicklesi* and at the base of the Zone of *Nicklesia pulchella.*

The origin of the two genera, *Metahoplites* SPATH, 1924 and *Holcodiscus* UHLIG, 1882 is not well known.

Metahoplites SPATH, 1924 appears at the top of the Zone of *Nicklesia pulchella,* with *Metahoplites* aff *fallax* (COQUAND *in* MATHERON, 1879), the ultimate species, *Metahoplites* aff. *henoni* (COQUAND, 1880), disappears in the Zone of *Heinzia sayni* ; this genera may be derives from *Almohadites* WIEDMANN, 1966 but one of both genera of this family present in the Zone of *Nicklesia pulchella* can also be the ancestor of *Metahoplites* SPATH, 1924.

Holcodiscus UHLIG, 1882 appears in the lower part of the Zone of *Kotetishvilia compressissima* with the type-species *Holcodiscus caillaudianus* (D'ORBIGNY, 1850) and then disappears in the Zone of *Heinzia sayni* (non described species). It derives either from *Almohadites* WIEDMANN, 1966, or *Metahoplites* SPATH, 1924.

1.1.3. *SILESITIDAE HYATT, 1900*

In the Barremian, only the genus *Silesites* UHLIG, 1883 is present. The first specimens appears at the base of the Zone of *Nicklesia pulchella*, therefore the origin of this family must be investigated from evolute forms present in the Zones of *Avramidiscus kiliani* and of *Kotetishvilia nicklesi,* probably deriving from *Abrytusites* NIKOLOV & BRESKOVSKI, 1969.

Remark: the understanding of *Patruliusiceras* AVRAM, 1990 is not easy ; the most species, as the type-species *Patruliusiceras crenulatum* AVRAM, 1990, are defined by young specimens having affinities with *Melchiorites* SPATH, 1923, while "*Patruliusiceras*" *uhligi* AVRAM, 1990 is a true *Silesites sensu stricto.*

1.2. ENDEMOCERATACEAE SCHINDEWOLF, 1966 *nom. transl.* VERMEULEN, 1996

Only the PULCHELLIIDAE DOUVILLÉ, 1890 *emend.* are present in the Barremian. More informations about this family can be taken in Vermeulen (2002).

1.2.1. *BUERGLICERATINAE VERMEULEN, 1995*

This subfamily appears at the base of the Upper Hauterivian; it is represented, in the lowermost Barremian which corresponds to the Zones of *Avramidiscus kiliani* and of *Kotetishvilia nicklesi*, by the genera *Discoidellia* VERMEULEN, 1995 and *Buergliceras* ETAYO-SERNA, 1968.

1.2.2. *PSILOTISSOTIINAE VERMEULEN, 1995*

This subfamily derives, at the top of the upper Hauterivian, from BUERGLICERATINAE VERMEULEN, 1995. It is represented in the lowermost Barremian, and probably in the latest beds of the uppermost Hauterivian, by the genera *Psilotissotia* HYATT, 1900 and *Arnaudiella* VERMEULEN, 1997, both deriving from *Discoidellia* VERMEULEN, 1995.

In this subfamily, from the base of the Barremian to the Zone of *Gerhardtia sartousiana*, three ways of evolution are shown up.

The first way, mainly confined in the lowermost Barremian, is characterized by the loss of the siphuncular keel, followed by the appearance, probably consequent, of two ventrolateral keels. *Subpulchellia* HYATT, 1903 were created for the bicarenate forms. There is not a main cladogenesis in this evolution and that allows to consider *Psilotissotia* HYATT, 1900 as a senior synonym of *Subpulchellia* HYATT, 1903.

The second way, confined in the lowermost Barremian, characterizes the genus *Arnaudiella* VERMEULEN, 1997. It makes species with rounded and wide ribs which cross a venter, either keeled or rounded in old species then rounded to flat in more recent species. The furthest species of this evolution are *Arnaudiella anglesense* (VERMEULEN, 1995) and *Arnaudiella schlumbergeri* (NICKLÈS, 1894).

The third begins from species with rounded venter classified into *Arnaudiella* VERMEULEN, 1997. It characterizes the genus *Kotetishvilia* VERMEULEN, 1997. It is marked by the gradual making, in the young stages, of two ventrolateral keels which will advance, on the ribs, toward the adult stage. On the ventrolateral area and on the venter, the reduction then the disappearance of the channels between the ribs, associated with the ventrolateral widening of the ribs imply the appearance of species with longitudinal continuous ventrolateral keels. The furthest species of this evolution are *Kotetishvilia nicklesi* (HYATT, 1903) and *Kotetishvilia brevicostata* (KOTETISHVILI, 1980).

1.2.3. PULCHELLIINAE DOUVILLÉ emend.

This subfamily takes his root into the genus *Arnaudiella* VERMEULEN, 1997.

From *Nicklesia pulchella* (D'ORBIGNY, 1841), with rounded venter, five ways of evolution are shown up.

The first way characterizes the genus *Coronites* HYATT, 1903 ; it makes species with opened umbilicus, siphuncular channel and ribs without keel. The furthest species of this evolution are *Coronites darsi* VERMEULEN, 1995 and *Coronites coronatoides* (SAYN, 1890).

The second way starts from the genus *Coronites* HYATT, 1903 and makes species with coma shape tubercles which are spined or rounded; it characterizes the genus *Curiolia* VERMEULEN, 1998.

The third way characterizes the genus *Heinzia* SAYN, 1890, *nom. transl.* HYATT, 1903; it makes, from the genus *Nicklesia* HYATT, 1903, from the base of the Zone of *Kotetishvilia compressissima* to the lower part of the Zone of *Heinzia sayni*, species with concave venter, with opening umbilicus and keeled ribs with peripheral structures. The furthest species of this evolution are *Heinzia communis* (BÜRGL, 1956) and *Heinzia sayni* HYATT, 1903.

The fourth way characterizes the genus *Memmiella* VERMEULEN, 1999; it shows an intermediate ornamentation between *Curiolia* VERMEULEN, 1998 and *Heinzia* SAYN, 1890; the umbilicus is opened.

The fifth way makes first, involute species with concave venter edged with ventrolateral keels on ribs (clavi) classified into the genus *Pulchellia* UHLIG, 1882. It carries on with species with open umbilicus, with peripheral structures well marked (Vermeulen, 2002) and, at last, by a siphuncular channel which excavates the concave venter, which are classified into the genus *Gerhardtia* HYATT, 1903. The furthest species of this evolution are *Pulchellia galeata* (VON BUCH, 1838) and *Gerhardtia provincialis* (D'ORBIGNY, 1850).

Remark: *Pulchellia* UHLIG, 1882 can be envisaged as senior synonym of *Gerhardtia* HYATT, 1903.

2.– SUBORDER ANCYLOCERATINA WIEDMANN, 1966

The barremian ANCYLOCERATINA are classified into two superfamilies, ANCYLOCERATACEAE GILL, 1878 and DESHAYESITACEAE STOYANOW, 1949.

2.1. ANCYLOCERATACEAE GILL, 1871

The barremian families are ACRIOCERATIDAE VERMEULEN, 2004, EMERICICERATIDAE VERMEULEN, 2004, HEMIHOPLITIDAE SPATH, 1924 and ANCYLOCERATIDAE GILL, 1871.

2.1.1. ACRIOCERATIDAE VERMEULEN, 2004

The barremian species of *Acrioceras* HYATT, 1900 are frequent in the Zones of *Avramidiscus kiliani* and of *Kotetishvilia nicklesi*. The ultimate species, *Acrioceras terveri* (ASTIER, 1851), disappears in the lower part of the Zone of *Nicklesia pulchella*.

Just before its disappearance, *Acrioceras* HYATT, 1900 give *Dissimilites* SARKAR, 1955. In the Zone of *Kotetishvilia compressissima*, from the base of the Subzone of *Subtorcapella defayi*, two main ways of evolution are shown up.

The first way makes species with shells close to those of the ancestors *Acrioceras* species.

The second way makes species with spindly shaft and probably reduced whorls ; it may be characterizes the genus*Toxoceratoides* SPATH, 1924.

On the two ways defined herein, the tuberculation moves forward the aperture.

Remark : New recent paleontological and biostratigraphical data imply to classify *Argvethites* ROUCHADZÉ, 1933 into the family ACRIOCERATIDAE VERMEULEN, 2004.

2.1.2. EMERICICERATIDAE VERMEULEN, 2004

The history of EMERICICERATIDAE VERMEULEN, 2004 begins in the Upper Hauterivian.

The first specimens of *Emericiceras* SARKAR, 1954 were collected in the lower part of the Zone of *Balearites balearis* but possible ancestors forms exist in the Zone of *Plesiospitidiscus ligatus*. This genus disappears in the lower part of the Zone of *Nicklesia pulchella*.

Honnoratia BUSNARDO *et al.*, 2003 derives from *Emericiceras* SARKAR, 1954 ; The original species *Honnoratia honnoratiana* (D'ORBIGNY, 1842), appears in the Zone of *Prieuriceras picteti* and *Honnoratia thiollierei* (ASTIER, 1851), the last species, disappears in the Zone of *Nicklesia pulchella*.

Paracrioceras SPATH, 1924 derives from *Emericiceras* SARKAR, 1954 ; it appears in the upper part of the Zone of *Avramidiscus kiliani*, in the Subzone of *Psilotissotia colombiana*, with forms close to *Paracrioceras fissicostatum* (ROEMER, 1840), and then it disappears with *Paracrioceras koechlini* (ASTIER, 1851) in the Zone of *Kotetishvilia nicklesi*.

2.1.3. HEMIHOPLITIDAE SPATH, 1924

Barrancyloceras VERMEULEN & BERT, 1998, derived from the genus *Honnoratia* BUSNARDO *et al.*, 2003, appears in the Zone of *Holcodiscus uhligi*. *Barrancyloceras barremense* (KILIAN, 1895), type-species, is preceded by a primitive population, not yet described, at the base of the Zone of *Heinzia sayni*. The main evolution of this family is characterized by an involutive process of the whorls and by the loss of the shaft and the

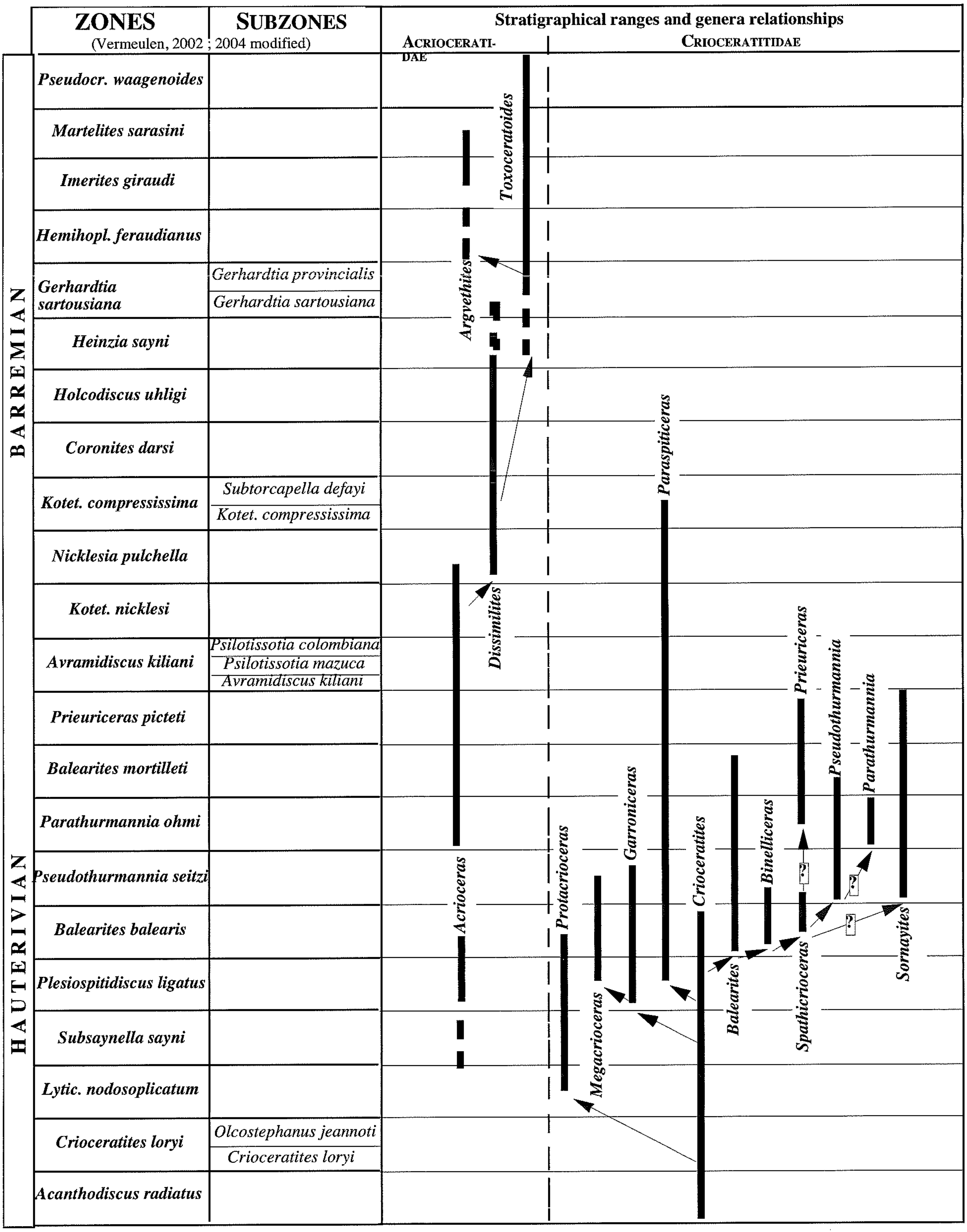

FIG. 84.- Evolution of the families ACRIOCERATIDAE and CRIOCERATITIDAE (ANCYLOCERATINA) during the Hauterivian and the Barremian.

hook, these two last present on the shells of original species of the family.

Ezeiceras VERMEULEN & BERT, 1998, which derives from *Barrancyloceras* VERMEULEN & BERT, 1998, appears about the middle of the Zone of *Heinzia sayni*; it is represented by several small species, with whorls in contact and with ribs non tuberculate to trituberculate.

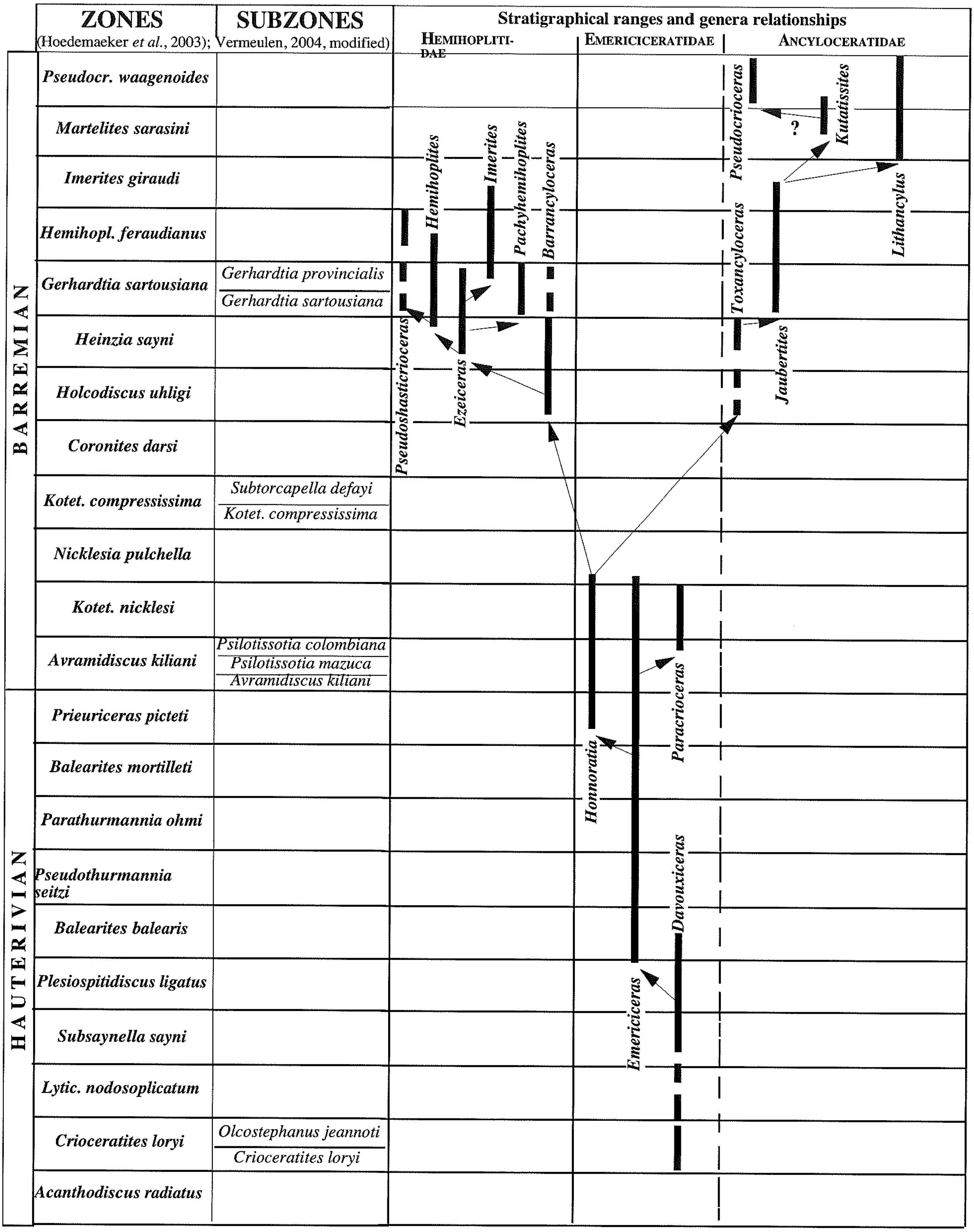

FIG. 85- Evolution of the families EMERICICERATIDAE VERMEULEN, 2004, HEMIHOPLITIDAE SPATH, 1924 and ANCYLOCERATIDAE GILL, 1871 during the late Hauterivian and the Barremian.

From the genus *Ezeiceras* VERMEULEN & BERT, 1998, between the upper part of the Zone of *Heinzia sayni* and the top of the Zone of *Hemihoplites feraudianus*, a complicated evolution process imply the birth of the genera *Hemihoplites* SPATH, 1924, *Pachyhemihoplites* DELANOY, 1992, *Imerites* ROUCHADZÉ, 1933, *Spinocrioceras* KEMPER, 1973 and *Pseudoshasticrioceras* DELANOY, 1999.

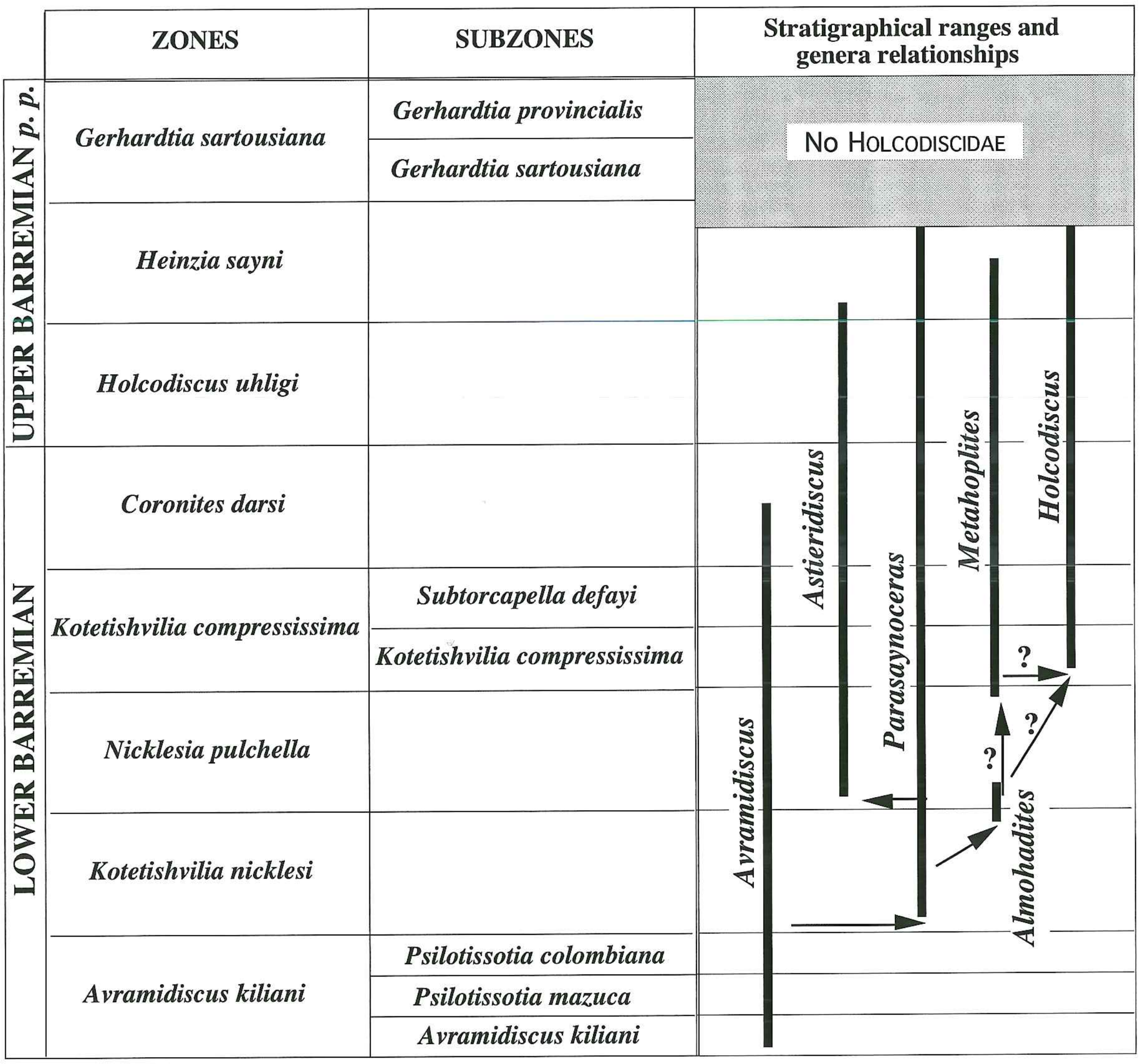

FIG. 86.- Evolution of the family HOLCODISCIDAE SPATH, 1923, according to Vermeulen and Thieuloy (1999), modified.

Remark : The whorls of the most species belonging to the genus *Pseudocrioceras* SPATH, 1924 show well marked hémihoplid characters, as for examples whorls in contact, whorls sections higher than wide, faintly convex venters and ventrolateral clavi, which take them away from the family ANCYLOCERATIDAE GILL, 1871. The origin from HEMIHOPLITIDAE SPATH, 1924, in particular from *Pseudoshasticrioceras* DELANOY, 1999, may be considered; in this case, it would imply the classification of *Pseudocrioceras* SPATH, 1924 into HEMIHOPLITIDAE SPATH, 1924.

2.1.4. ANCYLOCERATIDAE GILL, 1871

This family, derived from the genus *Honnoratia* BUSNARDO *et al.*, 2003, shows a quite different evolution than HEMIHOPLITIDAE SPATH, 1924. The shaft and the hook of the shells are always present and the whorls are very evolved and not so developed. In the Barremian they are first represented by sporadic populations, quantitatively well developed, then in the Bedoulian, their presence is more important and certainly made easy by the disappearance of HEMIHOPLITIDAE SPATH, 1924.

The oldest species known, *Toxancyloceras vandenheckii* (ASTIER, 1851), appears at the base of the Zone of *Heinzia sayni*; it is later followed, in the Zone of *Gerhardtia sartousiana*, by a population which can be overall represented by *Jaubertites audouli* (ASTIER, 1851). In the Bedoulian, this family is represented by species classified into the genera *Jaubertites* SARKAR, 1955 senior synonym of *Audouliceras* THOMEL, 1964, *Ancyloceras* D'ORBIGNY, 1842 and *Lythancylus* CASEY, 1960.

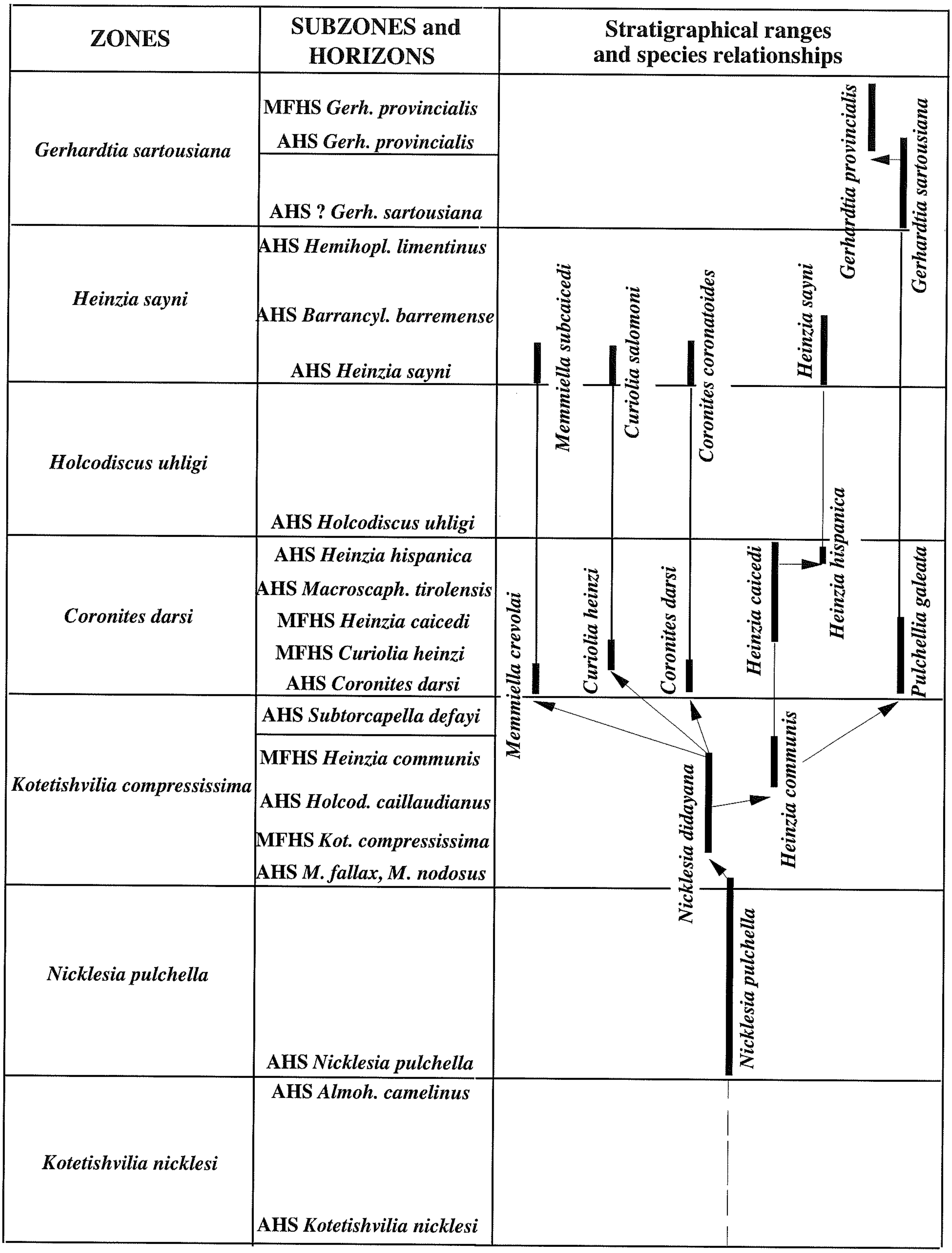

FIG. 87.- Evolution of the subfamily PULCHELLIINAE DOUVILLÉ, 1911, acording to Vermeulen (2002), modified.

2.2. DESHAYESITACEAE STOYANOW, 1949

The precise origin of HETEROCERATIDAE SPATH, 1922 is not yet established; they are therefore classified with DESHAYESITIDAE STOYANOW, 1949, which succeed them straight, into DESHAYESITACEAE STOYANOW, 1949.

2.2.1. Heteroceratidae Spath, 1922

In the Lower Cretaceous, HETEROCERATIDAE SPATH, 1922 are represented by three main populations classified into the genera *Pseudomoutoniceras* AUTRAN *et al.*, 1986, Upper Hauterivian, *Moutoniceras* SARKAR, 1955, Lower Barremian to the base of the upper Barremian, *Heteroceras* D'ORBIGNY, 1849 (= *Colchidites* DJANELIDZÉ, 1926 and *Martelites* CONTE, 1989), Upper Barremian.

Moutoniceras SARKAR, 1955 appears suddenly at the base of the Zone of *Nicklesia pulchella*; the last specimens of this genus, classified into *Moutoniceras moutonianum* (D'ORBIGNY, 1850), disappear in the lower part of the Zone of *Heinzia sayni*.

Heteroceras D'ORBIGNY, 1849 appears suddenly in the Upper Barremian, in the upper part of the Zone of *Hemihoplites feraudianus*, with *Heteroceras baylei* REYNÈS, 1876 and *Heteroceras astieri* D'ORBIGNY, 1851 (= *Heteroceras coulleti* DELANOY, 1994). This genus disappears in the Zone of *Martelites sarasini*; it is relayed by *Martelites* CONTE, 1989 which is the ultimate genus of this family which disappears in the Zone of *Martelites sarasini*.

Remark: fragments of HETEROCERATIDAE were collected in the Zone of *Gerhardtia sartousiana*, but their preserving do not allow specific attribution.

3.– Suborder Protancyloceratina nov.

The family BOCHIANITIDAE SPATH, 1922 is commonly classified (Wright *et al.*, 1996) into the suborder ANCYLOCERATINA WIEDMANN, 1966. The works of Thieuloy (1977) and Reboulet (1996) show that these ammonites are without link with the other families classified into the suborder created by Wiedmann. Therefore, the suborder *Protancyloceratina* nov. is created to keep out of ANCYLOCERATINA WIEDMANN, 1966 the linked families PROTANCYLOCERATIDAE BREISTROFFER, 1947 and LEPTOCERATOIDIDAE THIEULOY, 1966 *nom. transl.* VERMEULEN, this work.

Remark: the argumentation of this important taxinomic changing goes beyond the subject of this work; it will be enlarged in a later work.

3.1. Leptoceratoididae Thieuloy, 1966 *nom. transl.*

In the uppermost Hauterivian LEPTOCERATOIDIDAE THIEULOY, 1966 become very frequent, especially in the Zone of *Prieuriceras picteti*. Their descendants, in the lowermost Barremian, are classified into the genera *Hamulinites* PAQUIER 1901, *Manoloviceras* VASICEK, 1994, *Eoheteroceras* VASICEK, 1994, *Leptoceratoides* THIEULOY, 1966 and *Karsteniceras* ROYO Y GOMEZ, 1945 (Vasicek, 1994). In the Upper Barremian only *Hamulinites* PAQUIER 1901, *Karsteniceras* ROYO Y GOMEZ, 1945 and *Leptoceratoides* THIEULOY, 1966 remain. In the stratotype of Angles, LEPTOCERATOIDIDAE THIEULOY, 1966 are presents, with changes of frequency, in all the section, from the base of the Barremian to the Zone of *Martelites sarasini*; the ultimate species is *Leptoceratoides puzosianum* (D'ORBIGNY, 1842).

4.– Suborder Lytoceratina Hyatt, 1889

Three superfamilies are represented in the Barremian, LYTOCERATACEAE NEUMAYR, 1875, LYTOCRIOCERATACEAE VERMEULEN, 2000 and TETRAGONITACEAE HYATT, 1900.

4.1. Lytocerataceae Neumayr, 1875

The barremian species are classified into the genera *Lytoceras* SUESS, 1865 and *Eulytoceras* SPATH, 1927 belonging to the family LYTOCERATIDAE NEUMAYR, 1875. *Lytoceras subfimbriatum* (D'ORBIGNY, 1841) and *Eulytoceras anysoptychum* (UHLIG, 1883) are, in the Lower Barremian, the most frequent species. *Eulytoceras raricinctum* (UHLIG, 1883) and *Eulytoceras phestus* (MATHERON, 1878) appear in the upper part of the Zone of *Coronites darsi*. In the Upper Barremian, these two species will be more frequent.

4.2. Lytocriocerataceae Vermeulen, 2000

During the Barremian, the families HAMULINIDAE GILL, 1871, MACROSCAPHITIDAE HYATT, 1900 and PTYCHOCERATIDAE GILL, 1871 show their main evolutions and their higher quantitative developments.

4.2.1. Hamulinidae Gill, 1871

In the lowermost Barremian, the species *Anahamulina* aff. *subcylindrica* (D'ORBIGNY, 1850), *Anahamulina davidsoni* (COQUAND *in* MATHERON, 1879), *Amorina cincta* (D'ORBIGNY, 1849), *Vasicekina* gr. *paxillosa* (UHLIG, 1883) and *Hamulina astieri* (D'ORBIGNY, 1850) are the most frequent of the family; they disappear, in different levels, into this interval.

In the Zone of *Nicklesia pulchella*, *Vasicekina paxillosa* (UHLIG, 1883), typical form, and *Amorina subcincta* (UHLIG, 1883) are the most frequent species.

In the Zones of *Kotetishvilia compressissima* and of *Coronites darsi* the HAMULINIDAE GILL, 1871 become more rare. *Vasicekina* cf. *paxillosa* (UHLIG, 1883) has been collected in the bed n° 129/041 of the stratotype.

Rare specimens of the genus *Ptychohamulina* gen. nov. has been collected in the lower part of the Zone of *Heinzia sayni*. At the top of this zone and in the Zone of *Gerhardtia sartousiana*, HAMULINIDAE become once more frequent; the most frequent species can be classified into the genera *Ptychohamulina* gen. nov. and *Duyeina* gen nov.

I have not collected any specimen of this family up to the Zone of *Gerhardtia sartousiana*.

4.2.2. Macroscaphitidae Hyatt, 1900

This family appears suddenly at the top of the Zone of *Avramidiscus kiliani*, in the Subzone of *Psilotissotia colombiana*, with the genus *Lytocrioceras* Spath, 1924. The last most frequent barremian representants are *Macroscaphites yvani* (Puzos, 1831) and *Costidiscus recticostatus* (d'Orbigny, 1841).

From the genus *Lytocrioceras* Spath, 1924, a complicated evolution implies the birth of the genera *Rugacrioceras* Vermeulen, 1990, *Macroscaphites* Meek, 1876 and *Acantholytoceras* Spath, 1923.

Lineage *Lytocrioceras jauberti* (Astier, 1851)-***Lytocrioceras*** sp. nov.: *Lytocrioceras* sp. nov., of the Zone of *Heinzia sayni*, shows the existence of a lineage characteristic of the genus *Lytocrioceras* Spath, 1924 *sensu stricto*, in which, from *Lytocrioceras jauberti* (Astier, 1851), the whorls stay uncoiled and no tuberculate and the shaft and the hook acquire main trituberculate ribs.

Lineage Lytocrioceras-Rugacrioceras: from the Zone of *Nicklesia pulchella* to the Zone of *Gerhardtia sartousiana* , the species of *Lytocrioceras* regress in size and acquire tubercles which progress from the young uncoiled stage to the adult stage and therefore imply the birth of *Rugacrioceras* Vermeulen, 1990.

Lineage Lytocrioceras-Macroscaphites: the uncoiled whorls of ancestors *Lytocrioceras* quickly become in contact and the trituberculate main ribs progress from the youngest stages to the shaft; it permit the birth of *Macroscaphites tirolensis* Uhlig, 1887, at the top of the Zone of *Coronites darsi*. The bituberculate species, *Macroscaphites binodosus* Uhlig, 1883, is present in the lower part of the Zone of *Heinzia sayni*; a monotuberculate specimen, close to *Macroscaphites ectotuberculatus* Avram, 1984, has been collected in the Zone of *Gerhardtia sartousiana*; the untuberculate species *Macroscaphites yvani* (Puzos, 1832), appears in the Zone of *Gerhardtia sartousiana.* These data show that the regression of the tubercles is one of the main typical characteristics of the *Macroscaphites* evolution process.

The genus *Acantholytoceras* Spath, 1923: it derives from large species of the Zone of *Kotetishvilia nicklesi*, classified into *Lytocrioceras* Spath, 1924. This evolution is made by quick migration of the trituberculate main ribs on the whole shell. This evolution ends in the Zone of *Kotetishvilia compressissima*, at the base of the Subzone of *Subtorcapella defayi*, where I have collected *Acantholytoceras* aff. *longispinum* (Uhlig, 1883) in the bed n° 120/041 of Angles stratotype.

The case of the genus *Costidiscus* Uhlig, 1882: the origin of this genus is not yet established. A primitive specimen of this genus has been collected at the base of the Zone of *Heinzia sayni*; his ornamental characters take it away from subcontemporaneous *Macroscaphites* and bring it close to a non described species of the Zone of *Coronites darsi*.

4.2.3. Ptychoceratidae Gill, 1871

The precise classification of Ptychoceratidae Gill, 1871 is not yet established.

Supposing the relationship between *Anahamulina sensu lato* and *Ptychoceras*, this family is classified into Lytocriocerataceae Vermeulen, 2000. *Euptychoceras* Breistroffer, 1952, with trifid suture line, derives probably from *Bochianites* Lory, 1898; Therefore it must be classified into Bochianitidae Spath, 1922.

The barremian *Ptychoceras* become frequent only from the Zone of *Gerhardtia sartousiana* in which *Ptychoceras puzosianus* d'Orbigny, 1842 is the most frequent species. A specimen close to *Ptychoceras natrice* Anderson, 1938 and a not well preserved specimen close to *Ptychoceras laeve* Matheron, 1842 were collected also in this zone.

4.3. Tetragonitaceae Hyatt, 1900

Only the Tetragonitidae Hyatt, 1900 are present in the Barremian.

The recent discovery of the ancestor species *Eotetragonites lapitskii* sp. nov., in the Zone of *Kotetishvilia nicklesi*, implies a change of the classification of the related genera *Protetragonites* Hyatt, 1900 and *Eotetragonites* Breistroffer, 1947; they must be classified into Tetragonitidae Hyatt, 1900.

5.– Suborder Phylloceratina Arkell, 1950

Only the family Phylloceratidae Zittel, 1884 is present in the Barremian.

5.1. Phylloceratinae Zittel, 1884

In the lower Barremian, *Hypophylloceras* Salfeld, 1924 is the most frequent with *Hypophylloceras semistriatum* (d'Orbigny, 1841), senior synonym of *Hypophylloceras ponticuli* Rousseau, 1842 (Joly, 2000). Some small sporadic populations of the genus *Jolyceras* gen. nov. are also present and *Jolyceras paquieri* (Sayn, 1896), typical form, appears in the Zone of *Kotetishvilia compressissima*, at the base of the Subzone of *Subtorcapella defayi* and it is still present in the Gargasian. *Jolyceras terveri* (d'Orbigny, 1841) is a peripheral species (Vermeulen, 2004) ; it is confined to the Zone of *Kotetishvilia nicklesi*.

5.2. Phyllopachyceratinae Collignon, 1937

In the stratotype, from the base of the Barremian to the top of the Zone of *Gerhardtia sartousiana*, *Phyllopachyceras infundibulum* (d'Orbigny, 1841) is present in almost the whole beds. *Phyllopachyceras vergonsense* Delanoy & Joly, 1995 appears at the top of the Zone of *Heinzia sayni* (Joly, 2000) and *Phyllopachyceras baborense* (Coquand, 1880) is present in the Zone of *Imerites giraudi*.

6.– Short definitions of new taxa

The new classification used in this work requires the creation of new taxa, most of them classified into the family Hamulinidae Gill, 1871 still few studied on generic rank.

Family Hamulinidae Gill, 1871

Genus *Vasicekina* gen. nov.

Naming: this genus is dedicated to Zdenek Vasicek, Technical University of Ostrava, Czech Republic.
Type-species: *Vasicekina paxillosa* (Uhlig, 1883) = *Hamulina paxillosa* n. sp. *in* Uhlig, 1883, Pl. XIV, fig. 3.
Diagnosis: species with little rate of growth, with parallel to moderatly divergent proversum and retroversum. On the proversum the ribs are equal, thin and prorsiradiate. Near the bend, the ribs become a little more strong. In the middle, or near the middle, of the bend two coarse ribs are separated by a deep channel. On the retroversum the ribs are stronger than those of the proversum; they are rursiradiate at the beginning and gradually they become rectiradiate near the aperture.

Genus *Amorina* gen. nov.

Naming: this genus is dedicated to Henri Amor, gynecologist at Saint-Raphaël, Var, France.
Type-species: *Amorina cincta* (d'Orbigny, 1849) = *Hamulina cincta* d'Orbigny, 1849, Pl. VI, fig. 4-6.
Diagnosis: species with intermediate size between those of *Hamulina* and *Vasicekina*. Proversum and retroversum are parallel or little divergent. On the proversum the ribs are thin, a little prorsiradiate and some of them, less or more regularly spaced, are a little stronger than the others. On the bend, two or three grouped coarse ribs are separated by deep channels. On the retroversum, the ribs become quickly rectiradiate and some of them, less or more regularly spaced, are very stronger than the others.

Genus *Ptychohamulina* gen. nov.

Naming: for its species, sometimes close to those of the genus *Ptychoceras* d'Orbigny, 1842.
Type-species: *Ptychohamulina ptychoceroides* (Hohenneger *in* Uhlig, 1883) = *Hamulina ptychoceroides* Hohenneger *in* Uhlig, 1883, Pl. XIV, fig. 2.
Diagnosis: little size species, with very weak rate of growth. The proversum and the retroversum are less or more close and subparallel. On the proversum the ribs are thin to strong, less or more spaced and prorsiradiate. The bend wears only one coarse rib. On the retroversum the ribs are mainly rursiradiate and their strength is variable.

Genus *Duyeina* gen. nov.

Naming: this genus is dedicated to Jean Paul Duyé, Digne-les-bains, Alpes de Haute-Provence, France.

Type-species: *Duyeina glemmbachensis* (Immel, 1987) = *Anahamulina glemmbachensis* n. sp. *in* Immel, 1987, Pl. 14, fig.1.

Diagnosis: species with little rate of growth. The proversum and the retroversum are parallel to strongly divergent and close to distant. The ribs of the proversum are equal, strong, a little prorsiradiate and irregularly spaced depending on species. Near the bend the ribs become stronger. On the bend there is no coarse rib and all the ribs are equal, sometimes stronger on the venter than on the flanks. On the retroversum the ribs are similar or stronger than those of the bend ; they are rursiradiates ans sometimes they become rectiradiate near the aperture.

Family Tetragonitidae Hyatt, 1900

Genus *Eotetragonites* Breistroffer, 1947

Eotetragonites lapitskii sp. nov.

Naming: this species is dedicated to Sergei Lapitski, Lomonossov University , Faculty of Geology, Moscow, Russia.

Holotype: specimen n° LY001, bed n° 102/041, Zone of *Kotetishvilia nicklesi*, Angles stratotype, France.

Diagnosis: small-sized species, with diameter about 40-50 mm, as it may be sawn on collected specimens, with a wide umbilicus ; section of the whorls sub-quadrate, flat flanks, slighty rounded venter and abrupt peri-umbilical wall. On the youngest whorls the ornamentation is made of spaced constrictions and, from 9,5 mm to 11,5 mm of whorl height, thin ribs, well marked on the flanks appear against and in front of the constrictions. From 11,5 mm to the aperture, corresponding probably of adult stage, only thin ribs, regularly spaced out, are still present and they are very close to those of contemporaneous species belonging to the genus *Protetragonites* Hyatt, 1900. The suture line is unknown.

Family Phylloceratidae Zittel

Genus *Jolyceras* gen nov.

Naming: this genus is dedicated to B. Joly, paleontologist, spécialist of Phylloceratina Arkell, 1950.
Type-species: *Jolyceras paquieri* (Sayn, 1896) = *Phylloceras paquieri* Sayn, 1920, Pl. I, fig. 8-11.
Diagnosis: shell with whorl section less or more higher than wide, depending on age and species. The flanks are

slighty convex and the venter is rounded. Rectiradiate, prorsiradiate or flexuous constrictions, less or more numerous, either go across the flanks or just a part of the flanks; sometimes they can go across the venter. Between these constrictions there are very thin and flexuous ribs. The periumbilical wall is rounded. The umbilicus is less or more wide in the younger stages and the ratio umbilicus diameter/ height of whorl decreases with age. The suture line is close to *Hypophylloceras* (JOLY, 2000).

7.– CONCLUSIONS

Almost all the barremian ammonites families must be reviewed. Fiew specialists are now searching family by family and the knowledge of barremian ammonites families make progress slowly. Only the reviewing family by family of barremian ammonites can give new important data in order to have a better knowledge of the phylogenetical evolution of these ammonites and also in order to build a precise phylogenetical classification of them.

The main subdivisions of the stratotypical Barremian

The evolutions of the barremian ammonites allow to distinguish five main intervals in the stratotypical Barremian and, by extension, all over the mediterranean Barremian :

Barremian 1: in this interval, stretching from the base of the Zone of *Avramidiscus kiliani* to the top of the Zone of *Kotetishvilia nicklesi*, disappear numerous species and genera which was born in the upper Hauterivian, as for example *Discoidellia, Psilotissotia*, PULCHELLIIDAE, *Hamulina*, *Anahamulina*, HAMULINIDAE, *Plesiospitidiscus sensu lato*, BARREMITIDAE. ACRIOCERATIDAE, EMERICICERATIDAE and HAMULINIDAE show their most important developments; *Macroscaphitidae* appear.

Barremian 2: in this interval, stretching from the base of the Zone of *Nicklesia pulchella* to the top of the Zone of *Coronites darsi*, disappear EMERICICERATIDAE. The genera *Moutoniceras*, HETEROCERATIDAE, *Metahoplites* and *Holcodiscus*, HOLCODISCIDAE, and *Subtorcapella*, BARREMITIDAE, appear and show their most important developments. The last EMERICICERATIDAE, belonging to the genus *Paraspiticeras*, disappear.

Barremian 3: in this interval, stretching from the base of the Zone of *Holcodiscus uhligi* to the top of the Zone of *Hemihoplites feraudianus*, HETEROCERATIDAE regress strongly and they are replaced by HEMIHOPLITIDAE which are, in this interval, the most important stock of ANCYLOCERATINA. ANCYLOCERATIDAE appear but they are not so numerous as HEMIHOPLITIDAE. MACROSCAPHITIDAE show their maximum of diversification. Several new species of PTYCHOCERATIDAE appear. HOLCODISCIDAE disappear and PULCHELLIIDAE show their last diversifications.

Barremian 4: this interval, stretching from the base of the Zone of *Imerites giraudi* to the top of the Zone of *Martelites sarasini*, is characterized by the last and important diversification of HETEROCERATIDAE. HEMIHOPLITIDAE are gradually replaced by ANCYLOCERATIDAE. BARREMITIDAE are less numerous than in the previous intervals

Barremian 5: in this last interval, corresponding to the Zone of *Pseudocrioceras waagenoides* not yet defined in the stratotype, the different species of the genus *Pseudocrioceras* represent the main typical fauna of this interval. HETEROCERATIDAE and perhaps HEMIHOPLITIDAE, if *Pseudocrioceras* belongs to this family, disappear.

BARREMITIDAE, SILESITIDAE from their appearance, ACRIOCERATIDAE, PHYLLOCERATIDAE and LYTOCERATIDAE, less or more frequent, are regularly present along the stratotypical section.

Selected references

AGUADO R., COMPANY M., SANDOVAL J. & TAVERA J.M. (2001).– Caracterizacion bioestratigraphica del limite Hauteriviense-Barremiense en las Cordilleras Béticas. *Geotemas*, **3**, 2, 127-130.

BULOT L., ARNAUD H. & ARGOT M. *eds.* (1995).– Lower Cretaceous cephalopod biostratigraphy of the Western Tethys : recent developments, regional synthesis and outstanding problems. *Géologie Alpine*, Mém. H. S. n° **20**, 1-421, Grenoble.

BUSNARDO R. (1965).– Le stratotype du Barrémien. I. - Lithologie et macrofaune. *Mém. Bur. Rech. Géol. Min.*, **34**, 101-116, Paris.

BUSNARDO R., CHAROLLAIS J., WEIDMANN M. & CLAVEL B. (2003).– Le Crétacé inférieur de la Veveyse de Châtel (Ultrahelvétique des Préalpes externes ; canton de Fribourg, Suisse). *Revue Paléobiol.*, **22** (1) 1-174, 32 Pl., Genève.

COMPANY M., SANDOVAL J. & TAVERA J.M. (1995).– Lower Barremian ammonite biostratigraphy in the Subbetic Domain (Betic Cordillera, southern Spain). *Cretaceous Research*, **16**, 243-256

COMPANY M., SANDOVAL J. & TAVERA J.M. (2003).– Ammonite biostratigraphy of the uppermost Hauterivian in the Betic Cordillera (SE Spain). *Geobios*, **36**, 6, 627-792, 2 Pl., Lyon.

DELANOY G. (1998).– Biostratigraphie des faunes d'Ammonites à la limite Barrémien-Aptien dans la région d'Angles-Barrême-Castellane. Étude particulière de la famille des *Heteroceratidae* Spath, 1922 (Ancyloceratina, Ammonoidea). *Ann. Mus. Hist. Nat. Nice 1997*, **XII**, 1-270, 62 Pl., Nice.

EBBO L., POUPON A., DELANOY G. & GONNET R. (2000).– Nouvelles données sur le genre *Lytocrioceras* SPATH, 1924 dans le Barrémien inférieur du Sud-Est de la France. *Ann. Mus. Hist. Nat. Nice, 1999*, **14**, 1-25, Nice.

HOEDEMAEKER PH. J. & REBOULET S. (reporters), AGUIRRE-URRETA M., ALSEN P., AOUTEM M., ATROPS F., BARRANGUA R., COMPANY M., GONZALES C., KLEIN J., LUKENEDER A., PLOCH I., RAISOSSADAT N., RAWSON P., ROPOLO P., VASICEK Z., VERMEULEN J. & WIPPICH M. (2003).– Report on the 1st International Workshop of the IUGS Lower Cretaceous Ammonite Working Group, the "Kilian Group" (Lyon, 11 September 2002). *Cretaceous Research*, **24**, 89-94.

REBOULET S. (1996).– L'évolution des ammonites du Valanginien-Hauterivien inférieur du bassin vocontien et de la plate-forme provençale (Sud-Est de la France). Relations avec la stratigraphie séquentielle et implications biostratigraphiques. *Docum. Lab. Geol. Lyon*, **137**, 1-371, 38 Pl., Lyon.

THIEULOY J.-P. (1977).– La zone à *callidiscus* du Valanginien supérieur vocontien (Sud-Est de la France). Lithostratigraphie, ammonitofaune, limite Valanginien-Hauterivien, corrélations. *Géologie Alpine*, **53**, 83-143, 7 Pl., Grenoble.

THIEULOY J. P. (1979).– *Matheronites limentinus n. sp.* (*Ammonoidea*) espèce type d'un horizon repère Barrémien supérieur du Vercors méridional (Massif Subalpin Français). *Geobios*, Mémoire spécial **3**, 305-317, Lyon.

VERMEULEN J. (1999).– Nouvelles données sur les répartitions stratigraphiques, les évolutions et les classifications de trois familles d'ammonites du Crétacé inférieur. *Géologie Alpine*, **75**, 123-132, Grenoble.

VERMEULEN J. (2000).– Nouvelles données sur l'origine, l'évolution et la classification des Hemihoplitidae Spath, 1924 (Ammonoidea, Ancyloceratacea). *Ann. Mus. Hist. Nat. Nice*, **XV**, 91-101, Nice.

VERMEULEN J. (2002).– Étude stratigraphique et paléontologique de la famille des PULCHELLIIDAE (AMMONOIDEA, AMMONITINA, ENDEMOCERATACEAE).*Géologie Alpine* , Mém. H. S. n° **42**, 1-333, 57 Pl., Grenoble..

VERMEULEN J. (2004).– Vers une nouvelle classification à fondement phylogénétique des ammonites hétéromorphes du Crétacé inférieur méditerranéen. Le cas des CRIOCERATITIDAE GILL, 1871 *nom. correct.* WRIGHT, 1952, des EMERICICERATIDAE fam. nov. et des ACRIOCERATIDAE fam. nov. (ANCYLOCERATACEAE GILL, 1871). *Riviéra scientifique* , 69-92, 4 Pl., Nice.

WRIGHT C. W., CALLOMON J. H. & HOWARTH M. K. (1996).– Treatise on Invertebrate Paleontology. Cretaceous Ammonoidea, L, **4**, Revised, 1-362, Boulder, Lawrence.

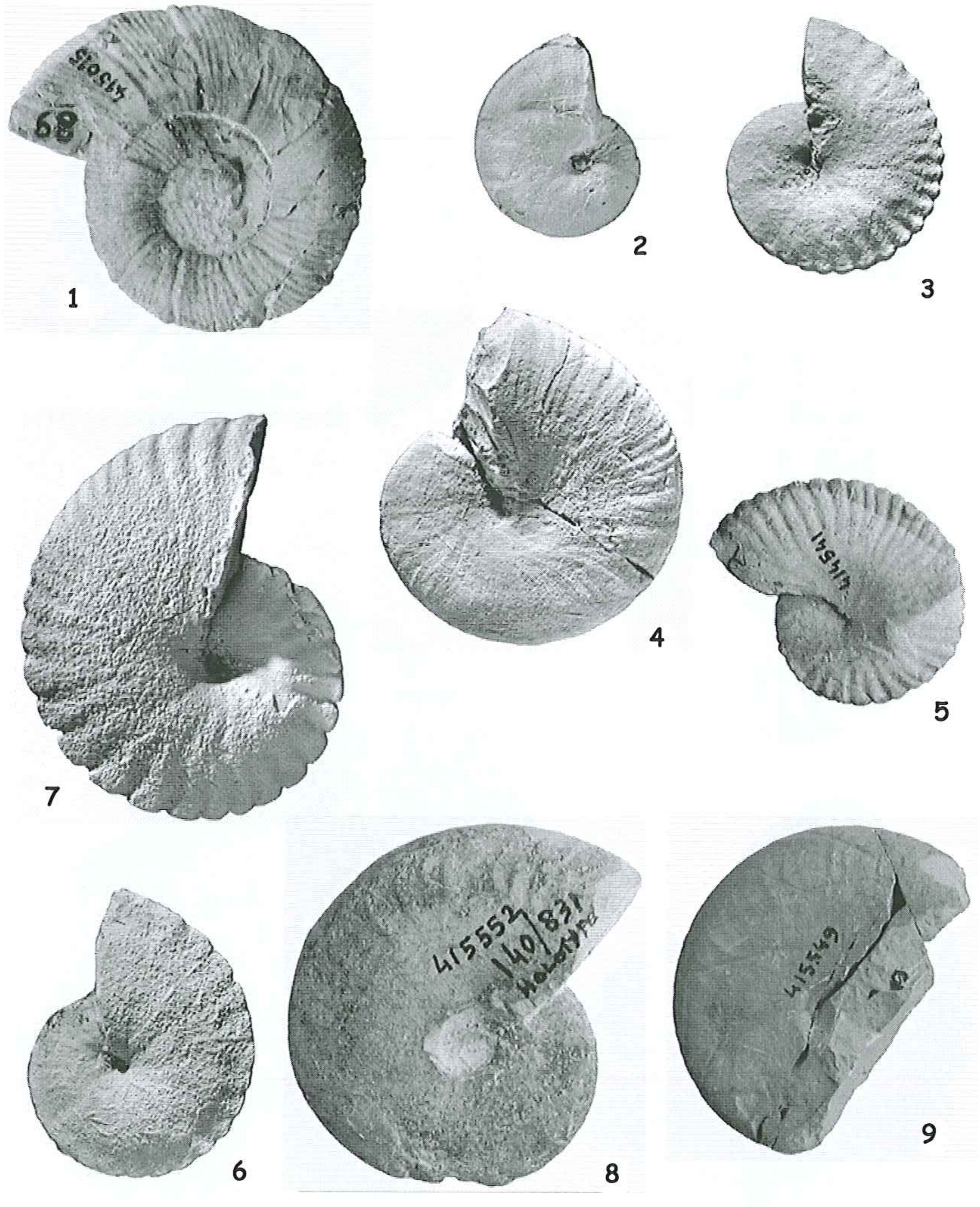

PLATE 42.- Fig. **1**, *Avramidiscus kiliani* (PAQUIER, 1900), HOLCODISCIDAE, specimen n°415015, bed n° 89/041, Angles section, x **1.2**. Fig. **2**, *Psilotissotia mazuca* (COQUAND, 1880), PULCHELLIIDAE, specimen n° 414652, **lectotype**, bed n° 76/041, Angles section, x **2**. Fig. **3**, *Psilotissotia colombiana* (D'ORBIGNY, 1842), PULCHELLIIDAE, specimen n° 414080, **neotype**, bed n° 89/041, Angles section, x **2**. Fig. **4**, *Kotetishvilia nicklesi* (HYATT, 1903), PULCHELLIIDAE, specimen n° 414029, bed n° 95/041, Angles section, x **2**. Fig. **5**, *Nicklesia pulchella* (D'ORBIGNY, 1841), PULCHELLIIDAE, specimen n° 414541, bed n° 109-1/041Angles section, x **1**. Fig. **6**, *Kotetishvilia compressissima* (D'ORBIGNY, 1841), PULCHELLIIDAE, specimen n° 414017, **hypotype**, bed n° 116/041, Angles section, x **2**. Fig. **7**, *Kotetishvilia compressissima* (D'ORBIGNY, 1841), PULCHELLIIDAE, specimen n° 414015, bed n° 116/041, Angles section, x **2**. Fig **8**, *Subtorcapella defayi* (Vermeulen, 2002), BARREMITIDAE, specimen n° 415552, **holotype**, bed n° 140/831, le Clos de Barral section, Var, x **1**. Fig **9**. *Subtorcapella defayi* (Vermeulen, 2002), BARREMITIDAE, specimen n° 415549, bed n° 120/041, Angles section, x **1**. All specimens: J. Vermeulen's collection.

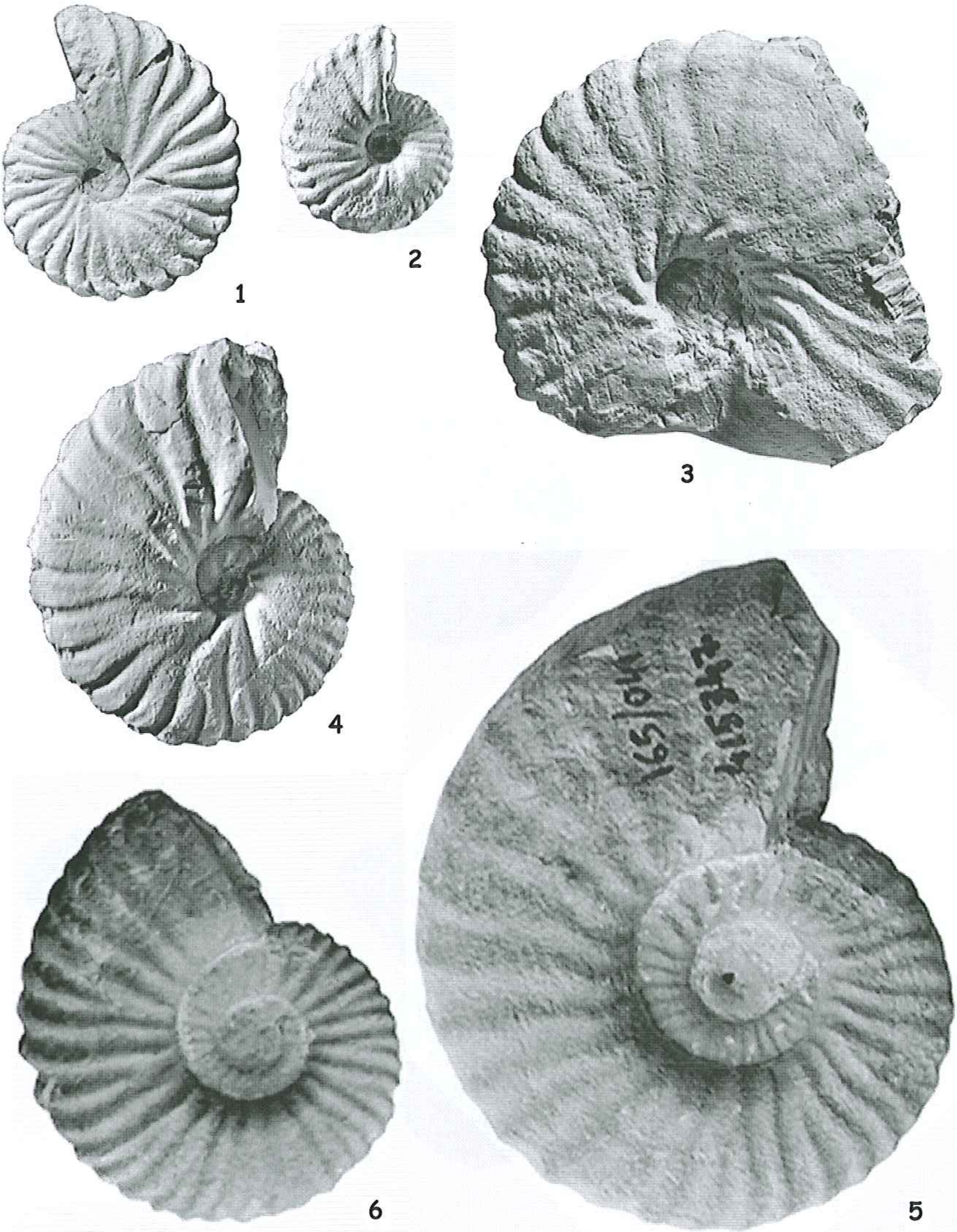

PLATE 43.- Fig. 1, *Coronites darsi* VERMEULEN, 1995, PULCHELLIIDAE, specimen n° 414008, **holotype**, bed n° 141/831, le Clos de Barral section, Var, x 2. Fig. 2, *Heinzia sayni* HYATT, 1903, PULCHELLIIDAE, specimen n° 414534, bed n° 151/831, le Clos de Barral section, Var, x 2. Fig. 3, *Gerhardtia sartousiana* (D'ORBIGNY, 1841), PULCHELLIIDAE, specimen n° 414531, **neotype**, bed n° 162/041, Angles section, x 2. Fig. 4, *Gerhardtia provincialis* (D'ORBIGNY, 1850), PULCHELLIIDAE, specimen n° 414983, bed n° 162/041, Angles section, x 2. Fig. 5, *Hemihoplites feraudianus* (D'ORBIGNY, 1841), HEMIHOPLITIDAE, specimen n° 415347, bed n° 165/041, Angles section, x 1,5. Fig. 6, *Hemihoplites feraudianus* (D'ORBIGNY, 1841), HEMIHOPLITIDAE, young specimen n° 415348, bed n° 165/041, Angles section, x 2. All specimens: J. Vermeulen's collection.

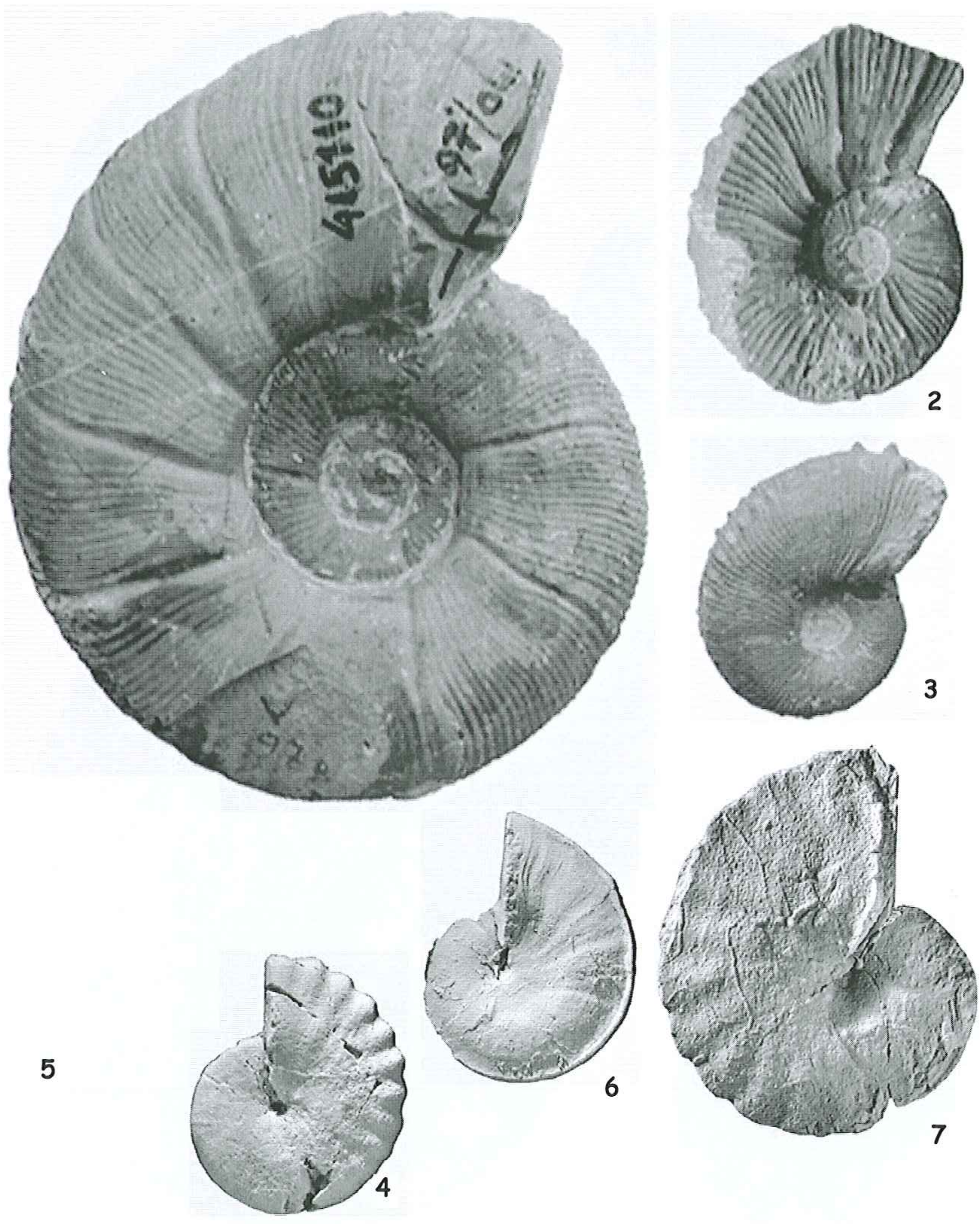

PLATE 44.- Fig. **1**, *Avramidiscus intermedius* (D'ORBIGNY, 1841), HOLCODISCIDAE, specimen n° 415110, bed n° 97/041, Angles section, Zone of *Kotetishvilia nicklesi*, x **2**. Fig. **2**, *Metahoplites fallax* (COQUAND *in* MATHERON, 1879), HOLCODISCIDAE, specimen n° 415031, bed n° 112-5/041,Angles section, Zone of *Kotetishvilia compressissima*, Subzone of *Kotetishvilia compressissima*, x **2**. Fig. **3**, *Metahoplites diverse-costatus* (COQUAND, 1880), HOLCODISCIDAE, specimen n° 415032, bed n° 120/041, Angles section, Zone of *Kotetishvilia compressissima*, Subzone of *Subtorcapella defayi*, x **2**. Fig. **4**, *Arnaudiella anglesense* (VERMEULEN, 1995), PULCHELLIIDAE, specimen n° 414651, **holotype**, bed n° 76/041, Angles section, Zone of *Avramidiscus kiliani*, Subzone of *Psilotissotia mazuca*, x **2**. Fig. **5**, *Arnaudiella schlumbergeri* (NICKLÈS, 1894), PULCHELLIIDAE, specimen n° 414035, bed n° 96/041, Angles section, Zone of *Kotetishvilia nicklesi*, x **2**. Fig. **6**, *Subpulchellia oehlerti* (NICKLÈS, 1894), PULCHELLIIDAE, specimen n° 414660, bed n° 97b/041, Angles section, Zone of *Kotetishvilia nicklesi*, x **2**. Fig. **7**, *Kotetishvilia changarnieri* (Sayn, 1890), PULCHELLIIDAE, specimen n° 414090, bed n° 140/041, Angles, Zone of *Holcodiscus uhligi*, x **2**. All specimens: J. Vermeulen's collection.

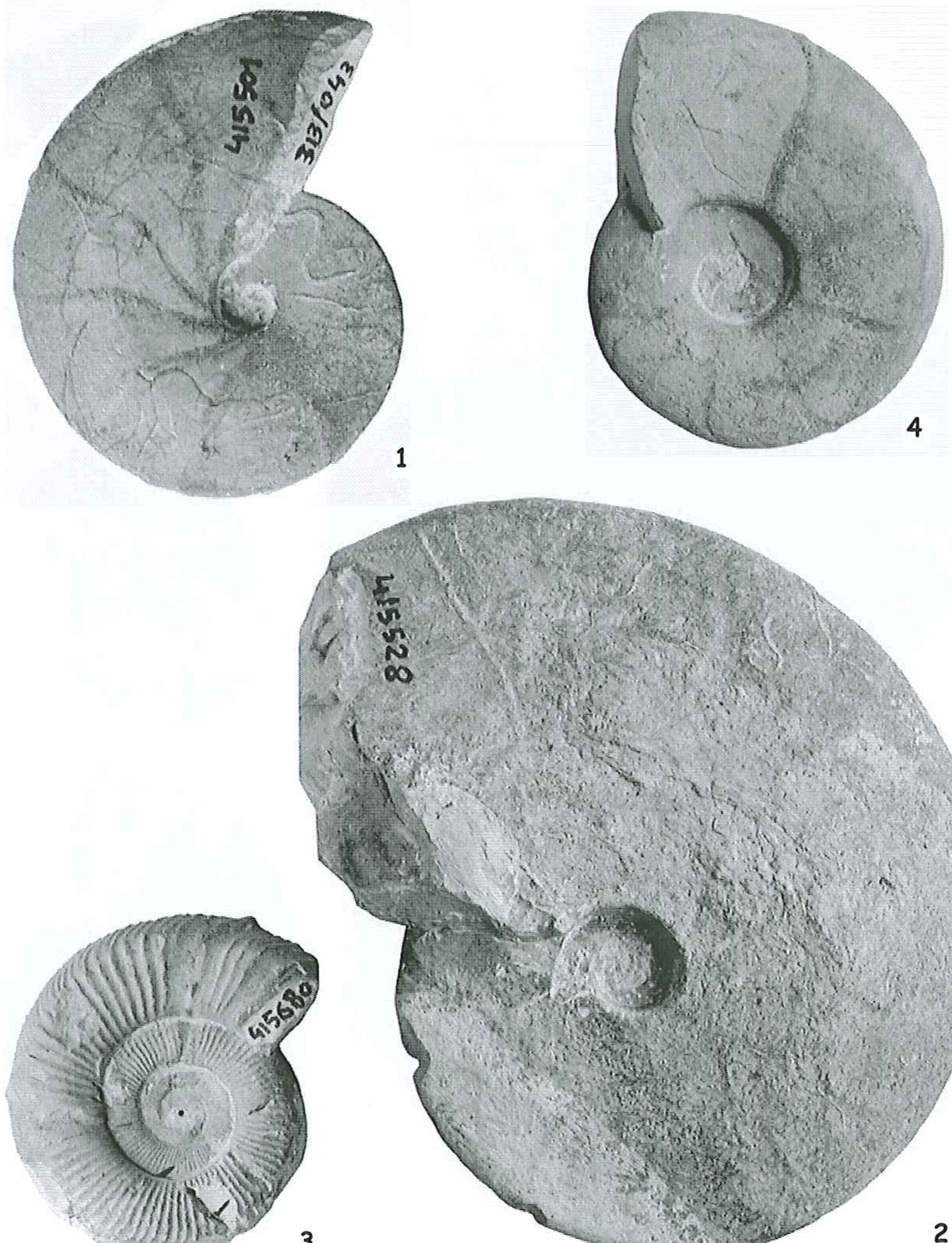

PLATE 45.- Fig. **1**, *Barremites difficilis* (d'Orbigny, 1841), BARREMITIDAE, le Saut du Loup near Barrême, specimen n° 415501, bed n° 313/043, Zone of *Gerhardtia sartousiana*, Subzone of *Gerhardtia provincialis*, x **1**, J. Vermeulen's collection. Fig. **2**, *Barremites strettostoma* (UHLIG, 1883), BARREMITIDAE, specimen n° 415502, bed n° 165/041, Angles section, Zone of *Hemihoplites feraudianus*, x **1**, J. Vermeulen's collection. Fig. **3**, *Silesites seranonis* (D'ORBIGNY), 1841, SILESITIDAE, specimen n° 415680, bed n° 282/045, Zone of *Gerhardtia sartousiana*, Subzone of *Gerhardtia provincialis*, Vergons section, x 1, J. Vermeulen's collection. Fig. **4**, *Melchiorites cassidoides* , BARREMITIDAE, specimen n° 8425/49c, Zone of *Gerhardtia sartousiana*, Subzone of *Gerhardtia provincialis*, Vergons section, x **1**, J.-P. Duyé's collection.

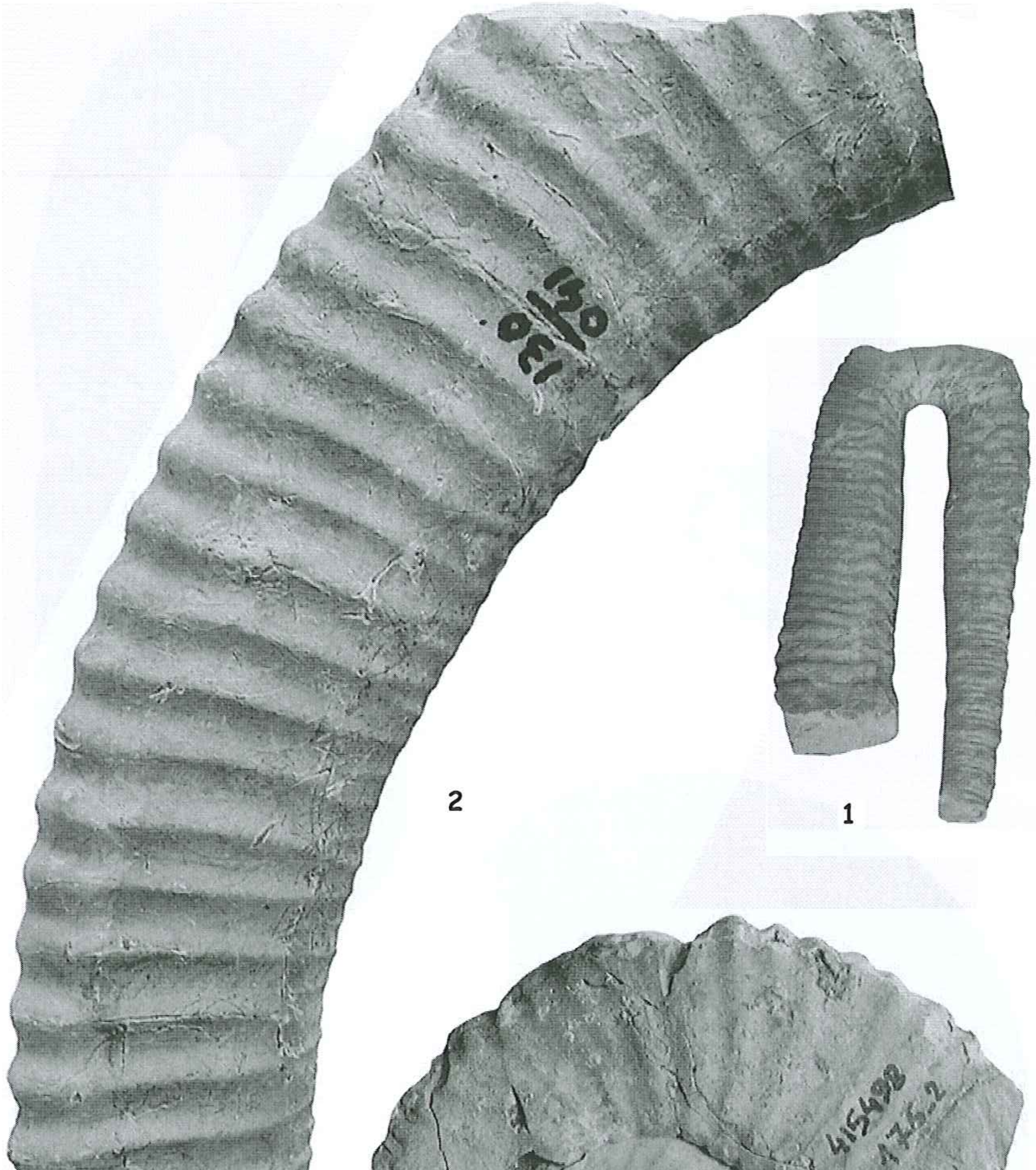

PLATE 46.- Fig. 1, *Dissimilites dissimilis* (D'ORBIGNY, 1842), ACRIOCERATIDAE, specimen n° 415369, bed n° 126/041, Zone of *Coronites darsi*, Angles, x 1. Fig. 2, *Moutoniceras moutonianum* (D'ORBIGNY, 1850), HETEROCERATIDAE, specimen n° 415499, bed n° 130/041, Zone of *Coronites darsi*, Angles section, x 1. Fig. 3, *Martelites sarasini* (ROUCHADZE, 1933), HETEROCERATIDAE, specimen n° 415498, bed n° 176-2/041, Zone of *Martelites sarasini*, Angles section, x 1. All specimens: J. Vermeulen collection.

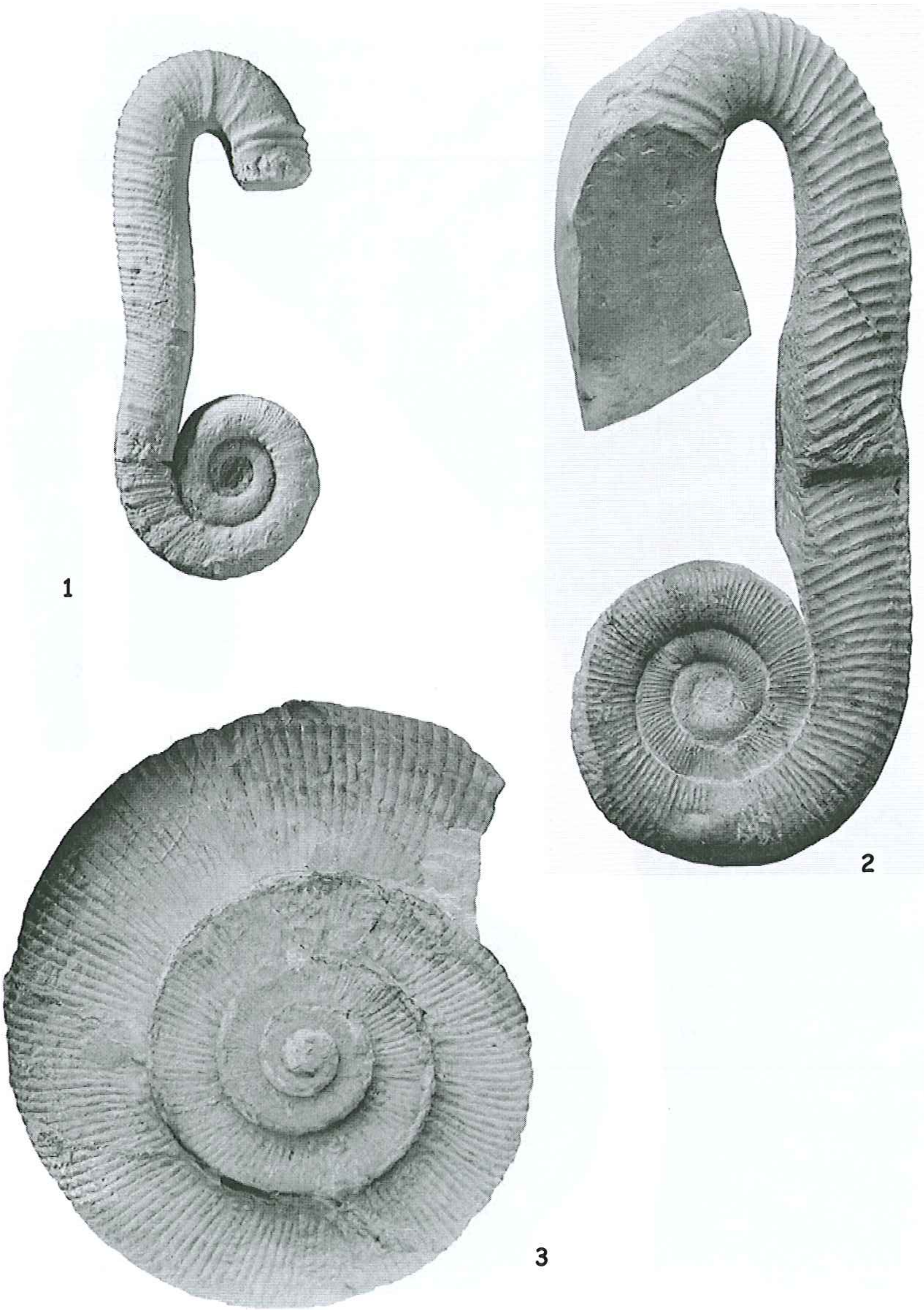

PLATE 47.- Fig. **1**, *Macroscaphites tirolensis* UHLIG, 1887, MACROSCAPHITIDAE, specimen n° 415302, bed n° 134/041, Zone of *Coronites darsi*, Angles section, J. Vermeulen's collection, x **1**. Fig. **2**, *Macroscaphites yvani* (PUZOS, 1832), MACROSCAPHITIDAE, specimen n° 8422/49c, Zone of *Gerhardtia sartousiana*, Subzone of *Gerhardtia sartousiana*, Vergons, J. P. Duyé's collection. Fig. **3**, *Costidiscus recticostatus* (D'ORBIGNY, 1841), MACROSCAPHITIDAE, specimen n° CT2, Angles, P. Lazarin's collection.

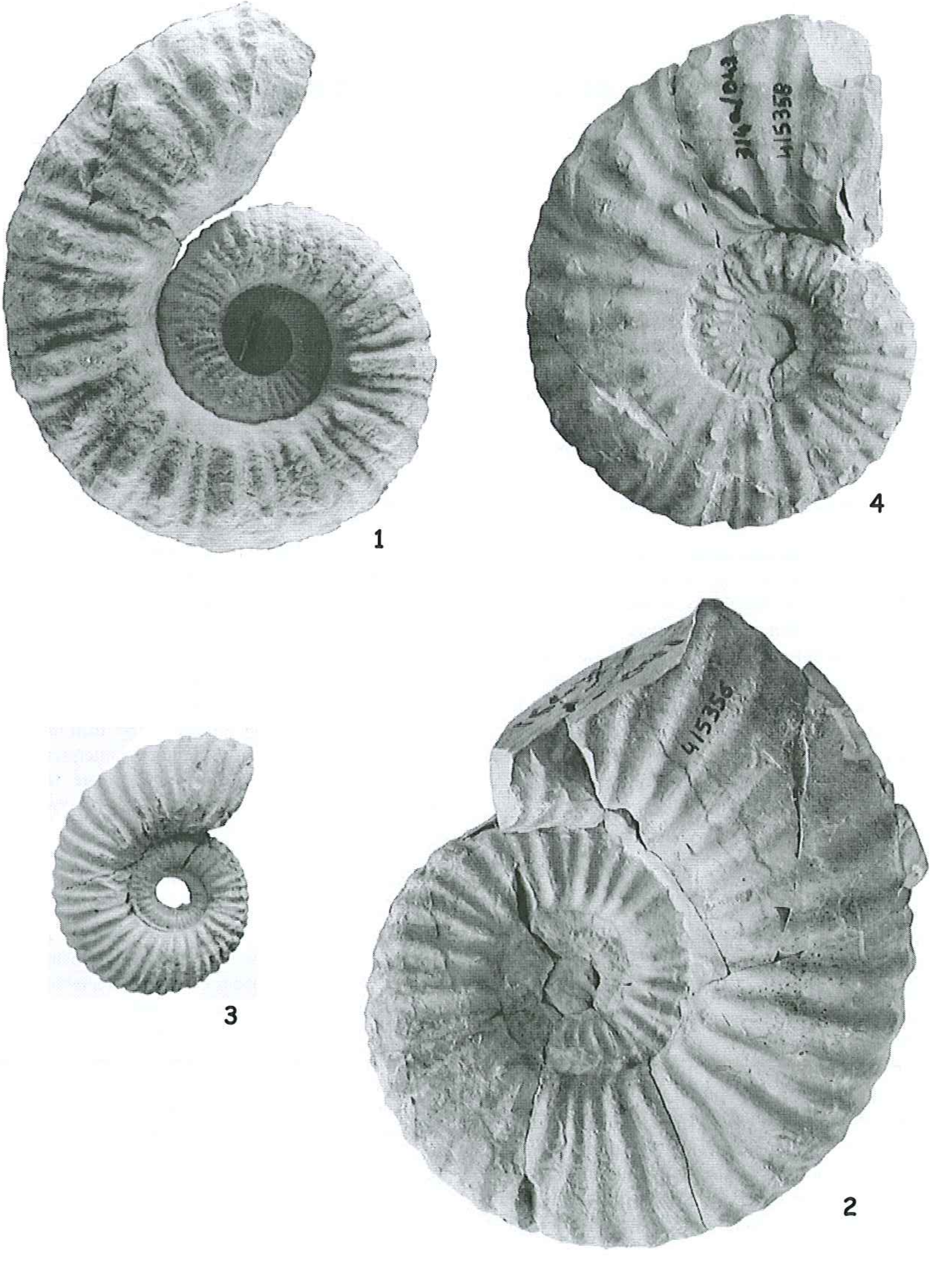

PLATE 48.- Fig. **1**, *Barrancyloceras barremense* (KILIAN, 1895), HEMIHOPLITIDAE, specimen n° 415300, **neotype**, bed n° 151-2/041, Zone of *Heinzia sayni*, Angles section, J. Vermeulen's collection, x **1,05**. Fig. **2**, *Hemihoplites intermedius* VERMEULEN, 2003, HEMIHOPLITIDAE, specimen n° 415356, **holotype**, bed n° 164X/041, Zone of *Gerhardtia sartousiana*, Subzone of *Gerhardtia provincialis*, Angles section, J. Vermeulen's collection, x **1**. Fig. **3**, *Hemihoplites feraudianus* (D'ORBIGNY, 1841), HEMIHOPLITIDAE, specimen n° ID 1019, Zone of *Hemihoplites feraudianus*, secondary road of Blieux, Alpes de Haute-Provence, Zürcher's collection, University of Grenoble. Fig. **4**. *Pachyhemihoplites gerthi* (SARKAR, 1955), HEMIHOPLITIDAE, specimen n° 415358, bed n° 314a/043, Zone of *Gerhardtia sartousiana*, Subzone of *Gerhardtia provincialis*, J. Vermeulen's collection.

Sequence stratigraphy interpretation

Hubert Arnaud

Using sequence stratigraphy at regional scale is not so easy as the sedimentation was dependant on different factors such as climate, nutrient and detrital inputs, depth and luminosity. On the other hand, sedimentation varies considerably in the different areas of the concerning region. For that reasons it is necessary to note what are the main results obtained both in the vocontian trough and on the Urgonian platform.

1.– The Angles section and the vocontian series

The early Cretaceous series of the vocontian trough is everywhere made of a succession of marl-limestone bundles as for the Barremian of the Angles section. Pelagic facies (facies F0) consists of fine-grained calcareous particles and detrital minerals as clays (see Bodin *et al.*, this volume). Calcareous particles are of planktic or platform origin, transported into the basin by storm or turbidity currents. In this kind of basinal section, sequence stratigraphy interpretations are based both on lithology and biostratigraphy.

1.1. Lithology

Owing to different authors, the presence of bundles is probably due to climatic cyclicity (20000 years cyclicity). Thicknesses vary all along the section, not only for the bundles themselves but also for the relative thicknesses of calcareous and marly parts of the bundles. These variations in thicknesses are clearly dependant of sedimentation rates (that is really true if each bundles was deposited during a 20000 years cycle). Sedimentation rates were linked with both 1) sea-level changes and 2) nutrient and detrital input variations.

Nutrient variations leads to the development of planktic microfossils, so that the quantity of calcareous ooze deposited in the basin is more important during period of high level than during period of low level of nutrient input.

Sea-level changes affect mainly the plaforms. During low sea-level periods, carbonate fabrik exists only on the bank margin, location which is good enough for the reworking of the carbonate particles toward the basin by storm or turbidity currents. For that reason lowstand periods are coeval with an increase of the quantity of allochtonous particles deposited in the basin, so that calcareous beds are thick. On the contrary, during high sea-level periods, the carbonate sedimentation backsteps on the platforms and far less particles are available to be transported toward the basin by currents: in that case, corresponding to late transgressive systems tracts (late TST) or early highstand systems tracts (early HST), calcareous beds are far thinner in the basin.

Detrital input variations are more dependant from climate changes, especially concerning the kind of mineral present in the bundles (see Bodin *et al.*, this volume). Nevertheless, the quantity of detrital elements transported to the basin depends also of the paleogeography: this quantity is more important during lowstand periods, when river mouthes are located along the bank margins than during highstand periods when a more or less part of the detrital material is deposited on the platforms.

In conclusion, it is clear that 1) bundles are generally thicker in LST than in TST an 2) both calcareous and marly beds are generally thinner in TST than in LST. It is a good way for sequence stratigraphy interpretation in the vocontian trough surrounded by huge Urgonian platforms. Unfortunatly, lithology is not everywhere so clear due to the interaction of other factors.

1.2. Fauna diversity and abundance

It is known for a long time that abundance and diversity of fauna is less important in LST than in TST. On that point, controversies exist above all owing to the lack of detailed knowledges available in the literature. Due to its richness in ammonite, the Angles section and some other belonging to the same SE France region are the only ones where the distribution of ammonites is well-known (see Vermeulen, this volume).Unfortunatly, these datas which result from a long and important work do not give indications for the relative abundance of specimens. Nevertheless, according to J. Vermeulen, it is clear that the maximum of abundance and diversity of ammonites is linked with set of bundles containing the maximum flooding surfaces (mfs). This increase of abundance is perhaps linked with the high level of nutrient input at the same time (Bodin *et al.*, this volume).

1.3. Main results

The Hauterivian-Barremian boundary is located in the depositional sequence HA7 and correspond approximatly to the transgressive surface (TS) of the

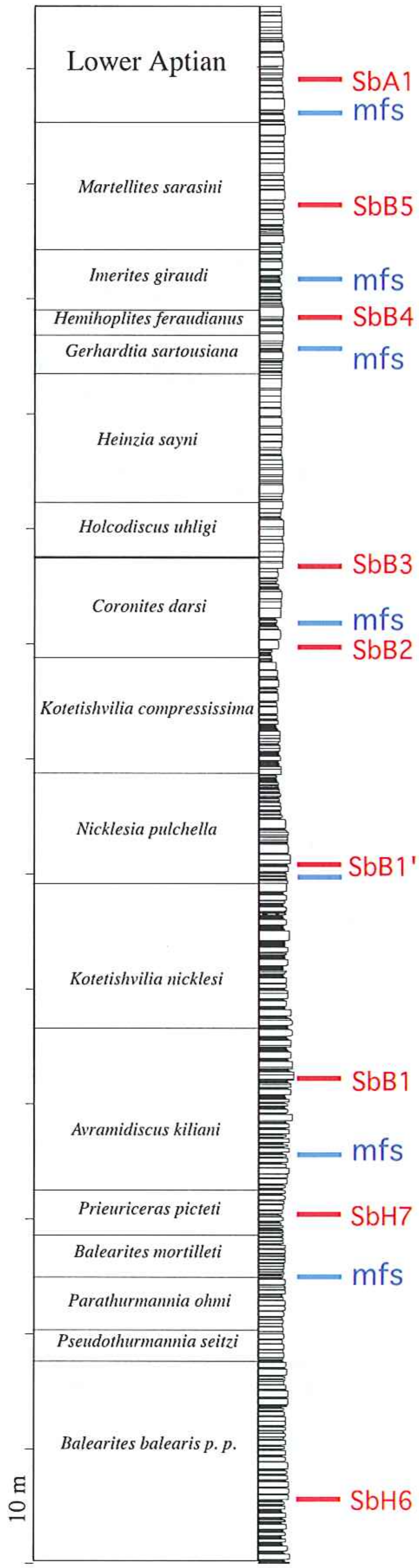

FIG. 88.- Angles section: sequence stratigraphy interpretation.

sequence. The overlaying Lower Barremian corresponds to the three depositional sequences BA1, BA1' and BA2. The two first (BA1 and BA1') are of the same thickness and duration, owing to the number of bundles. The last one (BA2) is approximately half of the first ones in thickness and number of bundles so that it significance seems to be far less important at the regional scale, a point which is proved by observations both on the Provence drowned platform and on the Urgonian platform(fig. 89 and 90).

Late Barremian is represented by three depositional sequences (BA3, BA4 and BA5). Sequence boundary SbB3 appears as the major lihtologic change of the whole Barremian series: it seems to be linked with a major geochimical change for the P content as for the $\delta^{18}O$ and $\delta^{13}C$ (see Bodin *et al.*, this volume). Depositional sequence BA3, as thick as the two last together, is made of a thick calcareous LST followed by a huge TST (these two parts correspond to the most calcareous interval of the series). Mfs is clearly located in the *Gerhardtia sarousiana* zone and the overlayed relatively thin HST from the upper part of this zone to the middle part of the *Hemihoplites ferausianus* zone. Due to the lack of some beds of the *H. feraudianus* zone in the Angles section, it is not possible here to know exactly what happens for the late HST of the BA3 sequence and for the LST and early TST of the depositional sequence BA4. The most marly interval of the series is recognized from the late TST of sequence BA3 to the early HST of sequence BA4: this lithologic feature could be linked with 1) the backstepping of the carbonate sedimentation on the surrounding Urgonian platforms, 2) the decrease of nutrient input (more oligotrophic conditions) and 3) the great change from hot and wet to arid climate (Bodin *et al.*, this volume). At the top of the Angles section, the depositional sequence AP1 is uncomplete due to faulting.

2.– THE CLOS DE BARRAL SECTION AND THE PROVENCE DROWNED PLATFORM

The Provence drowned platform is characterized, south from Castellane, by hemipelagic marl-limestone bundles rich in ammonites. As the Barremian series has been divided in 26 ammonite biohorizons by Vermeulen (2002 and this volume, fig. 71), this author is now able to propose a high resolution biostratigraphy for the Clos de Barral, near of Le Logis du Pin, and Escragnolles sections (fig. 89).

Near Escragnolles (north of the city of Grasse), the five metres-thick barremian series is mainly represented by several glauconitic and condensed beds. Gaps occur at different level of the series, corresponding to sequence boundaries. Depositional sequences are only represented by condensed sections (mfs).

The Clos de Barral section is thicker and sequence stratigraphy interpretation easier than in the basin sections like Angles.

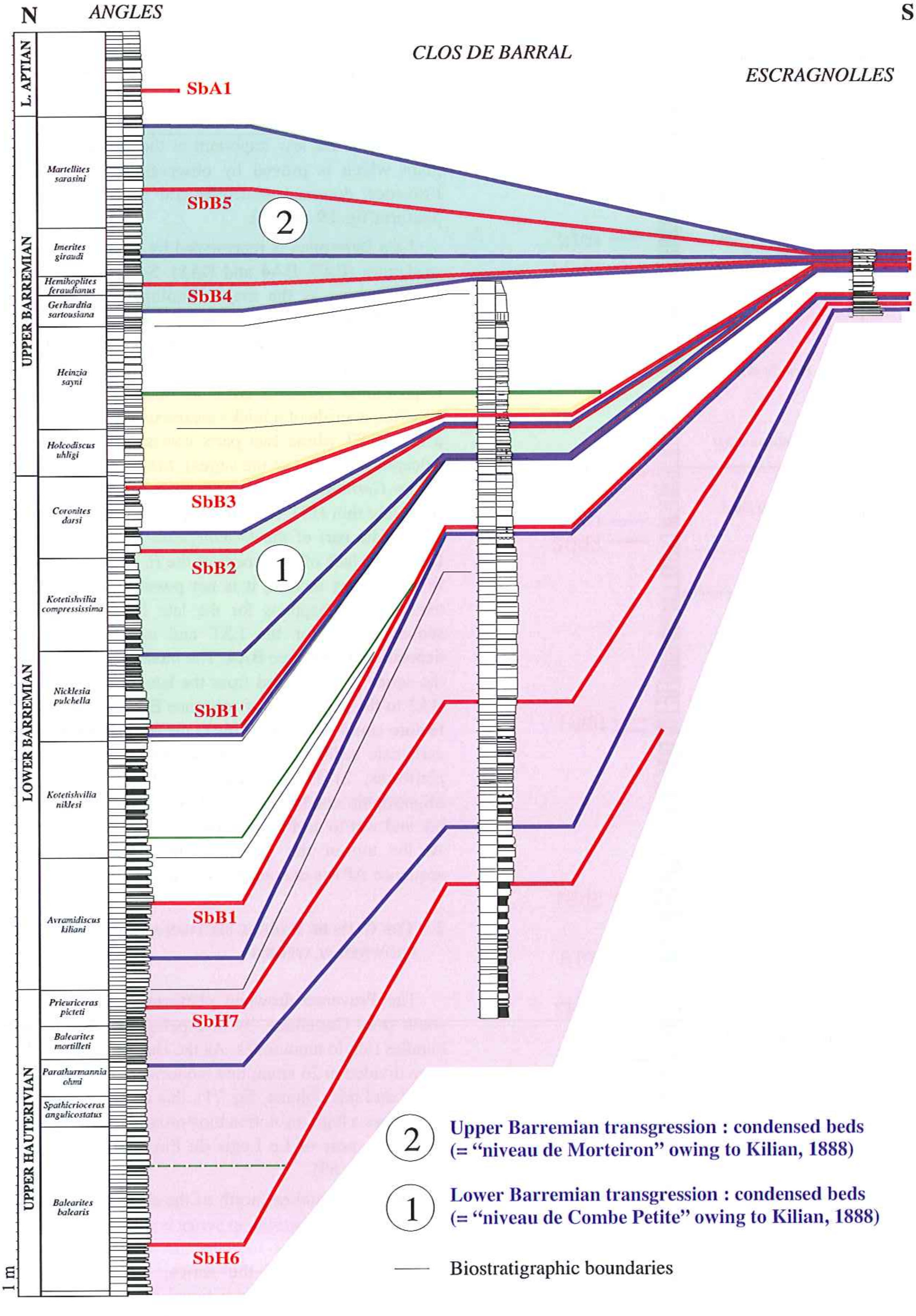

FIG. 89.- Sequence stratigraphy interpretation and correlations between the vocontian trough (Angles section) and the Provence drowned platform (Clos de Barral and Escragnolles sections).

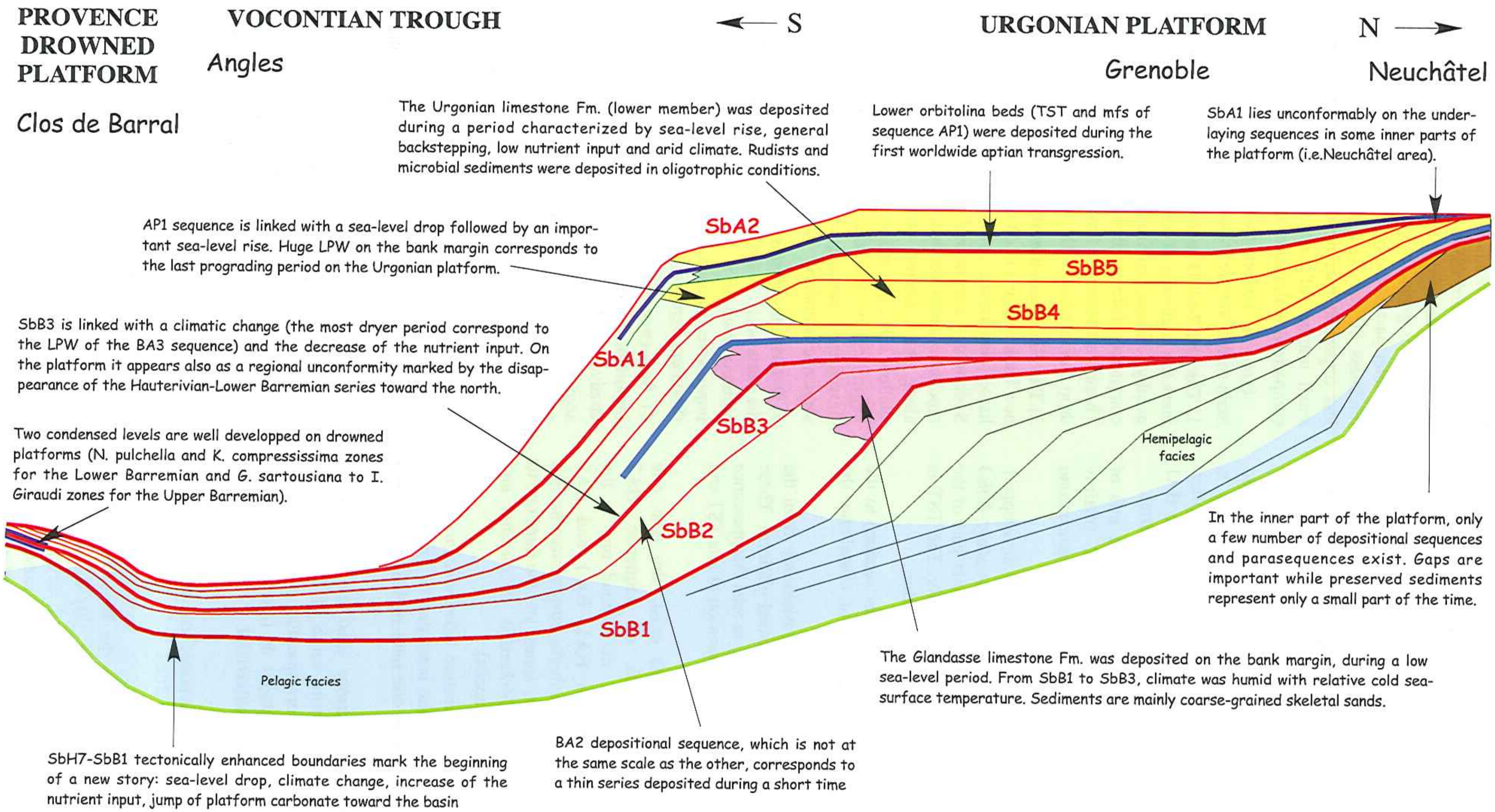

FIG. 90.- Schematic cross-section from the Provence drowned platform to the Urgonian platform (Northern subalpine chains and Jura) showing the sequence stratigraphy interpretation and the evolution of the urgonian platform at the regional scale.

– The upermost Hauterivian and lowermost Barremian is represented by two well developped depositional sequences (HA6 and HA7). Their total thickness is the same as for the Angles section while the repartition of thicknesses is different: the HA6 HST and the HA7 LST?-TST are thicker in Clos de Barral than in the Angles section. Late TST and early HST correspond to the first condensed beds of the region (*Avramidiscus kiliani* zone, lowermost Lower Barremian).

– The BA1 depositional sequence is the most constant unit of this region as its thickness and lithology is relatively the same from Angles to Escragnolles. Nevertheless, biostratigraphy data prove that the BA1 LST and early TST are lacking in Le Clos de Barral.

– A second condensed level occur from the mfs of sequence BA1' to mfs of sequence BA2 (mainly *Nicklesia pulchella* and *Kotetishvilia compressisima* zones, *Coronites darsi* zone at the top).

– The depositional sequence BA3 is well developped. As the first bed above the sequence boundary SbB3 belong to the *Heinzia sayni* zone, the main part of the LST (*Coronites darsi* zone) lack totally. The TST is more marly at the top of the visible section.

From the vocontian trough (Angles section) to the Provence drowned platform, south of Castellane, the following informations can be done.

1) The total thickness decrease considerably from the basin to the inner part of the drowned platform. These thicknesses variations are due both to total disappearance of LST and to progressive condensation of late TST and early HST.

2) Three condensed sections exist, the first one corresponding to the mfs of sequence HA7 (*Avramidiscus kiliani* zone), the second one to the stacked mfs of sequences BA1, BA'1 and BA2 (*Nicklesia pulchella, Kotetishvilia compressissima* and basal part of *Coronites darsi* zones) and the third one to the Upper Barremian (*Gerhardtia sartousiana* and *Hemihoplites feraudianus* zones).

3) The first condensed section (*Avramidiscus kiliani* zone) is known only on the inner part of the drowned platform and the second one (and probably the third) exists also basinward.

4) These condensed sections exist not only on the Provence drowned platform, south of Castellane, but also in other regions corresponding to hemipelagic domain, such as the Montagne de Lure, near Sisteron, and central and eastern Switzerland.

3.– The Urgonian platform of the Northern subalpine chains and Jura

The general section from the Provence drowned platform to the Swiss Jura (fig. 90) shows that the number of depositional sequences and, for each of them, the number of parasequences is far less important in the inner part than in the outer part of the platform or in the basin. As a consequence, gaps are more and more important toward the inner part of the platform. On the other hand, detailed studies show that the parasequence thickness is generally greatest in the inner part than in the outer part of the platform: the reason why the total thickness of carbonate platform deposits is generally less important basinward than seaward is due to the small number of parasequences in the first area in comparison with that of the second one.

From the bottom to the top of the Barremian, the main results are the following:

1) **The SbH7-SbB1 tectonically enhanced boundaries** mark the beginning of a new story: Baremian paleogeography, climate, environments and sedimentation are completely different from that of the Hauterivian time. These boundaries are linked with an important sea-level drop and increase of the nutrient input.

2) **The Glandasse limestones Fm.** was deposited on the new bank margin i.e. on the distally part of the previous hauterivian ramp, during a period of humid climate. Sediments correspond mainly to coarse-grained bioclastic sands deposited on narrow banks elongated along the emerged platform and characterized by shallow and open marine environments. Owing to the beginning of the sea-level rise during the early Barremian, parasequences onlap the underlaying sequence boundary.

3) **Depositional sequence BA2** does not appear to be at the same scale as the other (as observed on the Angles section) even if it corresponds locally to thick and impressive deposits such as on the Glandasse Plateau (Southern Vercors). Its significance is unclear until today.

4) **Sequence boundary SbB3** is one of the most important. In the inner part of the platform it is highly erosive: landward, all the depositional sequences and sequence boundaries are eroded until the Lower Hauterivian in the Neuchâtel area. SbB3 is also coeval with climate and nutrient input changes.

5) **The lower member of the Urgonian limestone Fm.** was deposited during a period characterized by sea-level rise, low nutrient input and arid climate. Carbonate deposits backstep on the bank margin, due to the sea-level rise (late Barremian transgressions). Oligotrophic environments are characterized by the development of rudist communities and microbial sedimentation.

6) **Sequence boundary SbA1** is the third most important boundary, at the top of the Barremian series. It is linked with an important sea-level drop during which carbonate sedimentation is only developped on the bank margin LST (for example Montagne de Belle Motte LST). At that time begins the Aptian story which is marked by rapid and more than 100 m changes of the sea-level (not only for SbA1, but also for SbA2 and SbA3 in the upper part of the early Aptian). At regional scale, SbA1 is highly erosive, not only in the Jura (inner part of the platform) but also in some parts of the Northern subalpine chains where some faults were active at that time.

7) **The Lower orbitolina beds**, TST of the depositional sequence SbA1, is the first of the worldwide aptian transgressions. *Palorbitolina lenticularis*-rich marly beds occur in the greatest part of the considered area.

8) **The sea-level variations**, which seems to be not so important during the Hauterivian time, are more and more important from the early Barremian to the early Aptian (fig. 7). At that timethey reach more or less 100 metres from the lowest to the highest sea level (depositional sequences AP1, AP2 and AP3).

9) **Incised valleys** are common during late Barremian-early Aptian times. In the Northern Vercors (l'Achard, Autrans syncline), the most impressive one is more than 60 m depth. It means that the elevation of the platform above the sea level was at least 60 m high at that time, i. e. far more than we have proposed the last decades. It is the reason why **everywhere in the platform series**, diagenetic complex stories due to emersion and fresh-water circulations, are evidenced below sequence boundaries: they give birth to reservoirs even if only the first stages of these stories correspond to synsedi-mentary events.

Summary